Analyzing and Modeling Capacity for Decentralized Air Traffic Control

Sunil, Emmanuel

Important note
To cite this publication, please use the final published version (if applicable).
Please check the document version above.

Analyzing and Modeling Capacity for Decentralized Air Traffic Control

Analyzing and Modeling Capacity for Decentralized Air Traffic Control

Proefschrift

ter verkrijging van de graad van doctor
aan de Technische Universiteit Delft,
op gezag van de Rector Magnificus Prof.dr.ir. T.H.J.J. van der Hagen,
voorzitter van het College voor Promoties,
in het openbaar te verdedigen
op maandag 1 april 2019 om 15:00 uur

door

Emmanuel SUNIL

ingenieur luchtvaart en ruimtevaart,
geboren te Thodupuzha, Kerala, India

Dit proefschrift is goedgekeurd door de

promotor: Prof. dr. ir. J.M. Hoekstra
copromotor: Dr. ir. J. Ellerbroek

Samenstelling promotiecommissie:

Rector Magnificus,	voorzitter
Prof. dr. ir. J.M. Hoekstra,	Technische Universiteit Delft, promotor
Dr. ir. J. Ellerbroek,	Technische Universiteit Delft, copromotor

Onafhankelijke leden:

Prof. dr. D. G. Simons	Technische Universiteit Delft
Prof. dr.-ing. H. Fricke	Technische Universität Dresden
Prof. dr. D. Delahaye	Ecole Nationale de l'Aviation Civile
Prof. dr.-ing. D. Kügler	Deutsches Zentrum für Luft- und Raumfahrt
Dr. B. Hilburn	Center for Human Performance Research
Prof. dr. ir. M. Mulder	Technische Universiteit Delft, reservelid

In memory of my dear little sister Ann-Mary
You will always be loved

Summary

The current system of Air Traffic Control (ATC) relies on a *centralized* control architecture. At its core, this system is heavily dependent on manual intervention by human Air Traffic Controllers (ATCos) to ensure safe operations. The capacity of this system is, therefore, closely tied to the maximum workload that can be tolerated by ATCos. Although this system has served the needs of the air transportation industry thus far, the increasing delays and congestion reported in many areas indicates that the current centralized operational model is rapidly approaching saturation levels.

To cope with the expected future increases of traffic demand, many researchers have proposed a transition to a *decentralized* traffic separation paradigm in en route airspaces. Although there are several variants of decentralized ATC, this thesis focuses on a variant known as *self-separation*. In self-separated airspace, each individual aircraft is responsible for its own separation with all surrounding traffic. To facilitate self-separation, significant research effort has been devoted towards the development of new algorithms for automated airborne Conflict Detection and Resolution (CD&R).

However, in spite of over two decades of active research highlighting its theorized benefits, decentralization/self-separation is yet to be deployed in the field. From a technical point of view a lack of understanding on three open issues namely airspace design, airspace safety modeling, and airspace capacity modeling, have impeded its further development and implementation. The goal of this research is to address these three open problems in order to bring self-separated ATC closer to reality. Consequently, the main body of this thesis is divided into three parts, with each part tackling one of the three aforementioned open problems.

The first part of this study focused on decentralized airspace design. Although airspace design elements such as airways and sectors are used by the current centralized ATC system, the use of similar design options to optimize decentralized operations have not been considered in detail by previous studies. In fact, there is no consensus in existing literature on whether or not some form of traffic structuring is also beneficial for decentralized ATC, with different studies on this topic presenting diametrically opposite conclusions. To gain a more thorough understanding of the relationship between airspace design and capacity for decentralized ATC, this study used fast-time simulations to empirically compare four airspace concepts of increasing structure. The four concepts, ranging from a completely unstructured direct routing airspace concept, to a highly structured tube network using 4-D trajectories, were subjected to multiple traffic demand conditions within the same simulation environment, for both nominal and non-nominal conditions.

The results of these simulations were highly unexpected; since previous studies had focused on only fully unstructured and fully structured airspace designs, one of these two extreme design options was hypothesized to lead to the highest capacity. The simulation results, on the other hand, indicated that a layered airspace design, which used heading-altitude rules to vertically separate cursing aircraft based on their travel directions, resulted in the best balance of all airspace metrics considered. This approach to organizing traffic not only lowered relative velocities between aircraft, it also permitted direct horizontal routes. As such the layered airspace concept led to the highest safety of all designs tested, without unduly reducing route efficiency relative to the completely unstructured design; the latter design option resulted in the second-best capacity. In contract, airspace concepts that imposed strict horizontal constraints on traffic caused a mismatch between the imposed structure and the traffic demand pattern. This in turn led to artificial traffic concentrations that reduced overall performance and capacity. To summarize, capacity for decentralization improved when structural constraints fostered a reduction of relative velocities, and when direct horizontal routes were permitted.

The second part of this thesis derived mathematical conflict count models that quantified the intrinsic safety of an airspace design, using unstructured and layered airspace concepts case studies. Here, the notion of intrinsic safety refers to the ability of an airspace design to prevent conflicts from occurring solely because of the constraints that it imposes on traffic motion. The models considered here are often referred to as 'gas models' in literature. As the name implies, this modeling approach treats conflicts between aircraft similar to the collisions that occur between ideal gas particles. Although such models are widely used within ATC research, most previous gas models have focused on only conflicts between cruising aircraft, limiting their applications.

This thesis, therefore, extends gas models such that they take into account the effects of both cruising and climbing/descending traffic on conflict counts. The developed method grouped aircraft according to flight phase, while also considering the interactions, as well as the proportion of aircraft, in different flight phases. This approach was combined with a simple, but novel, method to compute both the horizontal and vertical components of the weighted average relative velocity in an airspace. Fast time simulation experiments indicated that the resulting 3-D models estimated conflict counts with high accuracy for both unstructured and layered designs, for all tested conditions. Moreover, the results also indicated that climbing/descending aircraft are involved in the vast majority of conflicts for layered airspaces with a narrow heading range per flight level. The latter result emphasized the importance of considering all relevant flight phases when assessing the intrinsic safety of an airspace design.

In a related effort, this research also evaluated the effect of traffic scenario properties on the accuracy of gas models. The *analytical* gas models described previously make use of a number of idealized assumptions regarding the behavior of traffic that do not always reflect realistic operations, particularly with regard to the distributions of aircraft speed, heading, altitude and spatial locations. To address this limitation,

this research investigated the effects of such traffic scenario assumptions on the accuracy of analytical gas models using targeted fast-time simulations. Additionally, this work also developed and tested so called *numerical* 'model adjustments' that relaxed the dependency of the models on the idealized scenario assumptions. As before, conflict count models for unstructured and layered airspaces were used as cases studies for these purposes.

The results of these targeted simulations indicated that non-ideal altitude and spatial distributions of traffic had drastic negative effects on analytical model accuracy, while non-ideal heading distributions had a smaller negative effect on accuracy. In contrast, ground speed distribution did not meaningfully affect conflict counts for the airspace designs considered here; its effect, however, did increase in magnitude as the heading range per flight level was decreased for layered airspaces. The simulation results also indicated that the numerical model adjustments developed in this thesis increased accuracy for the more realistic scenarios to the levels found with the analytical model for the ideal scenario settings. Therefore, in addition to providing a physical understanding of the factors that affect intrinsic airspace safety, the adjusted conflict count models can also be used as tools for practical airspace design applications.

The third and final part of this thesis developed a quantitative method to determine the capacity limit of decentralized airspace concepts. The method considered here, named Capacity Assessment Method for Decentralized ATC (CAMDA), defined capacity as the traffic density at which conflict chain reactions propagate uncontrollably throughout the entire airspace. In other words, at the capacity limit, all aircraft exists in a persistent state of conflict, because every conflict resolution action leads to an infinite number of new conflicts. This critical density was identified using a semi-empirical approach whereby analytical models describing the intrinsic safety provided by an airspace design are combined with empirical models describing the actions of CD&R algorithms. Because conflict chain reactions affect both the safety and efficiency of travel, the approach used by CAMDA treats capacity as an intrinsic property of the airspace.

The CAMDA method is demonstrated here using fast-time simulations of decentralized unstructured and layered airspace designs that utilized a state-based method for conflict detection, and a voltage potential-based algorithm for conflict resolution. The simulation results confirmed the predictions of the CAMDA models; capacity was found to be higher for layered airspaces because it used predefined flight levels and heading altitude rules for cruising traffic. These two design elements reduced the number of possible combinations of two aircraft, and the average conflict probability between aircraft, when compared to unstructured airspaces, which in turn increased the maximum capacity for layered airspaces. The simulations also strongly indicated that the pairing between the selected airspace design and selected CD&R algorithm needs to be optimized to maximize decentralized airspace capacity.

The simulations used to demonstrate CAMDA also studied the effects of conflict detection parameters, conflict resolution dimension, conflict resolution priority, and the speed distribution of aircraft, on capacity. For all studied cases, CAMDA estimated the occurrence of conflict chain reactions with high accuracy, and therefore enabled capacity estimations using relatively non-intensive low density traffic simulations. Furthermore, because all CAMDA parameters have a physical interpretation, the effects of all tested conditions on capacity could be directly understood from the structure of the underlying models. For these reasons, in addition to providing a comparative capacity measurement metric, the CAMDA method can also be used to systematically select the experimental conditions necessary to assess the capacity limit of decentralized airspace designs.

Although the safety and capacity models derived in this work have focused on unstructured and layered airspace designs, it is important to realize that the underlying modeling methods are applicable to other airspace concepts. Any adaptations along these lines would require an analysis of how the constraints imposed by a particular airspace design affects the number of possible combinations of two aircraft, and the average conflict probability between any two aircraft, since these two basic factors are the starting point for all the safety and capacity models discussed here. Extensions of the models for other airspace designs is an interesting avenue for further research.

It should be noted that all the quantitative models described in this thesis have been validated under ideal weather conditions. Since weather is known to adversely affect the safety and the capacity of the airspace, the accuracy of the derived models for other, more realistic, weather conditions should be considered in future research. In this context, it is worth recognizing that the semi-empirical CAMDA capacity assessment method could, in theory, be used to quantify the capacity reductions caused by various whether phenomena, as long as such phenomena can be simulated with adequate realism. The use of the CAMDA method to assess the effects operational constraints, such as weather, on capacity represents another interesting topic for further analysis.

Lastly, it is necessary to consider the practical applications of this research. Before the safety conscious aviation authorities can be convinced of a radical transformation of en route airspace from a centralized to a decentralized design, it is likely that more practical experience needs to be gained with decentralized ATC. Thanks to the rapid emergence of *unmanned and personal aerial vehicles*, it may be possible to obtain such empirical data in the near future. The incredible traffic volumes forecasted for these new aircraft types, and the clean sheet approach to ATC that is required to facilitate their operation, has provided the necessary incentives for aviation authorities to investigate important some aspects of decentralization for the growing field of *urban airspace design*. Because of the generic nature of the airspace designs and of the quantitative safety and capacity models discussed in this thesis, the results of this work can be generalized beyond the specific conditions that have been considered here, for instance for the lower speeds of anticipated for unmanned aircraft. Therefore, in the short term, the methods developed in

this thesis to analyze and model the capacity of decentralized ATC could be useful towards the design of new concepts that enable low altitude urban air transport operations.

Contents

1

Introduction

At present, the safety of air travel is heavily reliant on manual intervention by ground-based air traffic controllers. Consequently, the capacity limits of the current system of air traffic control is closely tied to the maximum workload that an air traffic controller can tolerate. To cope with the ever increasing demand for air travel, many researchers have proposed a transfer of traffic separation tasks from the ground to each individual aircraft as a means to increase airspace safety and capacity over current operations. To facilitate the resulting decentralized traffic separation paradigm, previous studies have focused their attention on the development of advanced 'self-separation' automation. However, before the safety conscious aviation authorities can be convinced of a transition to a new, and as yet untested, mode of operations, it is also necessary to quantify the safety and capacity benefits of decentralized control. This chapter introduces the conceptual design of decentralized air traffic control and presents an overview of the previous literature in this domain. Subsequently, several open problems that have impeded the deployment of decentralized operations are used to motivate the main objectives of this thesis.

1

1.1. A Brief History of Air Traffic Control

In the early days of aviation, pilots relied on simple 'see-and-avoid' principles to prevent mid-air collisions, and navigated using landmarks such as roads, rivers and railway tracks [1]. As a result of numerous near misses and several high-profile accidents, these simple rules for collision avoidance and navigation were deemed to be no longer adequate as traffic demand increased in the 1920s [1].

To improve safety, and bolster public confidence in the fledgling air transportation industry, more formal systems and procedures for Air Traffic Control (ATC) were developed in the 1930s. These included, amongst others, the installation of rotating light beacons for navigation in low visibility conditions, which in turn led to the establishment of the first airways/air-routes between major cities [2].
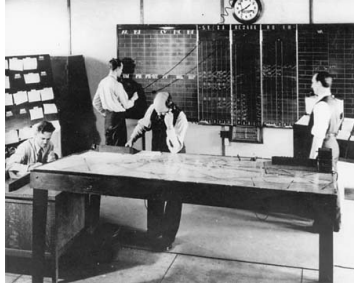
This era also saw the introduction of a new role in aviation, one that had a profound impact on the design and evolution of the entire current ATC system architecture. This was the role of the Air Traffic Controller (ATCo). Initially, ATCos were stationed only at airfields, see Figure 1.1, and their primary task was to coordinate the flow of aircraft in and around airports from air traffic control towers, or TWRs [3].
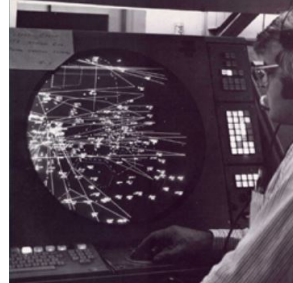
Figure 1.1: Archie William League, the first Air Traffic Controller (ATCo), at St. Louis airport in 1929. League's 'control tower' consisted of a wheelbarrow, a folding chair, an umbrella for shade, and colored flags for traffic control. League went on to earn a degree in Aeronautical Engineering, and was pivotal in the creation of many early ATC systems [4].

By the mid-1930s, ATCo responsibilities were extended to also separate high altitude aircraft in en route airspaces [2, 3]. These ATCos, located at Area Control Centers (ACCs)[1], used verbal position reports from pilots, and data from pre-filed flight plans, to identify and warn flight crews about potential collisions; see Figure 1.2(a). As cockpit avionics of the time did not provide any information about surrounding traffic, new regulations forced pilots to follow the instructions commanded by ATCos for the sake of safety [2, 3]. These regulations laid the foundations of a *centralized* ATC system in which final authority over aircraft separation and trajectory changes rested with ATCos, even though only pilots can directly manipulate aircraft flight paths.

---

[1]ACCs are known as Air Route Traffic Control Centers (ARTCCs) in the United States

(a) ATCos on duty at the first ACC in 1936, in Newark, USA

(b) Radar gave ATCos more active control of traffic from the 1940s

Figure 1.2: Evolution of en route Area Control Centers (ACC) [4]

After the Second World War, several technological innovations transformed the centralized ATC system. Most notably, radar technology gave ATCos more active control of the traffic [5]; see Figure 1.2(b). Ground navigation aids were also updated with radio beacons to further extend the network of airways to connect different parts of the world [2]. Additionally, to improve the transition between TWRs and ACCs, new Terminal Maneuvering Area centers (TMAs)[2] were established to separate climbing and descending aircraft around airports, and also from traffic in en route airspaces [5].

Although increasing levels of automation have been introduced over the years, from a system-design point of view, today's ATC has not changed substantially since the 1960s; controlled airspace is still structured into TWRs, TMAs and ACCs, and more importantly, traffic separation is still heavily reliant on manual intervention by ATCos [5]. For this reason, ATCo workload is often cited as one of the main capacity bottlenecks of the current centralized ATC system [6–11]. In fact, the need for ATCos to manage their workload explains the continued dependence on airway navigation during busy daytime operations. Although modern airliners can fly arbitrary routes accurately, airways limit aircraft flight paths along predefined trajectories, see Figure 1.3, and the resulting predictable and structured flow patterns make it easier for ATCos to monitor and deconflict traffic. However, as the airway structure is historically dependent on the location of radio navigation beacons, airway routing can add significant extra distance to flights (in relation to direct/great-circle routing) [12].

Due to such inefficiencies, the centralized ATC system is not expected to keep pace with the ever-increasing demand for air transportation [12–17]. Evidence for this can be found by studying delay statistics. In Europe, for instance, a moderate traffic demand increase of 2.4% in 2016 led a disproportionate 20.9% increase of en route delays [12]. In addition to costing airlines as much as 479 million euros, the trajectory deviations contributing to these delays also led a to a 25.3%

---

[2]TMAs are known as Terminal Radar Approach Control Centers (TRACONs) in the United States
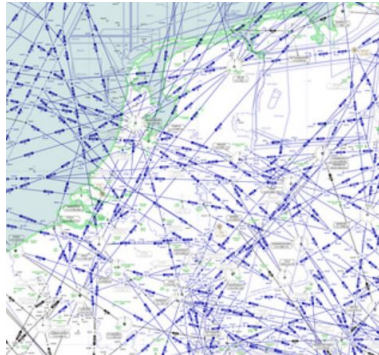
Figure 1.3: High altitude airway network over the Netherlands. Airways do not always allow direct routing, and thus reduces flight efficiencies. Source: skyvector.com

increase in the number of serious separation minima infringements, an indicator of safety [12]. These bleak statistics are likely to worsen in the future given the world-wide shortage of ATCos.

In response to the degrading performance of the current ATC system, novel approaches for ATC are being actively explored by large research projects in Europe and in the United States, known as SESAR and NextGen respectively [16–19]. While these programs aim to introduce incremental capacity improvements in the short-term, some of the proposed long-term plans call for a radical transformation of en route airspace from a centralized to a *decentralized* design.

1.2. What is Decentralized ATC?

To increase en route airspace capacity beyond the limitations of the current centralized system, many studies have proposed a decentralization of traffic separation responsibilities, from ground-based ATCos to each individual aircraft. A transition to decentralized ATC, therefore, implies a return to the early days of flight when pilots performed flying, navigation and collision avoidance tasks, but with the aid of modern surveillance and automation technologies. This section describes the conceptual design of decentralized ATC, its advantages over centralized ATC, and provides an overview of the previous research in this field.

1.2.1. Conceptual Design of Decentralized ATC

The change that decentralization brings to ATC can be best understood by comparing its conceptual design with that of the current centralized system; see Figure 1.4. As mentioned before, in centralized ATC, an ATCo on the ground is responsible for adequate separation between all aircraft in his/her airspace sector, see Figure 1.4(a). Hence, in centralized ATC, aircraft act as *passive agents* with respect to separation. On the other hand, in decentralized ATC, the separation task is trans-

(a) Centralized ATC   (b) Decentralized ATC
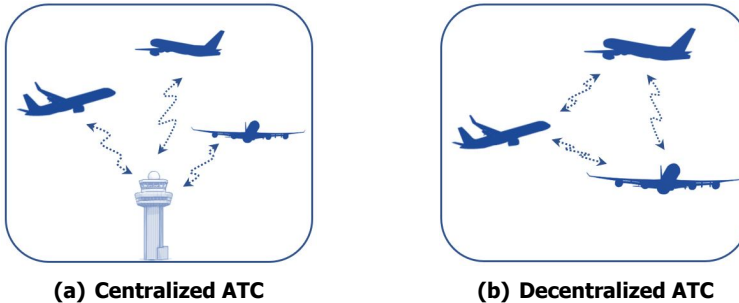
Figure 1.4: Difference between the conceptual designs of centralized and decentralized ATC.
Adapted from [20].

ferred to the cockpit. In this case, aircraft act as *active agents*, and each aircraft
is responsible for its own separation with all surrounding traffic, see Figure 1.4(b).
Consequently, this type of ATC is also referred to as 'self-separation'.

To enable self-separation, aircraft need to be made aware of the positions of all
neighboring traffic. In literature, this is often achieved using Automatic Dependent
Surveillance-Broadcast (ADS-B), a system for inter-aircraft communication [21, 22].
Using ADS-B transmitters, aircraft periodically broadcast their state information, in-
cluding their identification, 3D position, velocity and target state, using data gather
by onboard sensors. This functionality, known as ADS-B OUT, is already in use,
with many parts of the world mandating ADS-B transmitter equipage for flights
operating in controlled airspace by 2020 [23, 24].

Analogous to ADS-B OUT is ADS-B IN. Aircraft with ADS-B IN capability use receivers
to collect the state information transmitted by other aircraft in range, and this data
is presented to pilots using cockpit displays in real time. Subsequently, pilots can
identify and resolve conflicts manually, or do so with the support of automated
algorithms for airborne Conflict Detection and Resolution (CD&R). Recent studies
have shown that the ADS-B system and its signal quality are sufficiently robust for
self-separation applications [25, 26].
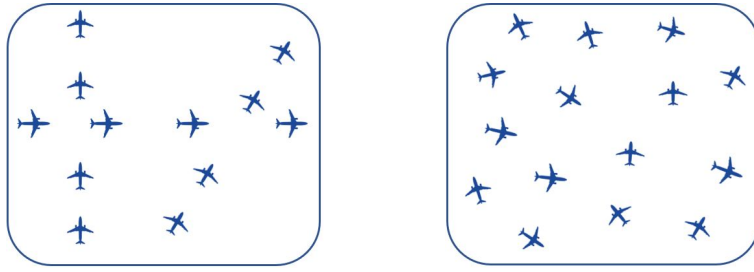
1.2.2. Advantages of Decentralized ATC

Decentralized separation in en route airspace is expected to yield several advan-
tages over centralized ATC in terms of efficiency, safety and capacity.

1.2.2.1. Efficiency

As indicated earlier, one of the major sources of delay in current operations has been
attributed to the use of airways [12]. Although airways reduce ATCo workload by
organizing traffic along predefined routes, see Figure 1.5(a), they can also increase
flight distances. Since ATCos are not actively involved with traffic separation in

(a) Centralized ATC relies on airway routing

(b) Decentralized ATC permits direct routing

Figure 1.5: Difference between aircraft routing in centralized and decentralized ATC. Adapted from [20].

decentralized ATC, aircraft would no longer be restricted to using airways for en route navigation. Instead, airspace users are free to fly arbitrary routes by making full use of the so called 'Area Navigation' (RNAV) capabilities of modern onboard Flight Management Systems (FMS), see Figure 1.5(b). In many cases, the lack of routing constraints will allow operators to choose direct horizontal routes, as well as the most fuel-efficient altitudes. Since deviations from such routes are only necessary if conflicts are encountered, the ability to fly *direct routes* is expected to minimize fuel usage and maximize efficiency [27].

Limited use of direct routing has already shown positive results in so called 'Free Routing Airspaces' (FRAs) in current European operations in areas with low traffic densities. In 2016, direct routing in FRAs yielded an average route efficiency increase of 1.6% per flight, with gains of up to 4% per flight in areas where FRAs were open 24 hours a day [12]. Further extending FRAs could, therefore, lead to substantial reductions to the total delay experienced when the corresponding efficiency gains are aggregated over all flights. It is hypothesized that the advantages of direct routing are even higher with decentralization as the traffic volume allowed into self-separated airspace would not be constrained by ATCo workload.

1.2.2.2. Safety and Robustness

In addition to improving route efficiency, arbitrary/direct routing is also expected to distribute traffic more uniformly over the available airspace [15]; compare Figures 1.5(a) and 1.5(b). This increased utilization of the available airspace has been shown to reduce conflict probability, thereby increasing the safety of decentralized airspace [15, 28, 29]. With centralized ATC, the opposite is true; airways artificially increase local traffic densities and therefore increase the chance of conflicts between aircraft on the same airway.

Although traffic patterns with decentralized ATC can appear chaotic, distributing the separation task among all aircraft not only increases the number of 'problem solvers'

1

in the airspace, it also increases the overall system robustness to *hardware failures* when compared to centralized ATC [15, 30]. For example, if the automated CD&R system of a self-separated aircraft fails, other aircraft would still be able to detect and resolve conflicts with such non-nominal aircraft, i.e., the implicit redundancy in the system reduces the chance of safety critical events. In contrast, hardware failures at a central node of the current ATC system could severely affect safety. For instance, if cyber-attacks cause the failure of radar and/or radio equipment at an ACC, ATCos would no longer be able to identify and/or warn *any* pilots in their sector of potential collisions, threatening the safety of *all* aircraft under their control.

1.2.2.3. Capacity

As ATCo workload is no longer a constraining factor with decentralization, and because of the numerous safety and efficiency benefits that arise from self-separation and direct routing (see above), many previous studies have suggested that a transition to decentralized ATC could substantially increase the capacity of en route airspace. However, *quantitative methods* to measure and analyze the absolute safety and capacity of decentralized ATC have not been well defined. The development of such methods is one of the main contributions of this thesis, see section 1.4 for more details.

1.2.3. Previous Research

Decentralized ATC is not a new idea. In fact, the notion of distributing traffic separation tasks have been debated in literature since the introduction of automated ATC systems and RNAV in the mid-1970s [2]. Such ideas were formalized by the Radio Technical Commission for Aeronautics (RTCA) in 1995 with the definition of the so called 'Free-Flight' concept. Free-Flight focused on increasing airspace capacity by providing operators with "the freedom to select their path and speed in real time" [31]. Furthermore, "traffic restrictions were only [to be] imposed to ensure separation...and safety" [31]. Since then, many studies on decentralized ATC have been performed under the banner of the Free Flight concept, and have focused on four main aspects: conceptual design and the role of ATCos, airborne CD&R algorithms, human factors issues surrounding self-separation, and the integration of unmanned/personal aerial vehicles into low altitude urban airspaces.

1.2.3.1. Conceptual Design and the Role of Air Traffic Controllers

Initial research in this domain focused on developing operational concepts for decentralized airspace that could viably reduce traffic flow constraints without affecting safety. Several different concepts emerged. These concepts mainly differed in terms of the roles assigned to ATCos, and the task-allocation that is required between ATCos and pilots to increase capacity. These concepts can be classified into three broad categories: partial delegation of separation tasks, full delegation of separation tasks, and the sector-less ATC concept.

1

With partial delegation, tactical separation responsibilities are transferred to only those pilots who request it, and the duration and scope of such delegation is determined by ATCos as part of their boarder control strategy [32–36]. Therefore, this approach aims to increase capacity by reducing ATCo workload, while continuing to provide ATCos with the overall strategic control of traffic.

In contrast, with full delegation, aircrews are entirely responsible for separation with all surrounding traffic, and this form of decentralization is often referred to as *self-separation* [30, 37–39]. Here, the aim is to increase capacity by allowing self-optimization of the routes of individual flights. In essence, this approach transforms controlled airspace into uncontrolled airspace where ATCos are not actively involved in separating aircraft (except when an emergency is declared). Instead, ATCos are required to regulate the number of aircraft allowed into self-separated airspace such that overall system safety is maintained at the required level, i.e., under this scenario, ATCos perform traffic flow management tasks.

In the recent past, a new type of decentralized ATC has been proposed that lies in between the current centralized system and fully self-separated airspace. This new concept is often referred to as the 'sector-less' ATC concept [40–42]. It is also sometimes referred to as the flight-centric ATC concept. In this concept, each ATCo is responsible for safely separating one (or more) aircraft for the entire duration of its flight through a large region of airspace, without handing over control to other ATCos as aircraft transit from sector to sector. In this sense, sector-less ATC can be thought of as a ground-based decentralized ATC concept. Research has shown that this approach improves capacity over current operations by providing airspace users with more freedom to select their own routes while also increasing ATCo efficiency.

It should be noted that this thesis is performed under context of fully automated and self-separated decentralized ATC. Section 1.5 provides more details on the scope of this thesis.

1.2.3.2. Conflict Detection and Resolution Algorithms

Because decentralizing ATC entails moving the traffic separation task to the cockpit, the vast majority of Free-Flight research has focused on developing automated algorithms for airborne Conflict Detection & Resolution (CD&R). As the name suggests, CD&R consists of conflict detection and conflict resolution elements.

Conflict Detection (CD) is the process of predicting future separation violations. In literature, CD algorithms are broadly classified as either state-based or intent-based. With state-based CD, linear extrapolations of aircraft positions over a prescribed 'look-ahead' time are used to predict losses of separation [20, 30]. On the other hand, with intent-based CD, aircraft states and flight plan information regarding the locations of a limited number of future waypoints are used in tandem to deduce potential separation infringements [43, 44].

Once conflicts are predicted, they need to be resolved to maintain safety; this process is known as Conflict Resolution (CR). A plethora of CR algorithms have been developed in the past, ranging from nature/physics inspired voltage-potential methods [20, 30, 45], to methods derived from differential game theory [46]. In addition to CR algorithms, literature also considers other related aspects such as the effect of the type of CR maneuver (horizontal/vertical/horizontal + vertical) [47], and the effect of priority rules [30, 48], on the safety, efficiency and practicality of decentralized operations. A review of CR algorithms can be found in [49, 50].

In conjunction to CD&R, a limited number of studies have investigated the use of Conflict Prevention (CP) algorithms. These algorithms, such as the Predictive Airborne Separation Assurance System (PASAS) [20, 30], aim to improve safety by preventing aircraft from turning into new conflicts when performing conflict resolutions (or nominal trajectory changes), thereby mitigating the possibility of conflict chain reactions. Such chain reactions have a detrimental effect on the stability of decentralized operations. The study of airspace stability, and its relationship to airspace capacity, is one of the main focuses of this thesis, see section 1.4 for more details.

1.2.3.3. Human Factors Research

Although it is technically feasible to realize a fully autonomous CD&R system on commercial aircraft, as per existing cockpit design principles, Free-Flight researchers have generally agreed that pilots should retain the final responsibility for ensuring separation with surrounding aircraft. To aid pilots with this additional task, many cockpit display interface concepts have been developed to help them visualize neighboring traffic and impending conflicts. Some display designs also directly portray potential conflict resolution options [20, 30], while other designs depict the constraints with which pilots should resolve conflicts manually [51, 52].

In many cases, the effectiveness of the proposed display interfaces have been validated using human-in-the-loop experiments. Some studies have used professional airline flight crews and flight simulator trials for a wide variety of cases, including final approach and landing [20, 30, 53, 54]. The results of such empirical investigations have indicated that the supplemental CD&R tasks do not significantly increase pilot workload, even for traffic densities that are three times greater, and for conflict rates that are nine times greater, than current European operations [20, 30]. In fact, the results of such experimental studies are often cited by Free-Flight researchers as evidence of the increased airspace capacity offered by decentralized ATC.

1.2.3.4. Integration of Unmanned and Personal Aerial Vehicles

Although decentralization was originally proposed to improve commercial air transport operations, the concept has become increasingly popular as a means to integrate unmanned and personal aerial vehicles into low altitude urban airspaces. In

1

fact, much of the latest research in this domain now focuses on this context. This is because many researchers and aviation authorities view the distribution of traffic separation tasks as a necessary step towards accommodating the incredible traffic volumes foreseen for these new aircraft types [55, 56].

Due to the lack of operational experience with unmanned and personal aerial vehicles, much of the initial research in this area has adapted or 'borrowed' methods from previous work on commercial decentralized ops. This includes the development of new decentralized operational concepts [57–60], as well as the development of new self-separation technologies for future aircraft types [50, 61, 62].

1.3. Open Problems with Decentralized ATC

Despite over two decades of active research, including successful flight demonstrations over Mediterranean airspace [63], decentralized ATC is yet to be applied in the field. From a technical point of view, a lack of understanding on three open issues, namely airspace design, airspace safety modeling, and airspace capacity modeling, have impeded its further development[3].

1.3.1. Airspace Design

Airspace design is the process of structuring, or organizing, traffic to achieve desired traffic flow patterns. For example, in current en route operations, airways are used to limit the occurrence of conflicts along predefined routes and at their intersections, and sectors are used to limit the area of airspace under the control of each ATCo. Both these airspace design elements are aimed at regulating ATCo workload to manageable levels, in order to balance demand with capacity.

However, the use of such airspace design options to optimize decentralized traffic flows has been largely overlooked in previous research. In fact, there is no consensus in existing literature on whether some form of traffic structuring is also beneficial for decentralized ATC; although Free-Flight researchers advocate that higher traffic densities can be achieved through a reduction of traffic restrictions (see section 1.2.3), other studies argue that capacity would benefit more from a further structuring of traffic [35, 64, 65]. Such diametrically opposed views indicate that there is no coherent understanding of the relationship between airspace structure and capacity in existing literature.

---

[3]Apart from technical challenges, there are legal and political obstacles that need to be tackled before decentralized operations can become routine. While these aspects also need to be considered, this thesis is only concerned with technical issues pertaining to decentralized ATC.

1

1.3.2. Safety Modeling

As implied above, airspace design can directly affect the probability of conflict between aircraft. To quantify this effect, literature introduces the notion of 'intrinsic safety' [66, 67]. This aspect of safety focuses on the ability of an airspace design to prevent (some) conflicts from occurring due to the constraints it imposes on traffic motion, without the aid of supplemental CR algorithms or actors such as pilots and ATCos.

Although previous studies have presented analytical methods to describe the intrinsic safety offered by an airspace design [66–70], most models have only considered conflicts between cruising aircraft. However, to fully quantify the intrinsic safety offered by decentralized en route airspace designs, particularly for those with relatively loose routing constraints, it is necessary to take into account interactions between aircraft in all relevant flight phases. Another limitation of many analytical safety models derived previously is that they make use of idealistic assumptions regarding the flow of traffic that do not always reflect realistic operations. Therefore, existing modeling approaches will need to be improved in relation to these two aspects before they can be used to accurately compare different airspace design options in terms of intrinsic safety.

1.3.3. Capacity Modeling

In ATC, it is often tempting to interrelate airspace safety and airspace capacity. Although these two metrics are closely related, an increase of safety does not always guarantee a corresponding increase of capacity. The difference between safety and capacity can be illustrated using the North Atlantic Organized Track System (NAT-OTS). This airspace design consists of a series of predefined trajectories, or 'tracks', that are used by traffic traveling between North America and Western Europe; see Figure 1.6. The safety of this system can be improved by increasing the spacing between these tracks. However, this would also reduce the *efficiency* with which the available airspace is utilized, which would in turn reduce the total number of available tracks, as well as the maximum capacity of NAT-OTS. For this reason, when evaluating the capacity of an ATC system, it is necessary to consider the effect of a design on multiple airspace performance metrics in unison, including safety and efficiency.

Because airspace safety and capacity are not equivalent, many previous studies have adopted simple *qualitative* methods to study the effect of decentralization on capacity. As indicated by Figure 1.7, in most cases, these qualitative methods measure capacity *indirectly* by analyzing the variation of safety and efficiency metrics, as well as other relevant performance metrics, with traffic density using simulation experiments. Although this approach facilitates a comparison of different designs, when it is used to determine the *capacity limit* of particular design, it is often necessary to use weighting factors to rank the relative importance of the considered metrics. Because such weights are often selected arbitrarily, this approach can lead to a biased estimation of airspace capacity. It is likely that more *quantitative*
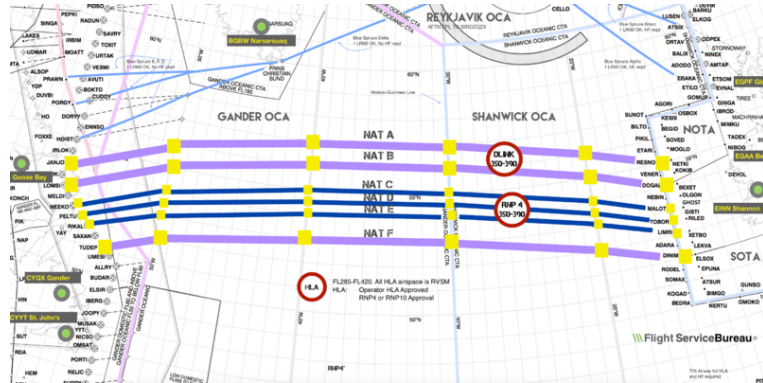
Figure 1.6: The North Atlantic Organized Track System (NAT-OTS) [71]. Increasing the spacing between the predefined tracks of this system increases safety, but decreases capacity. As such, airspace safety and capacity are not equivalent to each other.
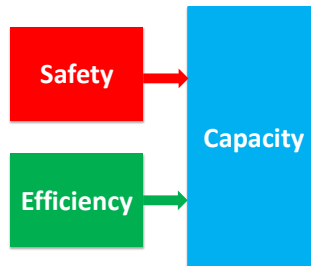
Figure 1.7: Most previous studies have used a qualitative approach to measure capacity indirectly by analyzing the rate of change of safety and efficiency metrics, as well as other relevant metrics, with traffic density. Because this approach requires the use of weighting factors, the resulting capacity estimates may be biased.

and unbiased capacity measurement methods would need to be developed before regulatory bodies could be convinced of a transition to decentralized ATC.

1.4. Research Objectives and Approach

This research aims to address the three open problems discussed above for decentralized ATC. More specifically, the primary objective of this thesis is to:

> **Primary Research Objective**
>
> Analyze and model the effects of *airspace design* and *airborne CD&R* on the *safety* and *capacity* of decentralized ATC

To meet this objective, the following three research activities, and associated research questions, have been defined.

1.4.1. Research Activity 1: Airspace Design

The first research activity aims to systematically study the effect of airspace design on the capacity of decentralized ATC. As mentioned in section 1.3.1, previous studies do not provide a definitive understanding on the relationship between airspace design and capacity for decentralization. Because a basic understanding of this relationship is necessary before quantitative safety and capacity models can be derived, the following research question has been defined:

> **Research Question on Airspace Design (Chapter 2)**
>
> RQ 1.   How does the *degree of structuring* of traffic by an airspace design affect the capacity of decentralized ATC?

It should be noted that in this thesis, the terms 'airspace structure' and 'airspace design' are used interchangeably. Both terms refer to procedural mechanisms for *a priori* separation and organization of traffic. Furthermore, the phrase 'degree of structuring' in RQ 1 denotes the number of constraints imposed on traffic motion by an airspace design. Correspondingly, if airspace design *A* is said to be 'more structured' than airspace design *B*, this implies that design *A* imposes a greater number constraints on traffic motion than design *B*.

To tackle RQ 1, in *chapter 2*, an empirical approach is used whereby four airspace concepts of increasing structure are compared using fast-time simulation experiments, for both nominal and non-nominal conditions. As particular emphasis is placed on determining whether the optimal method of structuring airspace varies with traffic density, multiple traffic demand scenarios are simulated. Subsequently, the structure-capacity relationship is inferred from the effect of traffic demand variations on a number of airspace performance metrics.

It is important to realize that the goal of this research activity is not to propose operationally ready airspace concepts, or to compute precise capacity limits for the four airspace concepts considered. Instead, the goal is only to study how the *degree of structuring* of traffic affects capacity for decentralization. A more quantitative method to estimate the capacity limit of a decentralized airspace concept is developed as part of research activity 3 (see below).

1.4.2. Research Activity 2: Safety Modeling

The second research activity is directed towards overcoming the shortcomings of existing analytical conflict count models described in literature. As explained in section 1.3.2, these models can be used to quantify and compare airspace designs in terms of the intrinsic safety they provide. However, most current models are limited by the fact that they only consider conflicts between cruising aircraft. Additionally, many such models make use of idealistic assumptions that limit the type of traffic

1

flow patterns, or 'traffic scenarios', for which they are applicable. To address these issues, the following two research questions are formulated as:

> ### Research Questions on Safety Modeling (Chapters 3-4)
>
> RQ 2. How can existing conflict count models be extended to take into account interactions between aircraft in *different flight phases* when assessing the overall intrinsic safety provided by an airspace design?
>
> RQ 3. How sensitive are conflict count models to the *traffic flow/scenario assumptions* upon which they are derived, and is it possible to relax the dependency of the models on these assumptions to further improve their accuracy?

The second research question (RQ 2) focuses on expanding current conflict count models from 2-D to 3-D airspaces by taking into account the effects of both the horizontal *and* vertical motion of aircraft on conflict counts. The developed method, described in *chapter 3*, groups aircraft according to their flight phase, takes into account the interactions that occur between aircraft in different flight phases based on the constraints imposed by a particular airspace design, while also considering the proportion of aircraft in each flight phase. The resulting 3-D models allow airspace designers to easily study the effects of physical airspace characteristics, such as airspace volume, number of flight levels, separation minima etc., on intrinsic safety. To investigate the accuracy of the derived models, model predictions are compared to the results of several fast-time simulation experiments.

The approach described above to model the intrinsic safety of an airspace design makes use of several assumptions regarding the distributions of aircraft speeds, headings, altitudes, and spatial locations. Collectively, these four distributions make up what is known as a 'traffic scenario'. The third research question (RQ 3) assesses the sensitivity of the 3-D analytical conflict count models to so called 'ideal' traffic scenario assumptions. This process, described in *chapter 4*, uses targeted fast-time simulation experiments to determine the impact of each traffic scenario assumption on the accuracy of the analytical conflict count models. The data collected from these simulations is also used to develop 'model adjustments' that aim to generalize the models such that they are applicable for a wider range of traffic scenarios. The model adjustments use numerical methods to compute complex integrals for non-ideal traffic scenarios.

It should be noted that two specific airspace designs, namely unstructured and layered airspace designs, described in section 2.2, are used as case studies in the context of RQs 2 and 3. This is because the output of RQ 1 indicated that these two modes of structuring leads to higher capacities when compared to the other structuring options initially considered. Nonetheless the methods developed in this thesis can also be applied to other airspace designs. The procedure to do so is described in the corresponding chapters.

Furthermore, it is also important to realize that the safety models derived in this thesis do not aim to define a target level of safety for decentralized airspace concepts. Instead, the goal of the models is to understand how the parameters of an airspace design, such as heading range per flight level, affect safety. Because the models provide such an understanding, the models developed here can be used to select the values of the design parameters of the airspace to achieve the desired target level of safety (whatever that target may be).

1.4.3. Research Activity 3: Capacity Modeling

The final research activity aims to develop a comprehensive capacity assessment framework for decentralized ATC, taking into account the combined effects of both airspace design and CD&R algorithms on the safety and efficiency of travel. To this end, the following research question has been defined:

> **Research Question on Capacity Modeling (Chapter 5)**
>
> RQ 4. How can the combined effects of *airspace design and airborne CD&R* on the *capacity limit* of a decentralized airspace concept be estimated without assigning weighting factors to safety and efficiency metrics?

To answer the fourth research question (RQ 4), this thesis uses the preexisting notion of airspace stability to define capacity. As defined in previous literature, in this thesis, airspace stability considers the occurrence and propagation of conflict chain reactions [32, 33]. Such chain reactions are often caused by the scarcity of airspace at high traffic densities, as well as due to the specific constraints imposed on traffic motion by the selected airspace design, and by the specific conflict resolution actions commanded by the selected algorithm for tactical CD&R. In addition to reducing the safety of the airspace, the route deviations that result from conflict chain reactions also decrease the efficiency of aircraft trajectories. Therefore, a study of the number of conflict chain reactions, or equally, a study of the rate of change of airspace stability with traffic density, can be used as a *direct* measure of airspace capacity, without the need for arbitrary weighting factors; see Figure 1.8.

To determine the capacity limit of a decentralized airspace concept from the viewpoint of airspace stability, a semi-empirical method is developed in *chapter 5* to compute the number of conflict chain reactions as a function of traffic density, airspace design and CD&R algorithm. This method defines the capacity limit of a decentralized airspace concept as the traffic density at which conflict chain reactions propagate uncontrollably throughout the entire airspace. In other words, at the capacity limit, all aircraft exist in a persistent state of conflict, as every conflict resolution maneuver triggers infinite number of new conflicts. The capacity limit is identified by combining analytical models that describe the safety performance of an airspace design (i.e., the output RQ 2) with empirical models that describe the actions of tactical CD&R algorithms. The resulting method is demonstrated
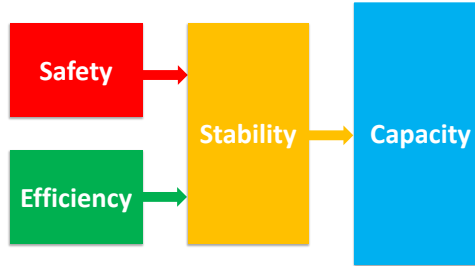
Figure 1.8: This thesis proposes a quantitative approach to measure capacity directly by analyzing the variation of airspace stability with traffic density. Because this approach implicitly takes into account the safety and efficiency of travel, it does not require arbitrary weighting factors to determine the capacity limit of a decentralized airspace concept.

for a number of interesting conditions using fast-time simulations of decentralized unstructured and layered airspace designs.

It should be noted that unlike currently used capacity metrics, which mainly focus on throughput, the capacity model developed in this thesis measures capacity as the *saturation density* of the airspace. As mentioned above, this saturation density is defined from the perspective of airspace stability. Therefore, capacity, as defined here, doesn't reflect the operational capacity of an airspace, but can be used instead to compare different (airspace) concepts with each other.

1.5. Research Scope

To ensure that the topics addressed in this thesis are dealt with in sufficient detail, the scope of this work has been limited in relation to the following seven aspects.

En Route Airspace
Results from previous studies have indicated that decentralization is most suitable for en route airspace. Consequently, the research questions of this thesis are considered only within the context of en route airspace, and the trajectories of aircraft outside this region of airspace are not considered in detail.

Decentralized Airspace Type
Although there are several types of decentralized ATC defined in literature, see section 1.2.3.1, this thesis limits its scope to the most extreme version of decentralization, namely airborne self-separation. This is because the fully automated nature of self-separated airspace is expected to yield the highest capacity increase relative to today's centralized ATC system, particularly since the capacity of centralized ATC is limited mainly by the manual workload constraints of human ATCos.

Because self-separation is radically different toady's ATC system, a potential introduction of a fully automated and self-separated decentralized ATC system is unlikely to occur overnight. However, aspects related to the practical issues related to the

implementation of self-separation is beyond the scope of this work. The reader is referred to [20, 72] for studies focusing on the issues related to a transition to decentralized ATC, including the ramifications of mixed equipage operations, i.e., operations in which aircraft with and without CD&R capability fly in the same airspace. Additionally, since the focus is on *fully automated* self-separation, human factors issues, including issues related to the role of ATCos, in this form of ATC, is outside the scope of this thesis.

Technical Systems

As mentioned before, ADS-B is regarded to be a key enabling technology for airborne CD&R. The ADS-B system is subject to communication delays and interference. Nevertheless, a recent study has shown that these limitations have little effect on the performance and robustness of the airborne CD&R algorithms considered in this work [25]. Consequently, to simplify the modeling needed for fast-time simulations, this work assumes perfect inter-aircraft communications.

On a similar note, human factors issues related to self-separation are not considered. Instead, it is assumed that CD&R tasks are performed fully autonomously. For a comprehensive review of the human factors implications of self-separation, the reader is referred to [53].

Non-Nominal Events and Weather

Non-nominal events and weather are known to have a significant effect on airspace capacity. For this reason, the empirical study undertaken as part of RQ 1 takes these elements into account using rogue aircraft and wind. Rogue aircraft, which do not respect the routing constraints imposed by an airspace design, are used to investigate the effects of deliberate rule breaking and aircraft that have suffered technical failures. These rogue aircraft are also simulated to have separation minima that are several times larger than nominal aircraft. Consequently, their motion through the airspace is somewhat comparable to 'no-go' areas caused by convective weather systems. The wind that was simulated was not taken into account during route planning. Hence, it was used to study the effects of wind prediction uncertainties on capacity.

Developing quantitative methods to predict the effects stochastic events, such as weather, on traffic flows is an ongoing area of research. Consequently, the safety models developed as part of RQs 2-3 are only applicable for ideal conditions. The semi-empirical capacity assessment method developed in response to RQ 4 can, on the other hand, be used to study the effects of such stochastic operational conditions on capacity, as long as adequately realistic simulation models can be developed for the required use cases.

Conflict Detection

Before the method used for Conflict Detection (CD) can be discussed, it is necessary to properly define the notion of a 'conflict', and how it differs from an 'intrusion'. A conflict occurs if the horizontal and vertical distances between two aircraft are expected to be less than the prescribed separation standards within a predetermined 'look-ahead' time. Conflicts, are therefore predictions of *future* separation

1

<div align="center">

(a) Conflict   **(b) Intrusion**

</div>
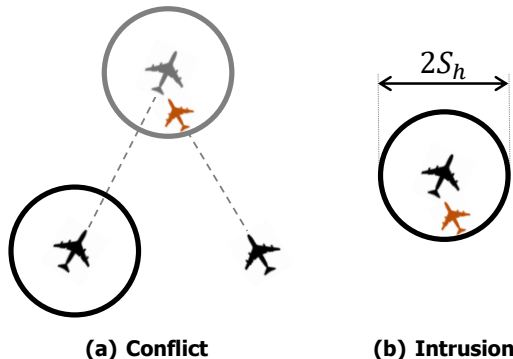
Figure 1.9: The difference between conflicts and intrusions, displayed here for the horizontal plane. Here, S_h is the horizontal separation requirement.

violations. Conflicts should not be confused with intrusions. Instead, intrusions, also referred to as losses of separation, occur when separation requirements are violated at the *present* time. This distinction between conflicts and intrusions is shown in Figure 1.9.

The so called 'state-based' CD method is used throughout this thesis. With this form of CD, conflicts are detected using linear extrapolation of aircraft positions, assuming constant velocity vectors within the predefined look-ahead time. State-based CD was selected for this study because it is an easy to understand and replicable form of CD, and as such it is used by the vast majority of research in this area. The mathematical formulation for state-based CD can be found in [20, 52]. The separation standards used are clearly described in the 'simulation design' sections of each chapter.

Conflict Resolution and Prevention
The Modified Voltage Potential (MVP) algorithm is used for tactical airborne Conflict Resolution (CR). This method uses the repulsion of similarly charged particles to resolve conflicts in a pair-wise fashion, and results in minimum deviation resolution maneuvers. MVP was selected because research performed along side this PhD showed that it resulted in the lowest number of conflicts when compared other types of algorithms, e.g. swarming. It was also found to be very effective for solving bottleneck scenarios in extreme densities. The reader is refereed to [25, 73] on studies investigating the performance of MVP.

The allowed resolution directions and priority are airspace design dependent, and are discussed in the appropriate chapters that follow. The procedure to calculate conflict resolution vectors using MVP can be found in [20]. In addition to tactical CR, the PASAS Conflict Prevention (CP) algorithm, described in section 1.2.3.2, has been used as part of the empirical study for RQ 1.

1

Simulation Platforms and Aircraft Types
This thesis uses two different fast-time simulation platforms, namely TMX and BlueSky. Additionally, Aircraft Performance Models (APMs) corresponding to Personal Aerial Vehicles (PAVs) and normal commercial airliners were used. The reason for the different simulation platforms and aircraft types has to do with the context of this work.

The first research question (RQ1) was performed as part of the Metropolis project (2014-2015). The Metropolis project focused on investigating the relationship between airspace structure and capacity using simulation experiments. To realize the extreme traffic densities needed to study this relationship using simulations alone, the Metropolis project adopted the context of a Personal Aerial Transportation System (PATS). For these simulations, the TMX software belonging to the National Aerospace Laboratory of the Netherlands (NLR), a member of the Metropolis consortium, was used. Furthermore, because Metropolis simulations were performed using the PATS setting, APMs for PAVs were used. Such PAV APMs were developed by modifying Eurocontrol's Base of Aircraft Data (BADA) APMs for fixed wing general aviation aircraft with the parameters of PAVs that were found on the internet. Therefore, for the most part, these PAV models behaved identical to normal fixed-wind aircraft (main difference was slower speeds).

After the Metropolis project, access to TMX was not allowed since it is a proprietary NLR software. Therefore, the studies related to RQs 2-4 used the BlueSky simulator developed at TU Delft. BlueSky is the open-source successor to TMX. BlueSky and TMX are extremely similar programs and the core of these simulators were both developed by Prof.dr.ir. Jacco Hoekstra, and therefore use the same underlying algorithms and models for many functions. In fact, from the user perspective, there is no difference since both programs use the same traffic command syntax. For this reason, the switch from TMX to BlueSky is not expected to affect the results.

In contrast to RQ 1, where simulations were used to study traffic dynamics, the simulations performed in the context of RQs 2-4 aimed to validate the safety and capacity models developed in this thesis. Because the goal of the latter simulations were to investigate model accuracy alone, a single APM corresponding to that of the Boeing 747-400 aircraft was used, as it is the default APM in BlueSky. Nonetheless, because of the generic nature of the models developed in this thesis, they can also be applied to the case with multiple aircraft types; the only requirement is that the average speed of all aircraft be known.

1.6. Thesis Outline

In line with the research approach described in section 1.4, the main body of this thesis is divided into three parts. The first part deals with decentralized airspace design, while the second and third parts focus on decentralized airspace safety and capacity modeling, respectively. Each part contains one or more chapters. To make the distinction between parts and chapters clear, parts are labeled using Roman

1

numerals, whereas chapters are labeled using Hindu-Arabic numbers. The structure of this thesis, including the relationships between the various parts and chapters, is depicted in Figure 1.10 below using the appropriate numbering format.

In addition to the main technical chapters, Chapter 6 discusses the results of this study in relation to the three main open problems identified for decentralized ATC. Subsequently, chapter 7 provides a concise summary of the main conclusions of this work. The procedure to produce the traffic scenarios required for fast-time simulation experiments is described in the appendix. Finally, the nomenclature (at the back) lists the mathematical symbols and acronyms used in this thesis.

1.7. Guide to the Reader

It should be noted that the main technical content of this thesis, i.e., chapters 2-5, are based on papers that are published (or submitted for publication). As such, these chapters can be read independently. This does, however, result is the repetition of some key definitions and concepts, particularly in the 'background' sections of of the following chapters. Cover-to-cover readers may choose to skip these repetitions without affecting the overall understanding of the work. Furthermore, to aid cover-to-cover readers, an unnumbered preamble paragraph is added to the start of each chapter that explains how each paragraph fits into the overall research line of this thesis. These preamble paragraphs also provide the publication history of each chapter, and mention sections contained within that are repeated from previous chapters.

1
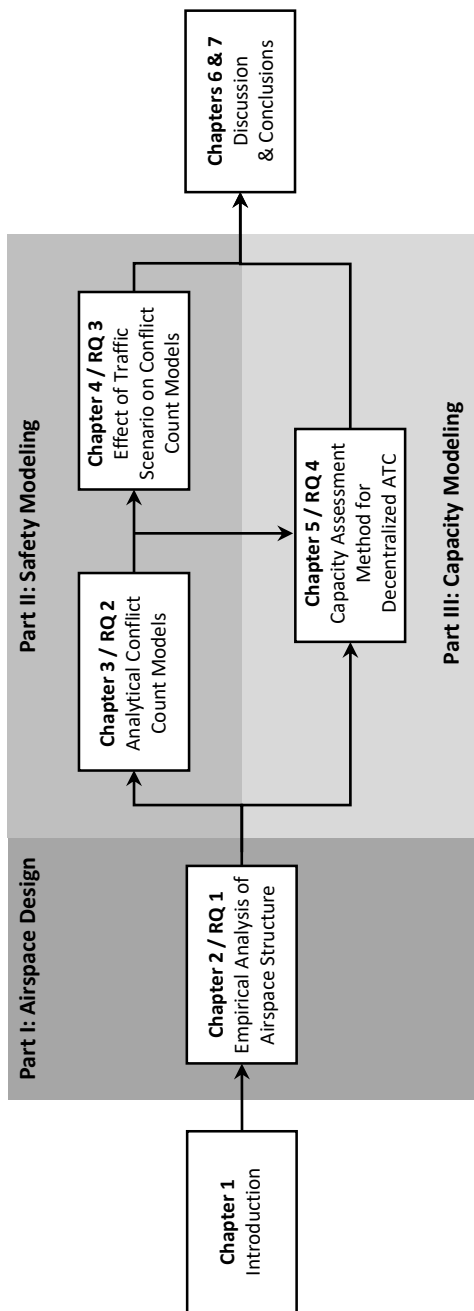
Figure 1.10: Overview of thesis structure. The Research Questions (RQ) tackled in each chapter are indicated. The thesis consists of three 'parts' that are labeled using Roman numerals, and seven chapters that are labeled using Hindu-Arabic numbers.

Part I:
AIRSPACE DESIGN

2

Analysis of Airspace Design for Decentralized Separation

As indicated in chapter 1, existing literature does not provide a definitive understanding on the relationship between airspace design and the capacity of decentralized ATC. A basic understanding of this relationship is necessary before quantitative safety and capacity modelling methods can be developed. This chapter aims to provide such an understanding by comparing four airspace design concepts of increasing structure using fast-time simulation experiments, for both nominal and non-nominal conditions, as well as for multiple traffic demand densities.

The work contained in this chapter was performed as part of the Metropolis project (2014-2015). To realize the extreme traffic densities needed to study the airspace structure-capacity relationship using simulations alone, the Metropolis project adopted the context of an urban Personal Aerial Transportation System (PATS). This context is different from the remaining chapters of this thesis where simulations are performed under the context of commercial air traffic operations.

Abstract

The work that is presented in this chapter is part of an ongoing study on the relationship between airspace structure and capacity. The present chapter investigates the degree of structuring needed to maximize capacity for decentralized en-route airspace. To this end, four decentralized en-route airspace concepts, which vary in terms of the number of constrained degrees of freedom, were compared using fast-time simulations, for both nominal and non-nominal conditions. The airspace structure-capacity relationship was studied from the effect of multiple traffic demand densities on airspace metrics. The results indicated that structuring methods that over-constrained the horizontal path of aircraft reduced capacity, as traffic demand displays no predominant patterns in the horizontal dimension for decentralization. The results also showed that capacity was maximized when a vertical segmentation of airspace was used to separate traffic with different travel directions at different flight levels. This mode of structuring improved performance over completely unstructured airspace by reducing relative velocities between aircraft cruising at the same altitude, while allowing direct horizontal routes.

2.1. Introduction

At present, traffic separation in en-route airspace is primarily performed by ground-based Air Traffic Controllers (ATCo), and relies on a rigid network of airways [75, 76]. The structure of this network historically depended on the physical location of radio navigation beacons, dating back to the early 1950s [1]. This airway system was devised to help pilots navigate safely under Instrument Flight Rules (IFR), using simple single channel radios [1]. Even though modern airliners have the necessary equipment to fly arbitrary routes accurately, airway navigation is still used during busy daytime operations in most parts of the world [13]. This is because airways limit aircraft flight paths along predefined trajectories, making it easier for the ATCo to monitor and de-conflict traffic flows [30, 45]. However, as airways do not always allow for efficient airspace usage, this *centralized* airspace design has been widely reported to be nearing saturation levels [13, 14, 18, 77].

In order to cope with the projected increases in traffic demand, a transfer of the traffic separation responsibility from the ground to the cockpit has been proposed as an alternative to the current operational model. To realize the resulting *decentralized* separation paradigm, sometimes referred to as 'self-separation', significant progress has been made towards the development of airborne Conflict Detection and Resolution (CD&R) algorithms [49]. However, little effort has been devoted towards decentralized *airspace design*. In particular, there is no consensus in existing literature if some form of traffic organization, or structuring, is also needed to maximize capacity for decentralized separation; while Free Flight researchers advocate that higher densities can be achieved through a reduction of traffic flow constraints [30, 39, 78], other studies argue that capacity would benefit more from a further structuring of airspace [35, 64, 65]. These diametrically opposed views

indicate that the relationship between airspace structure and capacity is not well understood for decentralization, i.e. does more or less structuring lead to a higher capacity? Or, does the degree of structuring required to maximize capacity vary with traffic density?

To answer these questions, this study analyzes the degree of structuring needed to maximize capacity for decentralized separation using fast-time simulations. To this end, four en-route airspace concepts, ranging from a completely unstructured direct routing concept, to a highly structured tube network using 4D trajectories, are compared within the same simulation environment, for multiple traffic demand scenarios. The effect of structure on capacity is subsequently analyzed from the effect of traffic demand variations on safety, efficiency, stability, arrival sequencing, complexity and noise pollution metrics. By including rogue aircraft that ignore concept dependent routing requirements in selected simulation runs, the robustness of the concepts to non-nominal conditions is also analyzed in this study.

The analysis described in this work is performed within the context of a hypothetical Personal Aerial Transportation System (PATS). This setting was adopted to provide the extreme traffic densities, up to 30,000 aircraft per 10,000 square nautical miles, needed to 'stress-test' and compare the four concepts in terms of capacity using a fast-time simulation approach. Note that the aim of this study is not to provide any specific conclusions regarding design options for a future PATS; the focus is only on the analysis of the airspace structure-capacity relationship for decentralized separation.

This chapter is structured as follows. Section 2.2 defines the notion of airspace structure, and describes the design of four decentralized airspace concepts of increasing structure. This is followed in section 2.3 with the setup of two separate simulation studies that are used to compare the concepts. The results of these simulations are presented and discussed in sections 2.4 and **??**, respectively. Finally the main conclusions are summarized in section **??**.

2.2. Design of Airspace Concepts

Airspace structure can be defined as a procedural mechanism for *a priori* separation and organization of en-route traffic. An example of this in current-day operations is the hemispheric rule, which separates east-bound from west-bound traffic at alternating vertical flight levels [79]. More generally, any a priori structuring of traffic implies *posing constraints* on one or more of the four degrees of freedom that describe aircraft motion (both spatial as well as temporal). Using this definition of airspace structure, four decentralized airspace concepts, named Full Mix, Layers, Zones and Tubes, have been designed by incrementally increasing the number of constraints applied. This section describes and compares the conceptual design of these four airspace concepts.

2

2.2.1. Full Mix

The Full Mix airspace concept can be most aptly described as 'completely unstructured airspace'. Here, no constraints are imposed on aircraft motion in this concept. Instead, this simplest form of airspace design focuses on maximizing overall system efficiency. Therefore, aircraft are free to use direct horizontal routes, as long as such routing is not obstructed by weather or static obstacles. Similarly, aircraft can also fly with preferred speeds and at optimum altitudes, based on their performance capabilities and trip distances. By offering greater freedom to aircraft operators, UA has been found to result in a more uniform distribution of traffic, both horizontally and vertically, reducing traffic concentrations and ensuing delays [29, 30].
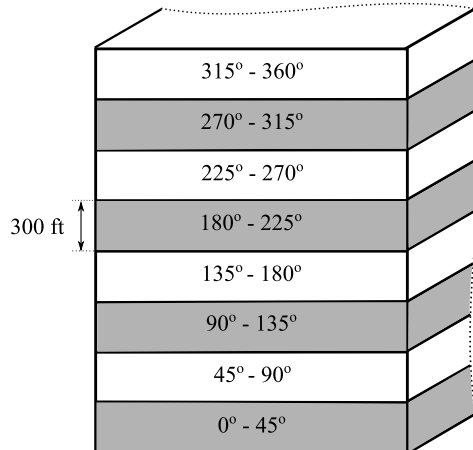
As no level of airspace structure is used to separate potentially conflicting trajectories in Full Mix, safe separation between aircraft is entirely dependent on airborne self-separation automation, see section 2.3.1.3. Since Full Mix imposes no constraints on the path of aircraft, combined heading, speed and altitude conflict resolution maneuvers are used to reduce deviations from the optimal route.

2.2.2. Layers

The Layers concept can be seen as an extension to the hemispheric rule [79]. In this concept, the airspace is segmented into vertically stacked bands, and heading-altitude rules are used to limit the range of travel directions allowed in each altitude layer. This segmentation of airspace is expected to improve safety when compared to the Full Mix concept, by reducing the probability of conflicts with crossing traffic for cruising aircraft. However, this increased safety comes at the price of efficiency; while direct horizontal routes are still possible, vertical flight profiles are dictated by the heading-altitude rules in-force. As a result, flights may not be able to cruise at their optimum flight levels, increasing fuel burn when compared to Full Mix. An exception to the heading-altitude rule is made for climbing and descending aircraft; these aircraft are allowed to maintain heading while climbing or descending to their destination altitude.

Figure 2.1 displays a schematic of the Layers concept. Here it can be seen that each altitude layer corresponds to a heading range of 45° and has a height of 300 ft. With these dimensions, two complete sets of layers fit within the airspace volume used to compare concepts, see section 2.3.2.1. As a result, short flights can stay at low altitudes while longer flights can improve fuel burn by flying at higher flight levels. This is expected to mitigate the efficiency drop of predetermined altitudes in this concept.

The Layers concept also makes use of the same self-separation automation utilized by Full Mix, albeit with restrictions on the allowed resolution maneuvers. While combined heading, speed and altitude resolutions are permitted for climbing and descending traffic, for cruising aircraft, altitude resolutions would create new conflicts with traffic in adjacent layers. Resolutions are therefore limited to combined heading and speed maneuvers for cruising aircraft.

Figure 2.1: Isometric view of the Layers concept with one complete set of altitude bands. Here, each altitude band constrains aircraft headings to within a predefined range.

2.2.3. Zones

Similar to Layers, the Zones concept separates traffic based on similarity of travel direction. However, in this case, a horizontal segmentation of airspace is used to separate traffic along pre-defined trajectories. In this respect, the Zones concept resembles the airway-based airspace design used today in that it facilitates travel towards and away from locations with high traffic demand.

The horizontal topology used by the Zones concept, see in Figure 2.2, consists of two major zone types: radial and ring zones. Radial zones separate inbound and outbound traffic from the center of the topology, which coincides with an area with high traffic demand. Concentric ring zones, on the other hand, function as connections between the radial zones, and separates clockwise and anti-clockwise traffic flows from each other. Aircraft can travel between any two points in the topology using a combination of radial and ring zones. As there is no vertical segmentation of airspace in this concept, optimum altitudes are selected based on the planned flight distance between origin and destination. The Zones concept used for simulations consisted of 41 rings. The number of radials depended on the distance from the center of the topology to ensure adequate separation between adjacent radials; 72 radials were used for distances up to 6 Nmi from the center, after which 216 radials were defined.

The Zones concept also uses self-separation automation to separate aircraft flying within the same zone, as well as to assist with the merging of aircraft between ring and radial zones. Since the Zones topology dictates the horizontal path of an aircraft, heading resolutions are not allowed for this concept.
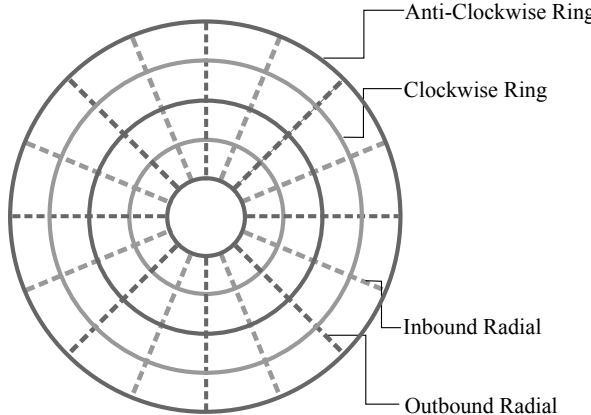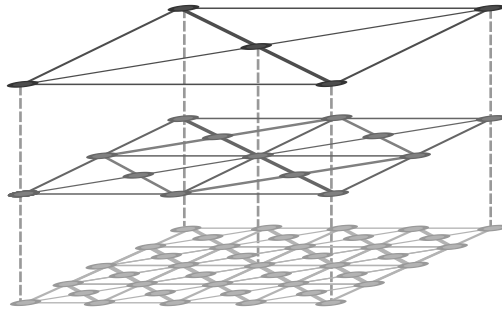
Figure 2.2: Top down view of an example Zones concept, which constrains traffic in the horizontal plane.

2.2.4. Tubes

As a maximum structuring of airspace, the final concept implements four-dimensional tubes that provide a fixed route structure in the air. Here, the aim is to increase the predictability of traffic flows by using preplanned conflict free routes.

The tube topology can be thought of as a graph with nodes and edges, see Figure 2.3. The nodes are connection points for one or more routes, while the edges are the tubes connecting two nodes. Tubes at the same horizontal level never intersect, except at the nodes, and are dimensioned to fit exactly one aircraft in the vertical and horizontal plane. To provide multiple route alternatives, the Tubes implementation uses a total of 13 tube layers that are placed above each other, with decreasing granularity. This way, short flights profit from a fine grid at the lowest layer, while at the same time, longer flights benefit from lengthier tubes at higher layers. Finally, it should be noted that aircraft are only allowed to climb/descend through one tube layer at a time.

Unlike the other concepts, the Tubes concept uses time-based separation. This mode of separation dictates that when an aircraft passes a node, it will 'occupy' that node for a prescribed time interval. Within this occupancy interval no other aircraft is allowed to pass through that node to prevent conflicts. For each node, an interval list is maintained that keeps track of the times at which that node is expected to be occupied. These lists are shared between all aircraft, and updated whenever new flights enter the network. Furthermore, new flights are only allowed to select routes that are not predicted to conflict with existing aircraft in the network. If no such route can be found, a pre-departure delay is applied in multiples of 10 seconds up to a maximum of 30 minutes. After this period, the tube network was considered to be saturated, and that particular flight is canceled. To ensure that separation at the nodes also guarantees separation within the tubes, all aircraft within the same layer are required to fly at the same velocity. This prescribed speed increases with

Figure 2.3: Isometric view of an example Tubes topology, which constrains traffic along all four dimensions of motion. The dashed lines are used to indicate the placement of nodes above each other.

the altitude of the layer to match the decreasing granularity of the tube network. A major advantage of this mode of separation is that it allows the tube network to be bidirectional, as the occupancy of a node is independent of travel direction. This simplifies its design, and enables a closer packing of tubes in the topology.

The time-based separation and the pre-planned routes used by the Tubes concept makes it somewhat similar to some 4D Trajectory Based Operations (TBO) concepts that have been discussed in literature. However, it should be noted that most TBO concepts utilize a *centralized* planning approach in which globally optimum routes are determined using an iterative process, after negotiations between an airspace user and an Air Navigation Service Provider (ANSP) [65]. Aircraft in the Tubes concept, on the other hand, use *decentralized* route planning whereby the shortest (conflict free) route is selected, given the availability of the tube topology at the time of flight plan calculation, i.e., routes are selected in Tubes using the 'first-come-first-served' principle. Moreover, the Tubes concept uses a predefined topology for route planning, while this is not strictly necessary for 4D TBO. Finally, (some) 4D TBO concepts offer the possibility of re-planning routes after take-off, whereas this functionality is not available for Tubes. Because of these differences, it is important not to equate Tubes and 4D TBO.

2.2.5. Concept Comparison

Figure 2.4 compares the four airspace concepts described above in terms of the number of constrained degrees of freedom. The figure shows that options for trajectory planning become increasingly restricted as the degree of structure is incrementally increased from Full Mix to Tubes; while all four degrees of freedom are available in Full Mix, in the Tubes concept, aircraft have no degrees of freedom, and are required to rigidly follow preplanned space-time routes through a predefined topology. Between these two extremes, the Layers and Zones concepts were defined to allow three and two degrees of freedom respectively. This choice was made such that the four concepts span the entire range from unstructured to structured airspace. Thus, a comparison of the four concepts using fast-time simu-

lations can be used to analyze the structure-capacity relationship for decentralized airspace. The goal of these simulations is not to arrive at precise capacity estimations for the four concepts, but rather to consider on how the degree of structuring affects capacity. Correspondingly, the concepts are subjected to multiple traffic demand densities, and a *relative capacity ranking* is performed by measuring the effect of traffic density changes on several airspace metrics.

Four Airspace Design Concepts of Increasing Structure

Full Mix	**Layers**	**Zones**	**Tubes**

0 Constrained Degrees of Freedom   **1 Constrained Degrees of Freedom**   **2 Constrained Degrees of Freedom**   **4 Constrained Degrees of Freedom**

- Altitude

- X Position
- Y Position

- X Position
- Y Position
- Altitude
- Speed
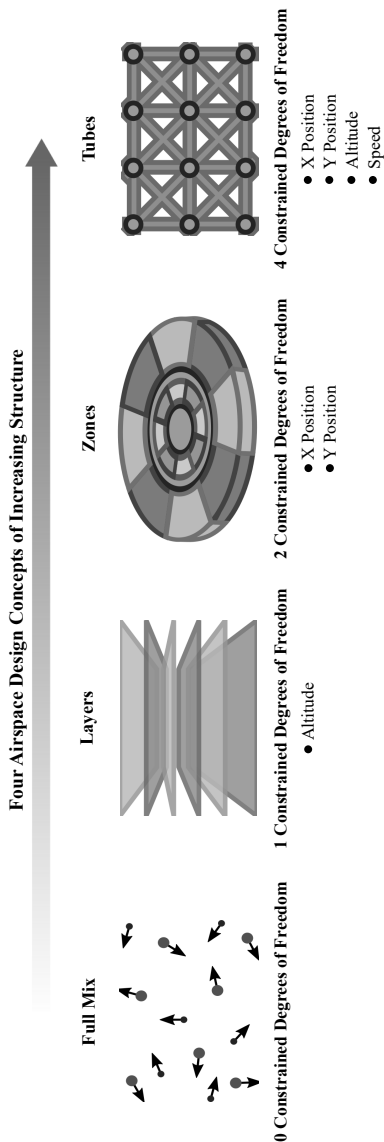
Figure 2.4: Four point airspace structuring framework. The level of structure is increased from Full Mix to Tubes by incrementally increasing the number of constraints applied.

2.3. Simulation Design

Two separate fast-time simulation experiments were conducted to compare the four airspace concepts in terms of capacity and robustness. This section describes the design of these two experiments.

2.3.1. Simulation Development

2.3.1.1. Simulation Platform and Vehicle Modeling

The Traffic Manager (TMX) software, developed by the National Aerospace Laboratory of the Netherlands (NLR), was used as the simulation platform in this research. The TMX simulator is well established in the ATM research community, and has been used in many previous Air Traffic Management (ATM) related simulation studies. For more information on TMX capabilities, the reader is referred to [80].

In order to simulate Personal Aerial Vehicle (PAV) dynamics, parameters of existing point-mass aircraft models in TMX, which are based on Eurocontrol's BADA Aircraft Performance Models (APM) [81], were adapted to match the performance specifications of several PAVs that are currently under development. In total, three different PAV types were used in the simulations.

2.3.1.2. Concept Implementation

The four concepts were implemented by modifying TMX's trajectory planning functions. The Full Mix concept used the direct horizontal route and the most fuel efficient altitude, as determined by the APMs. Layers also used the direct horizontal trajectory. However, altitude was selected based on the bearing to the destination and the matching altitude from a predefined list (see section 2.2.2). Additionally, distance determined the choice between the upper and lower layer sets; flights with a cruising distance less than 22 Nmi used the lower layer set.

For the Zones concept, the A* path planning algorithm was used to determine the shortest route over its predefined horizontal topology, while the most fuel efficient altitude was chosen by the APMs. Tubes also employed A* to calculate the shortest path, but in this case, it was also used to examine whether the selected route was conflict-free. Here, an instantaneous planning approach was used whereby the occupancy of each node along a proposed route was checked at traffic desired departure times. If any node along a proposed route was found to be occupied by another flight, the corresponding route was discarded, and the A* algorithm backtracked to evaluate the next best solution. If no route could be found, a pre-departure delay was applied in multiples of 10 seconds up to a maximum of 30 minutes. After this period, the tube network was considered to be saturated, and that flight was canceled. Once an appropriate route was found, aircraft were required to follow their preplanned routes as closely as possible, including arrival time intervals at each node.

For both Zones and Tubes, the A* algorithm used in this work had to be modified from the generic version. This was because origins and destinations for traffic were located outside the airspace volume used to design the concepts (see section 2.3.2.1). Consequently, the generic A* algorithm could yield unfeasible solutions due to aircraft bank angle limitations imposed by the APMs. To solve this problem, the A* implementation in this work differs slightly from the conventional algorithm by allowing already visited nodes to be rechecked if bank angle limits were exceeded, i.e., by remarking 'closed nodes' as 'open nodes'. A complete description of the A* algorithm can be found in [82].

2.3.1.3. Self-Separation Automation

The Full Mix, Layers and Zones concepts relied on airborne self-separation automation for tactical separation. It consisted of separate Conflict Detection (CD), Conflict Resolution (CR) and Conflict Prevention (CP) modules. CD was performed through linear extrapolation of aircraft positions over a prescribed 'look-ahead' time. Once conflicts were predicted, the Modified Voltage Potential (MVP) algorithm was used for CR in a pair wise fashion, resulting in implicit cooperative resolution strategies. Finally, the CP algorithm ensured that aircraft did not turn into conflicts, in an effort to mitigate conflict chain reactions. Previous research showed that this three pronged system was highly effective in solving multi-aircraft conflicts. Furthermore, this system was found to be computationally efficient as each aircraft is only concerned with its own separation with neighboring traffic. For more details, please consult [20].

Based on initial test runs, a look-ahead time of 60 seconds, as well as separation margins of 0.135 Nmi horizontally and 150 ft vertically, were found to be suitable for the APMs used here. Since the focus of this study is on decentralized en-route airspace, self-separation was performed only within the experiment airspace block, defined to be between 1650-6500 ft (see section 2.3.2.1). Additionally, aircraft were assumed to have perfect knowledge of the states of neighboring traffic to focus exclusively on the structure-capacity relationship.

2.3.1.4. Wind

In real-life operations, wind uncertainties are a common source of prediction error. To take this effect into account, wind was deliberately omitted from the simulation's trajectory planning functions to study the effect of uncertainties, which could cause deviations from the planned trajectory, on the four airspace concepts. To this end, wind was modeled as a uniform and time-invariant vector field in x, y and z, with random direction and random speed (12-22 kts). Although these conditions cannot be assumed by default, for a short time interval in a small observed area, and at sufficient altitudes to clear ground obstacles, as for the current study, this assumption is adequate for the purposes of this work.

2

2.3.2. Traffic Scenarios

2.3.2.1. Testing Region and Flight Profiles

To create high density traffic scenarios, a small square region, with an area of 1600 Nmi^2, was used for traffic simulations. Although this research focuses on en-route airspace design, arrival and departure operations were simulated to ensure that the results did not ignore the impact of ground constraints. Correspondingly, aircraft took-off from one of 1600 arrival/departure locations that were evenly distributed at ground level, against the direction of the wind. To prevent take-off conflicts, aircraft had a minimum creation interval of 60 seconds at each origin, corresponding to the CD look-ahead time.

After take-off, aircraft climbed to the 'experiment airspace block', defined between 1650 ft and 6500 ft. Once aircraft entered the experiment block, they followed concept dependent routing requirements, both horizontally and vertically. At a predetermined distance from their destination (which depended on the cruise altitude), aircraft descended out of the experiment block. Standardized climb/descent profiles were used below the experiment block for all airspace concepts, and were specified using the APMs. To simplify simulation development, runway capacity was not managed during landing. Instead, the effect of arrivals was analyzed using the 'arrival sequencing' metric, see section 2.3.5.4.

Relatively low altitudes were selected for the experiment block to limit the horizontal area needed for simulation. Given the constant climb/descent profiles below the experiment block, higher altitudes would have increased the horizontal area needed for the simulations. A larger area would in turn increase the traffic volumes needed to realize the desired densities, increasing computational effort without tangible benefits in terms of the primary research goals. On a similar note, all aircraft took-off from and landed at one of the 1600 arrival/departure locations that were defined in the square simulation area. Interactions with aircraft outside this area would not contribute heavily to an understanding of the airspace structure-capacity relationship, particularly for decentralization. Thus, such interactions are outside the scope of this work.

2.3.2.2. Traffic Demand

Four traffic demand scenarios of increasing density were used to compare the concepts, and were defined in terms of the instantaneous number of aircraft in the air, see Table 2.1. These scenarios had a an average trip distance and speed of 30 Nmi and 120 kts, respectively, and made use of assumptions for future per capita demand for PAVs, see [57] for more details.

In addition to different demand volumes, traffic scenarios were created with different demand patterns. Here, scenarios with largely converging, diverging and 'mixed' demand patterns were used. These different demand patterns were created by varying the ratio of origins and destinations that acted as sources and

Table 2.1: Instantaneous Traffic Volume of the Four Demand Scenarios

Scenario	Low	Medium	High	Ultra
Instantaneous Traffic Volume	2,625	3,375	4,125	4,875

sinks, and by varying the aircraft creation time intervals in different regions of the simulation area.

2.3.2.3. Rogue Aircraft

In a separate experiment, 'rogue aircraft' were introduced at random time intervals. Their separation requirements were seven times larger horizontally, and four times larger vertically, when compared to normal aircraft in the simulation. These aircraft flew haphazardly through the airspace with continuously varying heading and altitude. Furthermore, rogue aircraft were non-cooperative. This meant that normal aircraft were solely responsible for detecting and resolving conflicts with rogue aircraft using its self-separation automation, in all concepts. Although time based separation is used in Tubes, the self-separation automation described above is used with speed resolutions to resolve conflicts with rogue aircraft alone. By monitoring the effect of rogue aircraft on safety metrics, the robustness of the four concepts to non-nominal events can be analyzed.

2.3.3. Simulation Procedure and Data Logging

To enable a fair comparison between all concepts, standardized simulation conditions were used to minimize unsystematic variation in the results. For a particular repetition of a traffic demand volume, the creation times of aircraft, the origin-destination combinations, the strength and direction of the simulated wind, as well as the introduction and trajectories of rogue aircraft (in non-nominal experiment), were kept constant across all concepts. Additionally, scenarios had a duration of two hours, consisting of a 45 minute (traffic volume) build up period, a 1 hour logging period, during which the traffic volume was held constant at the required level, and a 15 minute wind down period, required to allow aircraft created during the logging hour to finish their flights, and prevent abnormally short flights from skewing the results.

Two types of logging were used. Event-driven logging kept track of the properties of conflicts and intrusions as they occurred. It was also used to store flight efficiency data when an aircraft arrived at its destination, including the time interval between consecutive arrivals at each destination. Periodic logging was used to monitor the status of all flights in the experiment airspace block every 30 seconds. This was required to monitor traffic volumes, as well as for computing structural complexity and noise pollution metrics.

2.3.4. Independent Variables

Two separate experiments were performed: the nominal experiment and the non-nominal experiment.

2

2.3.4.1. Nominal Experiment

The nominal experiment focused on the impact of airspace structure on capacity under ideal conditions; although traffic was subjected to a uniform wind field (see section 2.3.1.4), no other detriments to aircraft motion were included in this experiment. The two independent variables of this experiment, and their levels, are:

1. Airspace concept: Full Mix, Layers, Zones and Tubes

2. Traffic demand: Low, Medium, High and Ultra (see Table 2.1)

For each of the 16 experiment conditions, six repetitions were performed, consisting of two converging, two diverging and two mixed traffic demand patterns. Additionally, the scenarios were also simulated with and without tactical CR to measure airspace stability, resulting in a total of 192 nominal simulation runs (4 concepts x 4 demand scenarios x 6 repetitions x 2 CR settings).

2.3.4.2. Non-Nominal Experiment

The goal of the second experiment was to compare the relative robustness of the concepts to non-nominal situations. For this purpose, rogue aircraft were added to traffic scenarios during the logging hour, in addition to wind. The two independent variables of this experiment, and their levels, are:

1. Airspace concept: Full Mix, Layers, Zones and Tubes

2. Number of rogue aircraft: 4, 8, 16 and 32

The resulting 16 non-nominal experiment conditions were performed using the 'Medium' traffic demand scenario listed in Table 2.1. Once again, six repetitions, as well as simulations with and without tactical CR were performed, resulting in a total of 192 non-nominal simulation runs (4 concepts x 4 rogue scenarios x 6 repetitions x 2 CR settings).

To determine the number of rogue aircraft needed, pilot simulation runs were performed for testing purposes. These runs indicated that a minimum of 15 rogue aircraft per hour were needed to see some effect of rogue aircraft for unstructured airspace. Consequently 4, 8, 16 and 32 aircraft were selected to be below and above this threshold for a proper experiment design.

2.3.5. Dependent Variables

Six categories of dependent variables are used to compare the concepts: safety, efficiency, stability, arrival sequencing, structural complexity and noise pollution. The metrics used to access each category are described below.

2.3.5.1. Safety

Safety metrics focus on the ability of an airspace concept to maintain safe separation between aircraft. Separation performance is measured in terms of the number of intrusions and conflicts. Here, intrusions are defined as violations of minimum separation requirements, while conflicts are defined as predicted intrusions, i.e., when two (or more) aircraft are expected to violate separation requirements within a predetermined 'look-ahead' time (60 seconds in this research).

Intrusions do not imply collisions. Therefore, in addition to counting the number of intrusions, it is important to consider the severity of an intrusion. The severity of an intrusion, I_{sev}, is dependent on the path of an aircraft through the protected zone of another, see Figure 2.5, and is computed using the following expression:

$$I_{sev} = \max_{t_0 - t_1} \left[\min \left(\hat{I}_H(t), \hat{I}_V(t) \right) \right] \tag{2.1}$$

Here, $\hat{I}_H$ and $\hat{I}_V$ are the magnitudes of horizontal and vertical intrusions that are normalized with respect to the corresponding minimum separation requirements, while t_0 and t_1 are the start and end times of an intrusion. Using the above relation, the intrusion severity for the intrusion path shown in Figure 2.5 is equal to the normalized horizontal intrusion at point 'A'.

The last safety metric is Intrusion Prevention Rate (IPR). As the name suggests, this metric considers the proportion of intrusions that were successfully avoided, and is computed as follows:

$$IPR = \frac{C_{total} - I_{total}}{C_{total}} \tag{2.2}$$
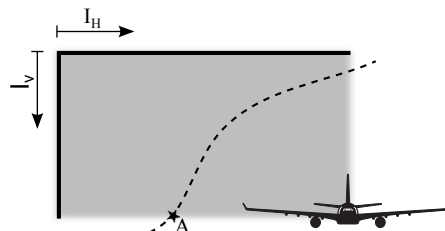
Figure 2.5: Front view of an intrusion. The dashed line shows the intrusion path of an aircraft through the protected zone of another.

Here, C_{total} and I_{total} are the total number of conflicts and intrusions, respectively.

2.3.5.2. Efficiency

The efficiency of the concepts is analyzed using the work done metric. This metric considers the optimality of an aircraft's trajectory, and therefore has a strong correlation with fuel/energy consumption. For each flight, the work done, W, is computed as:

$$W = \int_{path} \Gamma \cdot d\mathbf{s} \tag{2.3}$$

Here, Γ is the thrust vector and $\mathbf{s}$ is the displacement vector.

2.3.5.3. Stability

Resolving conflicts may cause new conflicts at very high traffic densities due to the scarcity of airspace. The stability of the airspace as a direct result of conflict resolution maneuvers has been measured in literature using the Domino Effect Parameter (DEP) [33, 78]. The DEP can be visualized through the Venn diagram pictured in Figure 2.6. Here, S1 is the set of all conflicts without resolutions, and S2 is the set of all conflicts with resolutions, for identical traffic scenarios. Furthermore, three regions can be identified in Figure 2.6 from the union and relative complements of the two sets, with $R1 = S1 \setminus S2$, $R2 = S1 \cap S2$ and $R3 = S2 \setminus S1$.

By comparing the number of R1 and R3 conflicts, the proportion of additional 'destabilizing' conflicts that were triggered by resolution maneuvers can be determined. Thus, the DEP is defined as [33]:

$$DEP = \frac{R3 - R1}{S1} = \frac{S2 - S1}{S1} = \frac{S2}{S1} - 1 \tag{2.4}$$
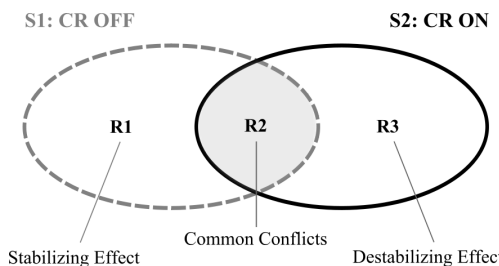
Figure 2.6: The Domino Effect Parameter (DEP) compares simulations with and without Conflict Resolution (CR) to measure airspace stability

It should be noted that the Tubes concept does not use tactical conflict resolution (expect with rogue aircraft). Hence, the DEP has no meaning for Tubes.

2.3.5.4. Arrival Sequencing

Although runway occupancy was not managed for landing traffic, the effect of airspace structure on approach sequencing is examined a posteriori by considering the time interval between successive arrivals at each destination. Both the number of arrivals within 60 seconds each other (equaling the CD look-ahead time), and the average time interval between successive arrivals, at each destination, has been used to measure arrival sequencing.

2.3.5.5. Structural Complexity

Complexity metrics are used to measure the difficulty of controlling a given traffic situation. Although complexity in ATM research often refers to ATCo workload, the class of intrinsic, or geographical, complexity metrics, which only consider the traffic patterns generated by an airspace concept, is most appropriate for this research.

Two indicators are used to measure intrinsic complexity. The proximity indicator, PR, describes the geographical distribution of aircraft within a specified volume of airspace, enabling the identification of spatial zones with high levels of aggregation, relative to the considered volume. On the other hand, the convergence indicator, CV, measures the geometric distribution of aircraft speed vectors to distinguish between converging and diverging traffic flows [83].

To compute intrinsic complexity, for each aircraft under consideration, a spatial weighting window that is centered on that aircraft is opened. Then, a complexity metric associated with the reference aircraft is determined by adding together the product of the two above complexity factors for all pairs of aircraft within the reference window:

$$CX_i = \lambda \sum_{j/CV_{ij} \leq 0} \overbrace{- \underbrace{\frac{\mathbf{P}_{ij} \cdot \mathbf{V}_{ij}}{D_{ij}}}_{CV_{r,ij}} \cdot \underbrace{e^{-\sigma D_{ij}^2}}_{PR_{ij}}}^{CX_{ij}} \tag{2.5}$$

Here, subscripts i and j represent the two aircraft considered, σ and λ are parameters fixed by the user, D_{ij} is the normalized distance between aircraft, and $\mathbf{P}_{ij}$ and $\mathbf{V}_{r,ij}$ represent the relative position and speed vectors, respectively.

2

Although aircraft positions are known accurately within the simulation, in real life operations, there is always some uncertainty regarding the precise location of aircraft. To ensure a reliable and robust complexity analysis, it is necessary to take this effect into account. Therefore, the complexity metric shown above is extended by considering all possible pairs of trajectory samples within a spatio-temporal window that is centered on each aircraft, i.e., by time averaging the complexity metric CX_{ij} from eq. 2.5 over all pairs of samples ij within a specified time interval. Finally, the robust complexity for a given traffic situation is calculated as the sum of the robust complexity metrics for all aircraft present in the airspace under evaluation.

Since complexity is defined for a particular traffic situation at a given time instant, for easier comparison of concepts, it is necessary to aggregate the robust complexity metric, $CX(t)$, over the total number of samples taken for each simulation run, n_s. This is done using a structural complexity metric, SCX, defined as:

$$SCX = \frac{1}{n^*} \sum_{t=0}^{n_s} CX(t) + \beta \max_t CX(t); \quad n^* = \max_s n_s \tag{2.6}$$

Here, β is a parameter fixed by the user to represent the relative importance of the maximum complexity compared to the average complexity, for a particular simulation run. In this work, $\beta = 0.05$ was selected. It should be noted that no differences to the trend of the SCX metric were found for β values between 0.01 and 0.3. For more details on the complexity metrics used, please refer to [84].

2.3.5.6. Noise Pollution

Although this study focuses on en route airspace design, because of the relatively low altitudes used by PAVs, the four airspace concepts are compared in terms of noise pollution. Noise pollution is analyzed using the LA_{eq} noise metric, calculated as [85]:

$$LA_{eq} = 10 \log_{10} \left(\frac{1}{t_{sim}} \int_0^{t_{sim}} 10^{\frac{LA(t)}{10}} dt \right) \tag{2.7}$$

where t_{sim} is equal to one hour, corresponding to the duration of the logging hour, and $LA(t)$ is the time dependent, A-weighted loudness level on the ground due to all the aircraft in a scenario, in dB(A). The computation of $LA(t)$ uses noise-power-distance relations that are similar to those found in environmental noise prediction programs such as the Integrated Noise Model (INM)) [86]. These relations (not shown) were established based on the data that is available for PAVs currently being designed, including the Maximum Take-Off Weight (MTOW) and FAA regulations governing the maximum noise that is allowed to be generated by tilt-rotor aircraft.

The footprints of the LA_{eq} metric are assessed by calculating iso-contour lines at the 68 dB(A) level. Although noise regulations in the Netherlands are based on the 48 and 58 dB(A) Loudness Day Evening Night (LDEN) sound levels, no requirements have been specified for the large amount of PAV traffic considered in this work. Hence, the next level, 68 dB(A), was selected for the current analysis. The encapsulated area of this contour can be used to compare concepts. A larger contour area implies a larger exposure to noise pollution. More details on the noise modeling method used in this work can be found in [87].

2.4. Results

In this section, the results of the nominal and non-nominal experiments are presented separately. For both experiments, the effect of the independent variables (airspace concept and traffic demand/number of rogue aircraft) on the dependent measures is analyzed using error bar charts, displaying the mean and the 95% confidence interval for each simulation condition. As identical scenarios were performed with and without tactical CR, whenever relevant, separate error bar charts are used to assess the need and the effect of CR on the four concepts. These charts are created by consolidating the demand data per concept.

2.4.1. Nominal Experiment

More than six million individual flights were simulated during the nominal experiment. Of these, data from approximately three million flights that flew during the logging hour have been analyzed. To gain a better sense on the amount of traffic simulated, as well as to explain the consequent implications on the analysis of the dependent variables, it is first necessary to consider the traffic volumes and densities that were actually realized during the experiment.

2.4.1.1. Traffic Volume and Density

Figure 2.7(a) shows the total traffic volume simulated during the logging hour, per simulation run, for all concept-demand combinations. Here it can be seen that the traffic volume simulated for the Full Mix, Layers and Zones concepts are the same and range from 12,000 aircraft in the Low scenario, to 22,000 aircraft in the Ultra scenario. On the other hand, the Tubes concept is shown to deviate from the other concepts for all demand conditions, even though all concepts were subjected to the same scenarios. In fact, the maximum traffic volume achieved by the Tubes concept in the Ultra scenario is less than the Medium demand volume realized by the three less structured concepts, indicating that demand could not be met by Tubes. This is because the Tubes concept used pre-departure delays and flight cancellations whenever conflict free routes could not be found at scenario specified departure times. As other concepts did not have the ability to delay or cancel flights, all flights in the demand scenarios were simulated.

2

<center>(a) Total traffic volume   (b) Average traffic density</center>
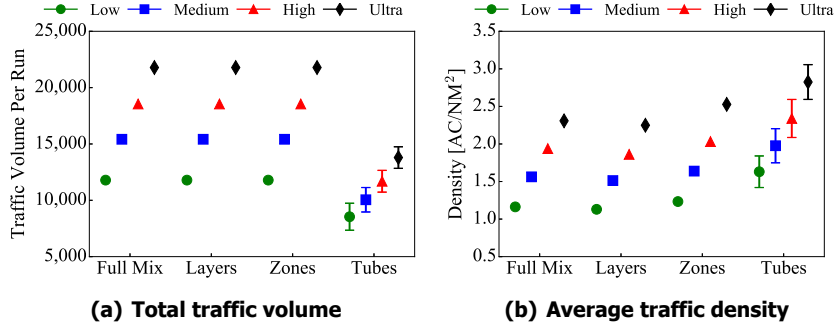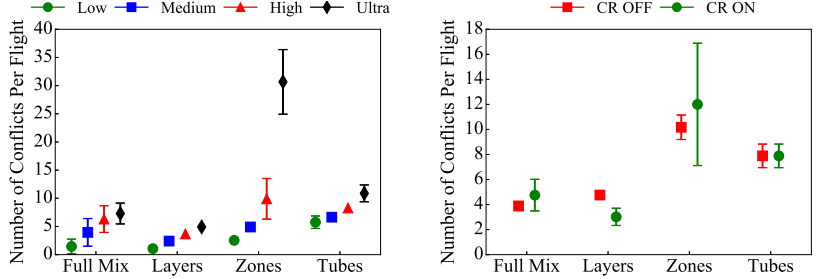
Figure 2.7: Means and 95% confidence intervals of the total number of flights and the average density per simulation run

In addition to total volume, it is also necessary to consider the traffic densities realized during the simulation, see Figure 2.7(b). Here it is clear that traffic density is fairly similar for the Full Mix, Layers and Zones concepts for all demand conditions. Conversely, the Tubes concept resulted in the highest traffic densities, despite the lower number of flights simulated for all demand scenarios (compare Figure 2.7(a) with Figure 2.7(b)). This paradoxical result can be explained by the fact that aircraft in the Tubes concept were often forced to use indirect and longer routes when the shortest path between an origin-destination pair was congested i.e., not conflict free prior to departure. Thus, average distances were much higher for Tubes (see efficiency metrics), causing aircraft to exist for longer durations in the experiment volume, which in turn resulted in higher densities than the other concepts.

These differences in traffic volume and density for the Tubes concept need to be taken into account when considering the other dependent variables. Although Figure 2.7(a) suggests that Tubes has a lower airspace capacity when compared to the other concepts, it should be noted that the figure does not imply that the other concepts are able to, for instance, facilitate the higher volumes safely. Therefore, conclusions with respect to capacity also depend on the other dependent variables discussed below, and cannot be based purely on the amount of traffic simulated. Moreover, whenever appropriate, these metrics are computed relative to the number of flights simulated to allow for a fair comparison between concepts.
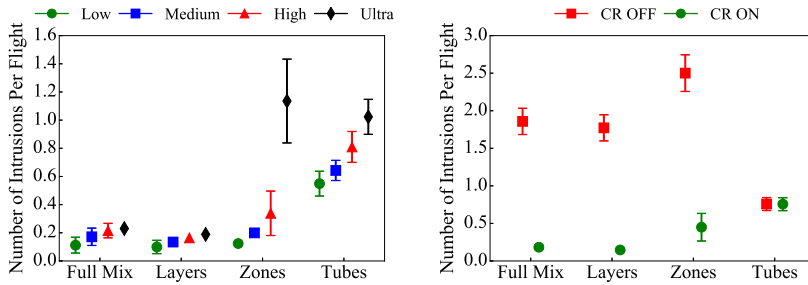
2.4.1.2. Safety

The number of conflicts and intrusions per flight for all simulation conditions are displayed in Figures 2.8 and 2.9, respectively. As expected, the number of conflicts and intrusions increased with traffic demand for all concepts, see Figures 2.8(a) and 2.9(a). Furthermore, the figures also show that the more structured Zones and Tubes concepts led to significantly higher numbers of conflicts and intrusions compared to the less structured Full Mix and Layers concepts.

(a) Effect of traffic demand (with conflict resolution)

(b) Effect of Conflict Resolution (CR)

Figure 2.8: Means and 95% confidence intervals of the number of conflicts per flight

(a) Effect of traffic demand (with conflict resolution)

(b) Effect of Conflict Resolution (CR)

Figure 2.9: Means and 95% confidence intervals of the number of intrusions per flight

The effect of tactical CR on the number of conflicts and intrusions is pictured in Figures 2.8(b) and 2.9(b), respectively. Here, the results with CR ON reflect the safety of each concept as a whole, whereas the results with CR OFF shows how well concepts are able to prevent conflicts from occurring. As Tubes did not use tactical CR, there were no differences between the ON and OFF conditions. For the other three concepts, the number of intrusions was considerably reduced with CR ON. However, the effect of CR on the number of conflicts did not follow the same trend. For Full Mix and Zones, the number of conflicts increased with CR ON. This was expected, as resolution maneuvers increase flight distances and the consequent probability of encountering other aircraft. However, for the Layers concept, the opposite was found, with CR ON leading to a lower number of conflicts. This unusual result is further analyzed using stability metrics.

It is also worth noting that the Tubes concept, which aimed at de-conflicting flights prior to take-off, resulted in a very high number of conflicts and intrusions for all scenarios. This was because the trajectory planning functions used in the Tubes concept did not take uncertainties, such as wind, into account. These uncertainties

2

caused aircraft to deviate from their planned flight paths during the simulation, resulting in a large number of conflicts due to the tight packing of the Tubes topology. As no tactical CR was used in the Tubes concept, these conflicts also resulted in a large number of intrusions.

To further analyze trends in the number of safety incidents, the relative velocity magnitudes between conflicting aircraft is computed, see Figure 2.10. Here, only conflicts between cruising aircraft, and data for simulations with CR OFF, are used, in order to consider the inherent safety of each concept. From this figure, it is clear that the vertical airspace segmentation used by the Layers concept significantly reduced relative velocities compared to the other three concepts, explaining the high safety of this concept.
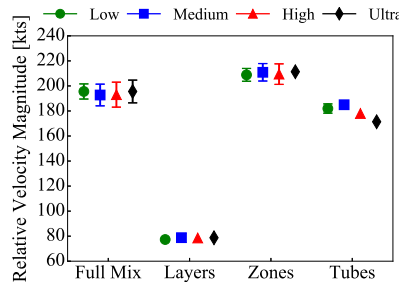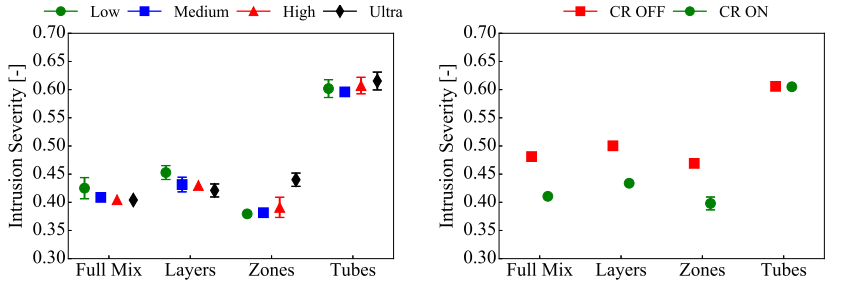
Figure 2.10: Means and 95% confidence intervals of the relative velocity magnitudes between conflicting aircraft in cruise (without conflict resolution)

The effect of the independent variables on intrusion severity is pictured in Figure 2.11. Here it can be seen that the Zones concept resulted in the lowest intrusion severity, despite experiencing the highest number of conflicts and intrusions. Furthermore, the figure shows that intrusion severity is not significantly dependent on traffic demand. This suggests that intrusion severity is more a function of the selected CR algorithm than airspace structure. Due to the resolution maneuvers initiated by the MVP algorithm, intrusion severity was reduced when CR was enabled for Full Mix, Layers and Zones, see Figure 2.11(b).
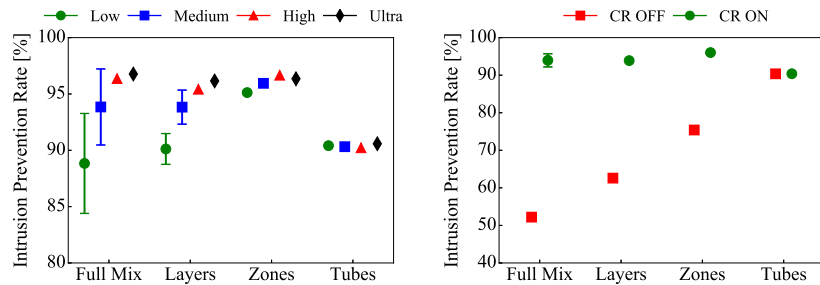
Figure 2.12 shows the results for the Intrusion Prevention Rate (IPR) metric, which measures the ability of a concept to solve conflicts without causing intrusions. For Full Mix, Layers and Zones, Figure 2.12(a) shows that IPR increases with traffic demand, while the rate of change of the metric appears to decrease with traffic demand and increasing airspace structure. This is because the rate of increase of intrusion number with traffic demand is less than that of conflict number, and the difference between the rates of change of conflicts and intrusions decreases with increasing demand and structure, compare Figures 2.8(a) and 2.9(a).

More interestingly, Figure 2.12(b) shows that IPR is non-zero for all concepts with CR OFF. These conflicts, termed 'false conflicts' as they were resolved without intervention from the tactical CR algorithm, were likely to have been caused by the state based CD method used in this work. As this CD implementation relied on

(a) Effect of traffic demand (with conflict resolution)

(b) Effect of Conflict Resolution (CR)

Figure 2.11: Means and 95% confidence intervals of the intrusion severity metric

(a) Effect of traffic demand (with conflict resolution)

(b) Effect of Conflict Resolution (CR)

Figure 2.12: Means and 95% confidence intervals of the Intrusion Prevention Rate (IPR) metric

linear extrapolation of aircraft trajectories to predict conflicts, aircraft, which were turning or climbing/descending to follow concept dependent routing requirements, would trigger conflicts if they were momentarily in the projected paths of other aircraft. Figure 2.12(b) also shows that IPR increased with airspace structure for CR OFF, and is the highest for Tubes. This suggests that increasing traffic structure does improve the *proportion* of intrusions that can be avoided as a result of the prescribed routing of the more structured concepts, even though the *absolute number* of conflicts and intrusions were found to increase with structure and demand.

On the other hand, IPR was found to be very high (greater than 90%) with CR ON for the three concepts that used tactical CR, see Figure 2.12(b). Although false conflicts can also be expected for CR ON, the CP algorithm, which was also activated with tactical CR, prevented aircraft from turning into conflicts, thus avoiding conflicts of the type mentioned for the CR OFF case. Additionally, the similarity of this metric for Full Mix, Layers and Zones indicates that the *relative* performance of the MVP CR algorithm remains constant. However, as indicated above, the *absolute* number of intrusions has a greater bearing on the safety comparison between concepts.

2.4.1.3. Efficiency

Efficiency, measured using the work done metric, is shown in Figure 2.13. Here, a positive correlation between work done, level of airspace structure and traffic demand can be seen. The Full Mix concept displays the lowest work done, and is closely followed by the Layers concept. The difference between these two concepts can be traced back to the inefficient altitudes used by the Layers concept, whereas Full Mix used the most optimum horizontal and vertical flight paths to improve efficiency. The Tubes concept led to the highest work done, implying that aircraft flew significantly longer distances in this concept. For the Full Mix, Layers and Zones concepts, work done was found to be higher with CR ON due to the extra distance flown during tactical CR maneuvers, see Figure 2.13(b). These trends were also seen when comparing the distance traveled between concepts (not shown). Thus, the results strongly indicate that efficiency decreases with increasing airspace structure and density, as well as when tactical CR is used.

(a) Effect of traffic demand (with con-   (b) Effect of Conflict Resolution (CR)
flict resolution)
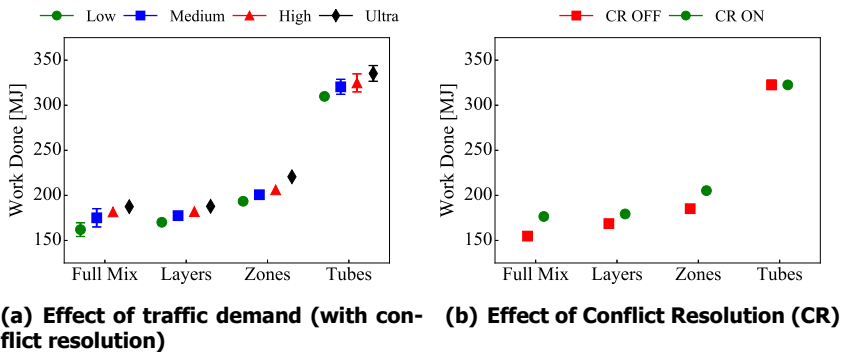
Figure 2.13: Means and 95% confidence intervals of the work done metric

2.4.1.4. Stability

The stability of the airspace as result a of CR maneuvers is measured using the Domino Effect Parameter (DEP). A negative DEP implies a net stabilizing effect of tactical CR whereby conflict chain reactions are outweighed by those that are solved without pushing aircraft into secondary conflicts, whereas a positive value indicates the opposite, with conflict chain reactions causing airspace instability. The DEP for all concept-scenario combinations is pictured in Figure 2.14. Note that the DEP is consistently zero for Tubes as it did not use tactical CR. For the other three concepts, the DEP for the Low demand scenario is similar and negative. However at higher demand levels, the DEP increases to positive values for the Full Mix and Zones concepts. This suggests that the maneuvering room available to solve conflicts decreases rapidly with increasing airspace density for these two concepts, making it progressively more difficult to avoid intrusions without triggering additional conflicts. This is particularly true for the Zones concept which experienced a very large
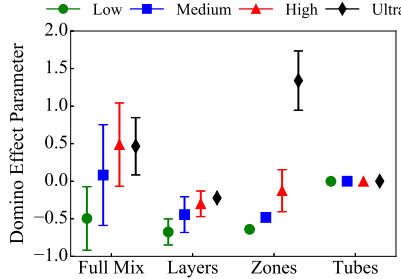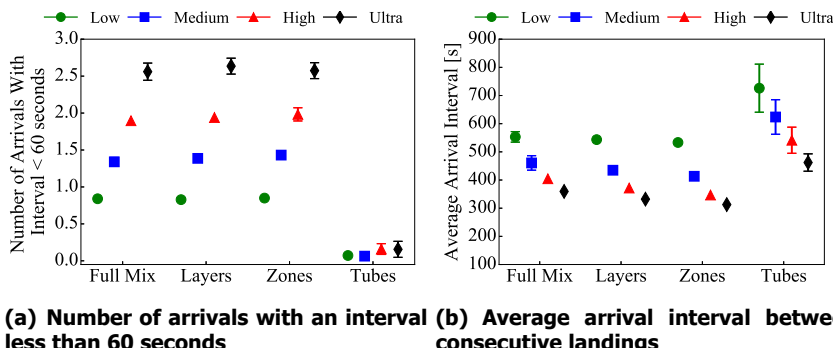
Figure 2.14: Means and 95% confidence intervals of the Domino Effect Parameter (DEP)

DEP increase between the High and Ultra demand scenarios, while for Full Mix, the DEP appears to settle at a value of approximately 0.5.

Although the DEP also increased with demand for Layers, it remained negative for the range of densities considered in this work, see Figure 2.14. This suggests that the vertical segmentation of traffic used by the Layers concept is more able to prevent conflict propagation from occurring, and is better at assisting the MVP CR algorithm in solving the conflicts that do occur by reducing conflict angles and relative velocities between aircraft cruising at the same altitude, i.e., through the alignment of neighboring traffic. This result explains the reduction in the number of conflicts with CR ON, noted earlier for Layers (see Figure 2.8).

2.4.1.5. Arrival Sequencing

The number of consecutive arrivals with a time interval smaller than 60 seconds (equaling the CD look-ahead time), per destination, is shown in Figure 2.15(a). This figure shows that the Tubes concept violated the 60 second threshold the least. This suggests that the time based separation used to separate traffic in the

(a) Number of arrivals with an interval less than 60 seconds

(b) Average arrival interval between consecutive landings

Figure 2.15: Means and 95% confidence intervals of the arrival sequencing between consecutive flights at each destination (with conflict resolution)

predefined tubes topology almost always ensured adequate separation at the run-way. This is because all aircraft used the same descent rates below the experiment volume. Hence a runway conflict could only occur if two or more aircraft attempted to land at the same runway at the same time from different nodes in the topology (a scenario with a low probability given the reduced traffic volume accommodated by Tubes). The other three concepts, however, resulted in up to 2.6 aircraft arriving with insufficient spacing at the runway for the Ultra demand scenario. Although this is partly due to the higher traffic volumes handled by these concepts, this result shows that some form of arrival metering may be necessary for Full Mix, Layers and Zones. But, as the average arrival interval between aircraft is always greater than 300 seconds for these three concepts, see Figure 2.15(b), arrival sequenc-ing can likely be managed by varying the speeds of conflicting aircraft during the final descent. Given the high average arrival intervals for all concepts, the differ-ent ways of structuring en-route airspace are not expected adversely impact arrival procedures.

2.4.1.6. Structural Complexity

Figure 2.16 displays the results for the Structural Complexity (SCX) metric, normal-ized with respect to the total number of flights simulated per concept. Here, high values corresponds to traffic situations that are more difficult to control, and those that are more sensitive to uncertainties. Figure 2.16(a) shows that SCX followed a similar trend to the number of conflicts and intrusions, with a clear distinction be-tween the two less structured concepts, which display a linear growth of SCX with demand, when compared to the two more structured concepts, which resulted in a quadratic increase of SCX with demand. This strongly suggests that little structur-ing of airspace, as used by Full Mix and Layers, results in traffic patterns that are easier to control than those produced by the predetermined routes of the Zones and Tubes concepts.

(a) Effect of traffic demand (with con-flict resolution)

(b) Effect of Conflict Resolution (CR)
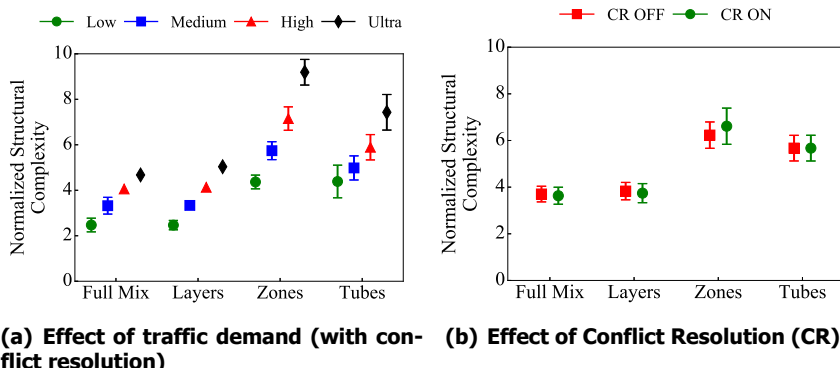
Figure 2.16: Means and 95% confidence intervals of the normalized Structural Complexity (SCX) metric
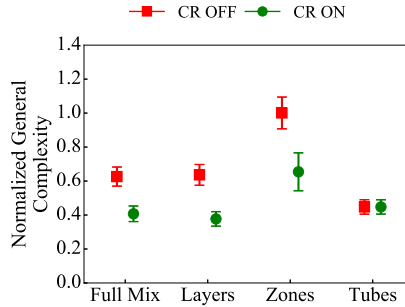
Figure 2.17: Means and 95% confidence intervals of the effect of Conflict Resolution (CR) on the normalized general complexity metric

The pre-planned routes used by the Tubes concept were expected to result in the lowest complexity. In fact, the absolute SCX values were the lowest for Tubes. However, when the results were normalized, the contribution of each flight to SCX was found to be much higher for Tubes than for the other concepts. The high complexity of the Zones concept can be traced to traffic convergence at the intersections between ring and radial zones.

As expected, no differences in SCX between CR ON and CR OFF were found for the Tubes concept, see Figure 2.16(b). However, the overlapping error-bars for the Full Mix, Layers and Zones concepts indicate that SCX was not significantly affected by CR maneuvers. This result can be explained by the fact that the computation of the SCX metric considers *all possible trajectory realizations/evolutions* between aircraft pairs within a predefined spatio-temporal window, negating the effect of the specific resolution maneuvers used to avoid intrusions. Therefore, it can be concluded that the SCX metric is not suitable to analyze the effect of CR maneuvers on intrinsic complexity.

To gain more insight on the effect of CR on complexity, the influence of CR maneuvers on the general complexity metric, described by eq. 2.5, is displayed in Figure 2.17. Here, it can be seen that CR ON reduced the general complexity metric for the Full Mix, Layers and Zones concepts, indicating that CR improves the controllability of a given traffic situation, as expected.

2.4.1.7. Noise Pollution

Noise footprints for all four concepts are displayed in Figure 2.18. This figure was created using data from a simulation for the 'Ultimate' demand volume and with a converging demand pattern, see Section 2.3.2.2. Figures 2.18(a) and 2.18(b) show that Full Mix and Layers resulted in very similar noise loads on the ground, consisting of a high intensity noise load at the main convergence point at the bottom of the simulation area, that decayed with increasing distance from that point. In contrast, the Zones and Tubes concepts resulted in footprints that clearly depicts the structuring of traffic used by these two concepts. For the Zones concept, Figure 2.18(c)

2

(a) Full Mix

(b) Layers

(c) Zones

(d) Tubes
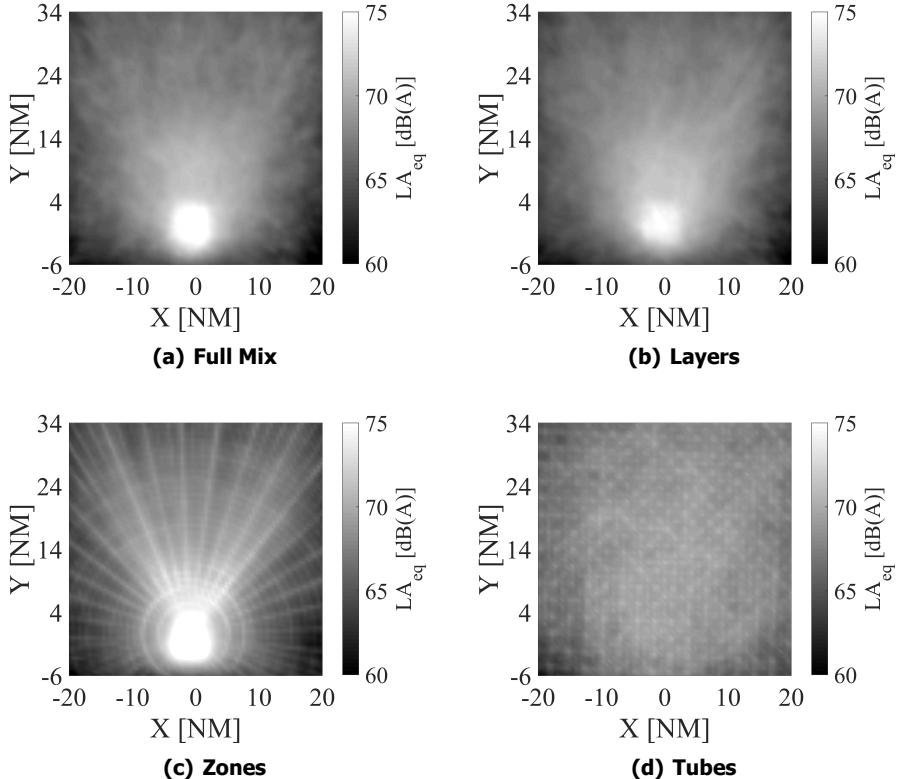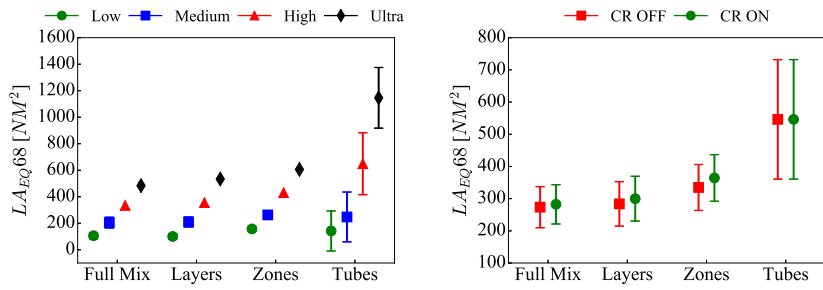
Figure 2.18: Noise footprints for an 'Ultimate' demand scenario with a converging traffic demand pattern

(a) Effect of traffic demand (with conflict resolution)

(b) Effect of Conflict Resolution (CR)

Figure 2.19: Means and 95% confidence intervals of the area encapsulated by the LA_{eq} noise metric for iso-contour lines at 68 dB

shows higher noise levels along the ground projections of the predefined ring and radial zones. This suggests that the Zones concept may allow for easier mitigation of noise pollution by defining its topology along less inhabited areas.

The Tubes concept is shown to have distributed sound evenly due to its grid-like structure, see Figure 2.18(d). Furthermore, Tubes appears to have caused the lowest noise impact on the ground and was the only concept without a high intensity noise load at the convergence point. However, these trends are related to the lower traffic volume that could be accommodated by the Tubes concept, see Figure 2.7(a). Unlike the other metrics discussed above, a linear normalization with respect to the total number of flights could not be used as noise is measured in dB, a logarithmic unit. This complicates a direct comparison with the Tubes concept in relation to noise pollution.

In addition to the noise footprints discussed above, the LAeq metric is used to quantitatively study the noise impact by computing the area encapsulated by iso-contour lines at the 68 dB(A) level. Figure 2.19(a) shows that noise pollution at 68 dB(A) is quite similar for Full Mix, Layers and Zones. On the other hand, the Tubes concept, which caused the lowest total noise impact on the ground, led to the largest area at the 68 dB(A) level for the higher demand scenarios. This suggests that the total noise on the ground would have been the highest for the Tubes concept had it been able to meet the required traffic demand. As expected, CR ON led to a slightly higher noise impact for the Full Mix, Layers and Zones concepts, see Figure 2.19(b), as resolution maneuvers increased flight distances for these three concepts.

2.4.2. Non-Nominal Experiment

As stated earlier, the purpose of the non-nominal experiment is to compare the relative robustness of the four airspace concepts when subjected to increasing numbers of rogue aircraft. Since rogue aircraft primarily affect safety metrics, the following

(a) Effect of number of rogue aircraft (with conflict resolution)

(b) Effect of Conflict Resolution (CR)
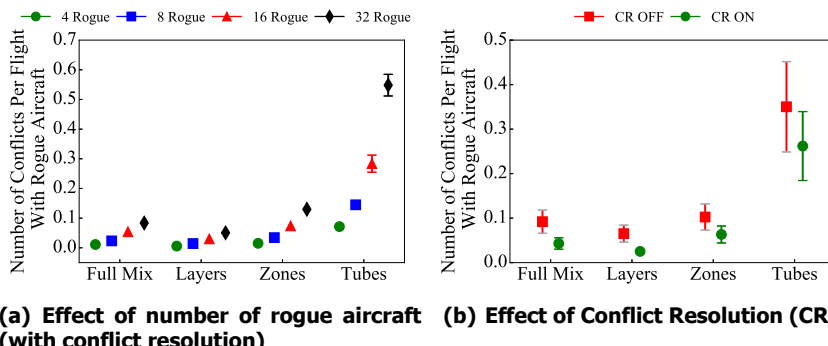
Figure 2.20: Means and 95% confidence intervals of the number of conflicts per flight with rogue aircraft alone

2

(a) Effect of number of rogue aircraft   (b) Effect of Conflict Resolution (CR)
(with conflict resolution)
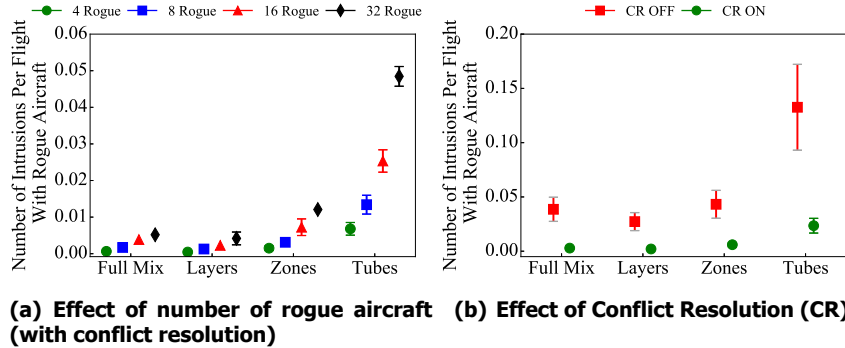
Figure 2.21: Means and 95% confidence intervals of the number of intrusions per flight with rogue aircraft alone

paragraphs discuss the number of conflicts and intrusions between rogue and 2.7 million normal aircraft that were logged during this experiment.

Figures 2.20 and 2.21 display the number of conflicts and intrusions per flight with rouge aircraft alone, i.e., only safety incidents between normal and rouge aircraft were counted for these two figures. Here it can be seen that increasing the number of rogue aircraft also increases the number of conflicts and intrusions for all concepts. Further analysis indicated that the nonlinear increase in the number of rogue aircraft only led to a linear increase in the number of conflicts and intrusions for all concepts, suggesting that all concepts are more robust than initially expected. Nonetheless, Figures 2.20(a) and 2.21(a) show that the safety of the Tubes concept is considerably more affected by rouge aircraft than it is for the Full Mix, Layers and Zones concepts.

As the trajectories of rogue aircraft were not known in advance, aircraft in the Tubes concept used the MVP CR algorithm to avoid intrusions with rogue aircraft alone. Since the tube topology specifies both the horizontal and vertical flight profiles, only speed resolution maneuvers were possible. Figures 2.20(b) and 2.21(b) shows that these resolutions did reduce the number of conflicts and intrusions with rogue aircraft for Tubes. As expected, CR ON also improved the safety of the other three concepts against rogue aircraft.

The above result may suggest that tactical CR can be used to complement the safety of the pre-planned Tubes concept. However, closer inspection of the simulation data indicated that CR maneuvers made it more difficult for conflict resolving (normal) aircraft to meet the specified Required Time of Arrival (RTA) at waypoints along pre-planned routes. This in turn resulted in additional intrusions between normal aircraft, that were avoided when rogue aircraft were not included in the simulations. In fact, the resulting break-down of the pre-planned routes caused the highest total number of intrusions per flight for the Tubes concept, while for the three less structured concepts, the total number of intrusions was not affected by the number
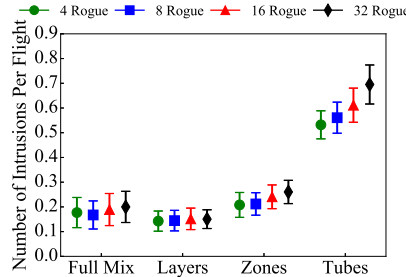
Figure 2.22: Means and 95% confidence intervals of the total number of intrusions per flight for the non-nominal experiment (with conflict resolution)

of rogue aircraft, see Figure 2.22. Therefore the simple addition of tactical CR is not guaranteed to improve the robustness of the Tubes concept. To improve robustness and safety, larger margins could be applied to time constraints at waypoints along a route. However, this would further decrease the efficiency of the Tubes concept, see Figure 2.13(a).

2.5. Discussion

In this chapter, four en-route airspace concepts of increasing structure, named Full Mix, Layers, Zones and Tubes, were compared using two fast-time simulation experiments that involved over eleven million flights. These simulations focused on the degree of structuring needed to maximize capacity for decentralized separation, and investigated whether the optimal mode of structuring depended on traffic density. The simulations also studied the robustness of the different structuring methods to non-nominal events. Here, capacity was inferred from the effect of multiple traffic demand scenarios on safety, efficiency, stability, arrival sequencing, structural complexity and noise pollution metrics, while robustness was assessed from the influence of increasing numbers of rogue aircraft on safety metrics.

As indicated previously, the goal of this work is not to propose an operationally ready airspace design, but to focus on how the level of structuring affects airspace capacity for decentralization. In relation to this specific goal, and considering the results of all metrics in unison, it can be concluded that some limited structure in the vertical dimension, as demonstrated by the Layers concept, can be beneficial in terms of capacity. This is because traffic demand, in addition to varying in time, displays no predominant patterns in the horizontal dimension for decentralization. Therefore, a strict horizontal structuring of airspace can cause a mismatch between the imposed structure and the demand pattern, as for the Zones and Tubes concepts. This in turn caused artificial bottlenecks at the intersection points of their predefined topologies, reducing overall performance. On the other hand, the vertical airspace segmentation used by the Layers concept dispersed traffic vertically, and grouped traffic by similarity of travel direction. This reduced the chance of

2

conflicts by lowering relative velocities between cruising aircraft when compared to the completely unstructured Full Mix concept, without unduly affecting efficiency, structural complexity or noise pollution metrics, as direct horizontal routes were still possible with Layers. These conclusions were not expected as previous research had focused primarily on either fully structured or fully unstructured airspace designs.

For the range of densities considered in this work, the results of the nominal simulations also indicate that the optimum method of structuring is independent of traffic density. In fact, the results show a clear distinction between the two less structured and the two more structured concepts; while performance degraded with increasing density for all concepts, it did so at a much higher rate for Zones and Tubes. In particular, the safety of the Zones and Tubes concepts deteriorated rapidly for the higher densities, indicating that the airspace had become saturated for these two highly structured concepts. When considering the fact that route planning was more computationally intensive for Zones and Tubes, the additional constraints imposed on traffic by these two concepts did not translate into benefits in terms of capacity.

The clear distinction between the two more and two less structured concepts was not, however, found for the results of the non-nominal simulations. In that experiment, the safety of the Full Mix, Layers and Zones concepts was not significantly affected by rogue aircraft. This suggests that tactical conflict resolution, which was used natively by these three concepts to resolve conflicts between nominal aircraft, could also effectively compensate for non-cooperative aircraft, without adversely affecting capacity. This was not the case for the Tubes concept. Here, the uncertainties caused by rogue aircraft made it difficult for nominal aircraft to adhere to time constraints at waypoints along a route. The resulting break down of the pre-planned space-time routes used by Tubes to separate aircraft caused a large number of unintended conflicts and intrusions. The performance of Tubes was also affected by wind for the same reason. While all concepts were negatively influenced by uncertainties, the current results show that the safety of highly structured and planned airspace concepts is particularly vulnerable to variations between the intended and actual flight trajectories.

For many metrics, the Full Mix and Layers concepts exhibited very similar behavior. The similarity between these two concepts was highlighted by their noise footprints, which were indistinguishable. The only difference between these two concepts is the method of altitude selection; aircraft in Full Mix used the most fuel-efficient altitude, while for Layers, altitude was dependent on the direction to the destination. Therefore, Full Mix was expected, and was also found, to be slightly more energy efficient. However, the similarity in efficiency between these two concepts may be a result of the short cruising distances used in this work, and longer distances may further increase the efficiency differences between Full Mix and Layers.

Although the vertical structuring used by Layers reduced efficiency relative to the unstructured Full Mix concept, it led to the highest stability of all four structuring

options. This high stability was reflected by the negative Domino Effect Parameter (DEP) values logged for all densities in the Layers concept. A negative DEP indicates a reduction in the number conflicts when tactical Conflict Resolution (CR) and Conflict Prevention (CP) algorithms are enabled, even though CR maneuvers increase flight distances and, correspondingly, the probability of encountering other aircraft. It is hypothesized that a negative DEP is caused by the alignment of neighboring traffic, and the consequent reduction of relative velocities that aids CR performance, a behavior that is further amplified by the limited heading ranges available to cruising aircraft in the Layers concept, and the use of CP. Although negative DEPs were also found for Full Mix and Zones at low demand levels, at higher densities, these modes of structuring transitioned to positive DEP vales, indicating a greater degradation of airspace stability with density. Hence, the stability analysis indicates that the altitude constraints utilized by Layers can accommodate even higher densities than what was considered in this work, without significantly reducing safety or efficiency. This reiterates the notion that a limited degree of vertical structuring can be beneficial for the capacity and robustness of decentralized airspace.

It should be noted that the results of this study are, to some degree, sensitive to the specific parameter settings selected for the concepts. However, given the magnitude of the differences in all of the results, as well as the consistency between results, it is unlikely that the overall trends are affected by different settings; capacity for decentralization was found to improve when structural constraints did not affect the horizontal path of aircraft. This conclusion is most applicable for traffic scenarios without any distinct horizontal patterns. For traffic demand cases with discernible horizontal patterns, such as for current hub-and-spoke operations, airspace concepts that permit flexible routing in the horizontal direction are also expected to perform well, as such structuring would not conflict with any demand pattern. Nonetheless, it may be possible to tailor the topologies of more structured concepts to match such scenarios.

2.6. Conclusions

This work investigated the degree of structuring needed to maximize capacity for decentralized en-route airspace. To this end, four decentralized en-route airspace concepts of increasing structure were compared using fast-time simulations. For the studied densities, the following conclusions can be drawn:

- *Capacity benefits when the horizontal path of aircraft is not over-constrained.* This is because traffic demand displays no predominant patterns in the horizontal dimension, for decentralization.

- *Capacity is maximized when vertical constraints are used to separate traffic with different travel directions at different flight levels.* This mode of structuring improved performance over completely unstructured airspace by decreasing relative velocities between aircraft cruising at the same altitude, while al-

2

lowing direct horizontal routes. The reduced relative velocities also increased the stability of the airspace to tactical conflict resolutions.

- *Conversely, structuring modes that imposed horizontal constraints caused a convergence of traffic at the intersections of structural elements.* These traffic concentrations reduced overall performance for such concepts.

- *The optimum method of structuring was found to be independent of density.* Capacity generally benefited from a reduction of structural constraints.

- *Robustness to uncertainties is significantly reduced when decentralization using time based separation is combined with a predefined and fixed three dimensional route structure.*

Part II:
SAFETY MODELING

3

Three-Dimensional Analytical Conflict Count Models

The results of the previous chapter indicated that airspace concepts that reduce the average relative velocities between aircraft, and those that avoid traffic concentrations, improve airspace safety and efficiency, and therefore, airspace capacity. Using this understanding as a starting point, this chapter develops analytical conflict count models to quantify the intrinsic safety provided by an airspace design, using unstructured and layered airspace concepts as case studies. These models compute the number of instantaneous conflicts in the airspace as a function of traffic demand and airspace design parameters such as traffic separation requirements. While previous similar models described in literature have focused mainly on conflicts between cruising aircraft, the present models also consider conflicts involving cruising as well as climbing/descending aircraft for a more comprehensive safety analysis. The resulting three-dimensional models are validated using fast-time simulation experiments.

Cover-to-cover readers may choose to skip sections 3.2.2 and 3.2.3 which describe the conceptual designs of unstructured and layered airspaces. These descriptions are essentially unchanged from their counterparts in chapter 2.

Abstract

This chapter presents analytical models that describe the safety of unstructured and layered en route airspace designs. Here, 'unstructured airspace' refers to airspace designs that offer operators complete freedom in path planning, whereas 'layered airspace' refers to airspace concepts that utilize heading-altitude rules to vertically separate cruising aircraft based on their travel directions. With a focus on the intrinsic *safety provided by an airspace design, the models compute instantaneous conflict counts as a function of traffic demand and airspace design parameters, such as traffic separation requirements and the permitted heading range per flight level. While previous studies have focused primarily on conflicts between cruising aircraft, the models presented here also take into account conflicts involving climbing and descending traffic. Fast-time simulation experiments used to validate the modeling approach indicate that the models estimate instantaneous conflict counts with high accuracy for both airspace designs. The simulation results also show that climbing and descending traffic caused the majority of conflicts for layered airspaces with a narrow heading range per flight level, highlighting the importance of including all aircraft flight phases for a comprehensive safety analysis. Because such trends could be accurately predicted by the three-dimensional models derived here, these analytical models can be used as tools for airspace design applications as they provide a detailed understanding of the relationships between the parameters that influence the safety of unstructured and layered airspace designs.*

Note on Nomenclature
The models described in this chapter compute *instantaneous* conflict counts as a measure of the intrinsic safety provided by an airspace design. As such, the following nomenclature simplifications are used to reduce the complexity of the equations presented in this chapter:
- C: Instantaneous conflict count without conflict resolution
- N: Instantaneous aircraft count without conflict resolution

---

3.1. Introduction

The sustained growth of air traffic in recent years has stressed several components of the current Air Traffic Management (ATM) system to near saturation levels. This is particularly true for en route airspace design where continued reliance on the fixed airway network has significantly reduced flight efficiencies [76]. This is because airway navigation often force aircraft to deviate from direct trajectories, which during peak demand periods can trigger artificial traffic concentrations and increased delays [13, 89]. Their use in Europe, for instance, has been linked to the 20% increase in en route delays in 2016, even though traffic demand grew by only 2.4% during the same time period [12]. Similar statistics reported in many other parts of the world have motivated several studies to explore alternate options for organizing en route traffic [18, 77, 90].

To overcome the capacity limitations posed by airway routing, some researchers have proposed a transition to less rigid route structures for en route airspace [30, 33, 91–93]. This approach has been adopted in some low-density areas of Europe with the creation of so called 'Free Route Airspaces' (FRAs) since 2008 [94]. FRAs aim to emulate the route selection flexibility offered to aircraft flying in unmanaged airspace, while continuing to provide air traffic controllers with control of the traffic within them. Analysis by Eurocontrol has shown that the limited use of FRAs thus far has yielded an average route efficiency increase of 1.6% per flight, with gains of up to 4% in some areas [12]. Further extending FRAs into more dense airspace sectors could, therefore, lead to substantial reductions in total delay, fuel consumption and emissions. As such, FRAs demonstrate the potential of utilizing procedural mechanisms to reorganize and improve the performance of en route airspace operations, without large capital investments in new hardware.

While reducing structural constraints can increase en route airspace capacity relative to airway routing for current traffic demand levels, a recent study has found that offering operators *complete* freedom in path planning is not optimal in terms of safety for higher densities [74]. In that study, several unmanaged en route airspace concepts, which varied in terms of the number of constrained degrees of motion, were compared qualitatively using simulation experiments. The results clearly showed that a layered airspace concept, which used a vertical segmentation of airspace to separate traffic with different travel directions at different flight levels, led to the highest safety. The increased safety for 'layers' was found to be a result of the reduction of relative velocities between cruising aircraft at the same altitude, which in turn reduced the number of conflicts when compared to a completely unstructured airspace design.

Using the qualitative understanding gained from [74] as a starting point, this chapter aims to develop quantitative models that describe the intrinsic safety provided by unstructured and layered en route airspace designs. Here the notion of intrinsic safety refers to the ability of an airspace design to reduce the occurrence of conflicts due to the constraints that it imposes on traffic motion. As such, the intrinsic safety provided by an airspace design is irrespective of whether or not conflicts are actually detected by aircraft; instead this aspect of safety considers the effect of the route structure imposed by a particular design on the number of 'truly occurring' conflicts. Consequently, intrinsic safety is directly proportional to the workload experienced by pilots and/or air traffic controllers in resolving any remaining conflicts that could not be prevented by a particular airspace design.

The modeling approach used in this work treats aircraft conflicts similar to the collisions that occur between ideal gas particles to determine instantaneous system-wide conflict counts as a measure of intrinsic safety. In comparison to previous studies, the models considered here take into account the effect of the horizontal *and* the vertical motion of aircraft on conflict counts. This is done by grouping the considered aircraft according to flight phase, while also considering the proportion of aircraft in different flight phases. This approach allows conflicts involving climbing and descending traffic, as well as those between aircraft, to be taken into account.

Because the resulting three-dimensional analytical models use measurable airspace characteristics, such as traffic demand and separation requirements, as inputs, they lend themselves well for airspace design applications as the interactions between the factors affecting safety can be directly understood from the structure of the models.

To assess the accuracy of the derived models, three separate fast-time simulation experiments have been performed, encompassing almost three million flights. The first experiment measures the accuracy of the models under ideal conditions, and analyzes the effect of the allowed heading range per flight level on the intrinsic safety of layered airspace concepts. The second experiment studies the effect of the proportion of aircraft in different flight phases on safety and on model accuracy. The final experiment focuses on the sensitivity of the models to a simplification made during the derivation process regarding the speed distributions of aircraft.

This chapter begins with an outline of the relevant background material and an overview of previous research in section 3.2. Next, in sections 3.3 and 3.4, the derivation of the models is presented. This is followed by the design of the simulation experiments used to assess model accuracy in section 3.5. Simulation results are presented in section 3.6, and discussed in section 3.7. Finally, a summary of the main conclusions is given in section 3.8.
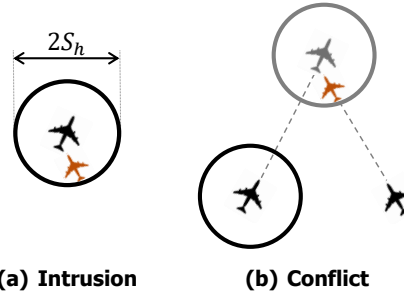
3.2. Background

This section summarizes the background material needed to follow the conflict count model derivations developed in this chapter. The sections begins by discussing the relationship between conflicts and intrinsic airspace safety. Additionally, descriptions of the conceptual design of unstructured and layered airspace concepts, as well as a review of previous studies that have used analytical models to measure intrinsic airspace safety, are provided.

3.2.1. Conflicts, Intrusions and Intrinsic Airspace Safety

Safety in ATM is often measured in terms of the number of intrusions and conflicts. Here, intrusions, also known as losses of separation, occur when minimum separation requirements are violated. Conflicts, on the other hand, are defined as *predicted* intrusions; they occur when the horizontal and vertical distances between aircraft are expected to be less than the prescribed separation standards within a predetermined 'look-ahead' time. Therefore, when a conflict occurs, some action needs to be taken by pilots and/or air traffic controllers to prevent that conflict from turning into an intrusion in the future. The distinction between intrusions and conflicts is illustrated in Figure 3.1.

Although a conflict is strictly speaking only defined between two aircraft, they can also occur between with more aircraft at the same time. Such 'multi-aircraft' conflicts can still be treated as several two-aircraft conflicts and are included in the

(a) Intrusion   (b) Conflict

Figure 3.1: The difference between intrusions and conflicts, displayed here for the horizontal plane. Intrusions are violations of separation requirements, whereas conflicts are predicted intrusions. Here, S_h is the horizontal separation requirement.
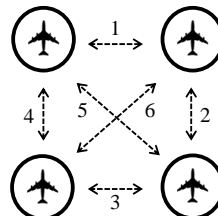
Figure 3.2: A multi-aircraft conflict can be decomposed into several two-aircraft conflicts. For example, a multi-aircraft conflict between four aircraft can result in up to six unique two-aircraft conflicts.

number of combinations based only on pairs of aircraft. For example, a multi-aircraft conflict involving four aircraft can result in *up to* six unique two-aircraft conflicts; see Figure 3.2. This combinatorial property is used by the modeling approach described in this work, see section 3.2.4.

As mentioned earlier, this work focuses on modeling the *intrinsic safety* of unstructured and layered airspaces. The notion of intrinsic safety focuses exclusively on the safety that is provided by the constraints imposed on aircraft motion by an airspace design. Since the type and number of constraints imposed directly affects the probability of intersecting trajectories, the intrinsic safety of an airspace design can be measured in terms of the number of conflicts that occur at any given moment in time, i.e., by the number of instantaneous conflicts. Although measurement and communication uncertainties can affect the number of observed, or perceived, conflicts for particular a aircraft, such uncertainties are unrelated to the design of an airspace. As such, the intrinsic safety provided by an airspace design is only concerned with the 'truly occurring' conflicts in an airspace.

Because intrinsic safety considers the situation *without* tactical conflict resolution, it can be used as an indication of the workload that is experienced by pilots and/or air traffic controllers in solving conflicts under the considered airspace concept. It can also be used to analyze the frequency of conflicts that any future automated conflict

resolution system should be able to handle. This flexibility allows the methods discussed in this chapter to be applied to current commercial air traffic operations, as well as for future operations integrating unmanned aircraft with automated detect-and-avoid systems.

3.2.2. Unstructured Airspace

As the name suggests, no constraints are imposed on aircraft motion in Unstructured Airspace (UA). Instead, this simplest form of airspace design focuses on maximizing overall system efficiency. Therefore, aircraft are free to use direct horizontal routes, as long as such routing is not obstructed by weather or static obstacles. Similarly, aircraft can also fly with preferred speeds and at optimum altitudes, based on their performance capabilities and trip distances. By offering greater freedom to aircraft operators, UA has been found to result in a more uniform distribution of traffic, both horizontally and vertically, reducing traffic concentrations and ensuing delays [29, 30].

3.2.3. Layered Airspace

Several different layered airspace concepts have been discussed in literature [95–97]. The specific variation under consideration in this work was developed in our prior work [74], and is known as the 'Layers' concept.

The Layers concept can be seen as an extension to the hemispheric/semicircular rule [79]. In this concept, the airspace is segmented into vertically stacked bands, and heading-altitude rules are used to limit the range of travel directions allowed in each altitude layer. Although the Layers concept dictates the vertical profile of a flight, operators are free to select direct horizontal routes when possible. Moreover, climbing and descending aircraft are exempted from the heading-altitude rules, and can violate them to reach their cruising altitude or destination. This exception avoids inefficient 'spirals' when climbing/descending.

An example Layers concept is shown in Figure 3.3. Two parameters define the topology of the Layers concept. The first parameter is the spacing between altitude bands, ζ. An important design requirement is that ζ is *at least* equal to the vertical separation requirement to prevent conflicts between aircraft cruising in adjacent flight levels. In this work, a vertical separation requirement of 1000 ft is used. Therefore, the altitude bands of the Layers concepts considered here are separated by $\zeta = 1100$ ft; the extra 100 ft is used to prevent so called 'false' conflicts that can sometimes occur due to any slight overshooting of altitude when aircraft level-off at their desired flight level. Such an offset is also necessary to account for any height-keeping errors, and because of turbulence.

The second design parameter of the Layers concept is the heading range allowed per altitude band, α. For the layered airspace shown in Figure 3.3, $\alpha = 45^o$, and thus eight flight levels are needed to define one complete 'set' of layers. Corre-

Figure 3.3: Isometric view of an example Layers concept, with an allowed heading range of $\alpha = 45^o$ per flight level, and a vertical spacing of $\zeta = 1100$ ft between flight levels

spondingly, for a layered design with $\alpha = 90^o$, only four flight levels would be needed to specify all possible travel directions. Therefore, for $\alpha = 90^o$, two complete 'sets' of layers would fit within the volume of airspace needed for $\alpha = 45^o$. When multiple sets of layers are available, the total trip distance of an aircraft is used in addition to its heading to determine its cruising altitude. In this way, short flights can use lower layer sets, and longer flights can use higher layer sets, to reduce the negative effect of predetermined altitudes on flight efficiencies.

3.2.4. Previous Research on Conflict Count Modeling

To model the total number of instantaneous conflicts in a given volume of airspace, it is necessary to take into account the total number of possible interactions between aircraft in that airspace, i.e., the maximum number of unique, two-aircraft combinations. Since any conflict can be decomposed into a series of one or more two-aircraft conflicts, see section 3.2.1, the maximum number of instantaneous conflicts possible is equal to the total number of unique two-aircraft combinations. However, in practice, not all aircraft are likely to be in conflict at the same time because the distance between corresponding aircrafts may be too large, or because the constraints imposed by a particular airspace design may prevent the trajectories of two specific aircraft from ever intersecting. Consequently, the total number of instantaneous conflicts can be estimated by scaling the *number of combinations of two aircraft* with the *average probability of conflict between any two aircraft*. This can be expressed in words as:

No. Inst. Conflicts =
No. of Combinations of Two Aircraft
×
Average Conflict Probability Between Any Two Aircraft

(3.1)

Here, different airspace designs can influence both the number of possible combinations of aircraft and the average conflict probability between any two aircraft.

In previous literature, this combinatorial characteristic, which is inherent to any system where all moving particles are equally likely to meet each other, has often been referred to as the 'gas model' since collisions between molecules in an ideal gas adhere to the same principle [98]. In the field of ATM, such models were first used to analyze the collision risk between adjacent routes of the North Atlantic track system [67, 99, 100]. Subsequently, they have also been used to investigate the safety of a wide variety of airspace types, including high altitude en route airways [101–103], low altitude terminal airspaces [69, 104–106], and for concepts that closely resemble unstructured and layered airspace concepts [66, 68, 70].

An important step in the derivation of a conflict model for a specific airspace design is the modeling of the *expected relative velocity* between aircraft, as this is needed to compute the average conflict probability between aircraft. Since aircraft move relative to each other in three-dimensional space, it is necessary to consider both the horizontal *and* vertical components of the relative velocity between aircraft. However, as most previous studies have only considered interactions between cruising aircraft, they have only presented models for the horizontal component of the expected relative velocity. Although a few studies have included climbing/descending traffic, they have done so by assuming a uniform distribution of flight-path angles, without adequate explanations for the distribution shape or the range of values selected [68, 69]. Moreover, a uniform distribution of flight-path angles is not a reasonable assumption for en route airspace design, the focus of this chapter. This is particularly the case for layered airspace designs which require aircraft to maintain fixed altitudes while cruising, see section 3.2.3. Consequently, the distribution of flight-path angles can be skewed, and depends on the proportion of aircraft in different flight phases.

Building on our earlier work [70], this chapter extends previous research on conflict count modeling, by developing analytical models for both the horizontal *and* vertical components of the expected relative velocity. While the derivation of the former is comparable to that in previous literature, a grouping of aircraft flight segments into climbing, cruising and descending phases is used in this chapter for the vertical direction. Consequently, the models derived here compute the total three-dimensional conflict probability as a function of the proportion of aircraft in different flight phases. This makes it possible to study how the proportion of cruising aircraft affects safety, or equally how the proportion of climbing/descending traffic affects safety. Conflicts involving climbing/descending aircraft are of particular interest to layered airspace designs, where constraints are imposed to only reduce conflicts between cruising aircraft.

In addition to extending the models to three dimensions, this chapter also presents extensive fast-time simulation experiments to test model accuracy for a wide variety of conditions. This includes an investigation of an assumption made during the derivation process regarding the speed distribution of aircraft. Additionally, it is also

shown how a numerical method can be used to augment the analytical models to further improve accuracy for cases where the speed distribution of aircraft violates modeling simplifications.

3.3. Modeling Conflict Probability

The goal of this section is to derive conflict probability expressions for direct-routing airspace concepts, such as unstructured and layered airspace designs, as a function of conflict detection parameters. Here, the conflict probability of an airspace design is defined as the likelihood that two randomly selected aircraft are in conflict, i.e., the likelihood that the trajectories of two arbitrary aircraft are predicted to be closer than the prescribed separation requirements within the conflict detection look-ahead time. Although the main contribution of this study is on the development of 3D conflict probability models, this section begins by considering the 2D case. This is because the 2D model is directly required to estimate conflict counts between cruising aircraft in layered airspaces. The 3D model is subsequently derived as an extension of the 2D case.

3.3.1. Conflict Probability for 2D Airspace

In 2D airspace, aircraft motion is restricted to the horizontal plane. Thus, aircraft velocities are purely horizontal, and all conflicts are between cruising aircraft.

Previous studies have proposed that the conflict probability between any two aircraft in 2D airspace, p_{2d}, can be computed by comparing the instantaneous *area searched* for conflicts by an aircraft, A_c, to the *total airspace area* under consideration, A_{total}; see Figure 3.4. Here it can be seen that A_c is approximated as a rectangular 'conflict search area', and its size is defined by the conflict detection look-ahead time, t_l, the horizontal separation requirement, S_h, and the expected horizontal relative velocity between aircraft, $\mathbf{E}(V_{r,h})$. Since a conflict is detected if the trajectory of another aircraft is predicted to pass through A_c, p_{2d} can be expressed as [69, 104, 106]:
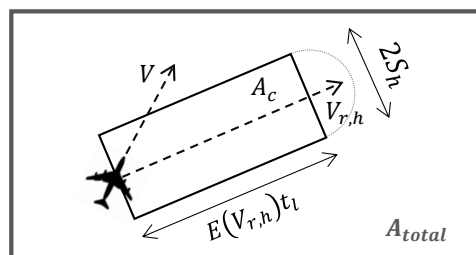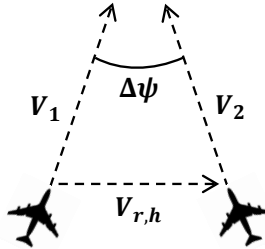
Figure 3.4: Area searched for conflicts, A_c, in 2D airspace. Here, A_{total} is the total airspace area under consideration.

Figure 3.5: The geometric relationships between velocity, V, relative velocity, V_r, and heading difference $\Delta\psi$ for two arbitrary aircraft

$$p_{2d} = \frac{A_c}{A_{total}} = \frac{2\,S_h\,\mathbf{E}\left(V_{r,h}\right)\,t_l}{A_{total}} \tag{3.2}$$

To arrive at a fully analytical expression for p_{2d}, it is necessary to quantify $\mathbf{E}\left(V_{r,h}\right)$. Because the goal of the derivation process is to determine the average conflict probability between a population of aircraft for a given airspace design, and not just between two specific flights, the *expected* horizontal relative velocity is used. More specifically, $\mathbf{E}\left(V_{r,h}\right)$ can be thought of as the weighted average of the horizontal relative velocities between *all* aircraft pairs (not just the conflicting pairs), given the aircraft speed and heading difference distributions in the airspace area of interest.

Nonetheless, to compute $\mathbf{E}\left(V_{r,h}\right)$, it is still useful to first consider the magnitude of the horizontal relative velocity between an arbitrary pair of aircraft, $V_{r,h}$; see Figure 3.5. Using the cosine rule, $V_{r,h}$ can be computed as:

$$V_{r,h} = \left(V_1^2 + V_2^2 - 2V_1 V_2 \cos\left(\Delta\psi\right)\right)^{1/2} \tag{3.3}$$

Here, V_1 and V_2 are the velocity magnitudes of the two aircraft pictured in Figure 3.5, and $\Delta\psi$ is the heading difference between these two arbitrary aircraft. Because the values of these variables can be different for every aircraft pair in the airspace, it is necessary to integrate equation 3.3 over all possible values of velocity and heading difference to compute $\mathbf{E}\left(V_{r,h}\right)$, while taking into account the probability density functions of velocity magnitudes and heading differences, $P\left(V_1\right)$, $P\left(V_2\right)$ and $P\left(\Delta\psi\right)$:

$$\mathbf{E}\left(V_{r,h}\right) = \int_{V_1} \int_{V_2} \int_0^\alpha \left(V_1^2 + V_2^2 - 2V_1 V_2 \cos\left(\Delta\psi\right)\right)^{1/2} P\left(\Delta\psi\right) P\left(V_1\right) P\left(V_2\right)\,d\Delta\psi\,dV_1\,dV_2$$
$$\tag{3.4}$$

In the above equation, α represents the maximum possible heading difference between any two cruising aircraft. Due to the complexity of equation 3.4, it can only be solved numerically [69]. However, an analytical solution is possible if all aircraft are assumed to have equal velocity magnitudes, i.e., if $V_1 = V_2 = V_o$. Under this assumption, the geometry between V_1, V_2 and $V_{r,h}$ in Figure 3.5 becomes an isosceles triangle. Thus, it is possible to rewrite equation 3.3 as:

$$V_{r,h} = 2 \, V_o \, \sin\left(\frac{|\Delta\psi|}{2}\right) \tag{3.5}$$

Since V_o is assumed to be a constant, the above simplified equation shows that $V_{r,h}$ is only dependent on the absolute heading difference between two aircraft, $|\Delta\psi|$. Therefore a simplified analytical expression for $\mathbf{E}\left(V_{r,h}\right)$ can be derived by integrating equation 3.5 for all possible $|\Delta\psi|$, while taking into account its probability density. In order to highlight the safety differences between unstructured and layered airspaces, traffic scenarios with a uniform distribution of aircraft headings between 0 and α are used in this work, since such scenarios have been shown in literature to maximize conflict counts [69]. For this type of scenario, the probability density function of the absolute heading difference, $P\left(|\Delta\psi|\right)$, takes on a triangular shape between 0 and α [107]:

$$P\left(|\Delta\psi|\right) = \frac{2}{\alpha}\left(1 - \frac{|\Delta\psi|}{\alpha}\right) \tag{3.6}$$

Using equations 3.5 and 3.6, a simplified expression for $\mathbf{E}\left(V_{r,h}\right)$ can be determined as [70]:

$$\begin{aligned}
\mathbf{E}\left(V_{r,h}\right) &= \int_0^\alpha 2V_o \sin\left(\frac{|\Delta\psi|}{2}\right) \cdot \frac{2}{\alpha}\left(1 - \frac{|\Delta\psi|}{\alpha}\right) \, d\,|\Delta\psi| \\
&= \frac{8V_o}{\alpha}\left(1 - \frac{2}{\alpha}\sin\frac{\alpha}{2}\right)
\end{aligned} \tag{3.7}$$

It should be noted that the above expression is only valid if all aircraft are assumed to have equal velocities. This assumption is used for all the analytical models derived in this chapter, and by all previous studies that have developed *analytical* conflict count models to analyze the safety of a particular airspace design, see section 3.2.4. Nevertheless, the sensitivity of this assumption on model accuracy is specifically analyzed by one of the fast-time simulation experiments performed in this work, see section 3.6.3.

3.3.2. Conflict Probability for 3D Airspace

In 3D en route airspace, cruising aircraft share the airspace with climbing and descending aircraft. Therefore in 3D, conflicts can occur between aircraft in different flight phases. Moreover, aircraft can have horizontal, as well as vertical velocity components.
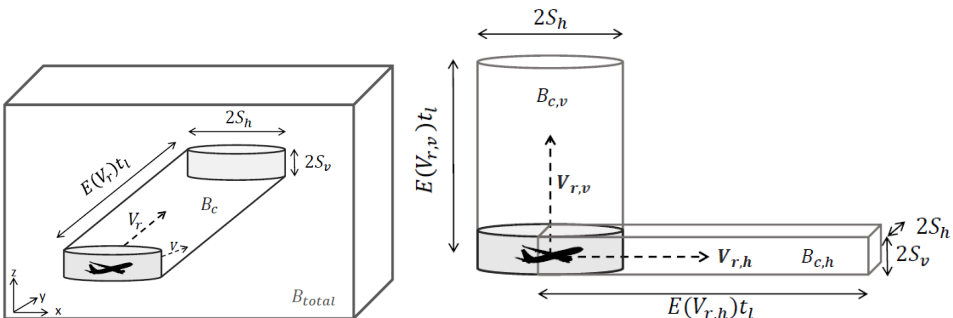
Analogous to the two-dimensional case, for 3D airspace, conflict probability can be defined as the ratio between the instantaneous *volume* of airspace searched for conflicts, B_c, and the total airspace volume under consideration B_{total}; see Figure 3.6(a). Furthermore, a conflict is defined to occur when the trajectory of another aircraft is predicted to pass through B_c, and its size is dependent on the conflict detection look-ahead time, t_l, the horizontal and vertical separation requirements, S_h and S_v, and the expected relative velocity, $\mathbf{E}(V_r)$.

It can be shown that volume B_c can be decomposed into two orthogonal components:

1. A horizontal cuboid, $B_{c,h}$, generated by the horizontal component of the expected relative velocity, $\mathbf{E}(V_{r,h})$

2. A vertical cylinder, $B_{c,v}$, generated by the vertical component of the expected relative velocity, $\mathbf{E}(V_{r,v})$

The horizontal and vertical components of B_c can be visualized in Figure 3.6(b). Because $B_c = B_{c,h} + B_{c,v}$, the total 3D conflict probability, p_{3d}, can be modeled as a summation of the horizontal and vertical 'volume searched' ratios:

$$p_{3d} = \frac{B_c}{B_{total}} = \frac{B_{c,h} + B_{c,v}}{B_{total}} = \frac{4\,S_h S_v\,\mathbf{E}(V_{r,h})\,t_l + \pi S_h^2\,\mathbf{E}(V_{r,v})\,t_l}{B_{total}} \quad (3.8)$$

(a) Volume searched for conflicts, B_c **(b) Horizontal and vertical components of volume searched for conflicts, $B_{c,h}$ and $B_{c,v}$**

Figure 3.6: Volume searched for conflicts by an aircraft, B_c, in 3D airspace. Here, B_{total} is the total volume of the airspace consideration. Note that $B_c = B_{c,h} + B_{c,v}$

To fully quantify p_{3d}, it is necessary to develop analytical formulations for the expected horizontal and vertical relative velocities. This is done in the following paragraphs.

3.3.2.1. Expected Horizontal Relative Velocity

To model the expected horizontal relative velocity in an airspace, $\mathbf{E}\left(V_{r,h}\right)$, it is first necessary to properly define what is meant as the 'horizontal velocity' of an aircraft, V_h; see Figure 3.7. This figure shows that V_h is a function of the of the total velocity of an aircraft, V, and its flight-path angle, γ :
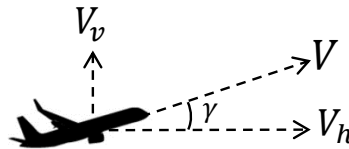
Figure 3.7: The flight path angle of an aircraft, γ, is defined in terms of its horizontal velocity, V_h, and its vertical velocity, V_v.

$$V_h = V \cos\left(\gamma\right) \tag{3.9}$$

As indicated previously, this chapter is concerned with modeling conflict counts for *en route* airspace. In en route airspace, aircraft generally climb/descend with flight-path angles less than six degrees. Based on the above equation, for such small angles, $V_h \approx V$. Therefore γ does *not* significantly affect V_h in en route airspace. For this reason, $V_{r,h}$ and $\mathbf{E}\left(V_{r,h}\right)$ can also be considered to be independent of γ in en route airspace. Thus, the expression for $\mathbf{E}\left(V_{r,h}\right)$ developed earlier for 2D en route airspace, given by equation 3.7, can also be used for 3D en route airspace.

It is important to note that the approach presented here to model $\mathbf{E}\left(V_{r,h}\right)$ is only applicable for small flight-path angles, as is the case in en route airspaces. For the rare cases where $\gamma >> 10^o$, it would be necessary to take γ into account when computing $\mathbf{E}\left(V_{r,h}\right)$. This would require a rewriting of equations 3.4 and 3.7 to include an additional integral that considers the probability density of γ when modeling $\mathbf{E}\left(V_{r,h}\right)$. However, as shown by the high model accuracy results in section 3.6, this added complexity is generally not required.

3.3.2.2. Expected Vertical Relative Velocity

Following a similar procedure to the horizontal direction, it is useful to first define the vertical velocity of an individual aircraft, V_v. Using Figure 3.7, V_v can be computed as:

$$V_v = V \sin\left(\gamma\right) \tag{3.10}$$

For small values of γ, as for en route airspace, the above equation can be simplified as $V_v \approx V\gamma$. Therefore, unlike the horizontal case, V_v is dependent on γ. If all aircraft are assumed to have equal total velocities, i.e., if $V = V_o$, then the magnitude of the vertical relative velocity between two arbitrary aircraft, $V_{r,v}$, is dependent on the flight path angles of each aircraft, γ_1 and γ_2:

$$V_{r,v} = |V_o \sin(\gamma_2) - V_o \sin(\gamma_1)| \tag{3.11}$$

Because the values of γ_1 and γ_2 can be different for every aircraft pair, to compute the expected vertical relative velocity, $\mathbf{E}\left(V_{r,v}\right)$, it is necessary to integrate equation 3.11 for all possible values of γ_1 and γ_2, while taking into account the probability density function of the flight path angles of each aircraft, $P\left(\gamma_1\right)$ and $P\left(\gamma_2\right)$:

$$\mathbf{E}\left(V_{r,v}\right) = \int_{\gamma_1} \int_{\gamma_2} |V_o \sin(\gamma_2) - V_o \sin(\gamma_1)| \; P\left(\gamma_1\right) P\left(\gamma_2\right) \; d\gamma_1 \, d\gamma_2 \tag{3.12}$$

To develop an analytical model for $\mathbf{E}\left(V_{r,v}\right)$, the following simplification is made in this chapter. In en route airspace, an aircraft can be considered to be either cruising or climbing or descending. Cruising aircraft generally fly with $\gamma_{cruise} \approx 0^o$. Furthermore, it is reasonable to assume a constant and equal $|\gamma|$ for all climbing and descending aircraft. Therefore, it is assumed that γ takes one of the following three values in en route airspace:

$$\gamma = \begin{cases} 0 & \text{for cruising aircraft} \\ +\gamma_{cd} & \text{for climbing aircraft} \\ -\gamma_{cd} & \text{for descending aircraft} \end{cases} \tag{3.13}$$

Using the above simplification, it is possible to rewrite equation 3.12 into its discretized form:

$$\mathbf{E}\left(V_{r,v}\right) = \sum_{\gamma_1} \sum_{\gamma_2} |V_o \sin(\gamma_2) - V_o \sin(\gamma_1)| \; P\left(\gamma_1\right) P\left(\gamma_2\right) \tag{3.14}$$

To utilize equation 3.14, it is necessary to determine discretized values for $V_{r,v}$ and $P\left(\gamma_1\right) \cdot P\left(\gamma_2\right)$. Discretized values of $V_{r,v}$ can be computed by evaluating equation 3.11 for all flight phase combinations of two arbitrary aircraft, see Table 3.1. This table shows that $V_{r,v}$ is zero when both aircraft have the same flight path angle, and that $V_{r,v}$ is highest when the two aircraft are flying with opposite flight path angles, as expected.

Discretized values for $P\left(\gamma_1\right) \cdot P\left(\gamma_2\right)$ can be computed by noting that the discretized probability distribution of γ is equivalent to the proportion of aircraft in cursing,

Table 3.1: Discretized vertical relative velocity, $\mathbf{V}_{r,v}$

AC 1 \ AC 2	Cruising	Climbing	Descending
Cruising	0	$V_o \sin(\gamma_{cd})$	$V_o \sin(\gamma_{cd})$
Climbing	$V_o \sin(\gamma_{cd})$	0	$2V_o \sin(\gamma_{cd})$
Descending	$V_o \sin(\gamma_{cd})$	$2V_o \sin(\gamma_{cd})$	0

climbing and descending flight phases. To this end, let ε be the proportion of cruising aircraft:

$$\varepsilon = \frac{N_{cruise}}{N_{total}} \tag{3.15}$$

Here, N_{cruise} is the number of instantaneous cruising aircraft, and N_{total} is the total number of instantaneous aircraft. Using ε, the proportion of climbing or descending aircraft can calculated be as $1 - \varepsilon$, and the probability of selecting two cruising aircraft at random is ε^2. Using this approach, the discretized values for $P(\gamma_1) \cdot P(\gamma_2)$ can be computed for all flight phase combinations of two arbitrary aircraft, see Table 3.2. Because this table represents a discrete probability density function, summation of the cells lead to a value of 1. Moreover, the table is symmetric along the leading diagonal as it assumes equal numbers of climbing and descending aircraft, which was in turn used to simplify the design of the simulation experiments, see section 3.5. However, the method described here can also be applied when this assumption is not true, as long as the proportion of aircraft in different flight phases are known.

Table 3.2: Discretized flight-path angle probability density distribution, $\mathbf{P}(\gamma_1) \cdot \mathbf{P}(\gamma_2)$

AC 1 \ AC 2	Cruising	Climbing	Descending
Cruising	ε^2	$\frac{\varepsilon - \varepsilon^2}{2}$	$\frac{\varepsilon - \varepsilon^2}{2}$
Climbing	$\frac{\varepsilon - \varepsilon^2}{2}$	$\frac{(1-\varepsilon)^2}{4}$	$\frac{(1-\varepsilon)^2}{4}$
Descending	$\frac{\varepsilon - \varepsilon^2}{2}$	$\frac{(1-\varepsilon)^2}{4}$	$\frac{(1-\varepsilon)^2}{4}$

Using equation 3.14 and the discretized values for $V_{r,v}$ and $P(\gamma_1) \cdot P(\gamma_2)$ in Tables 3.1 and 3.2, respectively, $\mathbf{E}(V_{r,v})$ can be computed. In essence, this involves an element-wise multiplication of the appropriate cells of Tables 3.1 and 3.2, followed by a summation of the resulting expressions. Since this process has to take into account the allowed flight phase combinations of interacting aircraft, the resulting $\mathbf{E}(V_{r,v})$ expressions are different for unstructured and layered airspace de-

signs; the corresponding equations are derived in sections 3.4.1 and 3.4.2, respectively.

3.4. Modeling Conflict Counts

This section presents the derivation of conflict count models for unstructured and layered airspace concepts. These derivations make use of the 2D and 3D conflict probability models developed in the previous section, and are adaptations of the generic conflict count model given by equation 3.1.

3.4.1. Unstructured Airspace

As indicated by equation 3.1, the number of instantaneous conflicts for Unstructured Airspace (UA), C_{ua}, can be modeled as the product of two factors, namely the *number of combinations of two aircraft*, and the *conflict probability between any two aircraft*. Because UA imposes no constraints on aircraft motion, an aircraft can conflict with any other aircraft in the airspace, regardless of the flight phase of either aircraft. Therefore, the total number of combinations of two aircraft can be expressed using the binomial coefficient, $\binom{N_{total}}{2}$, leading to the following model structure for C_{ua}:

$$C_{ua} = \binom{N_{total}}{2} p_{ua} = \frac{N_{total}\,(N_{total} - 1)}{2}\, p_{ua} \tag{3.16}$$

Here, N_{total} is the total number of instantaneous aircraft present in the volume of airspace under consideration. The conflict probability between any two aircraft, p_{ua}, scales the number of combinations of two aircraft such that only aircraft pairs that have intersecting trajectories within detection range are counted as conflicts. A model for conflict probability in 3D airspaces has been derived in section 3.3.2. It is repeated below for convenience, and uses the geometrical parameters defined in Figure 3.6:

$$p_{ua} = \frac{4\,S_h S_v\,\mathbf{E}\left(V_{r,h}\right) t_l + \pi S_h^2\,\mathbf{E}\left(V_{r,v}\right) t_l}{B_{total}} \tag{3.8}$$

To evaluate the above equation, expressions for the expected horizontal and vertical relative velocities between aircraft in UA, $\mathbf{E}\left(V_{r,h}\right)_{ua}$ and $\mathbf{E}\left(V_{r,v}\right)_{ua}$, are needed. Equation 3.7 shows that $\mathbf{E}\left(V_{r,h}\right)_{ua}$ is dependent on α, the maximum possible heading difference between two arbitrary aircraft. Since aircraft have complete route selection freedom in UA, conflicts can occur between aircraft flying in any direction. Thus for UA, $\alpha = 360^o = 2\pi$. Substitution of this value into equation 3.7 yields the following expression for $\mathbf{E}\left(V_{r,h}\right)_{ua}$:

$$\mathbf{E}\left(V_{r,h}\right)_{ua} = \frac{4V_o}{\pi} \tag{3.17}$$

Here, V_o is the assumed equal velocity of all aircraft in the airspace. As mentioned before, the effect of this assumption on model accuracy is analyzed using fast-time simulations, see section 3.6.3.

In the vertical direction, equation 3.14 can be used to compute $\mathbf{E}\left(V_{r,v}\right)_{ua}$. To use equation 3.14, expressions for the discretized vertical relative velocity, and the discretized flight-path angle probability density distribution, listed in Tables 3.1 and 3.2, respectively, are needed. Since the probability of conflict is independent of flight phase in UA, the expressions for all flight phases in Tables 3.1 and 3.2 should be used when evaluating equation 3.14. This results in the following for UA:

$$\begin{aligned}
\mathbf{E}\left(V_{r,v}\right)_{ua} &= 4\left(V_o \sin\left(\gamma_{cd}\right) \frac{\varepsilon - \varepsilon^2}{2}\right) + 2\left(2V_o \sin\left(\gamma_{cd}\right) \frac{(1-\varepsilon)^2}{4}\right) \\
&= V_o \sin\left(\gamma_{cd}\right)\left(1 - \varepsilon^2\right)
\end{aligned} \tag{3.18}$$

Here, γ_{cd} is the flight-path angle of climbing/descending traffic, and ε is the proportion of cruising aircraft in the airspace. Finally, the number of instantaneous conflicts for UA can be obtained by substituting equations 3.17 and 3.18 into equation 3.8, and then substituting the result into equation 3.16:

$$C_{ua,3d} = \frac{N_{total}\left(N_{total} - 1\right)}{2}\left(\frac{16\, S_h S_v V_o t_l + \pi^2 S_h^2 V_o t_l \sin\left(\gamma_{cd}\right)\left(1 - \varepsilon^2\right)}{\pi\, B_{total}}\right) \tag{3.19}$$

3.4.2. Layered Airspace

The structure of the Layers concept reduces the number of conflicts between cruising aircraft. However, there are no procedural mechanisms to separate cruising aircraft from climbing and descending traffic. Therefore, the conflict count model for layered airspaces needs to be split into three distinct parts based on the flight phase combinations of interacting aircraft:

$$C_{lay} = C_{cruise} + C_{cruise-cd} + C_{cd} \tag{3.20}$$

Here, C_{cruise} is the number of conflicts between cruising aircraft, $C_{cruise-cd}$ is the number of conflicts between cruising and climbing/descending aircraft, and C_{cd} is the number of conflicts between climbing/descending traffic. Each of these three conflict types are discussed in the paragraphs that follow.

3.4.2.1. Conflicts Between Cruising Aircraft

The number of instantaneous conflicts between cruising aircraft in the Layers concept can be modeled by taking into account the two aspects that differentiate layered airspaces from UA; the reduction of the number of possible conflict pairs, and the reduction of the relative velocity between cruising aircraft.

Conflict Pair Reduction

Since the vertical spacing between the predefined flight levels of the Layers concept is by definition at least equal to the vertical separation requirement, cruising aircraft at different altitude bands can not conflict with each other. This in turn reduces the number of possible conflict pairs for cruising aircraft. It also means that the conflict probability between cruising aircraft, p_{cruise}, is equal for all cruising flight levels. Thus, in a single flight level j, the number of conflicts between cruising aircraft, $C_{cruise,j}$, can be expressed as:

$$C_{cruise,j} = \frac{N_{cruise,j} \left(N_{cruise,j} - 1 \right)}{2} \, p_{cruise} \tag{3.21}$$

Here, $N_{cruise,j}$ is the number of cruising aircraft in flight level j. By summing equation 3.21 over all available flight levels, L, the total number of instantaneous cruising conflicts can be computed as:

$$C_{cruise} = \sum_{j}^{L} \frac{N_{cruise,j} \left(N_{cruise,j} - 1 \right)}{2} \, p_{cruise} \tag{3.22}$$

If cruising aircraft are uniformly distributed over all altitude bands, then $N_{cruise,j} = N_{cruise}/L$. This would be the case for layered airspaces if aircraft headings are also uniformly distributed, as for the traffic patterns considered in this work. In case of an uneven distribution of aircraft headings, a uniform vertical distribution of traffic can still be achieved by assigning multiple flight levels for the heading ranges with high demand. Using this assumption, equation 3.22 can be simplified to:

$$C_{cruise} = \frac{N_{cruise} \left(\frac{N_{cruise}}{L} - 1 \right)}{2} \, p_{cruise} \tag{3.23}$$

From the above equation, it can be concluded that increasing L increases the intrinsic safety offered by layered concepts to cruising aircraft. This is because higher values of L reduce the number of possible combinations of cruising aircraft pairs that can interact with each other.

Relative Velocity Reduction

As aircraft in the Layers concept are 'sorted' into different altitude bands based on their heading, the second beneficial effect of the Layers concept is the reduction of

the expected horizontal relative velocities between cruising aircraft, $\mathbf{E}\left(V_{r,h}\right)_{cruise}$. A reduction of $\mathbf{E}\left(V_{r,h}\right)_{cruise}$ leads to a reduction of p_{cruise}, which in turn increases safety. Since cruising aircraft are constrained to the horizontal plane, the 2D conflict probability model derived in section 3.3.1 can be used for p_{cruise} and $\mathbf{E}\left(V_{r,h}\right)_{cruise}$. They are restated below for convenience, and use the geometrical parameters defined in Figure 3.4:

$$p_{cruise} = \frac{2 \, S_h \, \mathbf{E}\left(V_{r,h}\right)_{cruise} \, t_l}{A_{total}} \tag{3.2}$$

$$\mathbf{E}\left(V_{r,h}\right)_{cruise} = \frac{8V_o}{\alpha}\left(1 - \frac{2}{\alpha}\sin\frac{\alpha}{2}\right) \tag{3.7}$$

Equation 3.7 shows that $\mathbf{E}\left(V_{r,h}\right)_{cruise}$ is a function of the heading range permitted per altitude band, α. As indicated in section 3.2.3, α is a design parameter for layered airspaces. To gain a sense of the effect of α on the safety of the Layers concept, equation 3.7 is plotted in Figure 3.8. Here it can be seen that the horizontal relative velocity varies non-linearly with α due to the $\sin\frac{\alpha}{2}$ term in equation 3.7. Furthermore, the figure shows that $\mathbf{E}\left(V_{r,h}\right)_{cruise}$ is lower for layered concepts with smaller values of α. Since reducing $\mathbf{E}\left(V_{r,h}\right)_{cruise}$ decreases p_{cruise}, reducing α is hypothesized to increase the intrinsic safety of layered concepts.
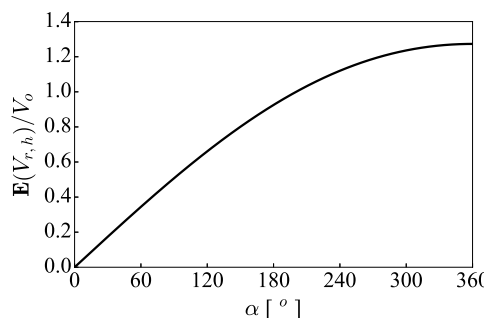
Figure 3.8: Hypothesized relationship between the expected horizontal relative velocity, $\mathbf{E}\left(V_{r,h}\right)$, and heading range per flight level, α

Substituting equations 3.2 and 3.7 into equation 3.23 leads to the following expression for the number of instantaneous conflicts between cruising aircraft in layered airspaces:

$$C_{cruise} = N_{cruise}\left(\frac{N_{cruise}}{L} - 1\right)\left(\frac{8\,S_h\,V_o\,t_l}{\alpha\,A_{total}}\right)\left(1 - \frac{2}{\alpha}\sin\frac{\alpha}{2}\right) \tag{3.24}$$

3.4.2.2. Conflicts Between Cruising and Climbing/Descending Aircraft

Because the Layers concept imposes no procedural constraints to prevent conflicts between cruising and climbing/descending traffic, the model for $C_{cruise-cd}$ is very similar to the model developed for UA, except for two minor differences:

1. The number of combinations of cruising and climbing/descending aircraft is $N_{cruise}\, N_{cd}$. This is because an aircraft can not be cruising and climbing/descending at the same time.

2. Since only cruising-climbing/descending conflicts are considered, the calculation of the expected vertical relative velocity, $\mathbf{E}\left(V_{r,v}\right)_{cruise-cd}$, should only consider cases where one aircraft is cruising, while the other is climbing/descending. This can be achieved by evaluating equation 3.14 for the four cases in Tables 3.1 and 3.2 where one aircraft is cruising, and the other is climbing/descending.

Application of these changes to the UA model leads to the following expressions for $C_{cruise-cd}$. These equations make use of the geometrical parameters displayed in Figure 3.6:

$$
C_{cruise-cd} \;=\; N_{cruise}\, N_{cd}\, p_{cruise-cd} \tag{3.25a}
$$

$$
p_{cruise-cd} \;=\; \frac{4\, S_h S_v\, \mathbf{E}\left(V_{r,h}\right)_{cruise-cd} t_l + \pi S_h^2\, \mathbf{E}\left(V_{r,v}\right)_{cruise-cd} t_l}{B_{total}} \tag{3.25b}
$$

$$
\mathbf{E}\left(V_{r,h}\right)_{cruise-cd} \;=\; \frac{4V_o}{\pi} \tag{3.25c}
$$

$$
\mathbf{E}\left(V_{r,v}\right)_{cruise-cd} \;=\; 4\left(V_o \sin\left(\gamma_{cd}\right)\frac{\varepsilon - \varepsilon^2}{2}\right) = 2V_o \sin\left(\gamma_{cd}\right)\left(\varepsilon - \varepsilon^2\right) \tag{3.25d}
$$

3.4.2.3. Conflicts Between Climbing/Descending Aircraft

The model describing the number of instantaneous conflicts between climbing/descending traffic, C_{cd}, is also remarkably similar to that derived earlier for UA. In this case, the only difference is in the computation of the expected vertical relative velocity between climbing/descending aircraft, $\mathbf{E}\left(V_{r,v}\right)_{cd}$. An expression for $\mathbf{E}\left(V_{r,v}\right)_{cd}$ can be obtained by applying equation 3.14 for the four cases in Tables 3.1 and 3.2 where both interacting aircraft are climbing/descending. This approach leads to

the following for expressions for C_{cd}. These equations make use of the geometrical parameters displayed in Figure 3.6:

$$C_{cd} = \frac{N_{cd}\,(N_{cd}-1)}{2}\,p_{cd} \tag{3.26a}$$

$$p_{cd} = \frac{4\,S_h S_v\,\mathbf{E}\left(V_{r,h}\right)_{cd} t_l + \pi S_h^2\,\mathbf{E}\left(V_{r,v}\right)_{cd} t_l}{B_{total}} \tag{3.26b}$$

$$\mathbf{E}\left(V_{r,h}\right)_{cd} = \frac{4V_o}{\pi} \tag{3.26c}$$

$$\mathbf{E}\left(V_{r,v}\right)_{cd} = 2\left(2V_o \sin\left(\gamma_{cd}\right)\frac{(1-\varepsilon)^2}{4}\right) = V_o \sin\left(\gamma_{cd}\right)(1-\varepsilon)^2 \tag{3.26d}$$

3.5. Fast-Time Simulation Design

To test the accuracy of the conflict count models developed in this work, three fast-time simulation experiments, named the 'primary experiment' the 'flight-path angle experiment' and the 'ground speed experiment', were performed. This section describes the design of these three experiments.

3.5.1. Simulation Development

3.5.1.1. Simulation Platform

The BlueSky open-source ATM simulator was used as the simulation platform in this research. It was developed at the Delft University of Technology (TU Delft) using the Python programming language. BlueSky has numerous features including the ability to simulate more than 5000 aircraft simultaneously, a suite of conflict detection and resolution algorithms, and extensive data logging functions. A complete overview of BlueSky is provided in [108].

In order to simulate aircraft performance dynamics, BlueSky uses point-mass Aircraft Performance Models (APMs) that are similar in structure to Eurocontrol's well known Base of Aircraft Data (BADA) models. The main difference between these two approaches is that BlueSky uses openly available data to quantify the APMS. To simplify the simulations, all traffic was simulated using a Boeing 744 model. A full description of the BlueSky APMs, including their validation, can be found in [109].

BlueSky uses a simulated Flight Management System (FMS) to provide horizontal and vertical navigation capabilities, as well as for aircraft speed control. Similar to real aircraft, the simulated FMS tries to fly an aircraft at the requested Calibrated Airspeed (CAS) or Mach number, if that is within the performance capabilities of the aircraft type, which is in turn specified in the APMs for different parts of the

flight envelope. Additionally, speed/heading changes occur while respecting the acceleration capabilities of aircraft.

3.5.1.2. Conflict Detection

In this study, the so called 'state-based' conflict detection method was used. This method predicts separation violations by linearly extrapolating aircraft positions over a predefined look-ahead time. Here, a look-ahead time of 5 minutes, as well as separation requirements of 5 nautical miles horizontally and 1000 ft vertically, were used.

As mentioned in section 3.2.4, the models derived in this chapter are concerned with the intrinsic safety provided by unstructured and layered airspace designs. Since the notion of intrinsic safety focuses on the number of *truly occurring* conflicts as a function of airspace design, conflict detection was performed assuming perfect knowledge of aircraft states. For the same reason, the simulations were performed without tactical conflict resolutions.

3.5.1.3. Airspace Concepts and Concept Implementation

Unstructured Airspace (UA) and four layered airspace concepts, each with a different allowed heading range per flight level, α, were used in the fast-time simulations. Table 3.3 displays the properties of the considered airspace concepts, and also indicates which concepts were used in each of the three experiments performed in this study.

Table 3.3: Properties of the airspace concepts used in the three simulation experiments

Symbol	Name	Heading Range Per Layer, α	Number of Layer Sets, κ
UA	Unstructured Airspace	-	-
L360	Layers 360	360°	8
L180	Layers 180	180°	4
L90	Layers 90	90°	2
L45	Layers 45	45°	1

The airspace concepts were implemented into BlueSky by modifying its trajectory planning functions. While direct horizontal routes were used in both unstructured and layered airspaces, the method used to determine the cruising altitude of an aircraft differed between the two airspace designs. For UA, the cruising altitude of an aircraft, $Z_{ua,i}$, was directly proportional to its trip distance, D_i:

$$Z_{ua,i} = Z_{min} + \frac{Z_{max} - Z_{min}}{D_{max} - D_{min}} \ (D_i - D_{min}) \tag{3.27}$$

Here, Z_{min} and Z_{max} are the minimum and maximum altitudes allowed for cruising aircraft in the simulation. Comparably, D_{min} and D_{max} are the minimum and maximum trip distances of aircraft in the simulation. Since traffic scenarios with a uniform distribution of trip distances were used, equation 3.27 resulted in a uniform vertical distribution of traffic.

On the other hand, for the Layers concept, the cruising altitude of an aircraft, $Z_{lay,i}$, depends on both its heading, ψ_i, and its trip distance, D_i, as indicated by the following heading-altitude rule:

$$Z_{lay,i} = Z_{min} + \zeta \left[\left\lfloor \frac{D_i - D_{min}}{D_{max} - D_{min}} \kappa \right\rfloor \beta + \left\lfloor \frac{\psi_i}{\alpha} \right\rfloor \right] \tag{3.28}$$

Here, β is the number of flight levels needed to define one complete set of layers, and κ is the number of complete layer sets. These two parameters are defined as $\beta = 360^o/\alpha$ and $\kappa = L/\beta$, where L is the total number of available flight levels. Note that the second term of equation 3.28 computes the cruising altitude of an aircraft as an *integer multiple* of the vertical spacing between flight levels, ζ, using the the floor operator ('$\lfloor$ $\rfloor$'). For all layered concepts in this study, $\zeta = 1100$ ft and $L = 8$. Correspondingly, for most layered concepts, $\kappa > 1$; see Table 3.3. For layered concepts with $\kappa > 1$, equation 3.28 uses trip distances to determine cruising altitudes such that short flights remain at lower altitudes, while longer flights use higher layer sets. This property, combined with traffic scenarios with a uniform distribution of trip distances and travel directions, resulted in a uniform of distribution of cruising aircraft over the eight predefined flight levels used by all layered concepts.

It should be noted that the only difference between the UA and L360 concepts is the use of predefined flight levels for cruising aircraft in L360, while any altitude could be selected by aircraft in UA. In fact, the L360 concept was specifically included in the simulations to investigate the effect of using fixed cruising flight levels while simultaneously allowing all possible headings in each flight level on intrinsic airspace safety.

3.5.2. Traffic Scenarios

3.5.2.1. Testing Region and Flight Profiles

A large three-dimensional en route sector was used as the physical environment for traffic simulations; see Figure 3.9. In the vertical dimension, the sector is divided into two parts; a 'transition zone' with a height of 4000 ft for climbing and descending traffic, and a 'cruising zone' with a height of 7700 ft. The eight predefined cruising flight levels for layered airspace concepts were within the latter zone (not shown).

In the horizontal plane, the sector had a square-shaped cross-section of 400 x 400 NM, and was divided into separate 'simulation' and 'experiment' regions; see
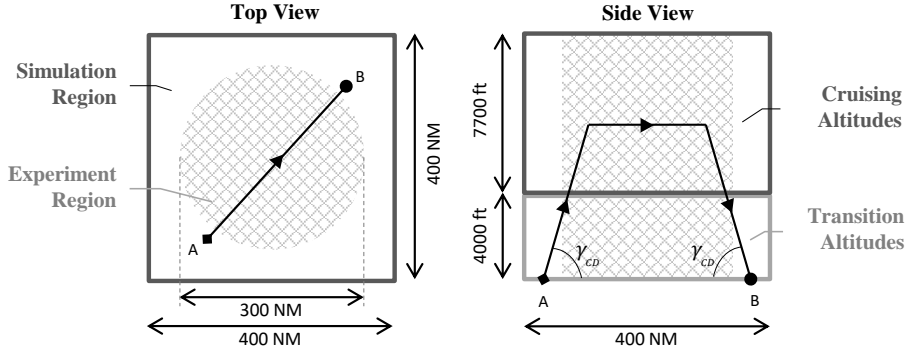
Figure 3.9: Top and side views of the simulation's physical environment. The trajectory of an example flight is shown.

Table 3.4: Common simulation parameters for all three experiments

Parameter	Value	Description
A_{total}	$7.0685 \cdot 10^4$ NM²	Area of 'experiment region'
B_{total}	$3.0533 \cdot 10^{16}$ ft ³	Volume of 'experiment region'
D_{min}	200 NM	Minimum trip distance
D_{max}	250 NM	Maximum trip distance
$\bar{D}$	225 NM	Average trip distance
t_l	5 mins	Conflict detection look-ahead time
S_h	5 NM	Horizontal separation requirement
S_v	1000 ft	Vertical separation requirement
L	8	Number of flight levels for layered airspaces
$\bar{V}$	400 kts	Average ground speed of aircraft

Figure 3.9. As no traffic was simulated outside the square sector, aircraft near the edges of the 'simulation region' were unlikely to interact with other traffic compared to flights near the center of the sector. To solve this issue, following the simulation design in [92], a smaller cylindrical 'experiment region', with a diameter of 300 NM, was defined at the center of the simulation region. The resulting gap between the experiment and simulation regions, which was sized such that it closely matched the length of the *horizontal volume of airspace searched for conflicts* by aircraft, see Figure 3.6(b), ensures that aircraft in the experiment region are surrounded by traffic in all directions. Correspondingly, only aircraft within the experiment region, and only conflicts with closest points of approach with the experiment region, were used to assess the accuracy of the models. The parameters of the experiment region needed to evaluate the models, as well as other parameters common to all three experiments, are listed in Table 3.4.

Figure 3.9 also shows the horizontal and vertical profiles of an example flight. Because the focus of this study is on en-route airspace design, take-off and landing

Table 3.5: Flight-path angle of climbing/descending aircraft (γ_{cd}) and proportion of cruising aircraft (ε) for the three experiments

Experiment	γ_{cd} [°]	ε
Primary	2.8	0.82
Flight-Path Angle	1.4	0.60
	2.8	0.82
	5.6	0.92
Ground Speed	2.8	0.82

Table 3.6: Aircraft ground speed distributions for the three experiments

Experiment	Distribution	Value [kts]
Primary	Equal	400.0
Flight-Path Angle	Equal	400.0
Ground Speed	Equal	400.0
	Normal	$\mathcal{N}(400.0,\ 16.7^2)$
	Uniform	$\mathcal{U}(350.0,\ 450.0)$

flight phases were not considered. Instead, aircraft entered the simulation at random sector entry-points located on the lower boundary of the 'transition zone'. Subsequently, they climbed to their assigned altitude in the 'cruising zone'. The specific cruising altitude of an aircraft depended on the airspace concept, and can be calculated using equations 3.27 and 3.28 for unstructured and layered airspaces, respectively. At a predetermined distance from their destination (which depended on the cruising altitude), aircraft began their descent. As aircraft descended through arbitrary sector exit-points on the lower boundary of the transition zone, they were deleted from the simulation.

It should be noted that all aircraft climbed/descended with equal flight-path angles, see Table 3.5 for the values used for each experiment. Furthermore, each aircraft maintained a constant ground speed during its flight. The speed distribution of aircraft for the three experiments is listed in Table 3.6.

3.5.2.2. Scenario Generation

A scenario generator was created to produce traffic scenarios with a desired and constant traffic density. Constant density scenarios were used so that the number of instantaneous conflicts logged during a simulation run could be attributed to a particular traffic density. Since aircraft were deleted from the simulation as they exited the sector, to realize constant density scenarios, aircraft were introduced into the simulation at a constant spawn rate equal to $\frac{\bar{V}}{\bar{D}} N$, where $\bar{V}$ is the average speed of aircraft, $\bar{D}$ is the average trip distance of aircraft, and N is the desired number of instantaneous aircraft. Using this approach, ten traffic demand scenarios of

Table 3.7: Number of instantaneous aircraft for the 10 traffic demand scenarios

#	Simulation Region	Experiment Region
1	80.0	58.3
2	111.6	81.5
3	155.7	112.2
4	217.2	158.7
5	302.9	218.4
6	422.6	304.9
7	589.4	422.3
8	822.2	588.1
9	1147.0	810.1
10	1600.0	1116.8

3

increasing density were defined, ranging between 5-100 aircraft per 10,000 NM^2 in the simulation region. This corresponds to an instantaneous traffic demand of between 80-1600 aircraft in the simulation region; see Table 3.7. Note that this table displays the number of instantaneous aircraft in both the 'simulation' and 'experiment' regions.

In addition to constant densities, scenarios had a uniform distribution of trip distances and aircraft headings. As explained previously, uniform distance distributions were required to ensure a uniform vertical distribution of traffic. Uniform heading distributions were used to maximize the number of instantaneous conflicts [69], thereby making it easier to understand the safety differences between unstructured and layered airspaces.

The horizontal routes for aircraft were selected such that these two requirements were met. This process began by randomly selecting the sector entry-point of an aircraft as any latitude-longitude combination within the simulation region. Subsequently, two uniform random number generators are used to output random values for the heading, ψ_i, and trip distance, D_i, of an aircraft. The sector exit-point of that aircraft is then determined as the end-point of of a straight line with length D_i and a bearing ψ_i from the entry-point. If the corresponding exit-point is outside the simulation region, it is discarded, and the above process is repeated until the entry- and exit-points for all aircraft are inside the simulation region.

It should be noted that all scenarios were generated off-line prior to the simulations. This ensured that all airspace concepts could be subjected to the same traffic demands and horizontal traffic patterns. Additionally, scenarios had a duration of 2 hrs, consisting of a 1 hour traffic volume buildup period, and a 1 hour logging period during which the traffic density was kept constant.

3.5.3. Independent Variables

Three separate experiments were performed. The independent variables of each experiment are discussed below.

3.5.3.1. Primary Experiment

The focus of the primary experiment was to validate the conflict count models for under ideal conditions, and to investigate the effect of the allowed heading range per altitude band on the safety of layered concepts. The independent variables of this experiment were:

1. 5 airspace concepts, see Table 3.3

2. 10 traffic demand scenarios, see Table 3.7

For each traffic demand scenario, ten repetitions were performed using different traffic realizations (i.e., different initial conditions). This resulted in a total of 500 simulation runs, involving over 950,000 flights.

3.5.3.2. Flight-Path Angle Experiment

The flight-path angle of climbing and descending traffic, γ_{cd}, is an important parameter that affects the proportion of aircraft in different flight phases, see section 3.3.2. Hence, an experiment was performed to test conflict count model accuracies for different values of γ_{cd}. The independent variables of this experiment were:

1. 2 airspace concepts, namely UA and L45, see Table 3.3

2. 10 traffic demand scenarios, see Table 3.7

3. 3 γ_{cd} settings, see Table 3.5

Ten repetitions were performed for each traffic demand condition. Therefore, a total of 600 simulations runs were performed for this experiment, using over 1.15 million flights.

3.5.3.3. Ground Speed Experiment

Since all aircraft were assumed to fly with equal ground speeds by the model derivations, this final experiment considered the sensitivity of the models to this assumption. The independent variables of this experiment were:

1. 2 airspace concepts, namely UA and L45, see Table 3.3

2. 10 traffic demand scenarios, see Table 3.7

3. 3 ground speed distributions, see Table 3.6

As before, ten repetitions were performed for each traffic demand condition, resulting in a total of 600 simulation runs for this experiment, involving over 1.15 million flights.

3.5.4. Dependent Variables

To determine the accuracy of the conflict count models derived in this chapter, model predictions were compared to actual conflict counts logged during the simulations. Model accuracy was quantified by introducing a model accuracy parameter, k, as illustrated below for the basic conflict count model:

$$\text{No. of inst. conflicts} = \text{Gas Model} \times k$$

In essence, k is a constant model term that accounts for any factor that was not considered during model derivations. The value of k is determined by fitting the model (right side of above equation) to the conflict count data logged during the simulations (left side of above equation) in a least-square sense. If $k = 1$, then the models, as derived, are able to predict conflict counts with 100% accuracy. On the other hand, if $k < 1$, then model output needs to be scaled down to fit the simulation data, and thus the models are *over-estimating* the measured conflict count. Conversely, if $k > 1$, then model output needs to be scaled up to fit the simulation data, and thus the models are *under-estimating* the measured conflict count.

Since the conflict count model for layered airspaces consists of three terms, see equation 3.20, three model accuracy parameters are used for layered airspaces, namely, k_{cruise}, $k_{cruise-cd}$ and k_{cd}. These parameters represent model accuracy for conflicts between cruising aircraft, for conflicts between cruising and climbing/descending aircraft, and for conflicts between climbing/descending aircraft, respectively. For UA, only one model accuracy parameter, k_{ua}, is used because no distinctions are made between aircraft in different flight phases by the corresponding conflict count model, see equation 3.19.

To determine the value of k using least-squares, during the simulations, the number of instantaneous conflicts, and the number of instantaneous aircraft were logged periodically every 15 seconds. Additionally only aircraft within the experiment region, and only conflicts with closest points of approach within the experiment region, were used to assess model accuracy. As mentioned earlier, this method for counting aircraft and conflicts is used because the scenarios used for the simulations had a traffic density of zero near the edges of the simulation region. A similar approach to analyzing simulation data was used in [68].

3.6. Results

In this section, the results of the three simulation experiments are presented separately. The analysis considers the accuracy of the models, and the intrinsic safety of unstructured and layered airspaces.

3.6.1. Primary Experiment

As stated previously, the goal of the primary experiment is to measure the accuracy of the conflict count models for both unstructured and layered airspace designs. Additionally, this experiment also investigated the effect of heading range per altitude band on the intrinsic safety of layered concepts. These aspects are considered below.

3.6.1.1. Validation of Model Structure

Before the absolute accuracy of the models can be evaluated, it is first necessary to examine whether the basic structure of the conflict count models derived in this work, described by equation 3.1, is sound. In essence, this aspect considers whether the models are able to correctly predict the *shape* of the relationship between the number of instantaneous aircraft and the number of instantaneous conflicts. Based on the structure of equation 3.1, it can be seen that the ability of the models to correctly describe the shape of the relationship between these two variables is entirely dependent on the *combinatorial* component of the models, which is, by definition, quadratic in nature; see for example equation 3.16. Therefore, the validity of the structure of the models can be analyzed by fitting simulation logged instantaneous conflict counts, C, to a simple quadratic equation of the form $C = aN^2$, where N is the number of instantaneous aircraft, and a is the quadratic coefficient that relates N to C.

This process is shown in Figure 3.10 for Unstructured Airspace (UA), and in Figure 3.11 for Layers 45 (L45). In these figures, the scatter points represent the raw
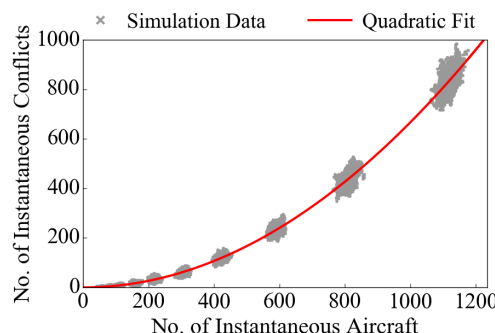
Figure 3.10: Total conflict count for Unstructured Airspace (UA), primary experiment
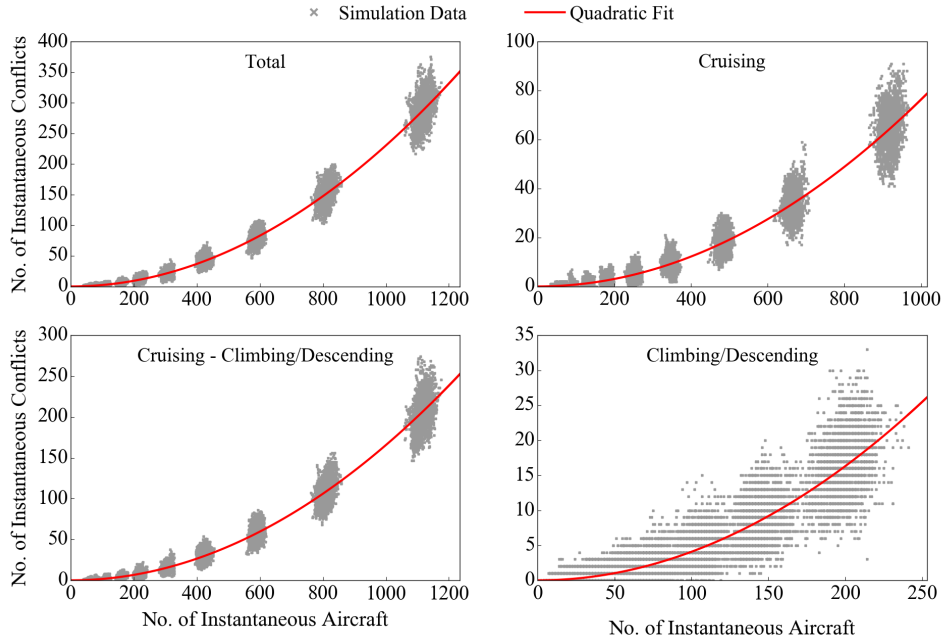
Figure 3.11: Conflict count per conflict type for Layers 45 (L45), primary experiment

simulation data, while the solid lines represent the least square fit of the aforementioned quadratic curve to the simulation data. Note that the raw data appears in 10 clusters since 10 traffic demand scenarios were used in the simulations, with each cluster representing data collected from all repetitions of a particular demand condition; see Table 3.7. In addition to the total conflict count, Figure 3.11 also shows the conflict count results for all flight phase combinations, as required by the model for layered airspaces. Accordingly, the x and y axes of the four graphs in Figure 3.11 vary according to flight phase; for example, for conflicts between cruising aircraft (top-right), the axes consider the number of instantaneous cruising aircraft and cruising conflicts in the airspace.

From Figures 3.10 and 3.11, it can be clearly seen that the number of conflicts does indeed increase quadratically with the number of aircraft in the airspace, confirming the combinatorial component of the models. This conclusion is equally true of the total conflict counts for UA and L45, as it is for the different conflict types of L45. This later result is particularly relevant for layered airspaces, since the corresponding model requires conflicts between aircraft in different flight phases to be treated separately; see equation 3.20. Because similar trends were found for the other layered airspace concepts, as well as for the flight-path angle and ground speed experiments (not shown), it can be concluded that the overall structure of the models derived in this work is sound.

3.6.1.2. Model Accuracy

Since this chapter proposes *analytical* conflict count models, in addition to checking the overall structure of the models, it is necessary to analyze the absolute accuracy of the models, i.e., the ability of the models to correctly estimate the number of instantaneous conflicts for a given number of instantaneous aircraft and known airspace design parameters (e.g. traffic separation requirements). While validation of the model structure focused on the combinatorial component of the models, see section 3.6.1.1, the absolute accuracy of the models is influenced by both the number of combinations of two aircraft, and the average conflict probability between any two aircraft. Absolute accuracy can be quantified using the model accuracy parameter, k. As described in section 3.5.4, these 'k-constants' can be thought of as a scaling factor, and thus a value close to 1 indicates high model accuracy, while $k < 1$ and $k > 1$ indicates over- and under-estimation of conflict counts, respectively.

The values of k for the primary experiment are given in Table 3.8 along with the corresponding percentage accuracy results. Here it can be seen that the overall accuracy of the models is high. For example, for UA (k_{ua}), and for conflicts between cruising aircraft in layered airspaces (k_{cruise}), model accuracy is greater than 90%. However, the table also indicates a consistent over-estimation of conflict counts for interactions involving climbing/descending aircraft, see $k_{cruise-cd}$ and k_{cd} rows of Table 3.8. This over-estimation is related to the design of the simulation experiments; a more detailed explanation is given with the results of the flight-path angle experiment.

Table 3.8: Model accuracy, primary experiment

	UA	L360	L180	L90	L45
k_{ua}	1.003 (99.7%)	-	-	-	-
k_{cruise}	-	0.986 (98.6%)	0.977 (97.7%)	0.909 (90.0%)	1.006 (99.4%)
$k_{cruise-cd}$	-	0.884 (86.9%)	0.882 (86.6%)	0.881 (86.5%)	0.867 (84.7%)
k_{cd}	-	0.796 (74.4%)	0.795 (74.1%)	0.791 (73.6%)	0.776 (71.1%)

3.6.1.3. Effect of Heading Range Per Flight Level on Intrinsic Airspace Safety

In addition to testing the accuracy of the models, data collected during the primary experiment was used to analyze the effect of the allowed heading range per flight level, α, on intrinsic airspace safety; see Figure 3.12. In this figure, conflicts are categorized according to the flight phases of interacting aircraft. Furthermore, for
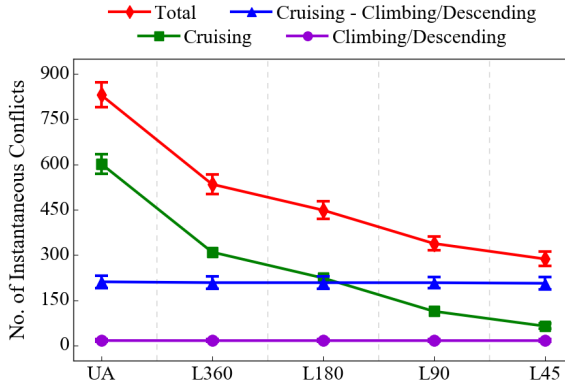
Figure 3.12: Means and 95% confidence intervals of the conflict count per conflict type at the highest traffic density, primary experiment

each airspace concept, the figure displays the means and the 95% confidence intervals of the number of instantaneous conflicts for all repetitions performed at the highest simulated traffic density. It should be noted that the same trends were observed for all traffic densities (other densities not shown).

Figure 3.12 shows that a decrease of α from L360 to L45 lowers the *total* conflict count (red line). Additionally, it can be seen that this safety improvement is entirely due to the reduction of conflicts between cruising aircraft when α is decreased (green line). Because all layered concepts used the same number of flight levels, based on the conflict count model for cruising aircraft in layered airspaces, given by equation 3.24, this increased safety can be explained by the reduction of horizontal relative velocities when α is decreased.

Interestingly, Figure 3.12 also shows that the number of conflicts involving climbing and descending traffic is invariant with α (blue and violet lines). This is because none of the airspace concepts considered here apply any constraints on the paths of climbing and descending traffic. While the absolute number of conflicts with climbing/descending aircraft remains constant, the proportion of such conflicts increases as α is decreased. This can be seen clearly for the L45 concept, for which 77.8% of the total conflicts is caused by climbing/descending traffic. This suggests that climbing/descending aircraft have a greater influence on the overall intrinsic safety of layered concepts with a narrow heading range per flight level.

Since α only affects the number of cruising conflicts, the corresponding conflict model for cruising aircraft, see equation 3.24, can be used to predict the beneficial effect of reducing α on the intrinsic safety of layered concepts; see Table 3.9. Note that this table shows the percentage reduction of conflicts relative to the case with the highest horizontal relative velocities, i.e, relative to $\alpha = 360^o$. Here it can be seen that linearly decreasing α results in a non-linear decrease in the number of conflicts. Furthermore, this table also shows that the model predicted reductions

are closely matched by the simulation logged conflict reductions. This once again demonstrates the high accuracy of the models, and also illustrates how the models can be used to understand the effects of other airspace design parameters, such as separation requirements, on intrinsic safety.

Table 3.9: Effect of heading range per flight level on predicted and actual conflict count reductions

Heading Range Per Layer,	Model Prediction	Simulation Results
360°	0%	0%
180°	27.3%	27.9%
90°	60.1%	63.3%
45°	79.6%	79.2%

Although the analysis thus far has focused on layered airspaces, Figure 3.12 can also be used to compare the safety of UA with that of layered concepts. In relation to this aspect, Figure 3.12 shows that UA results in significantly more (total) conflicts than for any of the layered concepts. This is also true when comparing UA to the L360 concept. Since there are no heading-altitude constraints, and therefore no reductions in relative velocities, for either of these two concepts, the increased safety of L360 can be attributed to the only other difference between UA and layered concepts, i.e., the use of predefined flight levels for cruising aircraft in layered concepts. As a result of these predefined flight levels, the model for layered airspaces predicts a 30.9% reduction of the total conflicts for L360 when compared to UA at the highest traffic demand (this matches well to the 35.5% reduction logged during the simulations).

3.6.2. Flight-Path Angle Experiment

For a given set of origins, destinations and cruising altitudes, the flight path angle of climbing and descending traffic, γ_{cd}, affects the ratio between the number of instantaneous of cruising vs. climbing/descending aircraft. This is because a higher value of γ_{cd} causes an aircraft to climb faster to its cruising altitude, leading to a higher proportion of cruising aircraft. Since the proportion of aircraft in different flight phases influences both the expected vertical relative velocity and the average conflict probability between aircraft, the effect of γ_{cd} on the intrinsic safety of the UA and L45 concepts has been analyzed in this experiment. To this end, simulations were repeated for $\gamma_{cd} = \{1.4^o, 2.8^o, 5.6^o\}$.

3.6.2.1. Effect of Flight-Path Angle on Intrinsic Airspace Safety

Total conflict count results for the flight-path angle experiment are displayed in Figure 3.13. For UA, Figure 3.13(a) shows that an increase of γ_{cd} increases the number of conflicts between cruising aircraft (green line). This trend is expected since the number of cruising aircraft increases with γ_{cd}. Additionally, an increase of γ_{cd} reduces the proportion of climbing/descending aircraft, leading to a corresponding

(a) Unstructured Airspace (UA)

(b) Layers 45 (L45)
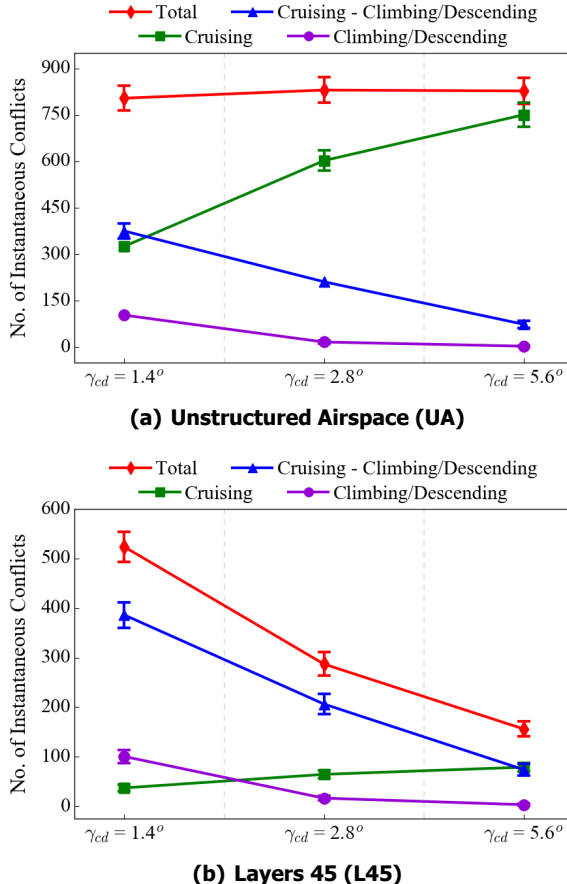
Figure 3.13: Means and 95% confidence intervals of the conflict count per conflict type for Unstructured Airspace and Layers 45 at the highest traffic density, flight-path angle experiment

decrease of such conflicts (blue and violet lines). Because these two effects are (nearly) equal, but opposite in magnitude, changes to γ_{cd} only have a minor effect on the total conflict count for UA (red line).

In contrast, Figure 3.13(b) shows that γ_{cd} has a substantial effect on the total conflict count for L45 (red line) , with safety increasing for higher γ_{cd}. Although the number of conflicts involving cruising aircraft increases for L45 (green line), it does so at a lower pace than for UA. In fact, the total conflict count for L45 is mainly influenced by conflicts between cruising and climbing/descending aircraft (blue line). This matches the trend found for the primary experiment, where the majority of conflicts for layered airspaces with a narrow heading range per flight level involve climbing/descending aircraft.

3.6.2.2. Effect of Flight-Path Angle on Model Accuracy

The effect of γ_{cd} on model accuracy is displayed in Table 3.10. As exemplified by the total conflict count in Figure 3.13, Table 3.10 shows only a minor effect of γ_{cd} on model accuracy for UA, and for conflicts between cruising aircraft in layered airspaces (see k_{ua} and k_{cruise} rows). However, accuracy for conflicts involving climbing/descending aircraft in layered airspaces appears to be significantly affected by γ_{cd}. As noted for the results of the primary experiment, the models show a tendency to over-estimate the number of such conflicts. Furthermore, the degree of this overestimation worsens as γ_{cd} increases.

Table 3.10: Model accuracy, flight-path angle experiment

		$\gamma_{cd} = 1.4^o$	$\gamma_{cd} = 2.8^o$	$\gamma_{cd} = 5.6^o$
UA	k_{ua}	0.973 (97.2%)	1.003 (99.7%)	1.003 (99.7%)
L45	k_{cruise}	1.081 (92.5%)	1.006 (99.4%)	0.991 (99.1%)
	$k_{cruise-cd}$	1.030 (97.1%)	0.867 (84.7%)	0.589 (30.1%)
	k_{cd}	0.916 (90.9%)	0.776 (71.1%)	0.681 (53.2%)

An explanation for this trend can be found by considering the design of the simulation experiments, and the relationship between γ_{cd} and the volume of airspace searched for conflicts during conflict detection. Since γ_{cd} affects the magnitude of the vertical relative velocity, it also affects the size of the *vertical volume* of airspace searched for conflicts by aircraft; see Figure 3.6(b). Furthermore, no traffic was simulated above and below the 'simulation' and 'experiment' regions; see Figure 3.9. Therefore, climbing/descending aircraft, with vertical conflict search volumes that extend outside the simulated sector, are less likely to detect conflicts when compared to similar aircraft in the middle altitudes of the simulation. Because an increase in γ_{cd} increases the size of the vertical conflict search volume, the number of climbing/descending aircraft that are negatively affected by this effect increases with γ_{cd}, leading to a greater over-estimation by the conflict count models.

It should be noted that, unlike the vertical direction, the model accuracy results for cruising conflicts is *not* affected by the fact that no traffic was simulated outside the simulated sector. Although cruising conflict counts are affected by the *horizontal volume* of airspace searched for conflicts in UA, and the *horizontal area* of airspace in layered concepts, only conflicts with closest points of approach within the 'experiment' region were considered for model accuracy analysis, as explained in section 3.5.4. Therefore, even if the horizontal conflict search volume/area extends beyond the 'experiment region', the gap between the 'experiment' and 'simulation'

regions; see Figure 3.9, compensates for this unrealistic aspect of the simulation's design.

However, a similar distinction between 'experiment' and 'simulation' regions is not feasible in the vertical direction since data from all cruising flight levels is needed to evaluate model accuracies for layered airspaces. Moreover, a sudden drop in densities is more realistic in the vertical direction; for example, commercial aircraft do not usually fly above 45,000 ft. On the other hand, changes in traffic density tend to be less abrupt in the horizontal direction for real operations (except near and over oceans), thus justifying the distinction between experiment and simulation regions used here in the horizontal plane.

3.6.3. Ground Speed Experiment

The analytical conflict count models derived in this chapter assume equal ground speeds for all aircraft. This assumption was required to simplify a complex expression that is used to compute the expected horizontal relative velocity between aircraft, see equation 3.4. However, this assumption is not representative of current day en route operations because optimum cruising speeds vary with aircraft type, and because wind direction and speed, which affects ground speed calculation, can vary significantly over large areas of airspace. Additionally, the equal ground speed assumption does not allow for the possibility of overtaking conflicts between aircraft. Consequently, to assess the sensitivity of the models to the equal ground speed assumption, simulations were repeated for cases where the grounds speeds of aircraft were normally and uniformly distributed for the UA and L45 concepts.

3.6.3.1. Effect of Ground Speed Distribution on Intrinsic Airspace Safety

Figure 3.14 shows that speed distribution has a negligible effect on conflict counts for UA. This is also largely true for L45, except for the slight increase in conflicts between cruising aircraft when the speed distribution changes from 'equal' to 'uniform' (green line). This invariance of conflict counts with speed distribution can be explained by the fact that the same average ground speed is used by all three distributions (to enable a fair comparison). Therefore, while the speed distribution of aircraft may have an effect at a per aircraft level, the overall intrinsic safety provided unstructured and layered airspaces is largely unaffected by the shape of the ground speed distribution, and is only dependent on the magnitude of the average speed of all aircraft in the airspace.

3.6.3.2. Effect of Ground Speed Distribution on Model Accuracy

The model accuracy results for the ground speed experiment are displayed in Table 3.11. Here it should be noted that the model was evaluated assuming equal ground speeds for all aircraft, regardless of the actual ground speed distributions

(a) Unstructured Airspace (UA)


(b) Layers 45 (L45)
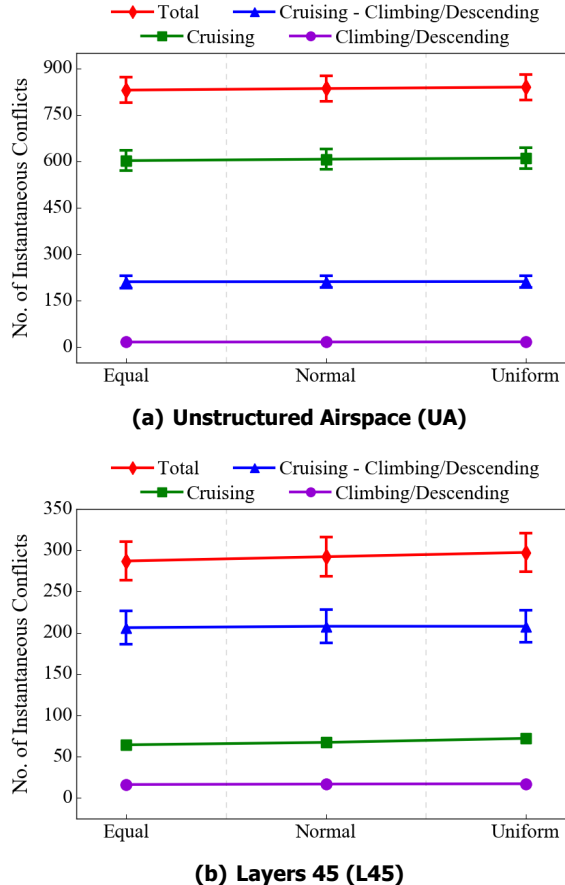
Figure 3.14: Means and 95% confidence intervals of the conflict count per conflict type for Unstructured Airspace and Layers 45 at the highest traffic density, ground speed experiment

Table 3.11: Model accuracy, ground speed experiment

		Equal	Normal	Uniform
UA	k_{ua}	1.003 (99.7%)	1.006 (99.4%)	1.006 (99.4%)
L45	k_{cruise}	1.006 (99.4%)	1.053 (95.0%)	1.118 (89.4%)
	$k_{cruise-cd}$	0.867 (84.7%)	0.873 (85.4%)	0.866 (84.5%)
	k_{cd}	0.776 (71.1%)	0.799 (74.8%)	0.809 (76.4%)

used in the simulations. The table shows that model accuracy for UA is not dependent on ground speed distribution. Similarly, for L45, model accuracy for conflicts involving climbing and descending aircraft is not significantly different to the condition with equal ground speeds. On the other hand, accuracy for conflicts between cruising aircraft decreases with increasing variation in aircraft ground speeds for L45. This suggests that restricting the heading range per altitude level negatively affects the accuracy of the models for layered concepts.

As mentioned above, the equal ground speed assumption affects the calculation of the expected horizontal relative velocity between aircraft, $\mathbf{E}\left(v_{r,h}\right)$. To gain a better sense on the effect of this assumption on $\mathbf{E}\left(v_{r,h}\right)$, equation 3.4 is evaluated numerically for all three speed distributions for the UA and L45 concepts, see Table 3.12. This table shows that changing the speed distribution has a much greater effect on $\mathbf{E}\left(v_{r,h}\right)$ for L45; a 10.3% increase occurs when the speed distribution is changed from 'equal' to 'uniform' for L45, while a similar change of speed distribution only results in a 0.5% increase for UA. Since $\mathbf{E}\left(v_{r,h}\right)$ directly affects the conflict count model for cruising aircraft in layered airspaces, the trends shown in Table 3.12 explain the model accuracy results noted above for this experiment.

Table 3.12: Numerically computed values of the expected horizontal relative velocities for Unstructured Airspace (UA) and Layers 45 (L45)

	Equal	Normal	Uniform
UA [kts]	509.30	507.42	511.66
L45 [kts]	103.92	107.46	114.66

Although this work focuses on developing fully *analytical* models, the *numerical* $\mathbf{E}\left(v_{r,h}\right)$ values listed in Table 3.12 can be used to increase model accuracy for cruising conflicts in layered concepts. To this end, Table 3.13 displays accuracy results for k_{cruise} for analytically and numerically computed $\mathbf{E}\left(v_{r,h}\right)$ for L45. Here it can be seen that accuracy for the normal and the uniform speed distributions increases to the level reported for the equal speed case when numerical values of $\mathbf{E}\left(v_{r,h}\right)$ are used. But for UA, as well as for conflicts involving climbing/descending aircraft in L45, using numerical values of $\mathbf{E}\left(v_{r,h}\right)$ does not significantly affect model accuracy (not shown). Therefore, based on the results shown in Figure 3.14, it can be concluded that the analytical models derived using the equal speed assumption

Table 3.13: Effect of analytical and numerical methods of estimating the expected horizontal relative velocity on model accuracy for Layers 45

	Equal	Normal	Uniform
k_{cruise} Analytical	1.006	1.053	1.118
	(99.4%)	(95.0%)	(89.4%)
k_{cruise} Numerical	1.006	1.018	1.013
	(99.4%)	(98.2%)	(98.7%)

can be used to understand and explain the factors that affect the intrinsic safety of unstructured and layered airspaces.

3.7. Discussion

In this chapter, analytical conflict count models were developed to analyze the intrinsic safety of unstructured and layered airspace designs. The models focused on quantifying the effect of airspace design parameters and traffic demand on the number of instantaneous system-wide conflicts. The models were validated using extensive fast-time simulation experiments that involved over three million flights. This section reflects on the intrinsic safety offered by unstructured and layered airspaces, and discusses the accuracy of the models. Additionally, important aspects related to model usage are also considered.

3.7.1. Intrinsic Safety of Unstructured and Layered Airspace Designs

The results of all simulation experiments performed in this study showed that aircraft in unstructured airspace are subject to more conflicts than aircraft in layered airspaces. The higher intrinsic safety of layered airspaces can be attributed to two factors that reduce the number of conflicts between cruising aircraft.

The first factor is related to the allowed heading range per flight level. For layered concepts that reduce the allowed heading range per flight level, relative velocities between cruising aircraft are reduced compared to unstructured airspace. This reduction in relative velocities, which stems from a greater alignment of cruising traffic in each flight level, reduces conflict probabilities between neighboring aircraft. While this effect was already hypothesized in our prior work [74], the current study quantifies this effect, and shows that the corresponding safety benefits are nonlinear with the allowed heading range. For example, lowering the heading range per flight level from 360° to 90° reduces the number of conflicts between cruising aircraft by approximately 60%. However, further halving the heading range per flight level to 45° only provides an additional 20% reduction in conflicts.

The second factor that improves the safety performance of layered airspaces is the use of predefined flight levels for cruising aircraft. Using predefined flight levels not only reduces the number of combinations of aircraft that can conflict with each other, it also reduces the conflict probability between aircraft. This is because in layered airspaces, conflicts can only occur between cruising aircraft if both aircraft are at the same flight level. Consequently, in layered concepts, conflict probability for cruising aircraft is a function of the *area* searched for conflicts. On the other hand, conflict probability is directly proportional to the *volume* searched for conflicts in unstructured airspace, since there are no vertical constraints on aircraft motion. The larger region of airspace searched for conflicts in unstructured airspace, therefore,

increases conflict probability and the number of conflicts encountered by cruising aircraft.

Although layered designs improve the overall safety of en route airspaces by reducing conflicts between cruising aircraft, it is worth noting that no differences were observed between unstructured and layered concepts in relation to the number of conflicts involving climbing/descending aircraft. In fact, the simulation results clearly showed that as the heading range per flight level is decreased, the *proportion* of conflicts involving climbing/descending aircraft is increased. Therefore, such conflicts can become more influential than conflicts between cruising aircraft, particularly for layered airspaces with a narrow heading range per flight level. While the magnitude of this trend is affected by the ratio of cruising vs. climbing/descending aircraft, which is in turn influenced by the flight path angles of climbing and descending traffic, this result does emphasize the need to take into account conflicts between aircraft in different phases when assessing the overall intrinsic safety of an airspace design.

3.7.2. Conflict Count Model Validation

By comparing simulation results to model predictions, model accuracy was determined to be high for both airspace designs. For example, in addition to correctly predicting the shape of the relationship between the numbers of instantaneous aircrafts and conflicts, the models could also estimate the effect of the allowed heading range per flight level on conflict counts with an accuracy greater than 90% the models could also calculate the effect of using predefined cruising altitudes on safety with a similar level of accuracy.

The accuracy of all models is, to some degree, affected by the assumptions upon which they are derived. The models derived here are no exception to this rule, and two assumptions negatively affected conflict count estimation. The first assumption was that all aircraft have equal ground speeds, and it was required to derive purely *analytical* conflict count models. Because this assumption does not consider the occurrence of over-taking conflicts, and because such conflicts are more likely to occur as the heading range per altitude band is decreased, model accuracy for layered airspaces was negatively affected by this assumption. Nevertheless, accuracy was shown to be increased to the level found for the equal speed assumption when the analytical models were augmented with numerically computed values of the expected horizontal relative velocity. It is hypothesized that the effect of other traffic scenario related assumptions, such as the uniformly distributed heading distributions used in this work, can also be compensated for in a similar manner. Such changes could be used to expand the models to account for the traffic flow and demand distributions of current-day operations.

Model accuracy was also affected by the fact that the models assume airspace to be infinite in extent, both horizontally and vertically. While this assumption is convenient for modeling purposes, it is an obvious deviation from reality. Therefore, the simulations performed to validate the models used a finite volume of airspace.

Although this approach made the simulations more realistic, it also caused traffic density to drop to zero at the boundaries to the simulated sector. Since traffic density rarely drops so drastically in the horizontal direction for real operations, the models were only validated for data logged within a horizontally defined experiment region at the center of the simulated sector. However, a similar approach in the vertical direction was deemed to be unrealistic, given the altitude related flight envelope limitations of aircraft. Therefore, the accuracy results presented in this chapter are representative of the range of values that could be obtained using the models for real operations, if such data were to become available in the future for unstructured and layered en route airspaces.

Despite these limitations, as noted above, model accuracy was generally quite high. This high accuracy allows the models to be used as tools to compare unstructured and layered airspaces, as well as to evaluate the effects of a number of safety relevant parameters, such as conflict detection look-ahead time and traffic separation requirements. Additionally, since the models derived here take into account the proportion of aircraft in different flight phases when computing conflict counts, they provide a more comprehensive understanding on the overall intrinsic safety provided by a particular airspace design when compared to previous studies that have only considered cruising aircraft. This aspect is particularly important during the design of layered airspaces where, as noted above, climbing/descending traffic can cause the majority of conflicts under certain design choices.

3.7.3. Additional Considerations

Although the models were tested within the context of high-altitude commercial operations, they can also be applied to the design and analysis of unstructured and layered airspace concepts for low-altitude unmanned aircraft ops. This is possible because the generic, analytical nature of the models allows a generalization of the results beyond the specific conditions that have been simulated in this study, for instance for the lower speeds anticipated for unmanned traffic. On a similar note, the underlying approach used here to model system-wide conflict counts could, with some additions, also be expanded to other airspace designs, including for concepts closer to today's mode of operations. Any adaptations along these lines would require an analysis of how the constraints imposed by a particular airspace design affect the number of combinations of two aircraft, and the average (horizontal and vertical) relative velocities between aircraft.

It is important to realize that the conflict count models considered here measure safety as a function of airspace design *only*. Other factors that affect safety, including uncertainties related to aircraft state measurement/communication, are not considered by the models since these aspects are not directly affected by the design of an airspace. Nevertheless, a recent study has concluded that the characteristics of the Automatic Dependent Surveillance-Broadcast (ADS-B) system, which is the system that is promoted by many ATM organizations to supplement, and eventually replace, radar-based surveillance, has little effect on the performance of the state-

based conflict detection method used here [25]. Therefore, uncertainties related to aircraft state measurement/communication are not expected to significantly affect the results presented here, particularly for future operations with ADS-B.

Another factor that is not considered by the notion of *intrinsic safety*, and by the models presented here, is the effect of tactical conflict resolutions on airspace safety. In fact, the *overall safety* of operations is affected by both the selected airspace design and the selected conflict resolution approach. This is particularly the case at high traffic densities because the scarcity of airspace could trigger conflict chain reactions when conflict resolution actions are taken. For a more detailed analysis on the effect of conflict chain reactions on safety, the reader is referred to [29].

Many ATM studies interrelate airspace safety and capacity. Although these two metrics are closely connected, airspace concepts that maximize safety need not be the optimum in terms of other relevant performance metrics, most notably airspace efficiency. The balance between safety and efficiency should be an important consideration when arguing for or against a particular airspace design, or when fine-tuning the parameters of the selected airspace design. This notion can be illustrated for the layers concept; although decreasing the heading range per flight level improves safety, it also increases the number of flight levels needed to specify all possible travel directions. Therefore, for a given volume of airspace, it may be more efficient to use a value for the heading range per flight level that allows multiple complete layer sets to be defined, since this approach could minimize the fuel penalty of using predefined cruising altitudes in layered airspaces. To summarize, when evaluating the *capacity* of an airspace design, it is necessary to consider the effect of a design on multiple airspace performance metrics in unison, including safety and efficiency. The approach used to model intrinsic airspace safety in this chapter is a good starting point to develop a capacity assessment method along these lines.

3.8. Conclusions

This chapter presented analytical conflict count models to measure the intrinsic safety of unstructured and layered en-route airspace designs. The models take into account the three-dimensional motion of aircraft, and therefore improve upon previous studies by considering conflicts between aircraft in different flight phases. Fast-time simulation experiments were performed to validate the models, and compare unstructured and layered airspaces in terms of the intrinsic safety they provide. The following conclusions can be drawn:

1. *Layered airspace concepts were found to be safer than unstructured airspace.* This is because layered airspaces restrict the heading range allowed per flight level, and because they use predefined flight levels to reduce the number of possible conflict pairs.

2. *The safety performance of layered airspaces increases as the heading range per flight level is reduced.* This can be explained by the reduction of relative velocities between cruising aircraft as the heading range per flight level is decreased. The relationship between the number of instantaneous conflicts and the heading range per flight level is nonlinear.

3. *The safety benefits of layered airspaces only apply to cruising aircraft,* and no differences were found between unstructured and layered airspaces with respect to the number of conflicts involving climbing/descending aircraft. For this reason, the safety of layered airspaces is more sensitive to the proportion of cruising aircraft. This result also emphasizes the need to consider aircraft in different flight phases when evaluating the overall safety of an airspace design.

4. *The 3D analytical conflict count models derived here were able to estimate conflict counts for both unstructured and layered concepts with high accuracy,* and were able to predict the aforementioned benefits of layered airspaces. Consequently, they can be used to understand the relationships between the parameters that affect safety for both these airspace concepts, including the effect of the proportion of aircraft in different flight phases on instantaneous conflict counts.

5. *Augmenting the analytical models with numerically computed values of the expected relative velocity between aircraft was shown to further increase model accuracy.* This approach can be used to take into account the effects of other traffic demand and flow conditions that have not been considered in this study.

3

4

Effect of Traffic Scenario Properties on Conflict Count Models

The analytical conflict count models derived in chapter 3 assume 'ideal' traffic scenario properties, namely equal ground speeds for all aircraft, as well as uniform aircraft heading, altitude and spatial distributions. The accuracy of these models for more realistic traffic scenarios is as yet unknown. The goal of this chapter is, therefore, twofold. Firstly, fast-time simulation experiments are used to evaluate model accuracies for non-ideal traffic scenario distributions. Secondly, data collected from these simulations is used to validate numerical approaches that aim to relax the dependency of the conflict count models to the ideal traffic scenario assumptions. As in chapter 3, these investigations are performed within the context of unstructured and layered airspace designs.

Cover-to-cover readers may choose to skip sections 4.2 and 4.3 which describe the conceptual designs of unstructured and layered airspaces, and the baseline analytical conflict count models for these two airspace designs. These sections are essentially unchanged from their counterparts in chapters 2 and 3.

Abstract

Closed-form analytical conflict count models have been derived in the previous chapter to quantify the safety performance of an airspace design. Although such models provide useful insights on the relationship between airspace design parameters, such as traffic separation requirements, and safety, they rely on idealized assumptions regarding the behavior of traffic that do not always reflect realistic operations. To address this limitation, this chapter: a) investigates the effect of traffic scenario assumptions on the accuracy of analytical conflict count models using targeted fast-time simulation experiments; and b) develops and tests so called 'model adjustments' that aim to relax the dependency of the models on the idealized assumptions. For these purposes, conflict count models for unstructured and layered en route airspace designs are used as case-studies. The simulation results indicate that the traffic scenario assumptions used to derive the analytical conflict count models do negatively affect model accuracy, with some assumptions leading to a substantial under-estimation of conflict counts. The results also show that the model adjustments developed here increased accuracy for the more realistic scenarios to the levels previously found for the ideal traffic settings. Therefore, in addition to providing a physical understanding of the factors that affect airspace safety, the adjusted models can also be used as tools for practical airspace design applications.

> **Note on Nomenclature**
> The models described in this chapter compute *instantaneous* conflict counts as a measure of the intrinsic safety provided by an airspace design. As such, the following nomenclature simplifications are used to reduce the complexity of the equations presented in this chapter:
> - C: Instantaneous conflict count without conflict resolution
> - N: Instantaneous aircraft count without conflict resolution

4.1. Introduction

The current system of Air Traffic Management (ATM) relies on a *centralized* control architecture. At its core, this system is heavily dependent on human Air Traffic Controllers (ATCos) to ensure safe separation between aircraft. While this system has served the needs of the air transportation industry thus far, the increasing delays and congestion reported in many parts of the world indicate that the current centralized operational model is rapidly approaching saturation levels [12, 17].

To cater for the expected future increases in traffic demand, several studies have proposed a transition to a *decentralized* traffic separation paradigm in en route airspace [30, 33, 91–93]. In decentralized airspace, each individual aircraft is responsible for its own separation with all surrounding traffic. To facilitate decentralization, many studies have focused on the development of automated airborne Con-

flict Detection and Resolution (CD&R) algorithms [49, 111–113]. Some researchers have also considered if such algorithms can be combined with alternate options for structuring traffic to further increase safety and capacity over current operations [57, 74, 114].

To evaluate the algorithms and the airspace designs that have been developed to implement decentralized control, most studies in this domain have used fast-time simulation experiments. Although fast-time simulations provide intuitive insights on the advantages and disadvantages of decentralized systems, they can be time consuming to develop, depending on the required level of realism. Furthermore, the results of such simulation studies can be very specific to the way they are performed, and this can make it difficult to extrapolate their results beyond the specific conditions that have been tested.

To overcome the aforementioned limitations of fast-time simulations, some researchers have derived mathematical models to gain a more *quantitative* and *generalizable* understanding of the interactions between aircraft in decentralized systems. When such methods are used to analyze the safety of an airspace design, they often make use of the so called 'gas modeling' approach [29, 66, 68–70]. This approach is inspired by the collisions that occur between ideal gas particles, and it determines instantaneous system-wide conflict counts between aircraft as a measure of airspace safety. Because this approach uses measurable airspace parameters, such as traffic demand and separation requirements, as inputs, gas models can be used to understand the factors that affect the safety of an airspace design.

However, to develop closed-form analytical expressions, most 'gas models' described in literature make use of idealized assumptions regarding the speed, heading, altitude and spatial/density distributions of traffic. Collectively, these four distributions describe what is often referred to as a *traffic scenario*. Typically, the following four traffic scenario assumptions are used in the derivation of analytical gas-models:

- Equal ground speed for all aircraft

- Uniform heading distribution

- Uniform altitude distribution

- Uniform spatial/density distribution

In practice, however, a traffic scenario with these exact combination of properties is unlikely to occur. This raises the question of the accuracy of such models for more realistic traffic scenarios.

In this research, the accuracy of analytical gas models is tested for cases that do not respect the above 'ideal' traffic scenario assumptions. For this purpose, three-dimensional analytical gas-models for unstructured and layered en route airspace designs, derived in our prior work [88], are used as case-studies. For both airspace designs, model accuracy was measured by comparing the predictions of the corresponding models to the results of four fast-time simulation experiments with varying

speed, heading, altitude and spatial distributions. In each experiment, one of the four traffic scenario assumptions is violated while respecting the other three assumptions in order to determine the effect of each assumption on model accuracy. The data collected from these simulations is also used to test so called 'model adjustments' that aim to relax the dependency of the conflict count models on the idealized traffic scenario assumptions. The adjusted models use numerical methods to evaluate complex integrals that can not be solved analytically for non-ideal traffic scenarios.

This chapter begins with a summary of the necessary background material in section 4.2. This is followed by an overview of the baseline analytical conflict count models for unstructured and layered en route airspaces in section 4.3. Next, in section 4.4, the effect of each traffic scenario assumption is analyzed, and a numerical approach is developed to generalize the models for more realistic traffic scenarios. The design of the simulation experiments used to assess model accuracy is described in section 4.5. The results of the simulations are presented and discussed in sections 4.6 and 4.7, respectively. Finally, the main conclusions of this study are summarized in section 4.8.

4.2. Background

This section presents the definitions and background material relevant to this chapter. It begins with descriptions of the two airspace concepts of interest to this study, namely unstructured and layered airspace designs. Additionally, this section defines the notion of a conflict between two (or more) aircraft, and also provides an overview of the 'gas-modeling' approach used to quantify the safety of an airspace design.

4.2.1. The Unstructured Airspace Design Concept

As the name suggests, no constraints are imposed on aircraft motion in Unstructured Airspace (UA). Instead, this simplest form of airspace design focuses on maximizing overall system efficiency. Therefore, aircraft are free to use direct horizontal routes, as long as such routing is not obstructed by weather or static obstacles. Similarly, UA permits aircraft to fly with preferred speeds and at optimum altitudes, based on their performance capabilities and trip distances. By offering greater freedom to aircraft operators, UA has been found to result in a more uniform distribution of traffic, both horizontally and vertically, relative to current day operations. This can in turn reduce traffic concentrations and ensuing delays [29, 30].

4.2.2. The 'Layers' Airspace Design Concept

Several different layered airspace concepts have been discussed in literature [95–97]. The specific variation under consideration in this work was developed in our prior work [74], and is known as the 'Layers' concept.

The Layers concept can be seen as an extension to the hemispheric/semicircular rule [79]. In this concept, the airspace is segmented into vertically stacked bands, and heading-altitude rules are used to limit the range of travel directions allowed in each altitude layer. Although the Layers concept dictates the vertical profile of a flight, operators are free to select direct horizontal routes when possible. Moreover, climbing and descending aircraft are exempted from the heading-altitude rules, and can violate them to reach their cruising altitude or destination. This exception avoids inefficient 'spirals' when climbing/descending.

Figure 4.1: Isometric view of an example Layers concept, with an allowed heading range of $\alpha = 90^o$ per flight level, and a vertical spacing of $\zeta = 1100$ ft between flight levels. This example layered concept is referred to as 'L90'.

An example Layers concept is shown in Figure 4.1. Two parameters define the topology of the Layers concept. The first parameter is the spacing between altitude bands, ζ. An important design requirement is that ζ is *at least* equal to the vertical separation requirement to prevent conflicts between aircraft cruising in adjacent flight levels. In this work, a vertical separation requirement of 1000 ft is used. Therefore, the altitude bands of the Layers concepts considered here are separated by $\zeta = 1100$ ft; the extra 100 ft is used to prevent so called 'false' conflicts that can sometimes occur due to any slight overshooting of altitude when aircraft level-off at their desired flight level. Such an offset is also necessary to account for any height-keeping errors, and because of turbulence.

The second design parameter of the Layers concept is the heading range allowed per altitude band, α. For the layered airspace shown in Figure 4.1, $\alpha = 90^o$, and consequently, this particular concept is referred to as Layers-90, or 'L90' for short. For L90, four flight levels are needed to specify all possible flight directions, and define one complete 'set' of layers. On the other hand, for a L180 concept (not shown), only two flight levels are needed to define a complete set of layers. Therefore, for L180, two complete sets of layers would fit within the volume of airspace needed for L90. When multiple sets of layers are available, the total trip distance of an aircraft is used in addition to its heading to determine its cruising altitude. In this way, short flights can use lower layer sets, and longer flights can

use higher layer sets, to reduce the negative effect of predetermined altitudes on flight efficiencies.

Previous research has shown that layered airspace designs are safer than UA [74]. The increased safety for layers has been attributed to a) the use of predefined flight levels to reduce the number of possible conflict pairs, and b) the use of heading-altitude rules to reduce the average conflict probability between cruising traffic [70, 88].

4.2.3. Conflicts vs. Intrusions

In ATM, safety is often measured in terms of the number of conflicts and intrusions. A conflict is defined to occur if the horizontal and vertical distances between two or more aircraft are expected to be less than the prescribed separation standards within a predetermined 'look-ahead' time. Conflicts are, therefore, predictions of *future* separation violations. Conflicts should not be confused with intrusions. Instead, intrusions, also referred to as losses of separation, occur when separation requirements are violated at the *present* time. This distinction between conflicts and intrusions is shown in Figure 4.2.

(a) Conflict   **(b) Intrusion**
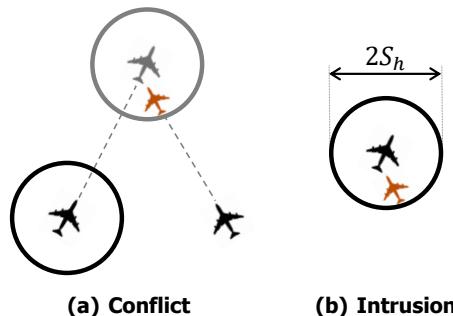
Figure 4.2: The difference between conflicts and intrusions, displayed here for the horizontal plane. Here, S_h is the horizontal separation requirement.

This chapter is concerned with the accuracy of *conflict* count models. Therefore, the rest of this chapter only deals with aspects that are relevant to conflicts.

4.2.4. Gas Models for Estimating Conflict Counts

As mentioned earlier, previous studies have presented so called 'gas-models' to compute the number of instantaneous conflicts that occur in a given volume of airspace. Gas models compute the number of instantaneous conflicts as a product of two factors; the number of combinations of two aircraft, and the average conflict probability between any two aircraft. In essence, the number of combinations of two aircraft is the maximum number of instantaneous conflicts that can occur,
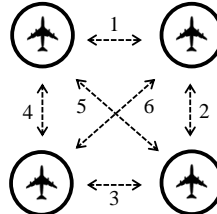
Figure 4.3: A multi-aircraft conflict can be decomposed into several two-aircraft conflicts. For example, a multi-aircraft conflict between four aircraft can result in up to six unique two-aircraft conflicts.

since multi-aircraft conflicts, i.e., conflicts involving more than two aircraft, can be decomposed into a series of unique two-aircraft conflicts; see Figure 4.3. The average conflict probability, on the other hand, scales down the number of combinations so that only those aircraft pairs that are within range each other, and/or those with intersecting trajectories, are counted as conflicts. Thus, the basic equation used by all gas models can be written out in words as:

$$\text{No. Inst. Conflicts} \quad = \quad \frac{\text{No. of Combinations of Two Aircraft}}{\text{Average Conflict Probability Between Any Two Aircraft}}$$

(4.1)

Here, different airspace designs can influence both the number of possible combinations of aircraft, as well as the average conflict probability between any two aircraft.

Gas models are named as such because the combinatorial characteristic that is central to this approach was initially used in the field of statistical mechanics to determine the number of collisions that can occur between the molecules of an ideal gas [98]. In ATM, gas models were first proposed in the 1960s to analyze the collision risk between adjacent routes of the North Atlantic track system [67, 99, 100]. Subsequently, they have also been used to investigate the safety of a wide variety of airspace types, including high altitude en route airways [101–103], low altitude terminal airspaces [69, 104–106], and for concepts that closely resemble unstructured and layered airspace concepts [20, 30, 66, 68, 70, 88].

It is important to note that gas models measure the so called 'intrinsic safety' provided by an airspace design. The notion of intrinsic safety focuses exclusively on the safety that is provided by the constraints imposed on aircraft motion by a particular airspace design. As such, intrinsic safety considers the situation *without* tactical conflict resolution. Nonetheless, because any conflict that could not be prevented by an airspace design requires some intervention, the notion of intrinsic safety can be used as an indication of the workload experienced by pilots and/or ATCos in

solving conflicts under the considered airspace concept. It is also important to note that although measurement and communication uncertainties can affect the number of observed, or perceived, conflicts for a particular aircraft, such uncertainties are unrelated to the design of an airspace. Consequently, the intrinsic safety provided by an airspace design is only concerned with the 'truly occurring' conflicts in an airspace.

As implied above, gas models are well established in the domain of airspace safety analysis. However, most previous studies have derived such models using idealized assumptions regarding the speed, heading, altitude and spatial distributions of traffic in order to obtain closed-form analytical expressions that are easy to use and understand. However, as a result of these assumptions, it is as yet unknown whether such models are applicable for more realistic traffic scenarios. To provide more clarity on this aspect, in this work, fast-time simulation experiments are used to examine the effect of each traffic scenario assumption on the accuracy of analytical gas models. Additionally, this chapter also presents the derivation of so called 'model adjustments' that can generalize gas models for a wider range traffic scenarios using a numerical approach. To these ends, analytical conflict count models for unstructured and layered en route airspace designs are used as case studies.

4.3. Baseline Analytical Conflict Count Models

This section summarizes the baseline analytical conflict count models for unstructured and layered en route airspace designs; the full derivation can be found in [88]. These analytical models assume equal ground speeds for all aircraft, as well as a uniform distribution of aircraft headings, altitudes and spatial locations.

4.3.1. Unstructured Airspace

As stated in section 4.2.4, gas models compute the number of instantaneous conflicts, C, as a product of the number of combinations of two aircraft, and the average conflict probability between any two aircraft, p. For UA, the number of combinations can be computed directly using the binomial coefficient, since this airspace design imposes no constraints on the motion of aircraft; see section 4.2.1. Therefore for UA, C_{ua} can be expressed as [70, 88]:

$$C_{ua} = \binom{N_{total}}{2} p_{ua} = \frac{N_{total}\,(N_{total} - 1)}{2}\,p_{ua} \qquad (4.2)$$

Here, N_{total} is the total number of instantaneous aircraft in the airspace of all flight phases. To model the conflict probability for UA, p_{ua}, it is necessary to consider the process of conflict detection. This study considers the so called 'state-based' conflict detection algorithm, which is the method used by most studies on decentralized control. In state-based CD, aircraft search for conflicts within a volume of airspace

in front of them. In essence, this involves a 4D extrapolation of aircraft position vectors over a predetermined 'look-ahead' time, t_l, assuming constant velocity vectors; see Figure 4.4(a). A conflict is said to have occurred if the extrapolated path of an another aircraft is predicted to pass through the slanted 'conflict search cylinder' pictured in Figure 4.4(a). If traffic density is uniform, and if aircraft are uniformly distributed in altitude, it can be shown that p_{ua} is equal to the ratio between the average volume of airspace searched for conflicts by aircraft, B_c, and the total volume of the airspace under consideration, B_{total}. For mathematical convenience, B_c can be decomposed into its horizontal and vertical components; see Figure 4.4(b). Using this approach, p_{ua} as can be expressed as [88]:

$$p_{ua} = \frac{B_c}{B_{total}} = \frac{B_{c,h}}{B_{total}} + \frac{B_{c,v}}{B_{total}} = \frac{4\,S_h S_v\,\mathbf{E}\left(V_{r,h}\right)_{ua} t_l + \pi S_h^2\,\mathbf{E}\left(V_{r,v}\right)_{ua} t_l}{B_{total}} \quad (4.3)$$

Here, S_h and S_v are the horizontal and vertical separation requirements. $\mathbf{E}\left(V_{r,h}\right)_{ua}$ and $\mathbf{E}\left(V_{r,v}\right)_{ua}$ are the horizontal and vertical components of the expected relative velocity of all aircraft pairs in UA. The expected relative velocity can be considered equivalent to the weighted average of the relative velocity between all aircraft pairs in the airspace, taking into account the heading and speed distributions of all aircraft. If aircraft are assumed to have equal ground speeds, and if aircraft headings are assumed to be uniformly distributed between 0°-360°, then the ex-

(a) Volume searched for conflicts, B_c (b) Horizontal and vertical components of volume searched for conflicts, $B_{c,h}$ and $B_{c,v}$
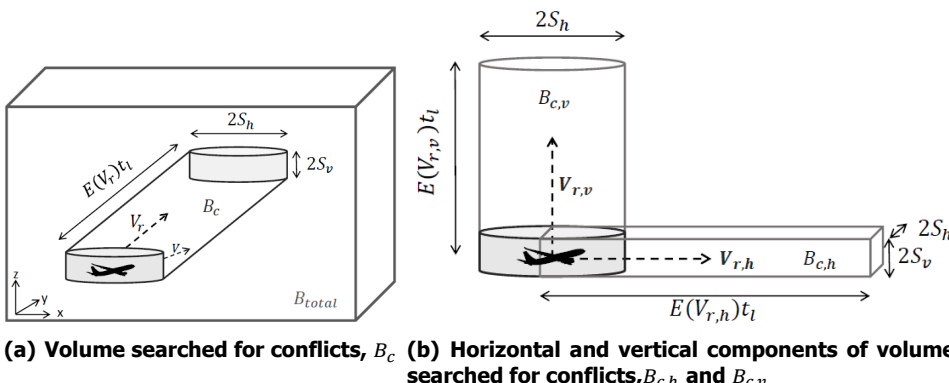
Figure 4.4: Volume searched for conflicts by an aircraft, B_c. Here, B_{total} is the total volume of the airspace. Note that $B_c = B_{c,h} + B_{c,v}$

pected relative velocity components for UA can be computed using the following expressions [88]:

$$\mathbf{E}\left(V_{r,h}\right)_{ua} = \frac{4V_o}{\pi} \tag{4.4a}$$

$$\mathbf{E}\left(V_{r,v}\right)_{ua} = V_o \sin\left(\gamma\right)\left(1 - \varepsilon^2\right) \tag{4.4b}$$

Here, V_o is average ground speed of all aircraft in an airspace, γ is the flight path angle of climbing/descending aircraft, and ε is the proportion of cruising aircraft in the airspace, i.e, $\varepsilon = N_{cruise}/N_{total}$, where N_{cruise} is the number of instantaneous cruising aircraft. Note that the derivation of the above equations for the expected relative velocities decomposes aircraft trajectories into cruising, climbing and descending flight phases [88]. While additional flight phases can be taken into account by the underlying derivation procedure, a segmentation into these three flight phases is considered to be adequate for en route airspaces [88].

4.3.2. Layered Airspace

The altitude constraints imposed by the Layers concept reduces the number of conflicts between cruising aircraft relative to UA. However, no procedural mechanisms are used to separate cruising aircraft from climbing and descending traffic in layered airspaces; see section 4.2.2. Therefore, the conflict count model for layered airspaces needs to be split into three distinct parts based on the flight phase combinations of interacting aircraft:

$$C_{lay} = C_{cruise} + C_{cruise-cd} + C_{cd} \tag{4.5}$$

Here, C_{cruise} is the number of conflicts between cruising aircraft, $C_{cruise-cd}$ is the number of conflicts between cruising and climbing/descending aircraft, and C_{cd} is the number of conflicts between climbing/descending traffic. Each of these three conflict types are discussed in the paragraphs that follow.

4.3.2.1. Conflicts Between Cruising Aircraft

Since the vertical spacing between the predefined flight levels of the Layers concept is, by definition, at least equal to the vertical separation requirement, cruising aircraft in different flight levels can *not* conflict with each other; see section 4.2.2. This in turn reduces the number of possible conflict pairs for cruising aircraft. If aircraft are uniformly distributed over all available flight levels, L, then the number of instantaneous cruising conflicts can be computed as [70, 88]:

$$C_{cruise} = \frac{N_{cruise}\left(\frac{N_{cruise}}{L} - 1\right)}{2} \, p_{cruise} \tag{4.6}$$

Here, p_{cruise} is the average conflict probability between two arbitrary cruising aircraft. Because cruising aircraft in layered airspaces are required to maintain constant altitudes, the velocities of cruising aircraft are purely horizontal. If traffic density is assumed to be uniform in each flight level, then it is possible to show that p_{cruise} is equal to the ratio between the average area of airspace searched for conflicts by an aircraft, A_c, and the total area of one flight level, A_{total}; see Figure 4.5. Using the geometric parameters displayed in Figure 4.5, p_{cruise} can be expressed as:
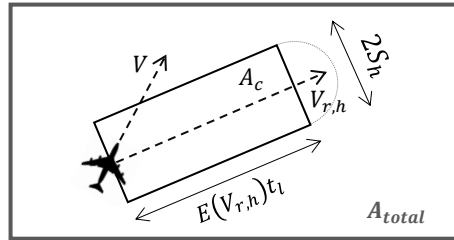
Figure 4.5: Area searched for conflicts, A_c, by cruising traffic in layered airspaces. Here, A_{total} is the total airspace area of one flight level.

$$p_{cruise} = \frac{2\ S_h\ \mathbf{E}\left(V_{r,h}\right)_{cruise}\ t_l}{A_{total}} \tag{4.7}$$

In the above equation, $\mathbf{E}\left(V_{r,h}\right)_{cruise}$ is the expected horizontal relative velocity between cruising aircraft. Previous research has shown that $\mathbf{E}\left(V_{r,h}\right)_{cruise}$ is dependent on the permitted heading range per flight level in layered airspaces, α, and that the relationship between these two variables is highly non-linear [70, 88]. If all aircraft are assumed to have equal ground speeds, and if aircraft headings are uniformly distributed between 0 and α, then $\mathbf{E}\left(V_{r,h}\right)_{cruise}$ can be computed as [70, 88]:

$$\mathbf{E}\left(V_{r,h}\right)_{cruise} = \frac{8V_o}{\alpha}\left(1 - \frac{2}{\alpha}\sin\frac{\alpha}{2}\right) \tag{4.8}$$

From the structure of the above equation, it can be seen that a reduction in α leads to a reduction to $\mathbf{E}\left(V_{r,h}\right)_{cruise}$. Because p_{cruise} is directly proportional to $\mathbf{E}\left(V_{r,h}\right)_{cruise}$, see equation 4.7, a reduction in α, therefore, improves the intrinsic safety provided by layered airspaces.

4.3.2.2. Conflicts Between Cruising and Climbing/Descending Aircraft

Because the Layers concept imposes no constraints to prevent conflicts between cruising and climbing/descending traffic, the model for $C_{cruise-cd}$ is very similar to the model developed for UA, except for two minor differences:

1. The number of combinations of cruising and climbing/descending aircraft is $N_{cruise}\, N_{cd}$. This is because an aircraft can not be cruising and climbing/descending at the same time.

2. Since only cruising-climbing/descending conflicts are to be considered, the calculation of the expected vertical relative velocity, $\mathbf{E}\left(V_{r,v}\right)_{cruise-cd}$, should only consider cases where one aircraft is cruising, while the other is climbing/descending. Using this logic, it can be shown that $\mathbf{E}\left(V_{r,v}\right)_{cruise-cd} = 2V_o \sin\left(\gamma_{cd}\right)\left(\varepsilon - \varepsilon^2\right)$ [88].

Application of these changes to the UA model leads to the following expressions for $C_{cruise-cd}$. These equations make use of the geometrical parameters displayed in Figure 4.4:

4

$$C_{cruise-cd} = N_{cruise}\, N_{cd}\, p_{cruise-cd} \tag{4.9a}$$

$$p_{cruise-cd} = \frac{4\, S_h S_v\, \mathbf{E}\left(V_{r,h}\right)_{cruise-cd} t_l + \pi S_h^2\, \mathbf{E}\left(V_{r,v}\right)_{cruise-cd} t_l}{B_{total}} \tag{4.9b}$$

$$\mathbf{E}\left(V_{r,h}\right)_{cruise-cd} = \frac{4V_o}{\pi} \tag{4.9c}$$

$$\mathbf{E}\left(V_{r,v}\right)_{cruise-cd} = 2V_o \sin\left(\gamma_{cd}\right)\left(\varepsilon - \varepsilon^2\right) \tag{4.9d}$$

4.3.2.3. Conflicts Between Climbing/Descending Aircraft

The model describing the number of instantaneous conflicts between climbing/descending traffic, C_{cd}, is also similar to that derived earlier for UA. In this case, the only difference is in the computation of the expected vertical relative velocity between climbing/descending aircraft, $\mathbf{E}\left(V_{r,v}\right)_{cd}$. Previous research has shown that $\mathbf{E}\left(V_{r,v}\right)_{cd} = V_o \sin\left(\gamma_{cd}\right)\left(1 - \varepsilon\right)^2$ for layered airspace designs [88]. This approach leads to the following for expressions for C_{cd}. These equations make use of the geometrical parameters displayed in Figure 4.4:

$$C_{cd} = \frac{N_{cd}\left(N_{cd} - 1\right)}{2} p_{cd} \tag{4.10a}$$

$$p_{cd} = \frac{4\, S_h S_v\, \mathbf{E}\left(V_{r,h}\right)_{cd} t_l + \pi S_h^2\, \mathbf{E}\left(V_{r,v}\right)_{cd} t_l}{B_{total}} \tag{4.10b}$$

$$\mathbf{E}\left(V_{r,h}\right)_{cd} = \frac{4V_o}{\pi} \tag{4.10c}$$

$$\mathbf{E}\left(V_{r,v}\right)_{cd} = V_o \sin\left(\gamma_{cd}\right)\left(1 - \varepsilon\right)^2 \tag{4.10d}$$

4.4. Traffic Scenario Adjusted Conflict Count Models

As indicated previously, the baseline *analytical* conflict count models rely on idealized assumptions regarding the speed, heading, altitude and spatial distributions of aircraft. If these assumptions are not respected, usage of the analytical models is expected to lead to inaccurate conflict count predictions. By analyzing the assumptions, as well as where they affect the equations, this section proposes *numerical* adjustments to increase the accuracy of the models for more realistic traffic scenarios, for both unstructured and layered airspace designs.

The accuracies of the baseline and adjusted models are determined in this study by comparing model predictions to empirical conflict count data obtained using fast-time simulation experiments. Because the adjustments use numerical methods to generalize model components, they are derived for the same traffic scenario distributions as used in the experiments. Note that all numerical integrations are performed here using the simple 'trapezoidal rule' [115]. Moreover, model adjustments are derived separately for each of the four traffic scenario assumptions. Consequently, each adjustment applies to the case where only one of the four ideal traffic scenario assumptions is violated, while respecting the other three assumptions.

4.4.1. Ground Speed Distribution Adjustment

An important step in the deviation of conflict count models is the computation of the expected relative velocity between aircraft, $\mathbf{E}\left(V_r\right)$, as it is needed to compute the average conflict probability between aircraft, p; see equation 4.3 for UA, and equations 4.7, 4.9b and 4.10b for layered airspaces. To derive expressions for $\mathbf{E}\left(V_r\right)$, the analytical conflict count models for both airspace designs of interest assume equal ground speeds for all aircraft. Because flight path angles are relatively small in en route airspaces, this assumption mainly affects the calculation of the expected *horizontal* relative velocity between aircraft, $\mathbf{E}\left(V_{r,h}\right)$.

To understand how the equal ground speed assumption affects the calculation of $\mathbf{E}\left(V_{r,h}\right)$, it is useful to first consider the magnitude of the horizontal relative velocity between two arbitrary aircraft, $V_{r,h}$; see Figure 4.6. If both aircraft are assumed to have equal speeds, i.e., if $V_1 = V_2 = V$, then the geometry between V_1, V_2 and $V_{r,h}$ becomes an isosceles triangle. Therefore, $V_{r,h}$ can be computed simply as:

$$V_{r,h\ baseline} = 2\ V\ \sin\left(\frac{|\Delta\psi|}{2}\right) \tag{4.11}$$

Since all aircraft are assumed to have equal speeds, equation 4.11 states that only the absolute heading difference between two aircraft, $|\Delta\psi|$, causes variations in $V_{r,h}$ between different aircraft pairs in the airspace. Consequently, to compute $\mathbf{E}\left(V_{r,h}\right)$,

the baseline analytical model integrates equation 4.11 over all possible values of $|\Delta\psi|$:

$$\mathbf{E}\left(V_{r,h}\right)_{baseline} = \int_0^\alpha 2\ V\ \sin\left(\frac{|\Delta\psi|}{2}\right) P\left(|\Delta\psi|\right)\ d\Delta\psi \qquad (4.12)$$

Here, α is the maximum heading difference between two arbitrary aircraft in the airspace. For UA, $\alpha = 360^o$ since there are no constraints on aircraft motion in this airspace design. On the other hand, in layered airspaces, the maximum heading difference between two arbitrary aircraft is dependent on the specific heading-altitude rule in force; for instance $\alpha = 90^o$ for the L90 concept pictured in Figure 4.1.

By using equation 4.12 to compute $\mathbf{E}\left(V_{r,h}\right)$, the baseline analytical conflict count models for both unstructured and layered airspaces assumes that $\mathbf{E}\left(V_{r,h}\right)$ is only dependent on one probability density function, i.e., that of the absolute heading difference between two arbitrary aircraft, $P\left(|\Delta\psi|\right)$. Evaluation of equation 4.12 using the appropriate values of α results in relatively simple analytical expressions for $\mathbf{E}\left(V_{r,h}\right)$; see equation 4.4a for UA, and equation 4.8 for layered airspaces.

However, for real-life operations, all aircraft in a given volume of airspace are unlikely to fly with equal ground speeds. This can be due to several reasons including the fact that different aircraft types have different optimum cruising speeds, and because standard operating procedures vary between different airlines. If aircraft are not assumed to fly with equal ground speeds, then the model for $\mathbf{E}\left(V_{r,h}\right)$ must be adjusted to take into account the actual speed distributions of all aircraft in the airspace.

To begin the derivation of the ground speed adjusted model for $\mathbf{E}\left(V_{r,h}\right)$, it is once again useful to reconsider the computation of $V_{r,h}$ for an arbitrary pair of aircraft, see Fig. 4.6. If $V_1 \neq V_2$, the cosine rule needs to be used to rewrite equation 4.11 as:
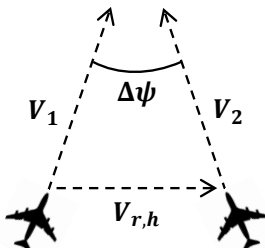
Figure 4.6: The relationship between velocity, V, relative velocity, V_r, and heading difference $\Delta\psi$ for two arbitrary aircraft

$$V_{r,h \ adjusted} = \left(V_1^2 + V_2^2 - 2V_1V_2 \cos(\Delta\psi)\right)^{1/2} \tag{4.13}$$

Since the values of V_1, V_2 and $|\Delta\psi|$ can be different for every aircraft pair in the airspace, to compute the ground speed adjusted version of equation 4.12, it is necessary to integrate equation 4.13 over all possible values of velocity and absolute heading difference, while taking into account the probability density functions of velocity magnitudes and absolute heading differences, $P(V_1)$, $P(V_2)$ and $P(|\Delta\psi|)$:

$$\mathbf{E}\left(V_{r,h}\right) = \int_{V_1}\int_{V_2}\int_0^\alpha \left(V_1^2 + V_2^2 - 2V_1V_2 \cos(\Delta\psi)\right)^{1/2} P(\Delta\psi)\,P(V_1)\,P(V_2)\ d\Delta\psi\,dV_1\,dV_2 \tag{4.14}$$

Due to the complexity of equation 4.14, the ground speed model adjustment can only be evaluated numerically. This has been performed for the four speed distributions displayed in Figure 4.7, while assuming a uniform distribution of aircraft headings (as stated previously, the model adjustments consider the effect of one scenario assumption at a time). Here the equal speed case corresponds to the assumption used by the baseline analytical model. The physical interpretation for the other three distributions corresponds to the hypothetical distributions of different aircraft types in a particular volume of airspace. For example, a bimodal speed distribution can occur if there are two dominant aircraft types in an airspace, e.g. 737s and A320s.
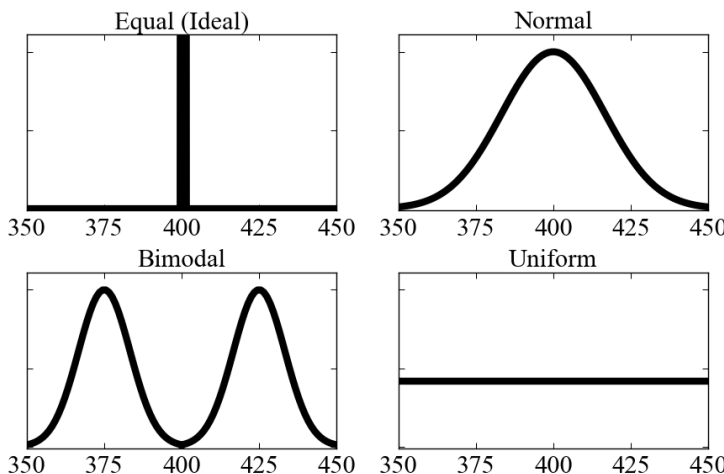
Figure 4.7: Probability density functions for the four speed distributions used for fast-time simulations

Table 4.1: Numerically computed expected horizontal relative velocities for the
ground speed distributions pictured in Figure 4.7

	Equal (Ideal)	Normal	Bimodal	Uniform
UA / L360 [kts]	509	507	509	512
L180 [kts]	370	370	373	374
L90 [kts]	203	205	208	210

Table 4.1 lists the numerically determined values of $\mathbf{E}\left(V_{r,h}\right)$ for the four speed
distributions displayed in Figure 4.7. Note that there are no differences between
the UA and the L360 concepts in terms of $\mathbf{E}\left(V_{r,h}\right)$, since $\alpha = 360^o$ in both cases (and
therefore no differences when evaluating the inner-most integral of equation 4.14).
More interestingly, the table indicates that ground speed distribution has a very
minor effect on $\mathbf{E}\left(V_{r,h}\right)$; varying the speed distribution from its 'ideal' setting only
causes slightly higher values of $\mathbf{E}\left(V_{r,h}\right)$ for all the airspace concepts considered
here. Consequently, ground speed distribution is not expected to have a significant
impact on the accuracy of the baseline analytical conflict count models for UA, or
for the layered airspace concepts considered in this work. This hypothesis is tested
using simulation experiments; see section 4.6.2.
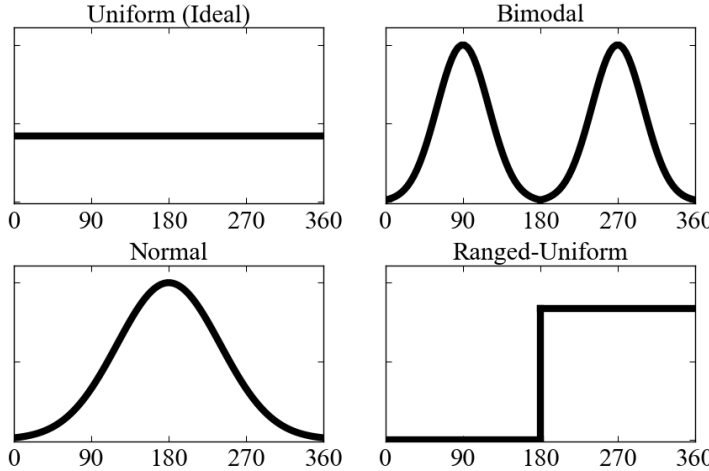
4.4.2. Heading Distribution Adjustment

As implied by equation 4.14, in addition to the speed distribution of aircraft, the
expected horizontal relative velocity between aircraft, $\mathbf{E}\left(V_{r,h}\right)$, is also affected by
the probability density function of the absolute heading difference between aircraft,
$P\left(|\Delta\psi|\right)$. The baseline analytical models assume a uniform distribution of aircraft
headings between 0 and α, where $\alpha = 360^o$ for UA, and depends on the spe-
cific heading-altitude rule selected for layered airspaces. For this 'ideal' heading
distribution, it can be shown that $P\left(|\Delta\psi|\right)$ has a triangular shape between 0 and
α [70]:

$$P\left(|\Delta\psi|\right)_{uniform} = \frac{2}{\alpha}\left(1 - \frac{|\Delta\psi|}{\alpha}\right) \tag{4.15}$$

Logically, the above expression for $P\left(|\Delta\psi|\right)$ should only be used to evaluate equa-
tion 4.14 when aircraft headings are uniformly distributed between 0 and α. How-
ever, the baseline analytical conflict count models assume a uniform distribution of
headings regardless of the actual heading distribution observed for a given traffic
scenario. Therefore, the accuracies of the analytical models are expected to be
reduced if aircraft headings are not uniformly distributed.

To ensure high model accuracy for other 'non-ideal' heading distributions, the ap-
propriate function for $P\left(|\Delta\psi|\right)$ should be used when numerically evaluating equa-
tion 4.14. In this work, the four heading distributions pictured in Figure 4.8 are

Figure 4.8: Probability density functions for the four heading distributions used for fast-time simulations

Table 4.2: Numerically computed expected horizontal relative velocities for the
heading distributions pictured in Figure 4.8

	Uniform (Ideal)	Bimodal	Normal	Ranged-Uniform
UA / L360 [kts]	509	485	395	370

used. In this figure, the uniform heading distribution matches the assumption made by the baseline analytical model. The normal and ranged-uniform heading distributions represent traffic scenarios with one, or a range of, predominant aircraft headings; these two cases are representative of traffic moving towards oceanic airspace. The bimodal distribution, on the other hand, is used to consider scenarios with head-on traffic. This could be indicative of the traffic pattern between the east and west coasts of the United States. For these cases, the following expressions describe $P\left(|\Delta\psi|\right)$:

$$P(|\Delta\psi|)_{normal} = \frac{\sqrt{2}}{\sigma\sqrt{\pi}} e^{-\frac{\Delta\psi^2}{2\sigma^2}} \tag{4.16a}$$

$$P(|\Delta\psi|)_{bimodal} = \frac{1}{2\sqrt{2\pi\sigma^2}} e^{\frac{(\Delta\psi-\pi)^2}{2\sigma^2}} + \frac{1}{\sqrt{2\pi\sigma^2}} e^{-\frac{\Delta\psi^2}{2\sigma^2}} \tag{4.16b}$$

$$P(|\Delta\psi|)_{ranged-uniform} = \frac{4}{\alpha^2}(\alpha - 2\Delta\psi) \tag{4.16c}$$

Table 4.2 displays the $\mathbf{E}\left(V_{r,h}\right)$ values for the four heading distributions pictured in Figure 4.8. These values were computed by numerically evaluating equation 4.14

using the appropriate expressions listed above for $P\left(|\Delta\psi|\right)$. As before, the effect of each traffic scenario assumption is considered on a case-by-case basis, and therefore, in this context, equation 4.14 is evaluated while assuming equal speeds for all aircraft, i.e., using the speed setting corresponding to the ideal traffic scenario. For a similar reason, only the UA and L360 concepts are used to assess the impact of heading distribution on model accuracy. This is because aircraft altitude is closely tied to aircraft heading for layered designs with $\alpha < 360^{o}$, see equation 4.25. Consequently, it is not possible to alter aircraft heading distribution without adversely affecting the altitude distribution from its ideal setting for such airspace designs.

Table 4.2 shows that $\mathbf{E}\left(V_{r,h}\right)$ is the highest for the uniform heading distribution, although there is no substantial difference between the uniform and bimodal cases. However, $\mathbf{E}\left(V_{r,h}\right)$ is significantly lower for the normal and ranged-uniform heading distributions when compared to the uniform/ideal case. Therefore, the baseline analytical models for both unstructured and layered airspaces are expected to *overestimate* conflict counts when aircraft headings are normally or ranged-uniformly distributed.

4.4.3. Altitude Distribution Adjustment

In en route airspace, most aircraft are in the cruise phase of flight. Therefore, the uniform altitude distribution assumption made by the baseline analytical models applies *mainly* to cruising aircraft. Although this is true for both unstructured and layered airspaces, unlike the other traffic scenario assumptions, the model adjustments required to take into account the altitude distribution of cruising traffic differs between these two airspace designs. The following paragraphs present the model adjustments needed for each airspace design separately.

4.4.3.1. Unstructured Airspace

For UA, equation 4.3 shows that conflict probability is computed as the summation of two ratios; 1) the ratio between the volume searched for conflicts in the horizontal direction, $B_{c,h}$, and the total airspace volume, B_{total}, and 2) the ratio between the volume searched for conflicts in the vertical direction, $B_{c,v}$, and B_{total}. The first of these two ratios assumes a uniform distribution of aircraft cruising altitudes. However, if traffic is not spread-out uniformly in the vertical direction, then aircraft in busier altitudes are more likely to experience conflicts than aircraft in less dense altitudes.

To take into account the vertical distribution of aircraft for a given traffic scenario, the altitude-related model adjustment for UA introduces a new variable p_v. This variable considers the effect of cruising altitude distribution on the average conflict probability between aircraft, p_{ua}, and it can be calculated as [69]:

$$p_v = \int_{Z_{min}}^{Z_{max}} P_z(h) \int_{h+S_v}^{h-S_v} P_z(u) \; du \; dh \tag{4.17}$$

Here, Z_{min} and Z_{max} are the minimum and maximum altitudes of the airspace volume of interest, and P_z represents the probability density function of aircraft cruising altitudes. Additionally, h is the altitude variable for an aircraft i, and u is the altitude variable for an aircraft j, where aircrafts i and j are two arbitrary aircraft in the airspace. In essence the inner integral in the above equation considers the probability that aircraft j is located within the vertical separation requirement of aircraft i, and the outer integral evaluates the probability that aircraft i is located within the upper and lower altitudes of the airspace volume of interest. If aircrafts i and j are both assumed to be located within the same airspace, then P_z is the same for both aircraft.

Using equation 4.17, it is possible to derive a generalized model for p_{ua} that takes into account the vertical distribution of traffic. To illustrate this process, it is useful reverse engineer the expression used by the baseline analytical model for p_{ua}. To this end, equation 4.17 is evaluated for the case where aircraft altitudes are uniformly distributed:

$$
\begin{aligned}
p_{v, \, uniform} &= \int_{Z_{min}}^{Z_{max}} \frac{1}{h} \int_{h+S_v}^{h-S_v} \frac{1}{u} \; du \; dh \\
&= \frac{2S_v \, (Z_{max} - Z_{min}) - S_v^2}{(Z_{max} - Z_{min})^2} = \frac{2S_v H - S_v^2}{H^2} \\
&\approx \frac{2S_v}{H} \quad \text{if } H \gg S_v
\end{aligned}
\tag{4.18}
$$

Here, H is the height of the airspace volume of interest. Note that the final expression shown above assumes that $H \gg S_v$, as is the case for most practical en route airspaces. The above expression was implicitly used during the derivation of the baseline analytical version of p_{ua} because:

$$p_{ua, \, uniform} = \frac{B_{c,h}}{B_{total}} + \frac{B_{c,v}}{B_{total}}$$

$$= \frac{4 \, S_h \, S_v \, \mathbf{E}\left(V_{r,h}\right) t_l}{B_{total}} + \frac{B_{c,v}}{B_{total}}$$

$$= \underbrace{\frac{2 \, S_h \, \mathbf{E}\left(V_{r,h}\right) t_l}{A_{total}} \cdot \frac{2 S_v}{H}}_{p_{v, \, uniform}} + \frac{B_{c,v}}{B_{total}} \qquad (4.19)$$

Here, the relationship between the area and the volume of a shape with a constant cross-section is used, i.e., $B_{total} = A_{total} \cdot H$. From the above derivation of $p_{ua, \, uniform}$, it is clear that the generalized version of p_{ua} can be written as:

$$p_{ua} = \frac{2 \, S_h \, \mathbf{E}\left(V_{r,h}\right) t_l}{A_{total}} \cdot p_v + \frac{B_{c,v}}{B_{total}} \qquad (4.20)$$

Here, p_v should be computed using equation 4.17 while taking into account the actual altitude distribution in a given traffic scenario. As for the other model adjustments, equation 4.17 can be evaluated numerically for cases where the altitude distribution is non-uniform. This approach has been taken for the four altitude distributions considered in this study; see Figure 4.9. As for the other traffic scenario properties, the uniform distribution corresponds to assumption made by the baseline analytical model. Normally distributed altitudes represent the case where most aircraft prefer to cruise within a narrow range of flight levels, a situation that is representative of current en route operations over continental airspace. A similar explanation can also be applied to the bimodal distribution when considering a mix of turbo-prop and jet aircraft; a set of lower altitudes for turbo-props, and a set of higher altitudes for jets. Finally, the ranged-uniform case approximates the preference of long distance flights over oceanic airspace to use only high altitude flight levels to minimize fuel burn.

The numerically computed values of p_v for the four considered altitude distributions are listed in Table 4.3. Unlike the heading distribution of aircraft, this table shows that a uniform distribution of altitudes leads to the lowest conflict probability between aircraft. Therefore, the baseline analytical model for UA is expected to *underestimate* conflict counts for cases with non-uniform altitude distributions.

4.4.3.2. Layered Airspace

Cruising aircraft in layered airspaces are required to fly at predefined altitudes; see section 4.2.2. Consequently, conflict probability for cruising aircraft in layered airspaces is a function of the *area* searched for conflicts by an aircraft. Since the
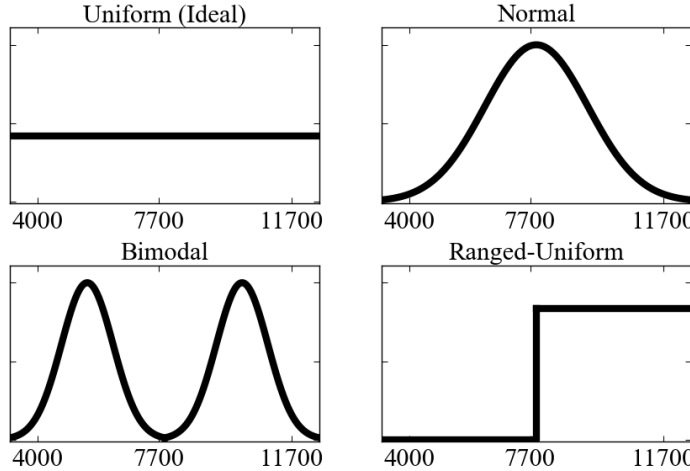
Figure 4.9: Probability density functions for the four altitude distributions used for fast-time simulations

Table 4.3: Numerically computed p_v values for Unstructured Airspace (UA) for the altitude distributions pictured in Figure 4.9

	Uniform (Ideal)	Normal	Bimodal	Ranged-Uniform
UA	0.171	0.289	0.289	0.342

area searched for conflicts is independent of the vertical separation requirement, the conflict probability between cruising aircraft is, in contrast to UA, *not* affected by altitude distribution; see equation 4.7.

Instead, the altitude distribution of traffic affects the computation of the total number of combinations of two cruising aircraft in layered airspaces, i.e., altitude distribution affects the maximum number of *possible* conflicts that can occur between cruising aircraft at each flight level in the Layers concept.

The baseline analytical model assumes an equal number of cruising aircraft in each altitude layer, and therefore, the total number of cruising aircraft in all layers, N_{cruise}, can be used to directly compute the total number of combinations of cruising aircraft in the entire airspace; see equation 4.6. However, if cruising aircraft are not uniformly distributed over all available flight levels, then number of combinations of cruising aircraft in each altitude band varies from layer to layer, and therefore, the number of combinations of cruising aircraft needs to be computed separately for each layer. If $N_{cruise,k}$ is the number of instantaneous cruising aircraft in altitude layer k, then the number of instantaneous cruising conflicts in layer k, $C_{cruise,k}$, is equal to:

$$C_{cruise,k} = \frac{N_{cruise,k}\left(N_{cruise,k} - 1\right)}{2}\, p_{cruise} \tag{4.21}$$

Here, p_{cruise} is the average conflict probability between any two cruising aircraft; see equation 4.7. If no assumptions can be made on the vertical distribution of traffic, then the total number of instantaneous cruising conflicts in the airspace, C_{cruise}, can be computed by summing up equation 4.21 over all available flight levels, L:

$$C_{cruise} = \sum_{k=1}^{L} \frac{N_{cruise,k}\left(N_{cruise,k} - 1\right)}{2}\, p_{cruise} \tag{4.22}$$

Equation 4.22 is the generalized version of equation 4.6, and as such, equation 4.22 can be applied to any altitude distribution as long as the number of cruising aircraft in each predefined flight level is known. On comparing these two equations, it can be see that any non-uniform altitude distribution will lead to an increase in the number of conflicts. As such, the baseline analytical model for layered airspaces is hypothesized to *under-estimate* the number of conflicts for non-ideal traffic scenarios.

4.4.4. Spatial Distribution Adjustment

Conflict probability computation by the baseline analytical models for both unstructured and layered airspace designs assume an equal likelihood of conflicts in all parts of the airspace. However, if the spatial/density distribution of traffic is not uniform, then more conflicts are likely to occur in airspace areas with higher traffic densities.

To deal with the effect of so called traffic density 'hot-spots' on conflict counts, the model adjustment for the spatial distribution of traffic discretizes the airspace into a number of smaller areas, each with a more uniform distribution of aircraft locations. Subsequently, the total conflict count for the entire airspace can be determined as the summation of the conflict counts for each sub-area, while taking into account the interactions that occur between with different the sub-areas:

$$C = \sum_{i=1}^{n} \frac{N_{area_i}\left(N_{area_i} - 1\right)}{2} p_{area_i} + \sum_{i=1}^{n}\sum_{j=1}^{n} N_{area_i} N_{area_j} p_{area_{i,j}} \tag{4.23}$$

Here, N_{area_i} is the number of aircraft in sub-area i, and p_{area_i} is the conflict probability in sub-area i. Because this approach presumes a constant, or near constant, density in each sub-area, p_{area_i} can be computed using the baseline analytical models for conflict probability, i.e., using equation 4.3 for UA, and equations 4.7, 4.9b

(a) Uniform (Ideal)

(b) Hot-Spot 1, Radius = 55 NM

(c) Hot-Spot 2, Radius = 40 NM
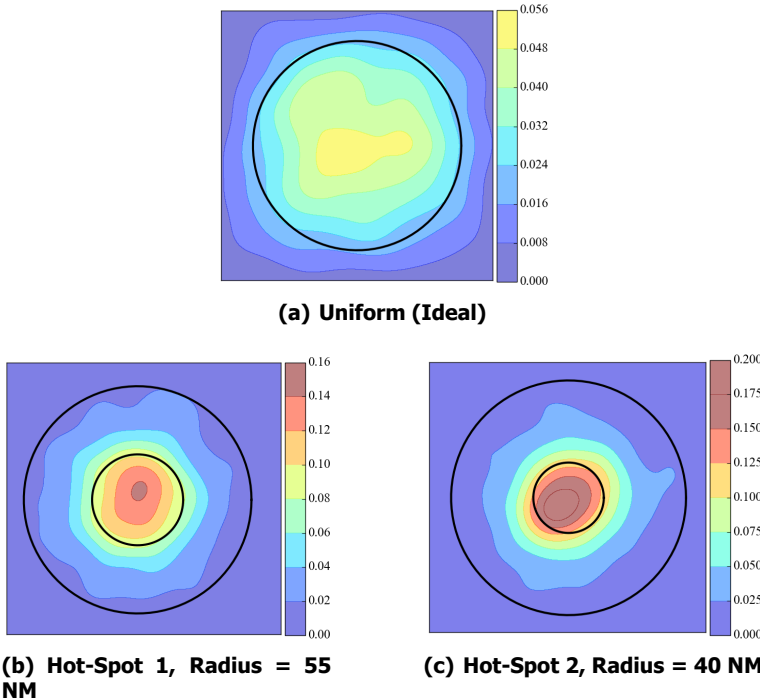
Figure 4.10: Traffic density heat-maps for the three spatial distributions used for fast-time simulations. The outer circle represents the boundary of the 'experiment region'. The inner circle represents the boundary of the hot-spot area.

and 4.10b for layered airspaces, but by taking into account the size of each sub-area i. A similar procedure can be followed for calculating $p_{area_{i,j}}$, except in this case the sum of the sizes of sub-areas i and j should be used.

It should be noted that the first summation term of equation 4.23 considers the number of conflicts that occur in each of the sub-areas, whereas the second summation term computes the number of conflicts that occur as a result of interactions between aircraft in different sub-areas. This logic applies to both UA and layered airspaces; the only difference for layered airspaces is that this approach should be applied separately to the three flight phase combinations taken into account by the corresponding baseline analytical model, see equation 4.5. A discretization into sub-areas can be achieved using clustering algorithms, such as the well-known DB-SCAN method [116], to detect airspace regions with near uniform traffic densities. Once the location and number of sub-areas are identified, recursive programming can be used to implement equation 4.23.

Heat-maps of the three spatial distributions considered in this study are pictured in Figure 4.10. Here it can be seen that traffic density is relatively uniform within the cylindrical 'experiment region' for the 'ideal' traffic scenario; see section 4.5.2

for more information on the design of the simulation's physical environment. On the other hand, the two hot-spot cases contain density concentrations at the center of the airspace, with a radius of 55 and 40 nautical miles, respectively. Such hot-spots can be trigged during real-life operations at the merge point of several traffic streams. Because the baseline analytical models for both unstructured and layered airspaces assume a constant density distribution, they are expected to underestimate the number of conflicts for the two hot-spot conditions, with the highest conflict count expected for hot-spot 2.

4.5. Fast-Time Simulation Design

Four fast-time simulation experiments were performed to investigate the accuracies of the analytical and adjusted conflict count models for unstructured and layered airspace designs, using traffic scenarios with varying speed, heading, altitude and spatial distributions. This section describes the design of these experiments.

4.5.1. Simulation Development

4.5.1.1. Simulation Platform

The BlueSky open-source ATM simulator was used as the simulation platform in this research. It was developed at the Delft University of Technology (TU Delft) using the Python programming language[1]. BlueSky has numerous features including the ability to simulate more than 5000 aircraft simultaneously, a suite of conflict detection and resolution algorithms, and extensive data logging functions. A complete overview of BlueSky is provided in [108].

In order to simulate aircraft performance dynamics, BlueSky uses point-mass Aircraft Performance Models (APMs) that are similar in structure to Eurocontrol's well known Base of Aircraft Data (BADA) models. The main difference between these two approaches is that BlueSky uses openly available data to quantify the APMS. To simplify the simulations, all traffic was simulated using a Boeing 744 model. A full description of the BlueSky APMs, including their validation, can be found in [109].

4.5.1.2. Conflict Detection

In this study, the so called 'state-based' conflict detection method was used. This method predicts separation violations by linearly extrapolating aircraft positions over a predefined look-ahead time. Here, a look-ahead time of 5 minutes, as well as separation requirements of 5 nautical miles horizontally and 1000 ft vertically, were used.

---

[1]BlueSky can be downloaded from `https://github.com/ProfHoekstra/blueksy`

As mentioned in section 4.2.4, the models derived in this chapter are concerned with the intrinsic safety provided by an airspace design. Since the notion of intrinsic safety focuses on the number of *truly occurring* conflicts as a function of airspace design, conflict detection was performed assuming perfect knowledge of aircraft states. For the same reason, the simulations were performed without tactical conflict resolutions.

4.5.1.3. Airspace Concepts and Concept Implementation

Unstructured Airspace (UA) and three layered airspace concepts, each with a different allowed heading range per flight level, α, were used in the fast-time simulations. Table 4.4 displays the properties of the considered airspace concepts, and also indicates which concepts were used in each of the three experiments performed in this study.

Table 4.4: Properties of the airspace concepts used in the three simulation experiments

Symbol	Name	Heading Range Per Layer, α	Number of Layer Sets, κ
UA	Unstructured Airspace	-	-
L360	Layers 360	360°	8
L180	Layers 180	180°	4
L90	Layers 90	90°	2

The airspace concepts were implemented into BlueSky by modifying its trajectory planning functions. While direct horizontal routes were used in both unstructured and layered airspaces, the method used to determine the cruising altitude of an aircraft differed between the two airspace designs. For UA, the cruising altitude of an aircraft, $Z_{ua,i}$, was directly proportional to its trip distance, D_i:

$$Z_{ua,i} = Z_{min} + \frac{Z_{max} - Z_{min}}{D_{max} - D_{min}} \ (D_i - D_{min}) \tag{4.24}$$

Here, Z_{min} and Z_{max} are the minimum and maximum altitudes allowed for cruising aircraft in the simulation. Comparably, D_{min} and D_{max} are the minimum and maximum trip distances of aircraft in the simulation.

On the other hand, for the Layers concept, the cruising altitude of an aircraft, $Z_{lay,i}$, depended on both its heading, ψ_i, and its trip distance, D_i, as indicated by the following heading-altitude rule:

$$Z_{lay,i} = Z_{min} + \zeta \left[\left\lfloor \frac{D_i - D_{min}}{D_{max} - D_{min}} \ \kappa \right\rfloor \beta + \left\lfloor \frac{\psi_i}{\alpha} \right\rfloor \right] \tag{4.25}$$

Here, β is the number of flight levels needed to define one complete set of layers, and κ is the number of complete layer sets. These two parameters are defined as

$\beta = 360^o/\alpha$ and $\kappa = L/\beta$, where L is the total number of available flight levels. Note that the second term of equation 4.25 computes the cruising altitude of an aircraft as an *integer multiple* of the vertical spacing between flight levels, ζ, and uses the the floor operator ('$\lfloor$ $\rfloor$'). For all layered concepts in this study, $\zeta = 1100$ ft and $L = 8$. Correspondingly, for all layered concepts, $\kappa > 1$; see Table 4.4. Therefore, equation 4.25 uses trip distances to determine cruising altitudes such that short flights remain at lower altitudes, while longer flights use higher layer sets.

It should be noted that the only difference between the UA and L360 concepts is the use of predefined flight levels for cruising aircraft in L360, while any altitude could be selected by aircraft in UA. Additionally, only the UA and L360 concepts are used for the 'Heading' and 'Altitude' experiments. This is because the aim of the experiments is to study the effect of each traffic scenario assumption on a case-by-case basis, and for these two concepts, heading and altitude distributions can be varied without directly affect the other traffic scenario distributions; for L180 and L90, the heading distribution influences the altitude distribution, and vice versa.

4.5.2. Traffic Scenarios

4.5.2.1. Testing Region and Flight Profiles

A large three-dimensional en-route sector was used as the physical environment for traffic simulations, see Figure 4.11. In the horizontal plane, the sector had a square-shaped cross-section of 400 x 400 nautical miles. In the vertical dimension, the sector is divided into two parts; a 'transition zone' with a height of 4000 ft for climbing and descending traffic, and a 'cruising zone' with a height of 7700 ft. Figure 4.11 also shows the horizontal and vertical flight profiles of an example flight.
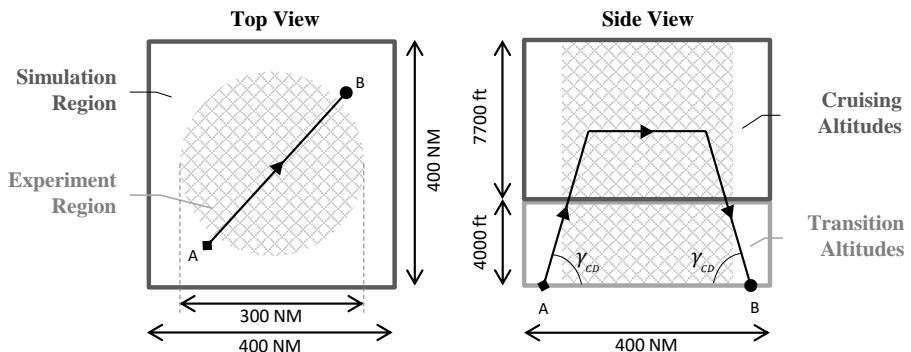
Figure 4.11: Top and side views of the simulation's physical environment. The trajectory of an example flight is shown.

As no traffic was simulated outside the simulated sector, aircraft near the edges of the 'simulation region' are unlikely to get into conflicts. To solve this issue, a smaller cylindrical 'experiment region', with a diameter of 300 nautical miles, was defined

Table 4.5: Common parameters for all four experiments

Parameter	Value	Description
A_{total}	$7.0685 \cdot 10^4$ NM²	Area of 'experiment region'
B_{total}	$3.0533 \cdot 10^{16}$ ft ³	Volume of 'experiment region'
D_{min}	200 NM	Minimum trip distance
D_{max}	250 NM	Maximum trip distance
$\bar{D}$	225 NM	Average trip distance
t_l	5 mins	Conflict detection look-ahead time
S_h	5 NM	Horizontal separation requirement
S_v	1000 ft	Vertical separation requirement
L	8	Number of flight levels for layered airspaces
$\bar{V}$	400 kts	Average ground speed of aircraft
γ_{cd}	2.82^o	Flight-path angle of climbing/descending aircraft
ε	0.82	Proportion of cruising aircraft

in the center of the 'simulation region'. The resulting gap between the experiment and simulation regions ensured that aircraft within the experiment region were surrounded by traffic in all directions. Correspondingly, only aircraft within the experiment region, and only conflicts with closest points of approach within the experiment region, were used to assess the accuracy of the conflict count models. The parameters of the experiment region needed to evaluate the models, as well as other parameters common to all four experiments, are listed in Table 4.5.

4.5.2.2. Traffic Demand Scenarios

A scenario generator was created to produce traffic scenarios with a desired and constant traffic density. Constant density scenarios were used so that the number of instantaneous conflicts logged during a simulation run could be attributed to a particular traffic density. Since aircraft were deleted from the simulation as they exited the sector, to realize constant density scenarios, aircraft were introduced into the simulation at a constant spawn rate equal to $\frac{\bar{V}}{\bar{D}} N$, where $\bar{V}$ is the average speed of aircraft, $\bar{D}$ is the average trip distance of aircraft, and N is the desired number of instantaneous aircraft. Using this approach, five traffic demand scenarios of increasing density were defined, ranging between 5-100 aircraft per 10,000 NM² in the simulation region. This corresponds to an instantaneous traffic demand of between 80-1600 aircraft in the simulation region; see Table 4.6. Note that this table displays the number of instantaneous aircraft in both the 'simulation' and 'experiment' regions. Furthermore, five repetitions, representing five random initial conditions, were tested for each traffic demand condition.

It should be noted that all scenarios were generated off-line prior to the simulations. This ensured that all airspace concepts could be subjected to the same traffic demand volumes. Additionally, scenarios had a duration of 2 hrs, consisting of a 1

Table 4.6: Number of instantaneous aircraft for the 5 traffic demand scenarios

#	Simulation Region	Experiment Region
1	80.0	58.3
2	302.9	218.4
3	589.4	422.3
4	1147.0	810.1
5	1600.0	1116.8

hour traffic volume buildup period, and a 1 hour logging period during which the traffic density was kept constant.

4.5.3. Independent Variables

Although the same five traffic demands were used for all experiments, the specific traffic patterns used varied between the four simulation experiments. This is because each experiment focused on analyzing the effect of one particular traffic scenario distribution on the accuracies of the baseline and adjusted conflict count models, for both unstructured and layered airspaces. The follow paragraphs describe the traffic speed, heading, altitude and spatial distributions used by each experiment.

4.5.3.1. Ground Speed Experiment

In this experiment, four different distributions were used to specify the ground speeds of aircraft, see Fig. 4.7. All speed distributions had a mean speed of 400 kts to allow for a fair comparison between conditions. Additionally, the scenarios of this experiment used uniform heading, altitude and spatial distributions, and considered the UA, L360, L180 and L90 concepts. This resulted in a total of 400 simulation runs, involving over 1,000,000 flights.

4.5.3.2. Heading Experiment

For the heading experiment, simulations were repeated for the four different heading distributions shown in Fig. 4.8. Each heading distribution was combined with uniform altitude and spatial distributions. Furthermore, this experiment used an equal ground speed of 400 kts for all aircraft, and considered the UA and L360 airspace designs. This resulted in a total of 200 simulation runs, using over 500,000 flights.

4.5.3.3. Altitude Experiment

The altitude experiment considered the effect of the four altitude distributions displayed in Fig. 4.9 on conflict counts. For this experiment, the ground speed of all aircraft equaled 400 kts, while the altitude and spatial distributions of traffic were

uniform. This experiment was repeated for the UA and L360 concepts. This resulted in a total of 200 simulation runs, with over 500,000 flights.

4.5.3.4. Spatial Experiment

The final experiment considered the effect of the spatial distribution of traffic on conflict counts. Therefore, the simulations were performed for three different spatial distributions; see Fig. 4.10. All spatial distributions were combined with traffic scenarios that had a uniform distribution of headings and altitudes, and with an equal ground speed of 400 kts for all traffic. This experiment was repeated for the UA, L360, L180 and 190 concepts. This resulted in a total of 300 simulation, using approximately 750,000 flights.

4.5.4. Dependent Variables

To determine the accuracy of both baseline and adjusted conflict count models, model predictions were compared to actual conflict counts logged during the simulations. Model accuracy was quantified by introducing a model accuracy parameter, k, as illustrated below:
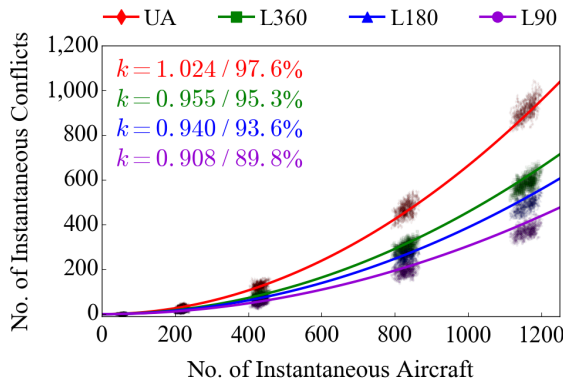
$$\text{No. of Inst. Conflicts} \ = \ \text{Gas Model} \ \times \ k$$

From the above, it can be seen that k acts as a constant scaling parameter to the models. The value of k is determined by fitting the models to the simulation data in a least-square sense. A value of k close to 1 indicates high model accuracy, while $k < 1$ and $k > 1$ indicates model over- and under-estimation of simulation data, respectively. For easy analysis of the results, model accuracy is also computed as a percentage by comparing the fitted k value to a reference value of 1. Furthermore, separate k values are computed for the analytical and 'adjusted' conflict count models for each simulation condition.

To determine the value of k using least-squares, during the simulations, the number of instantaneous conflicts, and the number of instantaneous aircraft were logged periodically every 15 seconds. Additionally only aircraft within the experiment region, and only conflicts with closest points of approach within the experiment region, were used to assess model accuracy. As mentioned earlier, this method for counting aircraft and conflicts is used because the traffic scenarios had a traffic density of zero outside the simulation region. A similar approach to analyzing simulation data was used in [68].

4.6. Results

The results of the fast-time simulation experiments are presented in this section. The analysis is primarily concerned with the effect of traffic scenario distributions

Figure 4.12: Empirical conflict counts (scatter points) and analytical model prediction (solid lines), ideal traffic scenario

on the accuracies on the analytical and the 'adjusted' conflict count models for unstructured and layered airspace designs.

4.6.1. Accuracy of the Baseline Analytical Model

Accuracy of the Baseline Analytical Model for the Ideal Traffic Scenario Before studying the effect of the four traffic scenario distributions on model accuracy, it is useful to consider the performance of the baseline analytical conflict count models for the 'ideal' traffic scenario. For the ideal case, all traffic scenario characteristics match the assumptions made during the derivation of the analytical models, i.e., all aircraft are assumed to fly with equal ground speeds, with uniform heading, altitude and spatial distributions. Therefore, the accuracies of the analytical models are expected to the highest for the ideal scenario. The corresponding results for both unstructured and layered airspaces are shown in Figure 4.12. In this figure, the scatter points represent the raw simulation data, whereas the solid lines represent the *predictions* of the analytical models. Note that the raw simulation data appears in 5 clusters since 5 traffic demand scenarios were used in the simulations, with cluster representing data collected from all repetitions of a particular demand condition; see Table 4.6. Additionally, model accuracies are listed in the top-left corner of this figure using the method described in section 4.5.4.

From Figure 4.12, it can be clearly seen that the baseline analytical model for UA, described in section 4.3.1, closely approximates both the shape and the scaling of the relationship between the number of instantaneous aircraft and the number of instantaneous conflicts. In fact, model accuracy for UA was determined to be as high as 97.6% for the ideal traffic scenario.

Although model accuracies for layered airspaces are shown to be high in an absolute sense, Figure 4.12 also indicates that the corresponding analytical model, described in section 4.3.2, is less accurate than the analytical model for UA. On close inspec-
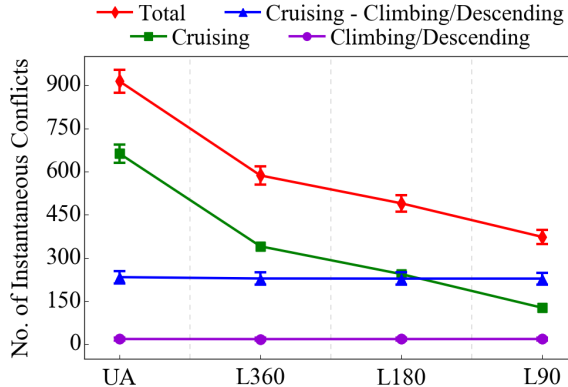
Figure 4.13: Means and 95% confidence intervals of the conflict count per conflict type at the highest traffic density, ideal traffic scenario

tion of this figure, the model for layered airspaces appears to over-estimate the number of conflicts, a conclusion that is confirmed by k values that are consistently less than 1 for all layered concepts. Moreover, the degree of over-estimation worsens as the heading range per flight level, α, is decreased; accuracy decreases by approximately 5% when α is reduced from 360° to 90°.

The lower accuracies for layered airspaces, as well as the reduction of accuracy for smaller values of α, can be explained by considering the interaction between two factors: the higher proportion of conflicts involving climbing/descending aircraft for layered airspaces, and the fact that no traffic was simulated above or below the considered sector during the experiments.

Before continuing with the explanation for the slightly lower model accuracies found for layered airspaces, we first provide evidence for the first factor mentioned above. To this end, Figure 4.13 displays error bars for conflict counts categorized according to the flight phases of interacting aircraft. Although this figure shows that a reduction of α reduces the total number of conflicts (red line), the number of conflicts involving climbing/descending traffic is found to be invariant with airspace concept (blue and violet lines). This is because none of the airspace designs considered here impose any constraints on the motion of climbing/descending traffic. Nonetheless, as the total conflict count decreases without affecting the number of climbing/descending conflicts, the relative importance of the latter conflict type increases for layered airspaces.

Although climbing/descending aircraft have a greater influence on the intrinsic safety of layered airspaces relative to UA, this fact by itself should not, in theory, negatively affect the accuracies of the corresponding models. It does, however, mean that climbing/descending conflicts have a larger weight on model accuracy for layered airspaces. Instead, the lower accuracy for layered airspaces is caused by the interaction between this fact and the design of the simulation experiments

which artificially suppresses the number of conflicts detected by climbing/descending traffic.

To understand this interaction, it is necessary to consider the process of conflict detection. As mentioned previously, aircraft search for conflicts within a predefined region of airspace that can be decomposed into separate horizontal and vertical 'conflict search volumes'; see Figure 4.4(b). For climbing and descending traffic, the *vertical* conflict search volume can extend beyond the upper and lower boundaries of the simulated sector. Since no traffic was simulated outside the considered sector, climbing and descending traffic are, therefore, less likely to detect conflicts, particularly near the edges of the simulation. Although this simulation artifact affects both unstructured and layered airspace designs, the higher proportion of climbing/descending conflicts in layered airspaces leads to a greater over-estimation by the corresponding analytical model, explaining the model accuracy results noted above. Previous research has validated this explanation by showing that decreasing the flight-path angle of climbing/descending aircraft increases model accuracy [88], as this reduces the size of the vertical conflict search volume.

In addition to assessing the accuracies of the analytical models, Figures 4.12 and 4.13 also shows that layered airspaces are safer than UA, and that the safety of layered airspaces increases as α is decreased. Although these trends have been predicted by previous studies [70, 88], it is as yet unclear how the safety performance of these two airspace designs are affected by traffic scenario characteristics. Therefore, in addition to quantifying the effects of scenario distributions on the accuracies of the analytical and adjusted conflict count models, the analysis that follows also examines whether the non-ideal traffic scenarios affect the relative safety differences between UA and layered airspaces.

4.6.2. Ground Speed Experiment

The analytical conflict count models assume that all aircraft fly with equal ground speed. Since this assumption deviates from realistic operations, the ground speed experiment investigated the sensitivity of the analytical model to four speed distributions displayed in Figure 4.7.

4.6.2.1. Effect of Speed Distribution on Conflict Counts

Before evaluating the effect of the equal speed assumption on model accuracy, it is useful to compare the actual conflict count results for the four simulated speed distributions. To this end, Figure 4.14 displays the means and the 95% confidence intervals of the number of conflicts logged at the highest traffic demand condition for all speed distributions. Here it can be seen that speed distribution has a negligible effect on conflict counts for all four airspace concepts considered in this study. Furthermore, as the vertical spacing between the four concepts is unaffected by changes in speed distribution, it can be concluded that speed distribution does

not alter the relative safety differences between unstructured and layered airspace designs.

The invariance of conflict counts with ground speed distribution can be explained by the fact that the same average ground speed is used by all four distributions. Therefore, this result indicates that the average conflict probability between pairs of aircraft, which is directly dependent on ground speed, is unaffected by *shape* of the ground speed distribution; instead, conflict probability is only affected by the magnitude of the average ground speed of all aircraft in the airspace.

4.6.2.2. Effect of Speed Distribution on Model Accuracy

The model accuracy results for the ground speed experiment are listed in Table 4.7 for both the analytical and adjusted models. Here it should be noted that the analytical model was evaluated while assuming equal speeds for all aircraft, regardless of the actual distribution used in the simulation. As evidenced by Figure 4.14, Table 4.7 indicates that the accuracy of the analytical model is unaffected by speed distribution, and it remains very high for all airspace concepts. This trend was hypothesized during the derivation of the ground speed model adjustment, where it was found that the expected horizontal relative velocity was largely unaffected by speed distribution; see Table 4.1. Nonetheless, the numerical ground speed adjustment described by equation 4.14, which is also shown in Table 4.7 to have produced high model accuracies, could be useful for layered airspaces with a very narrow heading range per flight level, i.e., for layered concepts with $\alpha < 90^o$, since overtaking conflicts are more likely to occur for such airspace designs. The speed model adjustment could also be required for cases where multiple traffic scenario distributions are varied from their ideal settings, i.e., for the case where the speed distribution is non-equal *and* the heading/altitude/spatial distribution is also non-uniform.
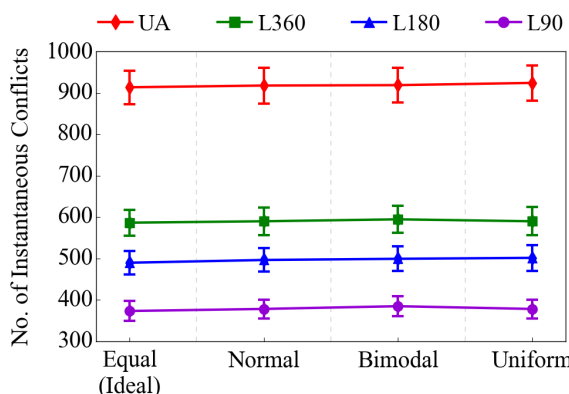
Figure 4.14: Means and 95% confidence intervals of the total conflict count at the highest traffic density, ground speed experiment

4

Table 4.7: Model accuracy for analytical and adjusted models, ground speed experiment

		Analytical	Adjusted
UA	Equal (Ideal)	1.024 (97.6%)	1.024 (97.6%)
UA	Normal	1.027 (97.4%)	1.030 (97.1%)
UA	Bimodal	1.021 (98.0%)	1.020 (98.0%)
UA	Uniform	1.027 (97.4%)	1.023 (97.8%)
L360	Equal (Ideal)	0.955 (95.3%)	0.955 (95.3%)
L360	Normal	0.958 (95.7%)	0.962 (96.0%)
L360	Bimodal	0.959 (95.7%)	0.958 (95.6%)
L360	Uniform	0.952 (94.9%)	0.948 (94.5%)
L180	Equal (Ideal)	0.940 (93.6%)	0.940 (93.6%)
L180	Normal	0.948 (94.5%)	0.950 (94.7%)
L180	Bimodal	0.951 (94.8%)	0.947 (94.4%)
L180	Uniform	0.951 (94.8%)	0.944 (94.1%)
L90	Equal (Ideal)	0.908 (89.8%)	0.908 (89.8%)
L90	Normal	0.917 (91.0%)	0.917 (91.0%)
L90	Bimodal	0.921 (91.4%)	0.912 (90.4%)
L90	Uniform	0.912 (90.4%)	0.899 (88.8%)

4.6.3. Heading Experiment

The heading experiment assessed the accuracy of the analytical conflict count models for the four heading distributions pictured in Figure 4.8.

4.6.3.1. Effect of Heading Distribution on Conflict Counts

Figure 4.15 displays the effect of heading distribution on conflict counts for the UA and L360 airspace concepts. Here it can be seen that conflict counts are the highest when aircraft headings are uniformly distributed, i.e., for the distribution assumed by the baseline analytical model. Although there are no significant differences between the uniform and bimodal distributions, the normal and ranged uniform distributions led to substantially lower conflict counts. These trends are displayed by both UA and L360. Moreover, the relative safety differences between the four heading distributions match the relative differences between the expected horizontal relative velocity between aircraft, see Table 4.2. These results strongly indicate that the heading distribution of traffic can have an effect on the intrinsic safety of unstructured and layered airspaces; the magnitude of this effect depends on the shape of the distribution used.
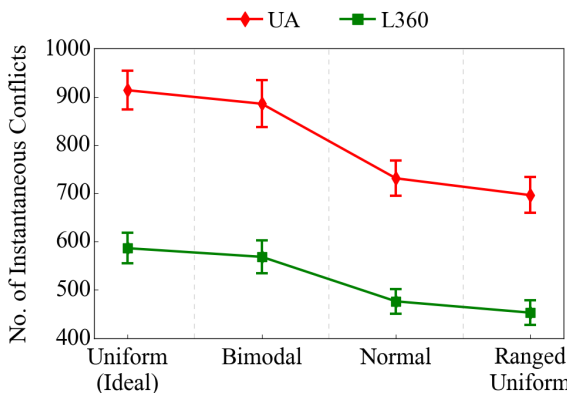
Figure 4.15: Means and 95% confidence intervals of the total conflict count at the highest traffic density, heading experiment

4.6.3.2. Effect of Heading Distribution on Model Accuracy

The model accuracy results for the heading experiment are listed in Table 4.8. As suggested by Figure 4.15, for both UA and L360, the analytical models, which assumes a uniform heading distribution for all simulation conditions, over-estimates conflict counts when the actual headings in the simulation followed normal and ranged-uniform distributions. This is indicated by k values that are significantly less than 1 for these two heading distributions. In addition to indicating the accuracy of the models, the k values computed for the analytical model can also be used to compute the relative differences between conditions; for example, for UA,

Table 4.8: Model accuracy for analytical and adjusted models, heading experiment

		Analytical	Adjusted
UA	Uniform (Ideal)	1.024 (97.6%)	1.024 (97.6%)
	Bimodal	1.005 (99.6%)	1.041 (96.0%)
	Normal	0.812 (76.9%)	0.982 (98.2%)
	Ranged-Uniform	0.769 (70.0%)	0.974 (97.4%)
L360	Uniform (Ideal)	0.955 (95.3%)	0.955 (95.3%)
	Bimodal	0.936 (93.1%)	0.977 (97.6%)
	Normal	0.769 (69.9%)	0.966 (96.5%)
	Ranged-Uniform	0.728 (62.6%)	0.969 (96.8%)

Figure 4.15 shows that the conflict count for the normal distribution condition is approximately 0.8 times lower than the count for the uniform condition, since $k \approx 0.8$ for the normal distribution, and $k \approx 1$ for the uniform condition.

Table 4.8 also indicates that the inaccuracies of the analytical model can be effectively compensated for by using the model adjustments for the heading distribution of traffic; the numerically adjusted model increased model accuracy for the normal and ranged-uniform heading distributions to the level found using the analytical model for the uniform case. This implies that the model adjustment for heading distributions, described in section 4.4.2, correctly determines the effect aircraft headings on the conflict probability between aircraft for both unstructured and layered airspaces.

4.6.4. Altitude Experiment

To evaluate the effect of altitude distribution conflict count model accuracy, in this experiment, traffic simulations were conducted for the four altitude distributions pictured in Figure 4.9.

4.6.4.1. Effect of Altitude Distribution on Conflict Counts

Figure 4.16 displays the conflict count results of the altitude experiment. Here it can be clearly seen that altitude distribution has a large impact on conflict counts
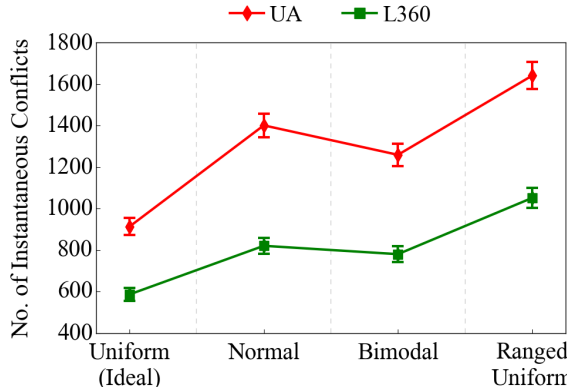
Figure 4.16: Means and 95% confidence intervals of the total conflict count at the highest traffic density, altitude experiment

for both UA and L360. In contrast to the heading experiment, the uniform (altitude) distribution condition, corresponding to the setting assumed by the baseline analytical model, led to the lowest number of conflicts. On the other hand, the ranged-uniform condition led to highest number of conflicts of all tested distributions. The figure also shows that changes in altitude distribution do not affect the relative differences between unstructured and layered airspaces.

4.6.4.2. Effect of Altitude Distribution on Model Accuracy

The effect of altitude distribution on model accuracy is shown in Table 4.9. The table indicates that the analytical model significantly under-estimates conflict counts ($k > 1$) for all non-uniform altitude distributions for both airspace designs. This result is unsurprising given the fact that the uniform altitude distribution was noted above to lead to the lowest number of conflicts of all studied conditions.

On the other hand, Table 4.9 indicates that model accuracies for the non-uniform altitude conditions are much higher when the predictions of the *adjusted* conflict count model are compared to logged simulation data. Nonetheless, in contrast to the adjustments made to account for the speed and heading distributions of traffic, the results for the altitude adjustment appears to be less consistent. This is particularly the case for the L360 concept when aircraft altitudes follow normal or bimodal distributions. These less consistent accuracy results can be attributed to the fact that the model adjustment for aircraft altitudes only considers the vertical distribution of cruising aircraft. Although the vast majority of aircraft in en route airspaces are in the cruise phase of flight, the vertical distribution of climbing/descending traffic will also affect the total conflict count in the airspace. However, because there are always more climbing/descending aircraft at lower altitudes, the vertical distribution of such aircraft is difficult to take into account since it always differs from that of cruising aircraft. Despite this limitation, it is important to note that the altitude related model adjustment derived in this work resulted in accura-

Table 4.9: Model accuracy for analytical and adjusted models, altitude experiment

		Analytical	Adjusted
UA	Uniform (Ideal)	1.024 (97.6%)	1.024 (97.6%)
UA	Normal	1.569 (63.7%)	1.103 (90.7%)
UA	Bimodal	1.416 (70.6%)	0.994 (99.4%)
UA	Ranged-Uniform	1.576 (63.4%)	0.958 (95.6%)
L360	Uniform (Ideal)	0.955 (95.3%)	0.955 (95.3%)
L360	Normal	1.336 (74.8%)	0.899 (88.7%)
L360	Bimodal	1.275 (78.4%)	0.906 (89.7%)
L360	Ranged-Uniform	1.448 (69.1%)	0.975 (97.5%)

cies that are generally quite high, with accuracies greater than 90% in most cases. As such, the adjusted models provide a significantly better estimate of the number of conflicts in the airspace when compared to the baseline analytical models.

4.6.5. Spatial Experiment

While the previous experiment considered the effect of the vertical distribution of traffic, this experiment investigated the effect of the horizontal distribution of traffic on the accuracy of the analytical conflict count models. Correspondingly, simulations were conducted for the three spatial distributions displayed in Figure 4.10.

4.6.5.1. Effect of Spatial Distribution on Conflict Counts

Unlike the other experiments, error-bars are not used to compare the conditions of this experiment. This is because the scenarios with hot-spots resulted in much higher traffic densities due to the fact that the hot-spot scenarios, by their very nature, aim to create traffic concentrations within the 'experiment region'. Because such density differences are not visible with error bars, the spatial conditions can be compared instead using Figure 4.17. In this figure, the simulation data (scatter points) is plotted together with the corresponding model *fits* (solid lines) for the four airspace concepts considered in this experiment.
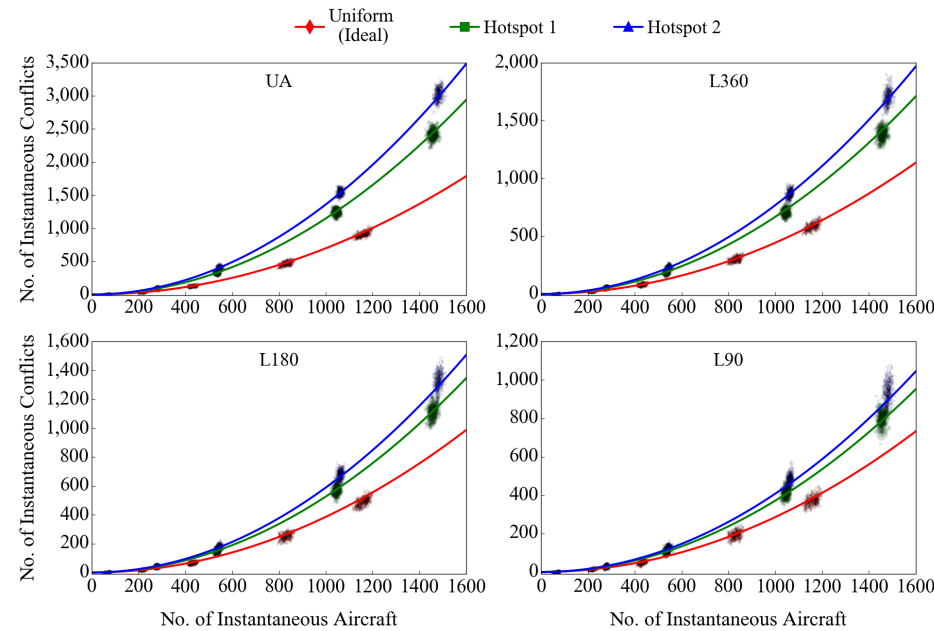
Figure 4.17: Empirical conflict counts (scatter points) and model fits (solid line), spatial experiment

The higher traffic densities for the hot-spot conditions are clearly evident in Figure 4.17; for all four concepts, the highest traffic demand scenario resulted in approximately 1100 instantaneous aircraft for the uniform spatial distribution, while it is greater than 1400 instantaneous aircraft for the hot-spot conditions. Furthermore, this figure indicates that the hot-spots led to a significantly higher number of conflicts, with hot-spot 2 resulting in the highest conflict count of all traffic scenario distributions considered in this work. This strongly implies that the spatial distribution of traffic can have a substantial effect on airspace safety.

4.6.5.2. Effect of Spatial Distribution on Model Accuracy

As expected, the model accuracy results for the spatial experiment, listed in Table 4.10, indicate that the analytical model grossly under-estimated the number of conflicts for the hot-spot conditions (k>1). On the other hand, model accuracy is significantly improved for the adjusted models. For instance, for UA, the accuracy for hot-spot 2 increased from 48.1% for the analytical model to 98.2% for the adjusted model. This indicates that the model adjustment procedure for the spatial distribution of traffic, which segments the airspace into a number of smaller areas, can be used to effectively improve conflict count model estimates for traffic scenarios with non-uniform density distributions.

Table 4.10: Model accuracy for analytical and adjusted models, spatial experiment

		Analytical	Adjusted
UA	Uniform (Ideal)	1.024 (97.6%)	1.024 (97.6%)
	Hotspot 1	1.725 (58.0%)	0.906 (89.6%)
	Hotspot 2	2.077 (48.1%)	1.018 (98.2%)
L360	Uniform (Ideal)	0.955 (95.3%)	0.955 (95.3%)
	Hotspot 1	1.432 (69.9%)	0.992 (99.2%)
	Hotspot 2	1.695 (59.0%)	1.019 (98.1%)
L180	Uniform (Ideal)	0.940 (93.6%)	0.940 (93.6%)
	Hotspot 1	1.362 (73.4%)	1.017 (98.3%)
	Hotspot 2	1.559 (64.1%)	1.020 (98.1%)
L90	Uniform (Ideal)	0.908 (89.8%)	0.908 (89.8%)
	Hotspot 1	1.249 (80.1%)	1.084 (92.2%)
	Hotspot 2	1.401 (71.4%)	1.089 (91.9%)

4.7. Discussion

This chapter investigated the effect of idealized traffic scenario assumptions on the accuracy of closed-form analytical conflict count models, often referred to as gas models in literature. To this end, model predictions for unstructured and layered airspace designs were compared with the results of four fast-time simulation experiments with varying speed, heading, altitude, and spatial traffic distributions. Data collected from these simulations was also used to test so called 'model adjustments' that aim to relax the dependency of the models on the idealized scenario assumptions. This section reflects on the intrinsic safety provided by unstructured and layered airspaces for 'non-ideal' traffic scenarios, and discusses the accuracies of the baseline analytical and adjusted conflict count models. Additionally, important aspects related model usage are also considered.

4.7.1. Effect of Traffic Scenario on Intrinsic Airspace Safety

Of the four traffic scenario distributions, the results showed that the altitude and spatial distributions of traffic had the greatest impact on the number of conflicts. Any deviation from the uniform altitude and spatial distributions assumed by the baseline analytical model led to a significant increases in the number of conflicts, with some spatial distributions leading to a doubling of conflict counts. While the heading distribution also affected intrinsic safety, the magnitude of its effect was strongly dependent on the shape of the distribution used. Moreover, in contrast to the altitude and spatial cases, non-uniform heading distributions led to a decrease in the number of conflicts. This is because non-uniform heading distributions generally result in one or more preferred directions of traffic flow, which in turn reduce the average relative velocities and average the conflict probabilities between aircraft.

On the other hand, variations of the ground speed distribution only resulted in minor differences in the number of instantaneous conflicts. Although this result may seem surprising at first, it can be explained by considering the effect of ground speed on the expected horizontal relative velocities between aircraft. The expected, or weighted average, horizontal relative velocity in a given volume of airspace is dependent on both the ground speed *and* the heading distributions in that airspace. Changes to the ground speed distribution, can therefore, be compensated for to some extent by the specific heading distribution used. In this study, all ground speed distributions were tested while using a uniform distribution of aircraft headings, since the experiments performed here only varied one traffic scenario property at a time from the so called 'ideal' setting. As mentioned above, uniform heading distributions resulted in the highest conflict counts by maximizing relative velocities. As a result, variations of the ground speed distribution did not yield significant changes to the expected horizontal relative velocities between aircraft, which in turn reduced its effect on conflict counts. It is hypothesized that ground speed distribution could have a larger effect on the safety of layered airspace designs with

a very narrow heading range per flight level, and for scenarios with non-uniform aircraft headings, since over-taking conflicts are more likely for such cases.

It should be noted that the trends discussed above were found for both unstructured and layered airspace designs. In fact, the relative differences between unstructured and layered airspaces were unaffected by the twelve different traffic scenarios that were tested in this work; unstructured airspace always resulted in higher conflict counts than layered airspaces, and the intrinsic safety of layered airspaces increased as the heading range per flight level was decreased. These results indicate that traffic scenario properties do not fundamentally alter the behavior of an airspace design. They may, however, exacerbate conflict counts for certain scenario distributions.

4.7.2. Accuracy of the Analytical and Adjusted Conflict Count Models

Although the accuracy of the baseline analytical model for both airspace designs was found to be very high for the ideal traffic scenario, accuracy was substantially degraded when the underlying scenario assumptions were violated. Because non-uniform altitude and spatial distributions led to the highest conflict counts, the accuracy of the baseline models was the lowest for these scenario properties, with some conditions resulting in accuracies as low as 50%, i.e., only half the actual number of conflicts could be predicted. The only exception to this trend was found for the speed experiment, since speed distributions, as mentioned above, only had a minor effect on conflict counts. Nonetheless, these results indicate that the predictions of analytical conflict count models should be considered with caution for non-ideal traffic scenarios.

In contrast, the accuracy of the numerically adjusted conflict count models was found to be very high for all tested scenario conditions. In fact, for most cases, the adjusted models resulted in accuracies that closely matched those produced by the baseline analytical model for the ideal traffic setting. Because the adjustments only affect the computation of certain components of the models, the basic structure of the adjusted models remains unchanged relative to the baseline analytical model. Therefore, in addition to providing a physical understanding of the parameters, and the relationships between the parameters, that affect intrinsic airspace safety, the adjusted models can be used to compute the highly accurate conflict count estimates necessary for practical airspace design applications.

4.7.3. Additional Considerations

Model adjustments have been derived in this study on an individual basis for each of the four traffic scenario assumptions. However, it should be noted that the four adjustments do not exclude each other, and therefore, multiple adjustments can be applied at the same time for cases where two or more traffic scenario properties deviate from their ideal settings. On a similar note, for mathematical conve-

nience, model adjustments have been tested here using relatively straightforward scenario distributions. Nevertheless, due to the numerical nature of all model adjustments, they can also be applied to other untested traffic scenarios, as long as the characteristics of the underlying distributions are known, or can be determined empirically.

This chapter has focused on analyzing and generalizing conflict count models for unstructured and layered airspace designs. The methods presented here to generalize the models can, however, be extended to other airspace designs. This is because all gas models can be described as a product of two factors, namely the number of combinations of two aircraft, and the average conflict probability between any two aircraft. The model adjustments derived here have considered the effects of non-ideal traffic scenarios on both these factors. As such, 'adjusted' conflict count models can be developed for other airspace designs using the approach outlined in this chapter, including for airspace concepts that are closer today's mode of operations.

4.8. Conclusions

This chapter analyzed the effect of traffic scenario properties on the accuracy of gas model inspired analytical conflict count models that have been used in the past to quantify the intrinsic safety provided by an airspace design. These analytical models were derived using idealized assumptions regarding the speed, heading, altitude and spatial distributions of traffic. The sensitivity of the analytical models to these assumptions was evaluated using four fast-time simulation experiments within the context of unstructured and layered airspace designs. Data from these simulations was also used to derive and test so called 'model adjustments' that aim to generalize the models beyond the specific traffic scenario assumptions upon which they were originally derived. The following conclusions can be drawn:

- *As found by previous research, the accuracy of analytical conflict count models was found to be very high for the ideal traffic scenario which respected all scenario related modeling assumptions.*

- *However, accuracy of the analytical models was substantially lower for traffic scenarios with non-ideal heading, altitude and spatial distributions of traffic.* These cases caused the analytical model to wrongly estimate one or both components of gas models, namely the number of combinations of two aircraft, and/or the average conflict probability between any two aircraft.

- Although the magnitude of the error between model predictions and simulation results depends on the specific distributions tested for each scenario property, for the studied conditions, it was found that the *altitude and spatial distributions of traffic had the largest negative impact on the accuracy of the analytical models.* This is because non-uniform altitude and spatial distributions resulted in traffic concentrations, either vertically or horizontally, which in turn caused a higher number of conflicts.

- On the other hand, the distribution of *aircraft ground speeds did not significantly impact the accuracy of the analytical models*, for the airspace concepts considered in this work. It is hypothesized that ground-speed distribution could have a greater impact on model accuracy for airspace concepts for which over-taking conflicts are more likely than what has been considered in this study.

- *The numerical model adjustments derived in this work increased model accuracy for all non-ideal traffic scenarios to the levels found with the analytical model for the ideal traffic scenario.* Consequently, the adjusted models can be used to accurately predict conflict counts for any traffic scenario, as long as the shapes of the underlying distributions are known, or can be determined empirically.

- *Variations in traffic scenarios did not affect the relative safety differences between unstructured and layered airspaces.* Unstructured airspace always led to a higher number of conflicts, and the safety of layered airspaces increased as the heading range per flight level was decreased, regardless of the specific traffic scenario tested.

Part III:
CAPACITY MODELING

5

Capacity Assessment Method for Decentralized Air Traffic Control

Using the outputs of chapters 2 and 3, this chapter develops the Capacity Assessment Method for Decentralized Air Traffic Control (CAMDA). The CAMDA method can be applied to data collected from fast-time simulation experiments to determine the maximum theoretical capacity of the pairing between the selected airspace design, and the selected algorithms for tactical conflict detection and resolution. It is demonstrated here for unstructured and layered airspace designs that use a state-based approach for conflict detection, and a voltage potential-based algorithm for conflict resolution. For this case, the CAMDA method is used to determine the effects of a number of interesting parameters on capacity, including the effects of conflict resolution dimension and conflict resolution priority.

Cover-to-cover readers may choose to skip sections 5.2.1, 5.2.3, and 5.2.4 as these sections repeat definitions, and the conceptual designs of unstructured and layered airspaces as stated previously in chapters 2 and 3. Readers may also chose to skip sections 5.3.3.1 and 5.3.4.1 which provide a summary of the analytical conflict count models of unstructured and layered airspace as previously shown in chapter 3.

Abstract

This chapter presents a semi-empirical method to determine the maximum theoretical capacity of decentralized airspace concepts using the notion of airspace stability. Here, airspace stability refers to the occurrence and propagation of conflict chain reactions. The method considered here, named Capacity Assessment Method for Decentralized Air Traffic Control (CAMDA), defines the capacity limit as the traffic density at which conflict chain reactions propagate uncontrollably throughout the entire airspace. In other words, at the capacity limit, all aircraft exists in a persistent state of conflict, because every conflict resolution action leads to an infinite number of new conflicts. CAMDA identifies this critical density using a semi-empirical approach whereby analytical models describing the safety performance of decentralized airspace designs are combined with empirical models describing the actions of decentralized conflict detection and resolution algorithms. The CAMDA method is demonstrated here using fast-time simulations of decentralized unstructured and layered airspace designs that utilize a state-based method for conflict detection, and a voltage potential-based algorithm for conflict resolution. The simulations studied how capacity is affected by a) the differences between unstructured and layered airspace designs; b) conflict detection parameters; c) conflict resolution dimension; d) conflict resolution priority; and e) the speed distribution of aircraft. The simulation results showed that CAMDA estimated the occurrence of conflict chain reactions with high accuracy for all studied cases, enabling capacity estimations using relatively non-intensive low density traffic simulations. Therefore, CAMDA can be used to speed up the airspace design process by reducing the number of time consuming high-density traffic simulations that are required when performing a trade-off between different airspace designs, or when fine-tuning the parameters of the selected airspace design.

5.1. Introduction

Despite the significant research and development efforts undertaken to overhaul aging Air Traffic Control (ATC) systems over the past decade, air traffic delays and congestion continue to rise at an alarming rate [12, 16, 17]. In response to this pressing issue, several researchers have advocated for a transfer of traffic separation responsibilities from ground based Air Traffic Controllers (ATCos) to each individual aircraft [30, 91–93]. The resulting decentralized traffic separation paradigm is expected to increase airspace capacity over current centralized operations by providing more flexing routing to aircraft operators, and thereby increasing the efficiency with which the available airspace is utilized.

To support decentralization, the research community has largely focused on the development of automated algorithms for Conflict Detection and Resolution (CD&R) [49, 111–113]. Some studies in this domain have also investigated if such algorithms can be combined with different options for structuring traffic to further improve capacity over todays operations [57, 74, 114].

However, in spite of over two decades of active research highlighting its theorized benefits, as well as successful test flights over Mediterranean airspace [63], decentralization is yet to be deployed in the field. From a technical point of view, one possible reason for the reluctance to introduce decentralization may be explained by the fact that most current capacity measurement tools, such as those related to ATCo workload, are not relevant for decentralized ATC. The absence of such tools has made it difficult to quantitatively analyze and compare the capabilities of the proposed decentralized airspace concepts and CD&R algorithms.

But before a comprehensive capacity assessment method can be developed for decentralized ATC, it is first necessary to consider what the term 'airspace capacity' refers to in a more general sense. At a fundamental level, airspace capacity, regardless of the type or location separation management, can be considered equivalent to the density at which the airspace becomes saturated, i.e., the density beyond which no additional traffic can be accommodated without significantly degrading system-wide macroscopic properties, properties such as the safety and efficiency of travel.

Using this view of airspace capacity as a starting point, previous research has identified airspace stability, which considers the propagation of conflicts as a result of tactical Conflict Resolution (CR) maneuvers, as an important factor when evaluating the saturation density of decentralized ATC concepts [32, 33]. These studies have shown that CR can destabilize the airspace at high traffic densities by triggering conflict chain reactions due to the scarcity of airspace, as well as due to the airspace design and CD&R algorithms used. To measure airspace stability, literature has presented the so called Domino Effect Parameter (DEP). The DEP was subsequently used by Jardin to relate airspace stability to airspace capacity for decentralization [28, 29]. Although Jardin's method provides an innovative approach for measuring capacity, it uses an oversimplified and inaccurate method to compute the expected relative velocity between aircraft, which is a key parameter of this approach. Additionally, Jardin's method is only applicable for the case where motion is restricted to the horizontal plane. Therefore the method, as derived previously, does not account for the effects of climbing and descending traffic on capacity. The latter shortcoming severely limits the application of Jardin's method, particularly as recent studies have indicated that climbing/descending traffic have a substantial impact on the safety of certain airspace configurations [88, 110].

In response to this limitation, the main goal of this chapter is to generalize the method proposed by Jardin, and to extend it for application in three-dimensional airspaces such the that effects of all aircraft flight phases on capacity can be taken into account. Additionally, we have used our past experiences in developing and validating analytical models that compute the expected relative velocity between aircraft as a function of airspace design to increase the accuracy and the realism of the method [88]. The resulting improved method, termed here Capacity Assessment Method for Decentralized ATC, or CAMDA for short, makes use of the DEP to define the *maximum theoretical capacity* of decentralized airspace designs as the density at which conflict chain reactions become uncontrollable. In other words, at

the capacity limit, all aircraft exists in a persistent state of conflict, because every conflict resolution action leads to an infinite number of new conflicts. Although the theoretical capacity limit cannot be realized in practice, it can be used as an unbiased metric to compare different airspace designs and/or CD&R algorithms in terms of capacity.

Because conflict chain reactions are caused by many interconnected factors that cannot be accurately described for all conditions in a purely analytical sense, CAMDA is a semi-empirical approach. Therefore CAMDA relies on empirical data, obtained through simulation, to apply its capacity definition, and to evaluate the capacity of a particular airspace design and CD&R algorithm combination. Nonetheless, because the underlying CAMDA models take into account the constraints imposed by airspace design concepts, and are based on the processes that govern CD&R, all its parameters have physical meaning. As such, the structure of the CAMDA models by themselves provide useful insights on the relationships between the factors that affect capacity for decentralization.

To demonstrate the CAMDA method, five fast-time simulation experiments are performed within the context of unstructured and layered airspace designs. Here, these two airspace designs are combined with the so called 'state-based' approach for decentralized conflict detection, and the Modified Voltage Potential (MVP) algorithm for decentralized tactical conflict resolution. The five experiments investigate how airspace capacity is affected by a) differences between unstructured and layered airspace designs; b) conflict detection parameters; c) conflict resolution dimension; d) conflict resolution priority; and e) the speed distribution of aircraft.

This chapter begins with a summary of the relevant background material in section 5.2. Subsequently, in section 5.3, the complete derivation of the CAMDA method is presented for both unstructured and layered airspaces. Section 5.4 describes the design of the simulation experiments that are used to demonstrate the utility of CAMDA method for the five cases mentioned above. The results of the experiments are presented and discussed in sections 5.5 and 5.6, respectively. Finally, the main conclusions of this study are listed in section 5.7.

5.2. Background

This section provides an overview of the definitions and background material used by the CAMDA method. Additionally, descriptions of the conceptual designs of unstructured and layered airspaces, the two airspace designs of interest to this study, are provided.

5.2.1. Conflicts vs. Intrusions

A conflict occurs if the horizontal and vertical distances between two aircraft are expected to be less than the prescribed separation standards within a predetermined 'look-ahead' time. Conflicts are, therefore, predictions of *future* separation

(a) Conflict   (b) Intrusion
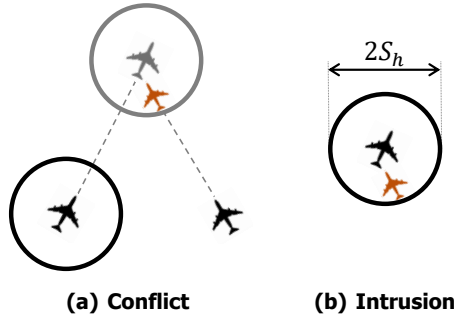
Figure 5.1: The difference between conflicts and intrusions, displayed here for the horizontal plane. Here, S_h is the horizontal separation requirement.

violations. Conflicts should not be confused with intrusions. Instead, intrusions, also referred to as losses of separation, occur when separation requirements are violated at the *present* time. This distinction between conflicts and intrusions is shown in Figure 5.1.

As mentioned earlier, CAMDA is concerned with the occurrences of conflict chain reactions. Therefore, the rest of this chapter only deals with aspects that are relevant to conflicts.

5.2.2. Airspace Stability and the Domino Effect Parameter

Airspace stability relates to the occurrence of conflict chains due to tactical Conflict Resolution (CR) maneuvers. At high traffic densities, such chain reactions can 'destabilize' the airspace by propagating conflicts throughout the entire airspace. To measure the propagation of conflict chain reactions, literature introduces the so called 'Domino Effect Parameter' (DEP) [32, 33]. The DEP can be visualized using the Venn diagram pictured in Figure 5.2. Here, $C_{total,nr}$ is the set of all conflicts without CR, and $C_{total,wr}$ is the set of all conflicts with CR, for identical traffic scenarios. Furthermore, three regions can be identified in Fig. 5.2; $R1$, $R2$ and $R3$. By comparing $R3$ with $R1$, the proportion of 'destabilizing' conflicts caused by CR can be determined. Thus, the DEP is defined as:

$$DEP = \frac{R3\left(\rho\right) - R1\left(\rho\right)}{C_{total,nr}\left(\rho\right)} = \frac{C_{total,wr}\left(\rho\right) - C_{total,nr}\left(\rho\right)}{C_{total,nr}\left(\rho\right)} = \frac{C_{total,wr}\left(\rho\right)}{C_{total,nr}\left(\rho\right)} - 1 \quad (5.1)$$

The number of conflicts that occur is dependent on the traffic density, ρ, regardless of whether CR is used, or not used. Hence, all parameters in the above equation are a function of ρ.
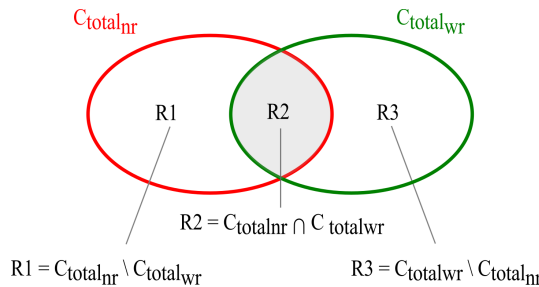
Figure 5.2: The Domino Effect Parameter (DEP) compares simulations with and without Conflict Resolution (CR) to measure airspace stability

To interpret the output of the above equation, it is useful to categorize conflicts in R_1, R_2, and R_3 subsets. First, conflicts that are common to both the CR OFF and CR ON cases are given by R_2. However, as soon as CR is applied, the aircraft that suffer conflicts will fly different routes, both spatially and temporally. Because of this, some conflicts that would have occurred with the original CR OFF trajectories will be avoided, and similarly, the altered CR ON trajectories can also trigger different conflicts. In Figure 5.2, R_1 represents the avoided conflicts, and R_3 corresponds to the additional, different conflicts, with CR ON. These additional conflicts can be either due to chance, or due to chain reactions, where a conflict resolution of a *primary* conflict immediately triggers a *secondary*, or knock-on, conflict. Therefore it follows that the numerator, $R_3 - R_1$, indicates the amount by which the number of additional conflicts outweighs the number of conflicts that are avoided with CR, and as such, the net destabilizing effect of CR (or stabilizing if $R_1 > R_3$). If it is assumed that conflict probability doesn't change due to CR, the *number* of primary conflicts can be considered equivalent to $C_{total,nr}$, i.e., the denominator of the above equation[1]. Consequently, based on the structure of equation 5.1, the DEP can be thought of as the *number of secondary conflicts per primary conflict*. Correspondingly, a higher value of DEP indicates higher airspace instability.

As the DEP is concerned with conflict chains, it is invariably linked to the safety of the airspace. But because conflict chain reactions also increase the flight distances of aircraft, the DEP, and consequently the notion of airspace airspace stability, also relates to airspace efficiency. The ability to simultaneously consider both the safety and efficiency of air travel makes the DEP a powerful tool for airspace capacity analysis purposes.

5.2.3. The Unstructured Airspace Design Concept

As the name suggests, no constraints are imposed on aircraft motion in Unstructured Airspace (UA). Instead, this simplest form of airspace design focuses on maxi-

---

[1]CR maneuvers are unlikely to reduce the *number* of conflicts compared to the no resolution case, expect for relatively low traffic densities when CD&R algorithms are combined with Conflict Prevention (CP) systems. CP is not considered in this work. Refer to [30] for more on CP.

mizing overall system efficiency. Therefore, aircraft are free to use direct horizontal routes, as long as such routing is not obstructed by weather or static obstacles. Similarly, UA permits aircraft to fly with preferred speeds and at optimum altitudes, based on their performance capabilities and trip distances. By offering greater freedom to aircraft operators, UA has been found to result in a more uniform distribution of traffic, both horizontally and vertically, relative to current day operations. This can in turn reduce traffic concentrations and ensuing delays [29, 30].

5.2.4. The 'Layers' Airspace Design Concept

Several different layered airspace concepts have been discussed in literature [95–97]. The specific variation under consideration in this work was developed in our prior work [74], and is known as the 'Layers' concept.

The Layers concept can be seen as an extension to the hemispheric/semicircular rule [79]. In this concept, the airspace is segmented into vertically stacked bands, and heading-altitude rules are used to limit the range of travel directions allowed in each altitude layer. Although the Layers concept dictates the vertical profile of a flight, operators are free to select direct horizontal routes when possible. Moreover, climbing and descending aircraft are exempted from the heading-altitude rules, and can violate them to reach their cruising altitude or destination. This exception avoids inefficient 'spirals' when climbing/descending.

Figure 5.3: Isometric view of an example Layers concept, with an allowed heading range of $\alpha = 45^o$ per flight level, and a vertical spacing of $\zeta = 1100$ ft between flight levels

An example Layers concept is shown in Figure 5.3. Two parameters define the topology of the Layers concept. The first parameter is the spacing between altitude bands, ζ. An important design requirement is that ζ is *at least* equal to the vertical separation requirement to prevent conflicts between aircraft cruising in adjacent flight levels. In this work, a vertical separation requirement of 1000 ft is used. Therefore, the altitude bands of the Layers concepts considered here are separated

by $\zeta = 1100$ ft; the extra 100 ft is used to prevent so called 'false' conflicts that can sometimes occur due to any slight overshooting of altitude when aircraft level-off at their desired flight level. Such an offset is also necessary to account for any height-keeping errors, and because of turbulence.

The second design parameter of the Layers concept is the heading range allowed per altitude band, α. For the layered airspace shown in Figure 5.3, $\alpha = 45^o$, and thus eight flight levels are needed to define one complete 'set' of layers. Correspondingly, for a layered design with $\alpha = 90^o$, only four flight levels would be needed to specify all possible travel directions. Therefore, for $\alpha = 90^o$, two complete 'sets' of layers would fit within the volume of airspace needed for $\alpha = 45^o$. When multiple sets of layers are available, the total trip distance of an aircraft is used in addition to its heading to determine its cruising altitude. In this way, short flights can use lower layer sets, and longer flights can use higher layer sets, to reduce the negative effect of predetermined altitudes on flight efficiencies.

Previous research has found that layered airspaces are safer than UA, and that the safety of layered airspaces increase as α is decreased [118]. One of the goals of this chapter is to determine whether the maximum theoretical capacity of layered airspaces also follows these trends.

5.3. The CAMDA Method

This section presents the complete derivation of the CAMDA method. It begins by introducing the airspace capacity definition used by CAMDA. This definition is subsequently used to derive components of the CAMDA approach for both unstructured and layered airspace designs.

5.3.1. CAMDA Capacity Definition

When a conflict is detected, a conflict resolution action needs to be taken to prevent that conflict from turning into an intrusion. In the case of decentralized ATC, these resolutions can be determined by pilots and/or by automated onboard CR algorithms. In either case, such tactical CR maneuvers can cause new conflicts, and in some cases, they can trigger conflict chain reactions. At low traffic densities, the ample maneuvering room available would, under normal conditions, allow such chain reactions to dissipate by themselves, i.e., without external intervention.

When extrapolating this logic for extreme traffic densities, it is likely that at a critical traffic density, the scarcity of airspace becomes so severe that conflict chain reactions propagate throughout the entire airspace. This would cause all aircraft to be inter-connected by a continuous, and perpetual conflict chain. Under such circumstances, it is unlikely that any CR maneuver by any aircraft could stabilize the airspace system. This would in turn result in an uncontrollable situation where all aircraft are resigned to continually perform meaningless CR maneuvers, without ever being able to solve any conflicts or fly to their actual destinations. The CAMDA

method defines the maximum *theoretical* capacity of a decentralized airspace design at this critical traffic density.

To pin-point the aforementioned hypothetical density at which conflict chain reactions become uncontrollable, CAMDA makes use of the DEP; if all aircraft are 'stuck' in conflict at the maximum theoretical density, then it follows that an *infinite* number of secondary conflicts would be triggered by the resolution of any primary conflict. Therefore, CAMDA defines the *maximum theoretical capacity* of the airspace as the traffic density at which the rate of change of the DEP with density approaches infinity. More formally, the CAMDA capacity definition can be stated as:

$$\lim_{\rho \to \rho_{max}} \frac{dDEP\left(\rho\right)}{d\rho} = \infty, \text{ where } \rho_{max} \equiv \text{capacity} \tag{5.2}$$

It should be noted that unlike currently used capacity metrics, which mainly focus on throughput, CAMDA measures capacity as the *saturation density* of the airspace. As mentioned above, this saturation density is defined from the perspective of airspace stability. Therefore, capacity, as defined here, doesn't reflect the operational capacity of an airspace, but can be used instead to compare different (airspace) concepts with each other.

5.3.2. CAMDA Framework

To evaluate the CAMDA capacity definition given by equation 5.2, it is necessary to express the DEP as a function of ρ. As indicated by equation 5.1, this requires the derivation of models for $C_{total,nr}$ and $C_{total,wr}$ as functions of ρ. CAMDA derives such expressions using a six-step sequential framework, see Figure 5.4. Here it can be seen that the framework consists of two main parts. The first part focuses on modeling $C_{total,nr}$, while the second focuses on modeling $C_{total,wr}$. Two assumptions, shown on the left side of Figure 5.4, are used to bridge these two main parts of the framework. The final step uses these models, and applies the CAMDA capacity definition to determine the maximum theoretical capacity, ρ_{max}, via the DEP.

Before proceeding with the derivation of the CAMDA model components, it is necessary to highlight three aspects.

Firstly, it should be noted that CAMDA is inspired by Jardin [28, 29]. In addition to formalizing Jardin's approach, this chapter extends his method for three-dimensional airspace, and applies it to determine the capacity of both unstructured and layered airspaces designs for a number of conditions, see section 5.4.3 for more details on the specific experiment conditions considered in this work. Furthermore, because CAMDA relies on a sequential framework, by using improved models for the first step of the CAMDA framework using results from our prior work [70, 88], the accuracy and realism of all subsequent steps is also expected to be higher than in [28, 29].

Secondly, it should be noted that CAMDA is a semi-empirical method as one of its parameters needs to be determined directly from simulation data. This is because conflict chain reactions, which are central to the CAMDA capacity definition, are dependent on a number inter-linked factors, and the effects of these interactions on capacity are difficult to model accurately using a purely analytical approach [119]. These include emergent behavior that results from interactions between the considered CD&R algorithms and the selected airspace design.

Finally, as stated previously, this work aims at demonstrating CAMDA for three-dimensional unstructured and layered airspace designs that are combined with a state-based CD algorithm, and a voltage potential-based CR algorithm. Hence the specific models, as derived here, are only applicable for these two airspace designs, and, to some extent, in combination with this particular CD&R algorithm. Nevertheless, the basic framework displayed in Figure 5.4 can be applied to any given decentralized airspace design. Because CAMDA is sequential, any adaptations along these lines mostly involves making appropriate modifications to the first step of the CAMDA framework.

5
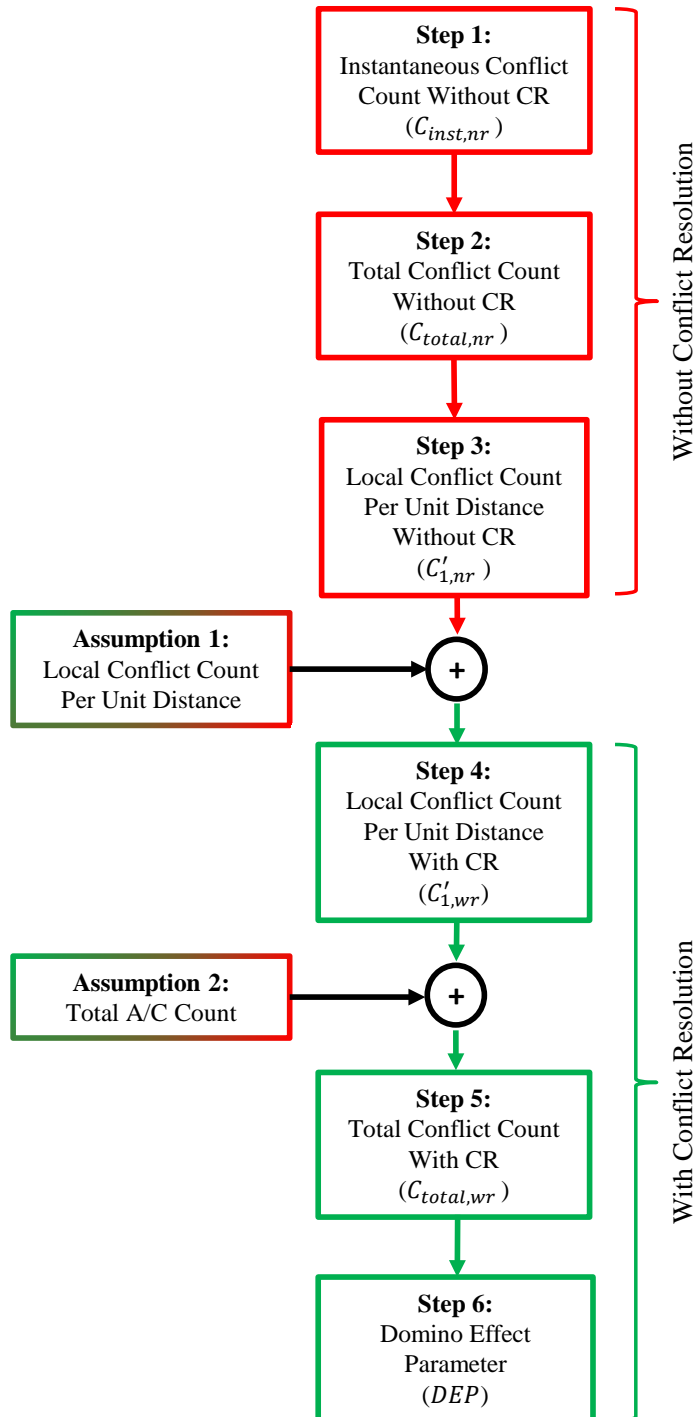
Figure 5.4: Six steps of the CAMDA framework. *Red* color indicates steps *without* Conflict Resolution (CR), and *green* color indicates steps *with* CR. The two assumptions are used to bridge the steps with and without CR.

5.3.3. Unstructured Airspace

The following paragraphs present the complete derivation of the six CAMDA steps for Unstructured Airspace (UA).

5.3.3.1. Step 1: Instantaneous Conflict Count Without Conflict Resolution

To be able to compute the total number of conflicts without CR, $C_{total,nr}$, it is necessary to first model the number of instantaneous conflicts in the entire airspace without CR, $C_{inst,nr}$, as a function of the number of instantaneous aircraft in the airspace without CR, $N_{inst,nr}$. Subsequently, in the second step of the derivation, the model for $C_{inst,nr}$ will be integrated over time to calculate $C_{total,nr}$.

For any airspace design, $C_{inst,nr}$ can be modeled as the product of two factors, namely the number of combinations of two aircraft, and the conflict probability between any two aircraft, p. In essence, the number of combinations of two aircraft is the maximum number of conflicts that can occur, since multi-aircraft conflicts, i.e., conflicts involving more than two aircraft, can also be decomposed into a series of two-aircraft conflicts. The conflict probability, on the other hand, scales down the number of combinations so that only those aircraft pairs that are predicted to violate separation requirements within the conflict detection look-ahead time are counted as conflicts.

For UA, the number of combinations can be computed directly using the binomial theorem, since this airspace design imposes no constraints on the motion of aircraft [70, 88]. Therefore, $C_{inst,nr_{UA}}$ can be expressed as:

$$C_{inst,nr_{UA}} = \binom{N_{inst,nr}}{2} p_{UA} = \frac{N_{inst,nr}\left(N_{inst,nr}-1\right)}{2} \, p_{UA} \qquad (5.3)$$

To model conflict probability for UA, p_{UA}, it is necessary to consider the process of CD. Most previous studies on decentralized ATC have the used so called state-based CD algorithm. In state-based CD, aircraft search for conflicts within a volume of airspace in front of them. In essence, this involves a 4D extrapolation of aircraft position vectors over a predetermined 'look-ahead' time, t_l, assuming constant velocity vectors. A conflict is said have occurred if the extrapolated path of an another aircraft is predicted to pass through the slanted 'conflict search cylinder' pictured in Figure 5.5(a) within t_l.. Since there are no constraints on aircraft motion in UA, conflicts can occur between aircraft in any flight phase in UA. Therefore, p_{UA} can be computed as the ratio between the volume of airspace searched for conflicts, B_c, and the total volume of the airspace under consideration, B_{total}. For mathematical convenience, B_c can be decomposed into its horizontal and vertical components, see Figure 5.5(b). Using this approach, p_{ua} as can be expressed as:

(a) Volume searched for conflicts, B_c (b) Horizontal and vertical components of volume searched for conflicts, $B_{c,h}$ and $B_{c,v}$
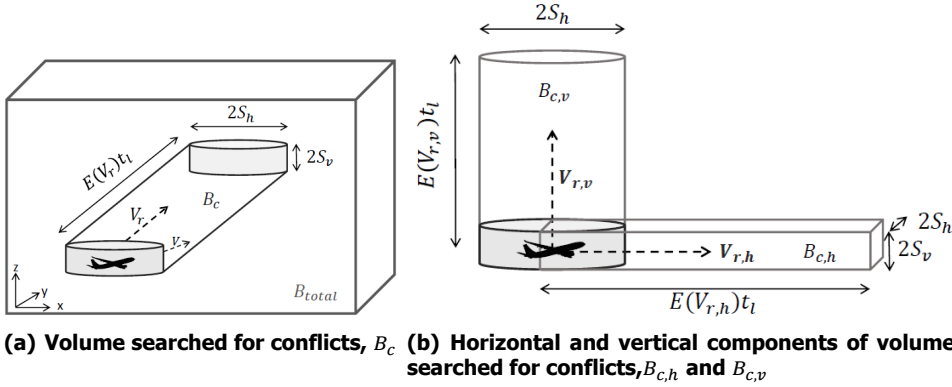
Figure 5.5: Volume searched for conflicts by an aircraft, B_c. Here, B_{total} is the total volume of the airspace. Note that $B_c = B_{c,h} + B_{c,v}$

$$p_{UA} = \frac{B_c}{B_{total}} = \frac{B_{c,h} + B_{c,v}}{B_{total}} = \frac{4 \, S_h S_v \, \mathbf{E}\left(V_{r,h}\right)_{UA} t_l + \pi S_h^2 \, \mathbf{E}\left(V_{r,v}\right)_{UA} t_l}{B_{total}} \tag{5.4}$$

Here, S_h and S_v are the horizontal and vertical separation requirements, and $\mathbf{E}\left(V_{r,h}\right)_{UA}$ and $\mathbf{E}\left(V_{r,v}\right)_{UA}$, are the horizontal and vertical components of the expected relative velocity of all aircraft pairs in UA. The expected relative velocity can be considered equivalent to the weighted average of the relative velocity of all aircraft pairs in the airspace, taking into account the heading, altitude, spatial and speed distributions of all aircraft. For UA, we have derived the following expressions for these two variables in our prior work [88]:

$$\mathbf{E}\left(V_{r,h}\right)_{UA} = \frac{4V_o}{\pi} \tag{5.5a}$$

$$\mathbf{E}\left(V_{r,v}\right)_{UA} = V_o \sin\left(\gamma\right)\left(1 - \varepsilon^2\right) \tag{5.5b}$$

Here, V_o is average ground speed of all aircraft in an airspace, γ is the flight path angle of climbing/descending aircraft, and ε is the proportion of cruising aircraft in the airspace, i.e, $\varepsilon = N_{inst,cr,nr}/N_{inst,nr}$, where $N_{inst,cr,nr}$ is the number of instantaneous cruising aircraft without CR.

Note that the derivation of the above equations for the expected relative velocities decomposes aircraft trajectories into cruising, climbing and descending flight phases. While additional flight phases can be taken into account by the underlying derivation procedure, a segmentation into these three flight phases is considered to be adequate for en route airspaces; the reader is referred to [88] for the complete

derivation. Furthermore, the specific version of equations 5.4 and 5.5 apply only for traffic scenarios with uniform heading, altitude, and spatial distributions. They also assume that all aircraft fly with equal ground speeds. Because CAMDA is a sequential method, these assumptions affect subsequent steps of the derivation. Nevertheless, the effect of the equal speed assumption on CAMDA is specifically tested in this research, see section 5.5.5. The reader is referred to [110] for alternate expected relative velocity expressions for cases where the above 'ideal' traffic scenario assumptions do not hold.

5.3.3.2. Step 2: Total Conflict Count Without Conflict Resolution

The total number of conflicts without CR, $C_{total,nr}$, can be computed by summing up the number of instantaneous conflicts detected at each time step during an analysis time interval T. The result of this summation should be divided by the average conflict duration, t_c, so that conflicts which occur over multiple time steps are only counted once. Since a continuous summation over time is equivalent to an integration over time, a model for $C_{total,nr}$ can be computed as:

$$
\begin{aligned}
C_{total,nr} &= \frac{1}{t_c} \int_0^T C_{inst,nr} \, dT \\
&= \frac{C_{inst,nr} T}{t_c}
\end{aligned}
\tag{5.6}
$$

To introduce traffic density, ρ, into the derivation process, the following simple relationship between the number of instantaneous aircraft, $N_{inst,nr}$, and the total area of the airspace, A_{total}, can be used:

$$
\rho = \frac{N_{inst,nr}}{A_{total}}
\tag{5.7}
$$

For UA, substitution of equations 5.3 and 5.7 into equation 5.6 leads to the following final expression for $C_{total,nr_{UA}}$:

$$
C_{total,nr_{UA}} = \frac{p_{UA} \; \rho \; T \; A_{total}^2 \left(\rho - \frac{1}{A_{total}} \right)}{2t_c} \approx \frac{p_{UA} \; \rho^2 \; T \; A_{total}^2}{2t_c} \quad \text{if } \rho \gg \frac{1}{A_{total}}
\tag{5.8}
$$

Note that the above equation has been simplified using the fact that $\rho - 1/A \approx \rho$ for practical values of ρ and A. Also note that under ideal conditions, t_c is equal to the look-ahead time, t_l, for state-based CD. However, simulation artifacts, such as pop-up conflicts between newly introduced aircraft and existing aircraft, can cause $t_c < t_l$. Because the frequency of such artifacts is very much dependent on the

design of the simulations themselves, and not by any naturally occurring interactions between aircraft, they are difficult to predict. Therefore, for the purposes of this derivation, t_c is considered to be a known input parameter. For the conditions studied here, t_c was found to be between 75-90% of t_l, depending on the value of t_l.

5.3.3.3. Step 3: Local Conflict Count Per Unit Distance Without Conflict Resolution

While the previous steps of the CAMDA framework have considered conflict counts for all traffic in the airspace (global), this step focuses on determining conflict counts, and conflict counts per unit distance flown, for a *single aircraft* without CR (local). These models are needed to bridge the CR OFF and CR ON parts of the CAMDA framework in subsequent steps.

Consider first the number of conflicts encountered by a single aircraft in UA without CR, $C_{1,nr}$. This can be calculated by dividing $C_{total,nr}$ by the total number of aircraft in the airspace during the analysis time interval T without CR, $N_{total,nr}$:

$$C_{1,nr} = \frac{C_{total,nr}}{N_{total,nr}} \tag{5.9}$$

Subsequently, the number of conflicts per unit distance for a single flight, $C'_{1,nr}$, can be computed by dividing equation 5.9 by the average flight distance in the airspace volume of interest without CR, D_{nr}:

$$C'_{1,nr} = \frac{\Delta C_{1,nr}}{\Delta D_{nr}} = \frac{C_{total,nr}}{N_{total,nr} \, D_{nr}} \tag{5.10}$$

Note that the CAMDA method considers D_{nr} to be a known input parameter. To express $C'_{1,nr}$ as a function of ρ, a model for $N_{total,nr}$ as a function of ρ is needed. This can be derived as follows; to maintain a constant density of one aircraft in an airspace, the aircraft replacement rate would have to be V_o/D_{nr}. Likewise, to maintain a density of $N_{inst,nr}$ aircraft, the replacement rate would have to be $N_{inst,nr} \cdot V_o/D_{nr}$. Correspondingly, the total number of aircraft introduced during an analysis interval of length T would be $T \cdot N_{inst,nr} \cdot V_o/D_{nr}$. By using equation 5.7, and the logic described here, $N_{total,nr}$ can be formulated as:

$$N_{total,nr} = \frac{TV_o \, N_{inst,nr}}{D_{nr}} + N_{inst,nr} = \rho A_{total} \left(\frac{TV_o}{D_{nr}} + 1 \right) \tag{5.11}$$

The first term on the right hand side of equation 5.11 is the number of aircraft that started their flights during the analysis time interval, while the second term is the number of aircraft that were already present in the airspace at the start of the

analysis time. Finally, $C'_{1,nr_{UA}}$ for UA can be derived by substituting equations 5.8 and 5.11 into equation 5.10:

$$C'_{1,nr_{UA}} = \frac{p_{UA}\rho\, T\, A_{total}}{2t_c\,(TV_o + D_{nr})} \tag{5.12}$$

5.3.3.4. Step 4: Local Conflict Count Per Unit Distance With Conflict Resolution

While the last three derivation steps considered the case *without CR*, the following three steps focus on conflict modeling *with CR*. Modeling the case with CR begins by developing an expression for the local conflict count per unit distance with CR, $C'_{1,wr}$, i.e., the 'with CR' counterpart of the previous step.

To model $C'_{1,wr}$, consider the motion of traffic within a decentralized system. In such a system, it is possible that there are no preferred directions, or because of a popular destination(s), there can be one or more preferred directions. Regardless of the type of heading distribution, CR maneuvers by a single aircraft, or by multiple aircraft in different parts of the airspace, are unlikely to affect the shape of the overall heading distribution of the total airspace. Because this logic can also be applied to all other traffic scenario distributions, such the altitude and spatial distribution of traffic, Jardin assumes that the number of conflicts *per unit distance* does not vary substantially with and without CR [28, 29]. More formally, the first assumption used by CAMDA can be stated as:

CAMDA Assumption 1
The local conflict rate per unit distance is unaffected by tactical conflict resolution maneuvers, i.e., $C'_{1,wr} = C'_{1,nr}$

Using assumption 1 and equation 5.12, $C'_{1,wr}$ for UA can be written as:

$$C'_{1,wr_{UA}} = \frac{p_{UA}\rho\, T\, A_{total}}{2t_c\,(TV_o + D_{nr})} \tag{5.13}$$

As stated above, assumption 1 was used by Jardin, but it was not verified [28, 29]. The results section of this chapter, on the other hand, will specifically investigate the validity of this assumption, and its effect on the final CAMDA capacity assessment, see section 5.5.1.

5.3.3.5. Step 5: Total Conflict Count With Conflict Resolution

As stated before, to compute the DEP, it is necessary to derive a model of the total number of conflicts in an airspace with CR, $C_{total,wr}$. This can be computed by first considering the average number of conflicts for a single aircraft with CR, $C_{1,wr}$, which can in turn be expressed as the product of the average flight distance with CR, D_{wr}, and the local conflict count per unit distance with CR, $C'_{1,wr}$:
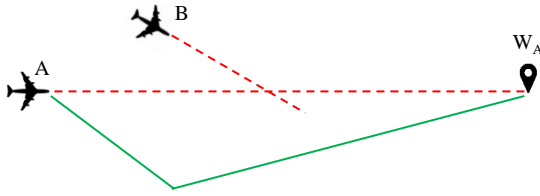
Figure 5.6: Conflict resolutions increase flight distances or flight times. Here, the former is depicted where the red-dashed line is the original, conflicted, path of aircraft A, while the green-solid line represents its path after conflict resolution. W_A is the target waypoint of aircraft A.

$$C_{1,wr} = D_{wr}\ C'_{1,wr} \tag{5.14}$$

Although $C'_{1,wr}$ was assumed to be not affected by CR, see assumption 1, this can not be assumed for D_{wr}. This is because CR maneuvers cause aircraft to deviate from their original paths, and these deviations will typically increase the total distance flown (and/or the total flight time) relative to the case without CR, regardless of the actual CR algorithm used[2]; see Figure 5.6. Therefore, D_{wr} can be expressed as:

$$D_{wr} = D_{nr} + D_{cdr}\ C_{1,wr} \tag{5.15}$$

The above equation states that the distance flown by an aircraft with CR increases with the number of conflicts detected. Here, the 'extra' distance flown as result of each conflict resolution maneuver, including the extra distance flown by an aircraft to recover its pre-conflict destination/waypoint, is denoted as D_{cdr}. As mentioned above, this parameter is primarily affected by the type of CD&R algorithm used, since the selected CD&R algorithm has a large influence on the initial deviation needed to resolve conflicts. For this reason, D_{cdr} is also heavily impacted by conflict chain reactions, because such conflict chain reactions increase the average deviation required to resolve conflicts. In addition to these two aspects, D_{cdr} is also affected by the airspace design in force. This is because the constraints imposed by a particular airspace design will affect the length of the trajectory recovery/turn-back path needed after conflict resolution. Because the interactions between these three elements are very difficult to quantify, D_{cdr} can not be computed accurately using an analytical approach. As such, D_{cdr} is the sole empirical parameter of the CAMDA method, and its value needs to be determined directly from simulation.

Substituting equation 5.15 into equation 5.14 leads to:

---

[2]If pure speed resolutions are used, then the derivation should be adjusted to take into account the extra time flown per conflict because of CD&R. However not all conflict geometries can be resolved using speed resolutions alone, given the speed related flight envelope restrictions of aircraft. As such pure speed resolutions are not considered here.

$$C_{1,wr} = \frac{D_{nr} C'_{1,wr}}{1 - D_{cdr} C'_{1,wr}} \qquad (5.16)$$

The total number of conflicts with CR, $C_{total,wr}$ can now be computed as the product of $C_{1,wr}$ and the total number of aircraft during the analysis time interval with CR, $N_{total,wr}$:

$$C_{total,wr} = C_{1,wr} N_{total,wr} \qquad (5.17)$$

To formulate $N_{total,wr}$ as a function of ρ, the following assumption is made; although CR is expected to increase ρ due to longer flights, CR is also expected to increase the average distance flown by a proportional amount. Thus, the total number of aircraft during the analysis time interval is assumed to be similar with and without CR, as can be seen when this logic is applied to equation5.11. More formally, the second assumption used by the CAMDA framework can be stated as:

CAMDA Assumption 2
The total number of aircraft during the analysis time interval is unaffected by tactical conflict resolution maneuvers, i.e., $N_{total,wr} = N_{total,nr}$

Using assumption 2 and equation 5.11, $N_{total,wr}$ can be written as:

$$N_{total_{wr}} = \rho A_{total} \left(\frac{TV_o}{D_{nr}} + 1 \right) \qquad (5.18)$$

As for assumption 1, the validity of assumption 2 is also tested is tested using simulation experiments, see section 5.5.1. Substitution of equation 5.13 into equation 5.16, and substitution of the resulting expression into equation 5.17 results in the following $C_{total,wr}$ model for UA:

$$C_{total,wr_{UA}} = \frac{p_{UA} \rho^2 \, TA_{total}^2 \, (TV_o + D_{nr})}{2t_c \, (TV_o + D_{nr}) - p_{UA} \rho \, T \, A_{total} \, D_{cdr_{UA}}} \qquad (5.19)$$

5.3.3.6. Step 6: Domino Effect Parameter and Capacity

The final step of the CAMDA framework uses the models developed above for $C_{total,nr}$ and $C_{total,wr}$ to express the DEP as a function of ρ. This allows the CAMDA capacity definition to be applied, which in turn enables the calculation of the maximum theoretical capacity of a given airspace design, ρ_{max}. The corresponding DEP model for UA can be computed by substituting equations 5.8 and 5.19 into equations 5.1:

$$DEP_{UA} = \frac{2t_c \, (TV_o + D_{nr})}{2t_c \, (TV_o + D_{nr}) - p_{UA}\rho \, T \, A_{total} \, D_{cdr_{UA}}} - 1 \qquad (5.20)$$

To apply the CAMDA capacity definition, it is useful to collect together all terms in the above equation that are *not* a function of ρ. To this end, η_{UA} and μ_{UA} are defined as:

$$\eta_{UA} = 2t_c \, (TV_o + D_{nr}) \qquad (5.21a)$$

$$\mu_{UA} = \frac{1}{p_{UA} \, T \, A_{total} \, D_{cdr_{UA}}} \qquad (5.21b)$$

Using equation 5.21, equation 5.20 can be simplified as:

$$DEP_{UA} = \frac{\rho}{\eta_{UA} \, \mu_{UA} - \rho} \qquad (5.22)$$

The CAMDA capacity definition, given by equation 5.2, can now be evaluated. This involves determining the density at which the rate of change of the DEP with ρ equals infinity:

$$\left. \frac{dDEP_{UA}}{d\rho} \right|_{\rho \to \rho_{max_{UA}}} = \frac{\eta_{UA} \, \mu_{UA}}{\left(\eta_{UA} \, \mu_{UA} - \rho_{max_{UA}} \right)^2} = \infty \qquad (5.23)$$

Based on the structure of equation 5.23, it can be seen that the rate of change of the DEP with density equals infinity if, and only if, the denominator is equal to zero, i.e., if $\eta_{UA}\mu_{UA} - \rho_{max_{UA}} = 0$. Therefore, the DEP is infinite, and an infinite number of secondary conflicts is triggered per primary conflict when $\rho_{max_{uA}}$ is equal to $\eta_{UA}\mu_{UA}$. Using equation 5.21, $\rho_{max_{uA}}$ equals:

$$\rho_{max_{UA}} = \eta_{UA} \, \mu_{UA} = \frac{2 \, t_c \, (TV_o + D_{nr})}{p_{UA} T \, A_{total} D_{cdr_{UA}}} \qquad (5.24)$$

A number of conclusions can be drawn from equation 5.24. Firstly, this equation shows that ρ_{max} is directly proportional to the average ground speed of aircraft, V_o, and inversely proportional to the expected relative velocity between aircraft via the conflict probability p_{UA}; see equation 5.4. Secondly, because $\frac{1}{p_{UA} A_{total}} = \frac{H}{B_c}$, where H is the height of the airspace, and B_c is the average volume of airspace searched for conflicts by an aircraft, the above equation also states that capacity increases with the height of the airspace volume under consideration; see Figure 5.5. Finally, the above equation indicates that ρ_{max} is dependent on the extra distance flown

per conflict due to CD&R, D_{cdr}, i.e., the empirical parameter of the CAMDA method. Therefore, a value for ρ_{max} can be determined by fitting simulation logged DEP data to equation 5.22 in a least-squares sense. Thus, even though all the parameters used by CAMDA have a physical meaning, and take into account the processes that govern CD&R, it is regarded as a *semi-empirical* method.

5.3.4. Layered Airspace

The following paragraphs present the derivation of the CAMDA sub-models for layered airspaces. Because the logic used to derive CAMDA steps 2-6 remains unchanged relative to UA, the derivation that follows focuses on the first step of the CAMDA framework for layered airspaces.

5.3.4.1. Step 1: Instantaneous Conflict Count Without Conflict Resolution

The altitude constraints imposed by the Layers concept reduces the number of conflicts between cruising aircraft relative to UA. However, there no procedural mechanisms used to separate cruising aircraft from climbing and descending traffic in layered airspaces; see section 5.2.4. Therefore, the computation number of instantaneous conflicts for this airspace design needs to be decomposed into three distinct parts based on the flight phase combinations of interacting aircraft:

$$C_{inst,nr_{LAY}} = C_{inst,cr,nr} + C_{inst,cr-cd,nr} + C_{inst,cd,nr} \qquad (5.25)$$

Here, $C_{inst,cr,nr}$, $C_{inst,cr-cd,nr}$ and $C_{inst,cd,nr}$ are the number of instantaneous conflicts between cruising aircraft, between cruising and climbing/descending aircraft, and between climbing/descending aircraft, respectively, without CR. These three conflict types are discussed separately below. Subsequently, the final expression for $C_{inst,nr_{LAY}}$ is computed by substituting the model for each conflict type into equation 5.25.

Conflicts Between Cruising Aircraft
Since the vertical spacing between the predefined flight levels of the Layers concept is, by definition, at least to the vertical separation requirement, cruising aircraft in different flight levels can not conflict with each other; see section 5.2.4. This in turn reduces the number of possible conflict pairs for cruising aircraft. If aircraft are uniformly distributed over all available flight levels, L, then the number of instantaneous cruising conflicts without CR can be computed as [70, 88]:

$$C_{inst,cr,nr} = \frac{N_{inst,cr,nr} \left(\frac{N_{inst,cr,nr}}{L} - 1 \right)}{2} \, p_{cr} \qquad (5.26)$$

Here, p_{cr} is the average conflict probability between two arbitrary cruising aircraft. Because cruising aircraft in layered airspaces are required to maintain constant al-
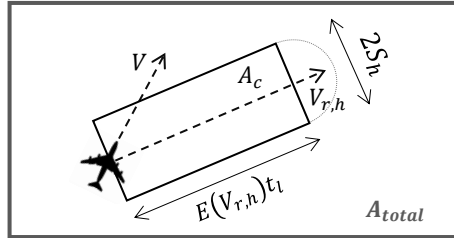
Figure 5.7: Area searched for conflicts, A_c, by cruising traffic in layered airspaces. Here, A_{total} is the total airspace area of one flight level.

titudes, the velocities of cruising aircraft are purely horizontal. Therefore, for state-based CD, p_{cr} can be computed as the ratio between the average *area* of airspace searched for conflicts by an aircraft, A_c, and the total *area* of one flight level, A_{total}; see Figure 5.7. Using the geometric parameters displayed in Figure 5.7, p_{cr} can be expressed as:

$$p_{cr} = \frac{2 \, S_h \, \mathbf{E}\left(V_{r,h}\right)_{cr} \, t_l}{A_{total}} \tag{5.27}$$

In the above equation, $\mathbf{E}\left(V_{r,h}\right)_{cr}$ is the expected horizontal relative velocity between cruising aircraft. Previous research has shown that $\mathbf{E}\left(V_{r,h}\right)_{cr}$ is dependent on the permitted heading range per flight level in layered airspaces, α, and that the relationship between these two variables is highly non-linear [70, 88]. If all aircraft are assumed to have equal ground speeds, and if aircraft headings are uniformly distributed between 0 and α, then $\mathbf{E}\left(V_{r,h}\right)_{cr}$ can be computed as [70, 88]:

$$\mathbf{E}\left(V_{r,h}\right)_{cr} = \frac{8V_o}{\alpha}\left(1 - \frac{2}{\alpha}\sin\frac{\alpha}{2}\right) \tag{5.28}$$

From the structure of the above equation, it can be seen that a reduction in α leads to a reduction to $\mathbf{E}\left(V_{r,h}\right)_{cr}$. Because p_{cr} is directly proportional to $\mathbf{E}\left(V_{r,h}\right)_{cr}$, see equation 5.27, a reduction in α, therefore, improves the intrinsic safety provided by layered airspaces in comparison to UA.

Conflicts Between Cruising and Climbing/Descending Aircraft

Because the Layers concept imposes no constraints to prevent conflicts between cruising and climbing/descending traffic, the model for $C_{inst,cr-cd,nr}$ is very similar to the corresponding model developed for UA, given by equations5.3-5.5, except for two minor differences:

1. The number of combinations of cruising and climbing/descending aircraft is $N_{inst,cr,nr} \cdot N_{inst,cd,nr}$. This is because an aircraft can not be cruising and climbing/descending at the same time.

2. Since only cruising-climbing/descending conflicts are to be considered, the calculation of the expected vertical relative velocity, $\mathbf{E}\left(V_{r,v}\right)_{cr-cd}$, should only consider cases where one aircraft is cruising, while the other is climbing/descending. Using this approach, it can be shown that
$\mathbf{E}\left(V_{r,v}\right)_{c-cd} = 2V_o \sin\left(\gamma_{cd}\right)\left(\varepsilon - \varepsilon^2\right)$ [88].

Application of these changes to the UA model leads to the following expressions for $C_{inst,cr-cd,nr}$. These equations make use of the geometrical parameters displayed in Figure 5.5:

$$C_{inst,cr-cd,nr} = N_{inst,cr,nr} \cdot N_{inst,cd,nr} \cdot p_{cr-cd} \tag{5.29a}$$

$$p_{cr-cd} = \frac{4\,S_h S_v\,\mathbf{E}\left(V_{r,h}\right)_{cr-cd} t_l + \pi S_h^2\,\mathbf{E}\left(V_{r,v}\right)_{cr-cd} t_l}{B_{total}} \tag{5.29b}$$

$$\mathbf{E}\left(V_{r,h}\right)_{cr-cd} = \frac{4V_o}{\pi} \tag{5.29c}$$

$$\mathbf{E}\left(V_{r,v}\right)_{cr-cd} = 2V_o \sin\left(\gamma_{cd}\right)\left(\varepsilon - \varepsilon^2\right) \tag{5.29d}$$

Conflicts Between Climbing/Descending Aircraft
The model describing the number of instantaneous conflicts between climbing/descending traffic, C_{cd}, is also similar to that derived earlier for UA. In this case, the only difference is in the computation of the expected vertical relative velocity between climbing/descending aircraft, $\mathbf{E}\left(V_{r,v}\right)_{cd}$. Previous research has shown that $\mathbf{E}\left(V_{r,v}\right)_{cd} = V_o \sin\left(\gamma_{cd}\right)\left(1 - \varepsilon\right)^2$ for layered airspace designs [88]. This approach leads to the following for expressions for $C_{inst,cd,nr}$. These equations make use of the geometrical parameters displayed in Figure 5.5:

$$C_{inst,cd,nr} = \frac{N_{inst,cd,nr}\left(N_{inst,cd,nr} - 1\right)}{2}p_{cd} \tag{5.30a}$$

$$p_{cd} = \frac{4\,S_h S_v\,\mathbf{E}\left(V_{r,h}\right)_{cd} t_l + \pi S_h^2\,\mathbf{E}\left(V_{r,v}\right)_{cd} t_l}{B_{total}} \tag{5.30b}$$

$$\mathbf{E}\left(V_{r,h}\right)_{cd} = \frac{4V_o}{\pi} \tag{5.30c}$$

$$\mathbf{E}\left(V_{r,v}\right)_{cd} = V_o \sin\left(\gamma_{cd}\right)\left(1 - \varepsilon\right)^2 \tag{5.30d}$$

Total Number of Instantaneous Conflicts for Layered Airspaces
Substitution of equations 5.26, 5.29, 5.30 into equation 5.25 yields the following expression for $C_{inst,nr_{LAY}}$:

$$C_{inst,nr_{LAY}} = \frac{p_{cr}\ N_{inst,nr}\ \varepsilon\left(N_{inst,nr}\ \varepsilon - L\right)}{2L}$$
$$+ \frac{2\ p_{cr-cd}\ N_{inst,nr}^2\ L\ \varepsilon\ \omega}{2L} \qquad (5.31)$$
$$+ \frac{p_{cd}\ N_{inst,nr}\ L\ \omega\left(N_{inst,nr}\ \omega - 1\right)}{2L}$$

In the above equation, ε is the proportion of cruising aircraft in the airspace, while ω is the proportion of climbing/descending aircraft. These two variables are defined as:

$$\varepsilon = \frac{N_{inst,cr,nr}}{N_{inst,nr}} \qquad (5.32a)$$

$$\omega = 1 - \varepsilon = \frac{N_{inst,cd,nr}}{N_{inst,nr}} \qquad (5.32b)$$

In preparation for the following steps of the CAMDA framework, traffic density, ρ, can be introduced into equation 5.31 by noting that $N_{inst,nr} = \rho \cdot A_{total}$:

$$C_{inst,nr_{LAY}} = \frac{p_{cr}\ \varepsilon\ \rho\ A_{total}^2\ (\rho\ \varepsilon - L/A_{total})}{2L}$$
$$+ \frac{2\ p_{cr-cd}\ \rho^2 A_{total}^2\ L\ \varepsilon\ \omega}{2L} \qquad (5.33)$$
$$+ \frac{p_{cd}\ L\ \omega\ \rho\ A_{total}^2\ (\rho\ \omega - 1/A_{total})}{2L}$$

Because $\rho\ \varepsilon >> 1/A_{total}$ and $\rho\ \omega >> 1/A_{total}$ for practical values of ρ, ε, ω and A_{total}, it is possible to further simplify equation 5.33 as:

$$C_{inst,nr_{LAY}} \approx \frac{p_{LAY}\rho^2 A_{total}^2}{2L} \qquad (5.34)$$

In the above expression, the p_{LAY} term can be thought of as the 'composite' conflict probability between any two aircraft in layered airspaces. It is computed as a weighted sum of three conflict probabilities considered by the model for layered airspaces, namely p_{cr}, p_{cr-cd} and p_{cd}:

$$p_{LAY} = \varepsilon^2\ p_{cr} + L\varepsilon\omega^2\ p_{cr-cd} + L\omega^2\ p_{cd} \qquad (5.35)$$

5.3.4.2. Steps 2 - 6 of the CAMDA Framework for Layered Airspaces

As mentioned before, the derivation of remaining steps of the CAMDA framework for layered airspaces is identical to that used by UA. As such, this chapter only presents the final expressions of steps 2-6 for layered airspaces. For the full derivation logic, the reader is referred to sections 5.3.3.2 - 5.3.3.6 where the corresponding models for UA are described in detail.

Step 2: Total Conflict Count Without Conflict Resolution

To compute the total number of conflicts that occurred without conflict resolution in layered airspaces, $C_{total,nr_{LAY}}$, equation 5.34 needs to be integrated over the analysis time interval T, while taking into account the average duration of a conflict, t_c:

$$
\begin{aligned}
C_{total,nr_{LAY}} &= \frac{1}{t_c} \int_0^T C_{inst,nr_{LAY}} \, dT \\
&= \frac{C_{inst,nr_{LAY}} T}{t_c} \\
&= \frac{p_{LAY} \rho^2 A_{total}^2 T}{2 \, L \, t_c}
\end{aligned}
\tag{5.36}
$$

Step 3: Local Conflict Count Per Unit Distance Without Conflict Resolution

The average number of conflicts experienced by a single aircraft per unit distance without CR in layered airspaces, $C'_{1,nr_{LAY}}$, can be calculated using the above expression for $C_{total,nr_{LAY}}$, and the model for the total number of aircraft in the analysis time interval without conflict resolution, $N_{total,nr}$, given by equation 5.11:

$$
\begin{aligned}
C'_{1,nr_{LAY}} &= \frac{C_{total,nr_{LAY}}}{N_{total,nr} \, D_{nr}} \\
&= \frac{p_{LAY} \rho \, T \, A_{total}}{2 \, L \, t_c \, (TV_o + D_{nr})}
\end{aligned}
\tag{5.37}
$$

Here, D_{nr} is the average flight distance of aircraft without CR, and it is considered to be a known parameter.

Step 4: Local Conflict Count Per Unit Distance With Conflict Resolution

Using CAMDA assumption 1, the local conflict count per unit distance with and without CR can be considered equivalent:

$$
\begin{aligned}
C'_{1,wr_{LAY}} &\approx C'_{1,nr_{LAY}} \\
&\approx \frac{p_{LAY} \rho \, T \, A_{total}}{2 \, L \, t_c \, (TV_o + D_{nr})}
\end{aligned}
\tag{5.38}
$$

Step 5: Total Conflict Count With Conflict Resolution

To compute the total number of conflicts with CR in layered airspaces, $C_{total,wr_{LAY}}$, it is necessary to take into account the average extra distance flown by a single aircraft to resolve each conflict and return to its pre-conflict waypoint. For layered airspaces, the corresponding parameters is denoted as $D_{cdr_{LAY}}$:

$$
\begin{aligned}
C_{total,wr_{LAY}} &= \frac{D_{nr} C'_{1,wr_{LAY}}}{1 - D_{cdr_{LAY}} C'_{1,wr_{LAY}}} N_{total_{wr}} \\
&= \frac{p_{LAY} \rho^2 \, TA_{total}^2 \, (TV_o + D_{nr})}{2 \, L \, t_c \, (TV_o + D_{nr}) - p_{LAY} \rho \, T \, A_{total} \, D_{cdr_{LAY}}}
\end{aligned}
\tag{5.39}
$$

Note that the total number of aircraft in the airspace during the analysis time interval, $N_{total,wr}$, is computed using equation 5.18 which is turn dependent on CAMDA assumption 2.

Step 6: Domino Effect Parameter and Capacity

Using the expressions derived above for $C_{total,wr_{LAY}}$ and $C_{total,nr_{LAY}}$, it is possible derive a model for the DEP in layered airspace by substituting equations 5.39 and 5.36 into equation 5.2:

$$
\begin{aligned}
DEP_{LAY} &= \frac{C_{total,wr_{LAY}}}{C_{total,nr_{LAY}}} - 1 \\
&= \frac{2 \, L \, t_c \, (TV_o + D_{nr})}{2 \, L \, t_c \, (TV_o + D_{nr}) - p_{lay} \rho \, T \, A_{total} \, D_{cdr_{LAY}}} - 1
\end{aligned}
\tag{5.40}
$$

To able to apply the CAMDA capacity definition given by equation 5.2, all terms that are not dependent on the traffic density ρ in the above expression are collected into two variables, η_{LAY} and μ_{LAY}:

$$
\begin{aligned}
DEP_{LAY} &= \frac{\rho}{\eta_{LAY} \mu_{LAY} - \rho} \\
\eta_{LAY} &= 2 \, L \, t_c \, (TV_o + D_{nr}) \\
\mu_{LAY} &= \frac{1}{p_{LAY} \, T \, A_{total} \, D_{cdr_{LAY}}}
\end{aligned}
\tag{5.41}
$$

Finally, a model for the maximum theoretical capacity of layered airspaces, $\rho_{max_{LAY}}$, can be determined by evaluating the CAMDA capacity definition:

$$
\left. \frac{dDEP_{LAY}}{d\rho} \right|_{\rho \to \rho_{max_{LAY}}} = \frac{\eta_{LAY} \mu_{LAY}}{\left(\eta_{LAY} \mu_{LAY} - \rho_{max_{LAY}} \right)^2} = \infty
\tag{5.42}
$$

Based on the structure of equation 5.42, $\rho_{max_{LAY}}$ is qual to:

$$\rho_{max_{LAY}} = \eta_{LAY}\mu_{LAY} = \frac{2\ L\ t_c\ (TV_o + D_{nr})}{p_{LAY}T\ A_{total}D_{cdr_{LAY}}} \tag{5.43}$$

On comparison of the final ρ_{max} equations for both UA and layered designs, given by equations 5.24 and 5.43, it can be seen that the two models are remarkably similar in structure. In fact, this is true for all final expressions computed for steps 2-6 of the CAMDA framework. The only two differences stems from the fact that conflict probability is computed differently, p_{UA} vs. p_{LAY}, and the fact that the models for layered airspaces are influenced by the number of flight levels available to cruising aircraft, L. Given the similarity between the models for these two airspace designs, it would be interesting is to determine what effect the heading-altitude rules and the pre-defined flight levels, i.e, the two design elements that distinguish layered designs from UA, have on the maximum theoretical capacity of the airspace. This is one of the goals of this study.

5.4. Fast-Time Simulation Design

This section describes the design of five fast-time simulation experiments that demonstrate the usage of the CAMDA method. These experiments were performed in the context of unstructured and layered airspace designs, and considered how capacity is affected by a) the differences between unstructured and layered airspaces; b) conflict detection parameters; c) conflict resolution dimension; d) conflict resolution priority; and e) the speed distribution of aircraft.

5.4.1. Simulation Development

5.4.1.1. Simulation Platform

The BlueSky open-source ATM simulator was used as the simulation platform in this research. It was developed at the Delft University of Technology (TU Delft) using the Python programming language[3]. BlueSky has numerous features including the ability to simulate more than 5000 aircraft simultaneously, a suite of conflict detection and resolution algorithms, and extensive data logging functions. A complete overview of BlueSky is provided in [108].

In order to simulate aircraft performance dynamics, BlueSky uses point-mass Aircraft Performance Models (APMs) that are similar in structure to Eurocontrol's well known Base of Aircraft Data (BADA) models. The main difference between these two approaches is that BlueSky uses openly available data to quantify the APMs. To simplify the simulations, all traffic was simulated using a Boeing 744 model. A full description of the BlueSky APMs, including their validation, can be found in [109].

---

[3]BlueSky can be downloaded from `https://github.com/ProfHoekstra/blueksy`

5.4.1.2. Conflict Detection

As stated before, the state-based Conflict Detection (CD) method was used in this study, see section 5.3.3.1. For most of the experiments performed in this study, a look-ahead time of 5 minutes, as well as separation requirements of 5 nautical miles horizontally and 1000 ft vertically, were used. The 'Conflict Detection' experiment, on the other hand, varied the values of these three parameters over multiple settings to study the effects of separation requirements and look-ahead time on airspace capacity; see Table 5.5.

It should be noted that CD was performed assuming perfect knowledge of aircraft states. This is in line with the findings of a recent study that concluded that ADS-B characteristics have little effect on the performance of the CD&R algorithms used in this work [25].

5.4.1.3. Conflict Resolution and Trajectory Recovery

Once conflicts were detected, the Modified Voltage Potential (MVP) algorithm was used for tactical Conflict Resolution (CR). MVP works similar to the repulsion that occurs between similarly charged particles to resolve conflicts between aircraft in a pairwise fashion. Furthermore, MVP uses minimum path deviations to reduce the effect of resolution maneuvers on flight efficiency; the resolution strategy used by MVP is illustrated in Figure 5.8 for the horizontal direction. A distinguishing characteristic of MVP is that it uses vector summation to determine the final CR avoidance maneuver for multi-aircraft conflicts. MVP has been used and validated by a number of previous studies [20, 30, 73, 74]. For a full description of the MVP algorithm, the reader is referred to [15, 20, 30].

For layered airspace designs, it is necessary to restrict conflict resolutions to the horizontal direction (using combined heading and speed maneuvers). This is because vertical resolutions could cause new conflicts with aircraft in adjacent flight levels, and thus negate the safety benefits offered by the predefined flight levels used in this airspace concept; see Figure 5.3. Therefore, conflict resolutions are limited to the horizontal direction for most experiments performed in this study, as this allows for a fair comparison between unstructured and layered airspace designs. However, because UA does not impose altitude constraints on traffic, the effects of both horizontal and vertical resolution maneuvers on its maximum theoretical capacity are specifically investigated in the 'Conflict Resolution Dimension' experiment; see sections 5.4.3.3 and 5.5.3. Regardless, the MVP algorithm is used for tactical CR in all cases. The resolution dimension used in each of the five experiments are summarized in Table 5.6.

It is also worth noting that the CR instructions issued by MVP took precedence over the routing constraints imposed by a particular airspace design. Nonetheless, after CR, aircraft flew directly to their pre-conflict sector exit waypoints in the horizontal direction, for both unstructured and layered airspaces. However, in the vertical direction, the trajectory recovery procedure differed between the two airspace designs. In UA, aircraft were allowed to directly return to their pre-conflict altitudes.

In layered airspaces, aircraft had to first check if the direct heading to their target waypoint conformed to the heading-altitude rules in force. If the direct path violated these rules, then aircraft were required to climb/descend to the closest flight level that permitted their desired horizontal travel directions.

5.4.1.4. Airspace Concepts and Concept Implementation

Unstructured Airspace (UA) and four layered airspace concepts, each with a different allowed heading range per flight level, α, were used in the fast-time simulations. Table 5.1 displays the properties of the considered airspace concepts.

Table 5.1: Properties of the airspace concepts used in this study

Symbol	Concept Name	Heading Range, α	Number of Layer Sets, κ
UA	Unstructured Airspace	-	-
L360	Layers 360	360°	8
L180	Layers 180	180°	4
L90	Layers 90	90°	2
L45	Layers 45	45°	1

The airspace concepts were implemented into BlueSky by modifying its trajectory planning functions. While direct horizontal routes were used in both unstructured and layered airspaces, the method used to determine the cruising altitude of an aircraft differed between the two airspace designs. For UA, the cruising altitude of an aircraft, $Z_{ua,i}$, was directly proportional to its trip distance, D_i:
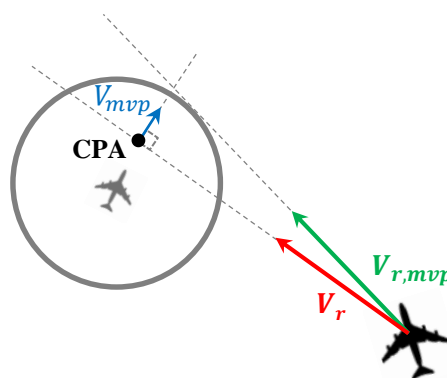
Figure 5.8: Conflict resolution strategy of the Modified Voltage Potential (MVP) algorithm. Here, 'CPA' is the closed point of approach, V_r is the original relative velocity vector between the two conflicting aircraft, V_{mvp} is the MVP conflict resolution velocity vector (perpendicular to V_r at the CPA), and $V_{r,mvp}$ is the resulting relative velocity vector commanded by MVP. Adapted from [15].

$$Z_{ua,i} = Z_{min} + \frac{Z_{max} - Z_{min}}{D_{max} - D_{min}} \ (D_i - D_{min}) \tag{5.44}$$

Here, Z_{min} and Z_{max} are the minimum and maximum altitudes allowed for cruising aircraft in the simulation. Comparably, D_{min} and D_{max} are the minimum and maximum trip distances of aircraft in the simulation.

On the other hand, for the Layers concept, the cruising altitude of an aircraft, $Z_{lay,i}$, depends on both its heading, ψ_i, and its trip distance, D_i, as indicated by the following heading-altitude rule:

$$Z_{lay,i} = Z_{min} + \zeta \left[\left\lfloor \frac{D_i - D_{min}}{D_{max} - D_{min}} \ \kappa \right\rfloor \beta + \left\lfloor \frac{\psi_i}{\alpha} \right\rfloor \right] \tag{5.45}$$

Here, β is the number of flight levels needed to define one complete set of layers, and κ is the number of complete layer sets. These two parameters are defined as $\beta = 360^o/\alpha$ and $\kappa = L/\beta$, where L is the total number of available flight levels. Note that the second term of equation 5.45 computes the cruising altitude of an aircraft as an *integer multiple* of the vertical spacing between flight levels, ζ, using the the floor operator ('⌊ ⌋'). For all layered concepts in this study, $\zeta = 1100$ ft and $L = 8$. Correspondingly, for most layered concepts considered here, $\kappa > 1$; see Table 5.1. For layered concepts with $\kappa > 1$, equation 5.45 uses trip distances to determine cruising altitudes such that short flights remain at lower altitudes, while longer flights use higher layer sets.

It should be noted that the only difference between the UA and L360 concepts is the use of predefined flight levels for cruising aircraft in L360, while any altitude could be selected by aircraft in UA. In fact, the L360 concept was specifically included in the simulations to investigate the effect of using fixed cruising flight levels while simultaneously allowing all possible headings in each flight level on the maximum theoretical capacity of the airspace.

5.4.2. Traffic Scenarios

5.4.2.1. Testing Region and Flight Profiles

A large three-dimensional en-route sector was used as the physical environment for traffic simulations, see Figure 5.9. In the horizontal plane, the sector had a square-shaped cross-section of 400 x 400 nautical miles. In the vertical dimension, the sector is divided into two parts; a 'transition zone' with a height of 4000 ft for climbing and descending traffic, and a 'cruising zone' with a height of 7700 ft. Figure 5.9 also shows the horizontal and vertical flight profiles of an example flight.

As no traffic was simulated outside the simulated sector, aircraft near the edges of the 'simulation region' are unlikely to get into conflicts. To solve this issue, a smaller
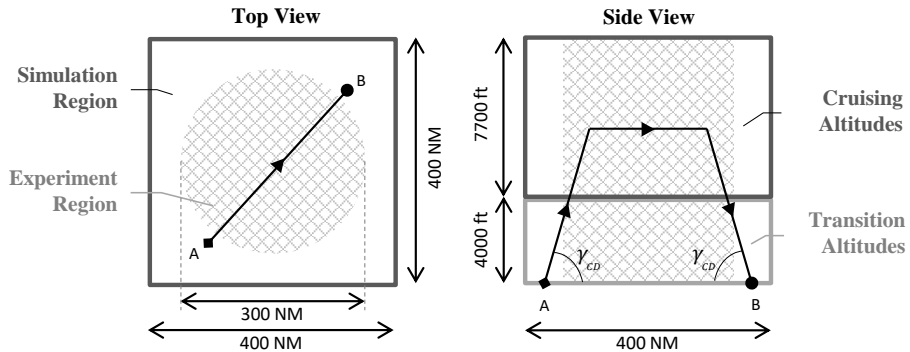
Figure 5.9: Top and side views of the simulation's physical environment. The trajectory of an example flight is shown.

Table 5.2: Common parameters for all five experiments

Parameter	Value	Description
A_{total}	$7.0685 \cdot 10^4$ NM²	Area of 'experiment region'
B_{total}	$3.0533 \cdot 10^{16}$ ft ³	Volume of 'experiment region'
D_{min}	200 NM	Minimum trip distance
D_{max}	250 NM	Maximum trip distance
$\bar{D}$	225 NM	Average trip distance
t_l	5 mins	Conflict detection look-ahead time
S_h	5 NM	Horizontal separation requirement
S_v	1000 ft	Vertical separation requirement
L	8	Number of flight levels for layered airspaces
$\bar{V}$	400 kts	Average ground speed of aircraft
γ_{cd}	2.82^o	Flight-path angle of climbing/descending aircraft
ε	0.82	Proportion of cruising aircraft

cylindrical 'experiment region', with a diameter of 300 nautical miles, was defined in the center of the 'simulation region'. The resulting gap between the experiment and simulation regions ensured that aircraft within the experiment region were surrounded by traffic in all directions. Correspondingly, only aircraft within the experiment region, and only conflicts with closest points of approach within the experiment region, were used to analyze results of the simulation and determine airspace capacity. The parameters of the experiment region needed to evaluate the models, as well as other parameters common to all five experiments, are listed in Table 5.2.

5.4.2.2. Traffic Demand Scenarios and Simulation Procedure

A scenario generator was created to produce traffic scenarios with a desired and constant traffic density. Constant density scenarios were used so that the number

Table 5.3: Number of instantaneous aircraft for the 10 traffic demand scenarios

#	Simulation Region	Experiment Region
1	80.0	53.0
2	103.3	69.3
3	133.5	89.0
4	172.4	114.1
5	222.6	147.4
6	287.5	189.3
7	371.3	244.3
8	479.6	316.7
9	619.4	403.4
10	800.0	521.1

of conflicts logged during a simulation run could be attributed to a particular traffic density. Since aircraft were deleted from the simulation as they exited the sector, to realize constant density scenarios, aircraft were introduced into the simulation at a constant spawn rate equal to $\frac{\bar{V}}{\bar{D}} N_{inst}$, where $\bar{V}$ is the average speed of aircraft, $\bar{D}$ is the average trip distance of aircraft, and N_{inst} is the desired number of instantaneous aircraft. Using this approach, ten traffic demand scenarios of increasing density were defined, ranging between 5-50 aircraft per 10,000 NM^2 in the simulation region. This corresponds to an instantaneous traffic demand of between 80-800 aircraft in the simulation region; see Table 5.3. Note that the maximum traffic density considered in the simulation is greater than the maximum density of 32 aircraft per 10,000 NM^2 in the upper airspace (> 18,000 ft) over the Netherlands in 2017 (computed using logged ADS-B data). Also note that Table 5.3 displays the number of instantaneous aircraft for both the 'simulation' and 'experiment' regions. Furthermore, ten repetitions, representing ten random traffic realizations (i.e, initial conditions), were tested for each traffic demand condition.

To ensure that all airspace concepts were subjected to the same traffic demand and horizontal traffic patterns, all scenarios were generated off-line prior to the simulations. Scenarios were created with a duration of 3 hours, consisting of a 1 hour traffic volume buildup period, a 1 hour logging period, and a 1 hour wind-down period. Traffic density was held constant at the required level during the logging and wind-down periods. The latter period was required to allow aircraft created during the logging hour to finish their flights, and thus prevent abnormally short flights from skewing the results. Moreover, all scenarios were repeated with and without CR such that the DEP could be computed using logged total conflict count data for the 'experiment region'. Furthermore, to enable analysis of all CAMDA sub-models, the number of instantaneous aircraft, and the number of instantaneous conflicts, within the 'experiment region', was logged periodically every 15 seconds.

5.4.3. Independent Variables

The independent variables of the five simulation experiments performed in study are discussed below.

5.4.3.1. Airspace Concept Experiment

The first experiment aimed to compare unstructured and layered airspace designs in terms of capacity. The independent variables of this experiment were:

- 5 airspace concepts; see Table 5.4

- 1 CD setting, namely 'Baseline; see Table 5.5

- 2 CR settings, namely 'CR OFF' and 'CR ON Horizontal'; see Table 5.6

- 1 priority setting, namely 'Cooperative'; see Table 5.7

- 1 speed distribution, namely 'Equal'; see Table 5.8

- 10 traffic demand scenarios; see Table 5.3

Ten repetitions were performed for each traffic demand condition. Therefore, this experiment resulted in a total of 1000 simulation runs, involving over 1.75 million flights.

Table 5.4: Airspace concepts used by the five experiments

Symbol	Concept Name	Aispace Concept Expt.	CD Expt.	CR Expt.	Priority Expt.	Ground Speed Expt.
UA	Unstructured Airspace	✓	✓	✓	✓	✓
L360	Layers 360	✓	-	-	-	-
L180	Layers 180	✓	-	-	-	-
L90	Layers 90	✓	-	-	-	-
L45	Layers 45	✓	✓	-	✓	✓

5.4.3.2. Conflict Detection Experiment

The purpose of this experiment was to determine the effect of conflict detection parameters, namely horizontal and vertical separation requirements, S_h and S_v, and look-ahead time, on airspace capacity. The independent variables for this experiment were:

- 2 airspace concepts, namely UA and L45; see Table 5.4

- 3 CD setting; see Table 5.5

- 2 CR settings, namely 'CR OFF' and 'CR ON Horizontal'; see Table 5.6

- 1 priority setting, namely 'Cooperative'; see Table 5.7

- 1 speed distribution, namely 'Equal'; see Table 5.8

- 10 traffic demand scenarios; see Table 5.3

As before, 10 repetitions were simulated for each traffic demand. As such, a total of 1200 simulation runs were performed for this experiment, using over 2.1 million flights.

Table 5.5: Conflict Detection (CD) parameters used by the five experiments

CD Condition Name	Horiz. Sep. S_h [NM]	Vert. Sep. S_v [ft]	Look-Ahead t_l [mins]	Concept Expt.	CD Expt.	CR Expt.	Priority Expt.	Speed Expt.
Baseline	5.0	1000	5.0	✓	✓	-	✓	✓
Half Separation	2.5	500	5.0	-	✓	✓	-	-
Half Look-Ahead	5.0	1000	2.5	-	✓	-	-	-

5.4.3.3. Conflict Resolution Experiment

This experiment considered the effect of conflict resolution dimension of the maximum theoretical capacity of UA. The independent variables of this experiment were:

- 1 airspace concepts, namely UA; see Table 5.4

- 1 CD setting,namely 'Half Separation'; see Table 5.5

- 3 CR settings, see Table 5.6

- 1 priority setting, namely 'Cooperative'; see Table 5.7

- 1 speed distribution, namely 'Equal'; see Table 5.8

- 10 traffic demand scenarios; see Table 5.3

Because 10 repetitions were performed for each traffic demand, this experiment resulted in a total of 300 simulations runs, using approximately 0.5 million flights.

Table 5.6: Conflict Resolution (CR) dimensions used by the five experiments

CR Condition Name	Resolution Dimension	Aispace Concept Expt.	CD Expt.	CR Expt.	Priority Expt.	Ground Speed Expt.
CR OFF	-	✓	✓	✓	✓	✓
CR ON Horizontal	Heading + Speed	✓	✓	✓	✓	✓
CR ON Vertical	Vertical Speed	-	-	✓	-	-

5.4.3.4. Priority Experiment

This experiment investigated the effect of conflict resolution priority on capacity. The independent variables of this experiment were:

- 2 airspace concepts, namely UA and L45; see Table 5.4

- 1 CD setting, namely 'Baseline'; see Table 5.5

- 2 CR settings, namely 'CR OFF' and 'CR ON Horizontal'; see Table 5.6

- 3 priority settings; see Table 5.7

- 1 speed distribution, namely 'Equal'; see Table 5.8

- 10 traffic demand scenarios; see Table 5.3

Note that in Table 5.7, the 'Cooperative' priority setting implies that all aircraft involved in a conflict share the task of conflict resolution. As the names suggest, for the 'Climb' and 'Cruise' priority settings, aircraft in these flight phases are excepted from performing resolution maneuvers, unless they are in conflict with another aircraft in the same flight phase (in which case a cooperative strategy is used). A total of ten repetitions were simulated for each traffic demand, resulting in 1200 simulation runs involving over 2.1 million flights.

5

Table 5.7: Priority settings used by the five experiments

Priority Condition Name	Resolving Aircraft	Aispace Concept Expt.	CD Expt.	CR Expt.	Priority Expt.	Ground Speed Expt.
Cooperative	Both	✓	✓	✓	✓	✓
Climb/Descend	Cruise	-	-	-	✓	-
Cruise	Climb/Descend	-	-	-	✓	-

5.4.3.5. Ground Speed Experiment

As the CAMDA models derived in this work assume that all aircraft fly with equal ground speeds, this final experiment considered the sensitivity of the models to this assumption. The independent variables of this experiment were:

- 2 airspace concepts, namely UA and L45; see Table 5.4

- 1 CD setting, namely 'Baseline'; see Table 5.5

- 3 CR settings, see Table 5.6

- 1 priority setting, namely 'Cooperative'; see Table 5.7

- 3 speed distribution; see Table 5.8

- 10 traffic demand scenarios; see Table 5.3

A total of 1200 simulation runs were performed for this experiment, using 10 repetitions for each traffic demand scenario, and involving over 2.1 million flights.

Table 5.8: Aircraft ground speed distributions used by the five experiments

Speed Distribution	Value [kts]	Aispace Concept Expt.	CD Expt.	CR Expt.	Priority Expt.	Ground Speed Expt.
Equal	400	✓	✓	✓	✓	✓
Normal	$\mathcal{N}(400.0, 16.7^2)$	-	-	-	-	✓
Uniform	$\mathcal{U}(350.0, 450.0)$	-	-	-	-	✓

5.4.4. Dependent Variables

In addition to computing the maximum theoretical capacity of the airspace, ρ_{max}, for all experiments, data collected from the 'Airspace Concept Experiment' was also used to assess the accuracies of the CAMDA sub-models. The specific approach used to measure accuracy varied between the analytical and semi-empirical components of the CAMDA framework. The appropriate methods are discussed with the corresponding results in the following section.

5.5. Results

This section presents the results of the five fast-time simulation experiments. As indicated previously, the results are applicable for decentralized unstructured and layered airspace designs that utilize the state-based CD method, and the MVP CR algorithm.

5.5.1. Airspace Concept Experiment

Heading-altitude rules and predefined flight levels differentiate layered airspaces from Unstructured Airspace (UA). The goal of this experiment, therefore, was to examine how these two differences between unstructured and layered airspaces affect the maximum theoretical capacity of the airspace. Additionally, the data gathered from this experiment is also used to analyze the accuracy of all CAMDA sub-models, and to validate the two assumptions that were made during their derivation. The following paragraphs discuss the results of the analytical and the semi-empirical components of the CAMDA framework separately.

5.5.1.1. Analytical Model Components

Figure 5.10 displays the simulation results for the analytical components of the CAMDA method. Here, the scatter points represent the raw data collected from the simulations, while the solid lines represent the predictions of the corresponding analytical CAMDA components. Note that the simulation data appears in 10 clusters as 10 traffic demand conditions were simulated, with each cluster representing data collected from all repetitions of a particular demand condition; see Table 5.3.

To measure the accuracy of the analytical models, a model accuracy parameter, k, is introduced:

$$\text{Simulation Measurement} = \text{Analytical Model} \times k$$

Here it can be seen that k acts as a constant scaling parameter to the analytical models. Its value is determined by fitting the models to the simulation data in a least-square sense. A value of k close to 1 indicates high model accuracy, while $k < 1$ and $k > 1$ indicates model over- and under-estimation of simulation data, respectively. Model accuracy is also computed as a percentage by comparing the fitted 'k value' to a reference value of 1. The k values are indicated on the top-left corner of the four graphs displayed in Figure 5.10.

Step 1: Instantaneous Conflict Count Without Conflict Resolution, $\text{C}_{\text{inst,nr}}$

The results for $C_{inst,nr}$ are displayed in Figure 5.10(a). The figure shows that the analytical models for $C_{inst,nr}$, given by equations 5.3 and 5.25 for unstructured and layered airspaces, are able to predict both the shape and the magnitude of the simulation data for all airspace concepts. This high accuracy is reflected by k values that are very close to 1, particularly for UA and L360. Although accuracies for all airspace concepts are greater than 85%, the k values for layered airspaces indicates that the corresponding model slightly over-estimates the number of conflicts, and that the degree of overestimation increases as the heading range per flight level, α, is decreased.

The reduction of model accuracy for smaller α can be explained by considering the simulation's design, and the process of conflict detection for climbing/descending aircraft. As indicated by Figure 5.5(b), in state-based CD, the volume of airspace searched for conflicts by an aircraft can be decomposed into separate horizontal and vertical components. For climbing/descending aircraft, the *vertical* conflict search volume can extend beyond the upper and lower boundaries of the simulated sector. Since no traffic was simulated outside the considered sector, climbing/descending aircraft are, therefore, less likely to detect conflicts, particularly near the edges of the sector. Although this simulation artifact affects both airspace designs, previous research has shown that the significant increase in the proportion of conflicts involving climbing/descending aircraft in layered airspaces leads to a greater over-estimation by the corresponding model, explaining the accuracy results noted above. Previous research has also validated this explanation by showing that a decrease of the flight-path angles of climbing/descending aircraft increases model accuracy, as this reduces the size of the vertical conflict search volume [118].

Because Figure 5.10(a) considers the situation without CR, it can be used to compare the five airspace concepts in terms of the 'intrinsic safety' that they provide. Here, the notion of intrinsic safety focuses purely on the effect of the constraints imposed by an airspace design on the number of instantaneous conflicts. Figure 5.10(a) shows that layered airspaces are intrinsically safer than UA, and that the safety of layered airspaces increases as α is decreased. In addition to the

beneficial effect of reducing α on intrinsic safety, comparison of the UA and L360 concepts indicates that the use of predefined flight-levels also decreases the number of instantaneous conflicts.

Step 2: Total Conflict Count Without Conflict Resolution, $\mathbf{C_{total,nr}}$

Figure 5.10(b) shows the results for the second model of the CAMDA framework, namely $C_{total,nr}$. As for $C_{inst,nr}$, this figure shows that layered airspaces reduced the total number of conflicts without CR relative to UA, and that smaller values of α lead to lower total conflict counts. This is unsurprising because $C_{total,nr}$ is computed by integrating the model for $C_{inst,nr}$ over the analysis time interval (1 hour in this case), while taking into account the average duration of a conflict (which is in turn dependent on the look-ahead time); see equation 5.8 for UA and equation 5.36 for layered airspaces.

Although the model curves in Figure 5.10(b) closely follow the trend between $C_{total,nr}$ and traffic density, it can be seen that the corresponding models for both airspace designs underestimate the total conflict count without CR. This underestimation is also indicated by $k > 1$ for all airspace concepts. This result can be

(a) Inst. Conflict Count Without CR

(b) Total Conflict Count Without CR

(c) Local Conflict Rate, Layers 45 (L45)

(d) Total Aircraft Count, Layers 45 (L45)
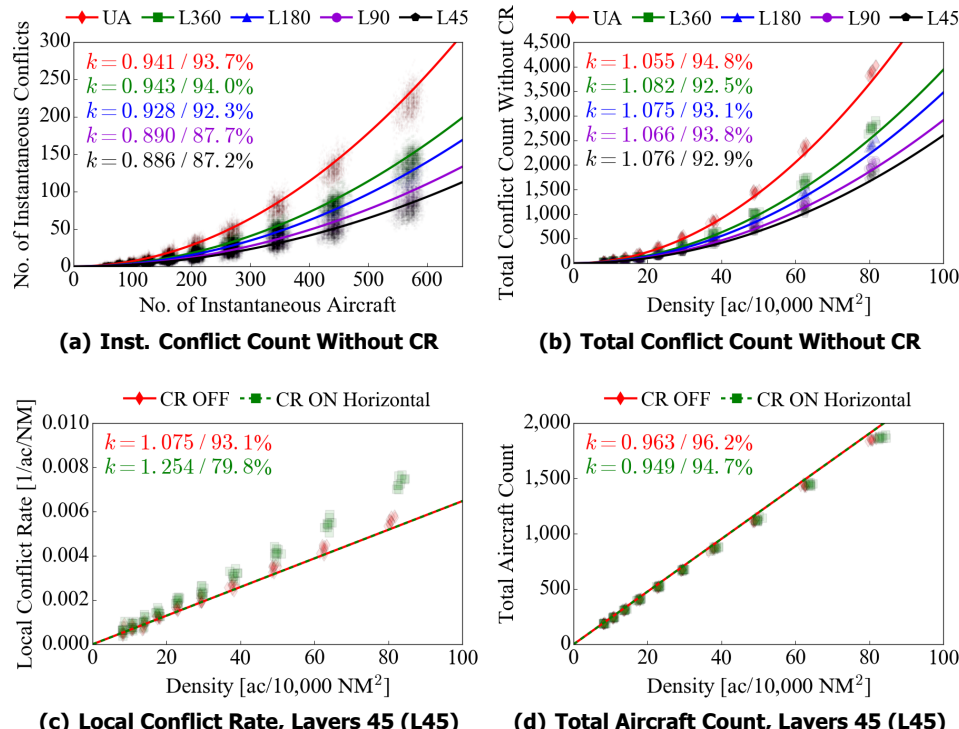
Figure 5.10: Simulation data (scatter points) and model *predictions* (solid lines) for analytical components of the CAMDA framework, airspace concept experiment

attributed to the occurrence 'pop-up' conflicts, which are short-term conflicts often caused by climbing aircraft when they first enter the simulated sector. Because such pop-up conflicts reduce the average conflict duration in the simulation, and because of the effects of pop-up conflicts are not taken into account by the models for $C_{total,nr}$, the models under-estimate the total number of conflicts.

Steps 3&4 + Assumption 1: Local Conflict Rate With and Without Conflict Resolution, C'_1

The results for C'_1 with and without CR are pictured in Figure 5.10(c). Note that due to limited space, the figure only displays the results for the Layers 45 (L45) concept; the results for the other airspace concepts are similar. Moreover, the L45 concept led to the lowest model accuracy of all considered concepts.

An important assumption made by the CAMDA method to bridge the cases with and without CR is that $C'_{1,wr} = C'_{1,nr}$, see assumption 1. Analysis of Figure 5.10(c) shows that this assumption is true up to a density of approximately 40 aircraft per 10,000 NM^2. But beyond this density, the simulation data indicates that $C'_{1,wr} > C'_{1,nr}$. Furthermore, the difference between the model predictions and the simulation results appears to increase beyond this density. It is hypothesized that the larger number of conflict chain reactions that occur at higher densities leads to a break-down of this assumption; for instance, if such conflict chains are concentrated in one or more parts of the airspace, then it is logical that, on average, the local conflict count per unit distance with CR would increase relative to the case without CR.

Regardless, Figure 5.10(c) indicates that the first assumption made by the CAMDA framework, that $C'_{1,wr} = C'_{1,nr}$, is only valid for densities that are comparable to todays peak densities (32 aircraft per 10,000 NM^2 over the Netherlands in 2017). For densities that are approximately three times greater than today, this assumption does not hold in a purely mathematical sense. However, because the absolute difference between model and simulation at the highest simulated density is less than 2e-3 conflicts per aircraft per nautical mile, the violation of this assumption is not likely to significantly affect the final CAMDA capacity estimate; at this level of difference, an aircraft would have to fly an additional 500 NM, which is double the average flight distance of aircraft in the simulation, for it to encounter just one additional conflict relative to the model prediction for Layers 45. This conclusion is further exemplified model accuracies which are approximately 80% for all airspace concepts.

Assumption 2: Total Aircraft Count, N_{total}

The second assumption used by the CAMDA framework to bridge the cases with and without CR is that $N_{total,wr} = N_{total,nr}$. To validate this assumption, results the corresponding results for L45 are displayed in Figure 5.10(d); the results for the other airspace concepts are identical but are not shown in the interest of space. The figure shows that the model for N_{total}, given by equation 5.11, closely matches the simulation data for the cases with and without CR. The high accuracy is further emphasized by k values that are very close to 1. Therefore it can be concluded

that the second assumption used by CAMDA is valid for all considered densities and airspace concepts.

It is interesting to note that Figures 5.10(c) and 5.10(d) show that CR increased traffic densities even though the exact same traffic scenarios were used for simulations with and without CR. This is because CR maneuvers increase the flight distances of aircraft, which in turn increases the average number of instantaneous aircraft within the simulated sector at any given moment in time. The increase of flight distance (and/or flight time) with CR is central to the derivation of the CAMDA capacity framework; see section 5.3.3.5.

5.5.1.2. Semi-Empirical Model Components

The last two models of the CAMDA framework, namely $C_{total,wr}$ and the DEP, are influenced by D_{cdr}. This parameter describes the extra distance flown by an aircraft to resolve each detected conflict and to return to its pre-conflict sector exit waypoint; see Figure 5.6. Because D_{cdr} is affected by conflict chain reactions, its value can only be determined by fitting the model for $C_{total,wr}$, or equally the model for the DEP, to the simulation data in a least-squares sense. As these two models are semi-empirical, it is, therefore, not possible to measure model accuracy using the procedure outlined earlier for the analytical components of the CAMDA framework.

Instead, the accuracy of the semi-empirical models can be determined by considering two aspects. The first aspect is *qualitative*, and it considers the ability of the models to predict the shape of the relationship between traffic density and the airspace state of interest, in this case $C_{total,wr}$ and the DEP. This aspect can be studied visually by checking whether the shape of the fitted model curve follows the trends displayed by the raw simulation data. If the fitted model curve matches well with the simulation data for all experiment conditions, then the basic structure of the model can be regarded to be sound.

The second aspect is *quantitative*, and it aims to measure the accuracy of the fitting process. To this end, the available simulation data is split into two datasets of equal size, known as the 'training' and the 'validation' datasets. Only the training dataset is used to determine the value of the semi-empirical parameter, D_{cdr}. Subsequently, the Root Mean Square (RMS) error between model predictions and the empirical data is computed for both training and validation datasets. If the RMS error for the training dataset is small, then the fitting accuracy is considered to be high. If the RMS errors for both training and validation datasets are comparable, then the model fitting process was not significantly affected by simulation artifacts and noise, i.e, over-fitting was limited.

Step 5: Total Conflict Count With Conflict Resolution, $\text{C}_{\textbf{total,wr}}$

Figure 5.11(a) shows the results for $C_{total,wr}$, i.e., the with CR counterpart of Figure 5.10(b). Unsurprisingly, this figure shows that the total number of conflicts with CR was the highest for UA. However, on comparing Figures 5.10(b) and 5.11(a),

(a) **Total Conflict Count With CR**

(b) **RMS Error of Total Conflict Count With CR**

(c) **Domino Effect Parameter**

(d) **RMS Error of Domino Effect Parameter**
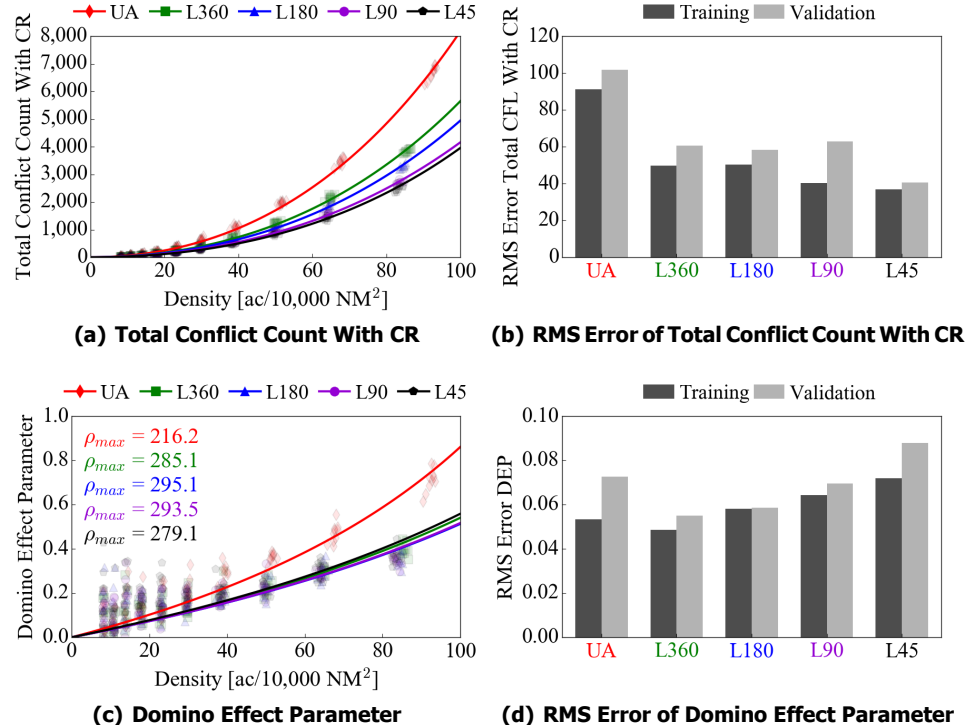
Figure 5.11: Simulation data (scatter) and model *fits* (solid lines) for semi-empirical components of the CAMDA framework, airspace concept experiment

it can be seen that CR appears to have reduced the relative differences between the concepts, particularly between the layered concepts; compare, for instance, the difference between the L90 and L45 concepts in Figures 5.10(b) and 5.11(a). Nonetheless, as the fitted model curves closely approximate the shape and the magnitude of the simulation data, it can be concluded that the corresponding models, given by equations 5.19 and 5.39 for unstructured and layered concepts, well represent the trends between $C_{total,wr}$ and traffic density.

To quantify the accuracy of the model fits for $C_{total,wr}$, Figure 5.11(b) displays the RMS errors for the training and validation datasets. Here, it can be see that the errors for the training dataset are quite low relative to the average number of conflicts logged for each airspace concept. For example, the RMS error of 90 conflicts for the training dataset of UA corresponds to an error of only 6% relative to the average number of conflicts logged for this airspace design (across all traffic densities and repetitions). On a similar note, the errors for the training and validation datasets are comparable for each airspace concept. For these two reasons, the accuracy of the model fits can be considered to be high.

Step 6: Domino Effect Parameter (DEP) and Airspace Capacity

The results for the DEP are pictured in Figure 5.11(c). As expected, the figure shows that the DEP, which considers the occurrence and propagation of conflict chain reactions, increases nonlinearly with traffic density for all airspace concepts. However, the empirical DEP values, i.e., scatter points in Figure 5.11(c), appear to be very noisy at low densities. This can be attributed to the fact that the empirical DEP values are obtained by *dividing* simulation logged conflict counts for scenario repetitions with and without CR, and the output of this division process is particularly sensitive to the relatively few conflicts that occur at low traffic densities; see equation 5.1. Nevertheless, Figure 5.11(c) indicates that the fitted model curves for all airspace concepts closely approximate the shape and magnitude of the empirical DEP data at high traffic densities. The accuracy of the model fitting process is further highlighted by the low RMS errors found for both training and validation datasets, given the 'noisy' empirical data; see Figure 5.11(d).

Using the DEP results, it is possible to apply the CAMDA capacity definition, given by equation 5.2, to determine the maximum theoretical capacity, ρ_{max}, of all airspace concepts considered in this experiment. From a graphical point of view, this entails determining the traffic density corresponding to the vertical asymptote of the fitted model curves. The corresponding ρ_{max} results are shown on the top left corner of Figure 5.11(c). As for all previous CAMDA steps, there is a clear distinction between unstructured and layered airspace designs, with UA resulting in the lowest capacity. However, no significant differences can be found between the capacities of the layered concepts. In fact, capacity *decreased* as α was reduced below 180°, a trend opposite to that reported above for the number of conflicts with and without CR; see Figures 5.10(a) and 5.10(b).

This unexpected result can be understood by considering equation 5.43, which describes the relationship between ρ_{max}, the (weighted) conflict probability between aircraft in layered airspaces, p_{LAY}, and the average extra distance flown to resolve each conflict in layered airspaces due to CD&R, $D_{cdr_{LAY}}$. It is restated below for convenience:

$$\rho_{max_{LAY}} = \eta_{LAY}\mu_{LAY} = \frac{2\ L\ t_c\ (TV_o + D_{nr})}{p_{LAY}T\ A_{total}D_{cdr_{LAY}}} \qquad (5.43)$$

From the above equation it can be seen that ρ_{max} is inversely proportional to both p_{LAY} and $D_{cdr_{LAY}}$. The values of both these parameters, as well as the average distance to the Closest Point of Approach (CPA) between conflicting aircraft, D_{cpa}, are listed in Table 5.9 for all four layered airspace concepts considered in this experiment.

Table 5.9 indicates that p_{LAY} reduces with α; this can be explained by the reduction of relative velocities between cruising aircraft for smaller α; see equation 5.28. On the other hand, a reduction of α is shown to increase $D_{cdr_{LAY}}$, indicating that aircraft fly longer routes for smaller α. This trend can be explained by considering

Table 5.9: Values for p_{LAY}, $D_{CDR_{LAY}}$ and D_{cpa} for layered designs, airspace concept experiment

Concept Name	Heading Range, α	p_{LAY}	$D_{CDR_{LAY}}$ [NM]	D_{cpa} [NM]
Layers 360	360°	0.0070	32.05	31.15
Layers 180	180°	0.0058	35.04	32.11
Layers 90	90°	0.0044	37.97	34.36
Layers 45	45°	0.0037	52.56	37.26

the behavior of the MVP CR algorithm used in this study. As indicated by the V_{mvp} vector in Figure 5.8, MVP acts by 'pushing' conflicting aircraft pairs away from each other in a direction that is *perpendicular* to the relative velocity vector, V_r, at the CPA, such that minimum separation requirements are just met. As constant aircraft velocities are assumed within the look-ahead time, the magnitude of the 'push' that is necessary to resolve conflicts in this manner is inversely proportional to D_{cpa}. However, because smaller values of α reduce conflict angles between aircraft, smaller values of α increase D_{cpa}, see Table 5.9. This in turn increases the length of the MVP commanded resolution path for smaller α. Therefore, in contrast to the number of conflicts with and without CR, reducing α does not increase of the capacity of layered airspaces that use MVP because the safety benefits of lowering α are counteracted by the efficiency drop caused by longer CR trajectories.

5.5.2. Conflict Detection Experiment

The goal of the Conflict Detection (CD) experiment is to study the effects of horizontal and vertical separation requirements, and look-ahead time, on the maximum theoretical capacities of the UA and L45 airspace concepts. Figure 5.12 displays the corresponding DEP and capacity results for this experiment. Here it can be seen that separation requirements have a significantly larger effect on capacity than look-ahead time for both airspace concepts. As for the airspace concept experiment, this trend can be understood by considering the effects of CD parameters on conflict probability, p, and the extra distance flown by aircraft due to each conflict resolution maneuver, D_{cdr}.

The effect of CD parameters on p can be studied using equation 5.4. This equation states that a halving of the look-ahead time leads to a halving of p, while a having of horizontal and vertical separation requirements leads to a quartering of p. This indicates that separation requirements have a much larger effect of on p, and therefore, on ρ_{max}, than look-ahead time.

Separation requirements and look-ahead time also affect ρ_{max} via the D_{cdr} parameter; see equations 5.24 and 5.43. However, because D_{cdr} is an empirical parameter, the exact relationship between it and CD parameters is unknown. But for both airspace designs, Figure 5.12 indicates that D_{CDR} minimizes the capacity benefits of reducing CD parameters. This is particularly the case when look-ahead time is halved for L45; instead of doubling capacity relative to the baseline condition, a
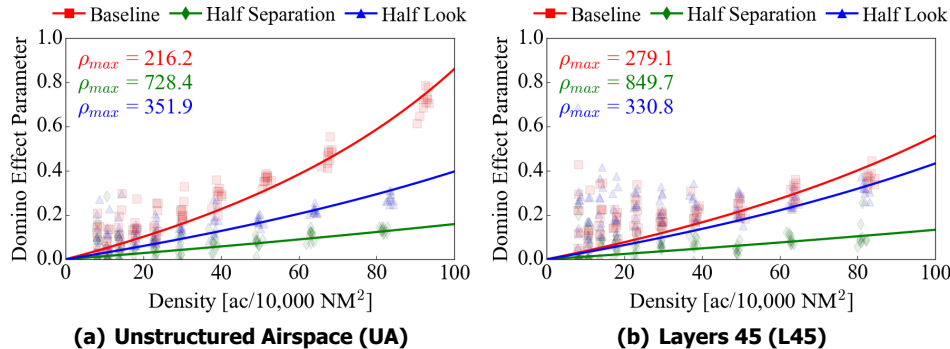
Figure 5.12: Domino Effect Parameter (DEP) and airspace capacity (ρ_{max}) results, conflict detection experiment

halving of look-ahead time increases D_{cdr} such that capacity is only increased by approximately 18%. This indicates that D_{CDR} actually increases as the look-ahead time is reduced, and this increase in D_{CDR} reduces the beneficial capacity effect of reducing the look-ahead time on conflict probability. Moreover, an inverse relationship between D_{CDR} and look-ahead time is logical since a larger heading deviation, and therefore a larger path deviation, is needed when conflicts are detected and resolved later in time.

5.5.3. Conflict Resolution Experiment

The third experiment investigated the effect of conflict resolution dimension on airspace capacity. To this end, simulations for UA were repeated for the cases where conflict resolution was a) limited to the horizontal direction and b) limited to the vertical direction. The DEP and capacity results for this experiment are shown in Figure 5.13. Here it can be seen that the airspace becomes more unstable when vertical conflict resolutions are used. In fact, limiting CR to the vertical direction decreases airspace capacity by more than a third.

Although the horizontal separation requirement is 30 times larger than the vertical separation minima for the settings used in this experiment, see Table 5.5, this unusual result can be explained by considering the horizontal and vertical density distributions of aircraft. In en route airspace, aircraft tend to be more closely packed in the vertical direction than in the horizontal plane. For example, most long-distance flights cruise between FL300-FL400, whereas aircraft can be separated in the horizontal direction by many nautical miles. As a result of the closer packing of aircraft along the vertical direction, vertical conflict resolution maneuvers are more likely to trigger new conflicts, and therefore, more like to cause conflict chain reactions. Consequently, vertical resolutions reduce the maximum theoretical capacity of the airspace.
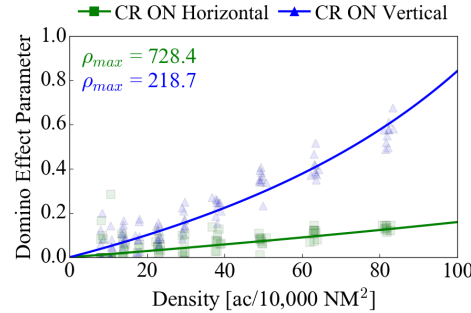
Figure 5.13: Domino Effect Parameter (DEP) and airspace capacity (ρ_{max}) results for Unstructured Airspace (UA), conflict resolution experiment

5.5.4. Priority Experiment

While all other experiments used cooperative conflict resolutions, this experiment considered the impact of conflict resolution priority on airspace capacity. Therefore, in addition to cooperative resolutions, simulations were performed for the cases where priority was assigned to either climbing/descending aircraft or to cruising aircraft; see Table 5.7. The corresponding DEP and airspace capacity results for the UA and L45 concepts are displayed in Figure 5.14. This figure shows that priority had different effects on the two airspace concepts. For UA, capacity was the highest when cruising aircraft had priority, but for L45, the situation was reversed, and capacity was maximized when climbing/descending aircraft were given priority.

(a) Unstructured Airspace (UA)   **(b) Layers 45 (L45)**
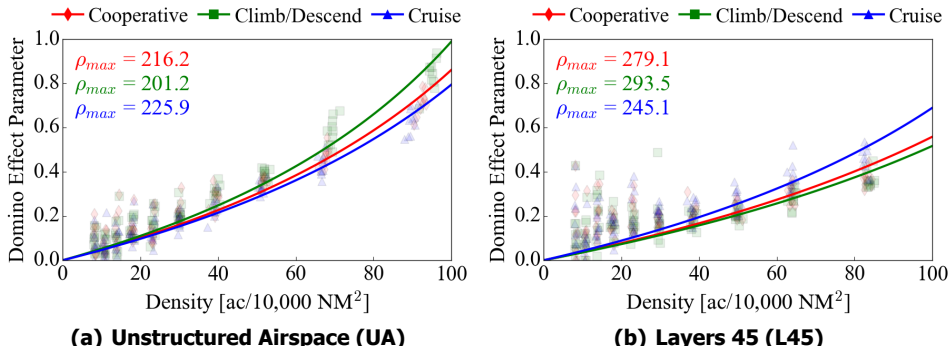
Figure 5.14: Domino Effect Parameter (DEP) and airspace capacity (ρ_{max}) results, priority experiment

The opposite trends displayed by the UA and L45 concepts can be understood by considering two factors: a) the process of CD and b) the proportion of aircraft in different flight phases. In UA, all aircraft, regardless of flight phase, search for conflicts within a *volume* of airspace in front of them, see Figure 5.5. Although this

volume is slightly larger for climbing and descending aircraft, conflict probabilities for all flight phases are comparable in magnitude as aircraft horizontal speeds are much higher than their vertical speeds in en route airspaces. Instead, capacity is maximized in UA when priority is given to cruising aircraft because the vast majority of aircraft are in the cruise phase (82% in the simulations considered here). Therefore, by shifting the burden of conflict resolutions to the minority of aircraft, i.e., climbing/descending aircraft, capacity is increased by approximately 10% (compare green and blue lines in Figure 5.14(a)).

However, in layered airspaces, conflict probability is significantly dependent on the flight phases of interacting aircraft. This is because conflict probability is a function of the *area* of airspace searched for conflicts for cruising aircraft, whereas for climbing/descending aircraft, it is dependent on the volume of airspace searched for conflicts. As a result of the smaller region of airspace searched for conflicts, conflict probability is significantly smaller for cruising aircraft in layered airspaces. For this reason, even though there are vastly more cruising aircraft in the airspace, resolution maneuvering by cruising aircraft is less likely to trigger new conflicts and conflict chains. This in turn improves airspace stability, explaining the nearly 20% increase in maximum capacity when climbing/descending aircraft are assigned priority over cruising traffic in layered airspaces (relative to all other priority settings).

5.5.5. Ground Speed Experiment

To reduce the complexity of the derivation process, the models described in this chapter assume equal grounds speeds for all aircraft. This assumption ignores possibility of overtaking conflicts, and it primarily affects the computation of the expected horizontal relative velocities between aircraft, $\mathbf{E}\left(V_{r,h}\right)$; see equations 5.4 and 5.27. To study the effect of this assumption on airspace capacity, simulations for the UA and L45 airspace concepts were performed for the conditions where aircraft speeds were a) equal, b) normally distributed and c) uniformly distributed; see Table 5.8.

The DEP and capacity results for the ground speed experiment are displayed in Figure 5.15. As for the previous experiment, this figure shows that ground speed variations between aircraft had different effects on UA and L45. For UA, Figure 5.15(a) shows no substantial differences between the three speed distributions tested. But for L45, Figure 5.15(b) indicates that capacity decreases for non-equal speed conditions; capacity decreases by approximately 10% for the uniform speed distribution relative to the equal speed case.

To better understand these results, $\mathbf{E}\left(V_{r,h}\right)$ has been computed using the numerical approach described in [110] for all three speed distributions, and for both airspace concepts; see Table 5.10. Here it can be seen that speed distribution has a much greater effect on $\mathbf{E}\left(v_{r,h}\right)$ for L45; a 10% increase occurs when the speed distribution is changed from 'equal' to 'uniform' for L45, while a similar change of speed distribution only results in a 0.5% increase for UA. Because speed distribution has a larger effect on the $\mathbf{E}\left(V_{r,h}\right)$ for L45, it also has a larger effect on the capacity of
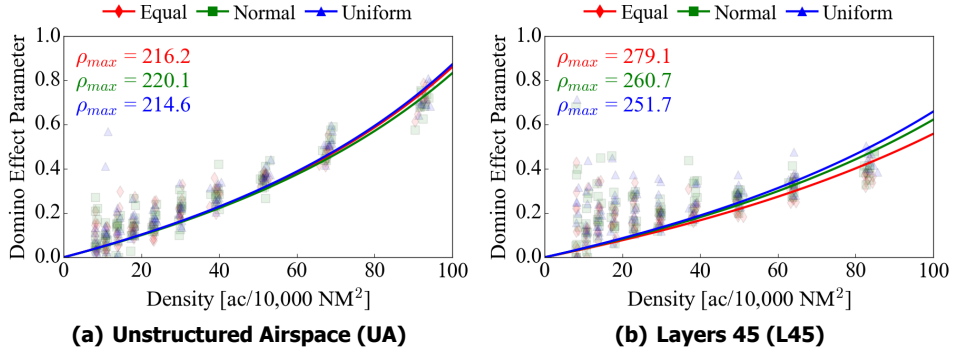
Figure 5.15: Domino Effect Parameter (DEP) and airspace capacity (ρ_{max}) results, ground speed experiment

L45, explaining the trends described in Figure 5.15. Furthermore, this result indicates that the capacity of layered airspaces are directly proportional to the heading range permitted per altitude band, as overtaking conflicts are more likely for smaller heading ranges.

Table 5.10: Numerically computed values of the expected horizontal relative velocities for Unstructured Airspace and Layers 45

	Equal	Normal	Uniform
Unstructured Airspace [kts]	509.30	507.42	511.66
Layers 45 [kts]	103.92	107.46	114.66

5.6. Discussion

This chapter presented the derivation of the Capacity Assessment Method for Decentralized Air Traffic Control (CAMDA). CAMDA is a semi-empirical method, and it was demonstrated here using fast-time simulations of unstructured and layered airspace designs that utilized the state-based Conflict Detection (CD) method, and the Modified Voltage Potential (MVP) Conflict Resolution (CR) algorithm. This section reflects on the results of the simulations and discusses the accuracy of the underlying models of the CAMDA framework. Additionally, important aspects related to the usage of the CAMDA method are also considered.

5.6.1. Unstructured vs. Layered Airspace Designs

Analogous to the safety trends reported by previous studies, analysis of the current experimental results using the CAMDA approach indicated that the capacity of layered airspace designs is higher that of the unstructured airspace concept. The

increased safety and capacity of layered concepts can be attributed to the two aspects that differentiate unstructured and layered airspaces: the use of predefined flight levels, and the use of heading-altitude rules. Because these two design elements reduce the average conflict probability and the number of possible conflict pairs, both the number of conflicts and the number of conflict chain reactions were found to be lower for layered airspaces. As the CAMDA framework defines capacity to be inversely related to the number of conflict chain reactions, capacity was determined to higher for layered airspaces.

However, a direct correlation between safety and capacity was *not* found for the different layered airspace concepts considered here, which differed in terms of the heading range allowed per flight level. Although decreasing the heading range lowered the total number of conflicts, reductions of this parameter did not lead to a consistent improvement of the number of conflict chain reactions. In fact, the CAMDA computed capacity estimate actually decreased slightly when the heading range per flight level was decreased below 180°.

Detailed analysis of the simulation data traced this unexpected result to the behavior of the MVP CR algorithm when it is used in combination with layered airspace designs. The MVP algorithm acts by 'pushing' conflicting aircraft pairs away from each other at their Closest Point of Approach (CPA) such that separation requirements are just satisfied. For unstructured airspaces, this approach does not negatively affect CR performance. But for layered airspaces, a reduction of the heading range per flight level increases the distances between conflicting aircraft pairs and their CPAs. This in turn increases the length of CR trajectories as the heading range per flight level is reduced for layered airspaces. Therefore, the capacity of layered airspaces that use MVP for CR does not increase as the heading range per flight level is decreased because the corresponding safety benefits are negated, and in some cases, outweighed, by the increasing inefficiency with which conflicts are resolved.

From the above analysis, it can be concluded that the *maximum* airspace capacity is strongly dependent on both the safety and efficiency of travel, and that both these performance measures are affected by the selected airspace design, and the selected algorithms for Conflict Detection and Resolution (CD&R). Here, the airspace design affects the safety and efficiency of the *planned* flight routes, whereas the algorithms for CD&R contributes to the safety and efficiency of the *actually flown* trajectories. As such, an optimization of airspace capacity requires an optimization of both airspace design and CD&R algorithm. If this is not the case, the beneficial characteristics of an airspace design, can for instance, be bottlenecked by the chosen CD&R method, as was the case for the pairing between layered airspaces and the MVP algorithm in this study.

5.6.2. Unexpected Results

In addition to the trends described above, analysis of the simulation results led to two particularly unexpected conclusions. These were related to the effects of CR priority and CR dimension on maximum airspace capacity.

Conventional ATM wisdom suggests that CR priority, when dependent on the flight phases of aircraft, should be assigned to the flight phase exhibited by the majority of aircraft. As most aircraft in en route airspaces are in the cruise phase of flight, this reasoning suggests that assigning priority to cruising traffic would maximize en route airspace capacity. While this was indeed the case for unstructured airspace, for layered airspaces, capacity was higher when climbing/descending aircraft were given priority. This counterintuitive result can be explained by the fact that the predefined flight levels used by layered airspaces leads to significantly lower conflict probabilities for cruising traffic than for climbing/descending aircraft. As such, any maneuvering by cruising traffic is less likely to trigger additional 'secondary' conflicts during the resolution of a 'primary' conflict. For this reason, even though 82% of aircraft in the simulations were cruising at any given moment in time, capacity was increased by around 20% when the burden of CR was shifted to cruising traffic in layered airspaces.

Because vertical separation requirements are often an order of magnitude smaller than their horizontal counterparts, vertical CR is expected to be more efficient, and therefore, lead to higher capacities relative to resolutions that are limited to the horizontal direction. This logic is indeed true when considering an isolated conflict between *two* aircraft. However, for a *population* of aircraft, it is also necessary to consider the horizontal and vertical distributions of aircraft locations when examining the influence of CR dimension on capacity. Because aircraft in en route airspaces tend to be packed more closely together in the vertical direction than in the horizontal plane, vertical CR is more likely to trigger conflict chains. As a result, the simulations performed here indicated a threefold increase in the number of conflict chain reactions, as well as a corresponding decrease of capacity, when conflicts were resolved using vertical speed changes alone. If skewed separation standards are also proposed for future unmanned aircraft operations in low altitude urban airspaces, this conclusion suggests that maximum capacity would benefit significantly from the use horizontal conflict resolutions for such scenarios.

As implied above, the initially surprising results can be explained using the underlying models of the CAMDA framework, as well as by using the associated capacity definition that measures capacity from the perspective of conflict chain reactions. As such, the two cases described above illustrate the utility of the CAMDA method; because the all the parameters of the underlying models are derived with a physical interpretation, the effect of a number of factors on capacity can be directly understood from the structure of the models themselves. This in turn allows for a more systematic selection of the required experimental conditions, and thus speeding up the analysis of a new decentralized airspace concept.

5.6.3. Accuracy of CAMDA Models

The CAMDA framework is composed of six sequential steps, consisting of four analytical and two empirical models. The accuracies of the analytical models were computed by comparing simulation results to model predictions. This approach re-

vealed high accuracies for the first three analytical models. However, the accuracy of the fourth analytical model, which calculates the conflict rate per aircraft with CR, varied with traffic density; accuracy was high for densities up to today's peak demand, but it degraded for higher densities. Nevertheless, as overall accuracy for all considered densities was found to be approximately 80% for this parameter, this error did not significantly affect the accuracy of the final empirical components of the CAMDA framework. This is because minor errors from the preceding analytical steps are absorbed into the value estimated for the one empirical parameter of the framework, which considers the extra distance flown per CR maneuver. Furthermore, qualitative and quantitative methods indicated that the empirical models were capable of accurately describing the relationship between traffic density and the number of conflict chain reactions in the airspace, for all tested conditions and airspace concepts. Therefore, the final CAMDA computed capacity estimate can be considered to be sufficiently accurate for performing tradeoffs between different airspace designs and/or CD&R algorithms.

5.6.4. Additional Considerations

As mentioned previously, CAMDA is a semi-empirical method. It is reliant on empirical data, obtained through simulation, to assess the capacity of an airspace design and CD&R algorithm combination. Although simulations can be time consuming, this reliance on empirical data increases versatility of the method; by applying appropriate changes to the first step of the method, the CAMDA framework can be adapted to assess the capacities of airspace designs and CD&R algorithms other than those considered in this study. In fact, this approach was used here to derive the required models for layered airspaces using the models initially developed for the unstructured airspace concept. This versatility also allows it to be used to investigate the effects of a number of operational conditions that were not tested here, such as the effects of hardware failures and/or various weather phenomena on capacity, as long as adequately realistic simulation models can be developed for the required use cases.

It is important to realize that there is a clear distinction between the theoretical and the operationally relevant practical capacity of the airspace. The CAMDA method developed in this work focuses on the theoretical capacity limit. The theoretical capacity limit can be used as a metric to compare different airspace design options. Furthermore, the CAMDA approach makes it possible to understand how the features of a particular airspace design contribute to its theoretical capacity. However this theoretical capacity limit is hypothetical, as it represents a situation where aircraft never reach their destination, but are in a persistent state of conflict. This theoretical capacity limit on its own therefore has no operational relevance.

For an operational capacity limit, it is necessary to define thresholds on safety and efficiency. Here, thresholds on safety, e.g., target levels of safety (e.g. 10^{-7} incidents per hour), are dependent on what we as a society find an acceptable risk of an incident occurring. Efficiency limits are dictated by economic demands

of the airspace users. Such targets are independent of the airspace design selected. Nevertheless, using such desired targets, it is possible to use the CAMDA relations to determine corresponding operational capacity for the selected airspace concept.

5.7. Conclusions

This study focused on the development and demonstration of the Capacity Assessment Method for Decentralized Air Traffic Control (CAMDA). CAMDA was tested here using fast-time simulations of decentralized unstructured and layered airspace concepts that utilized the state-based method for conflict detection, and the Modified Voltage Potential (MVP) algorithm for conflict resolution. The following conclusions can be drawn:

1. *CAMDA defines the maximum theoretical capacity of the airspace as the traffic density at which the Domino Effect Parameter (DEP), a measure of airspace stability, approaches infinity.* At this critical density, all aircraft exist in a persistent state of conflict due to uncontrollable conflict chain reactions. As such, CAMDA implicitly takes into account the safety and efficiency of travel when estimating capacity.

2. *Fast-time simulation results showed that the underlying CAMDA models can accurately predict the occurrence and propagation of conflict chain reactions.* Therefore, CAMDA can be used to perform tradeoffs between decentralized airspace concepts in terms of their maximum theoretical capacities.

3. *The vertical structuring used by layered airspaces provides higher capacities than for unstructured airspace.* But, decreasing the heading range per flight level of layered airspaces did not significantly improve capacity as it does safety. This is because the conflict resolution algorithm used here increased flight distances as the heading range per flight level was decreased. This indicates that safety and capacity should not be considered to be equivalent; capacity is also affected by the efficiency with which conflicts are resolved.

4. *Separation requirements have a larger effect on airspace capacity than conflict detection look-ahead time.* This is because separation requirements have a larger effect on the average conflict probability between aircraft.

5. *Cooperative horizontal conflict resolutions result in higher capacities than cooperative vertical conflict resolutions.* This is because aircraft are more closely packed together in the vertical direction than in the horizontal direction in en route airspaces. Therefore, cooperative vertical conflict resolution maneuvers cause a larger number of conflict chain reactions, decreasing capacity relative to cooperative horizontal conflict resolutions.

6. *Although the capacity of unstructured airspace is increased by assigning conflict resolution priority to cruising aircraft, this approach decreases capacity for layered airspaces.* This is because conflict probability is significantly lower

for cruising aircraft when compared to climbing/descending traffic in layered airspaces, while flight phase only has a minor effect on conflict probability in unstructured airspace. Therefore shifting the conflict resolution responsibility to cruising aircraft increases capacity for layered airspaces.

7. *The capacity of layered airspaces are more sensitive to variations in the ground speed between aircraft.* This is because the heading-altitude rules used by this airspace design is more like to trigger over-taking conflicts than for unstructured airspace.

5

6

Discussion

The current centralized system of Air Traffic Control (ATC) is widely reported to be operating near its capacity limits. In response to this pressing issue, many studies have proposed a decentralization of traffic separation responsibilities, from ground-based Air Traffic Controllers (ATCos) to each individual aircraft, as a means to increase airspace safety and capacity over today's operations. To facilitate decentralized control, the research community has mainly focused its attention on the development of airborne Conflict Detection and Resolution (CD&R) automation. However, the further development and the implementation of this novel approach to ATC has been hindered by three technical[1] open problems related to decentralized airspace design, airspace safety modeling, and airspace capacity modeling. The goal of this study was to address these open problems, in order to bring decentralized ATC closer to reality. More specifically, the primary objective of this thesis, as formulated in chapter 1, was to:

> **Primary Research Objective**
>
> Analyze and model the effects of *airspace design* and *airborne CD&R* on the *safety* and *capacity* of decentralized ATC

To meet this research objective, this thesis was divided into three parts, with each part focusing on one of the three open problems mentioned above. This chapter provides a comprehensive discussion on all components of this thesis. Additionally, recommendations for future work are also presented.

---

[1]The political and legal barriers to decentralized ATC are not considered in this thesis

6.1. Discussion

6.1.1. Airspace Design

The first part of this thesis focused on the effect of airspace design on the capacity of decentralized ATC. Although airspace design elements, such as airways and sectors, are used by the current centralized ATC system to reduce ATCo workload, the use of similar design options to optimize decentralized operations have not been considered in detail in the past. Moreover, the few previous studies on this topic have provided contradictory conclusions; some studies have suggested that a complete reduction of traffic flow constraints is necessary to improve travel efficiency and thereby increase airspace capacity [30, 37–39], while other studies have argued that a further structuring of traffic is required to increase traffic predictability and achieve higher densities [35, 64, 65].

To gain a more concrete understanding of the relationship between airspace design and capacity for decentralized separation, *chapter 2* used fast-time simulation experiments to empirically compare four airspace concepts of increasing structure. The four concepts, named Full Mix, Layers, Zones and Tubes, differed in terms of the number of constrained degrees of motion; see Figure 6.1. The concepts were subjected to multiple traffic demands, for both nominal and non-nominal conditions.
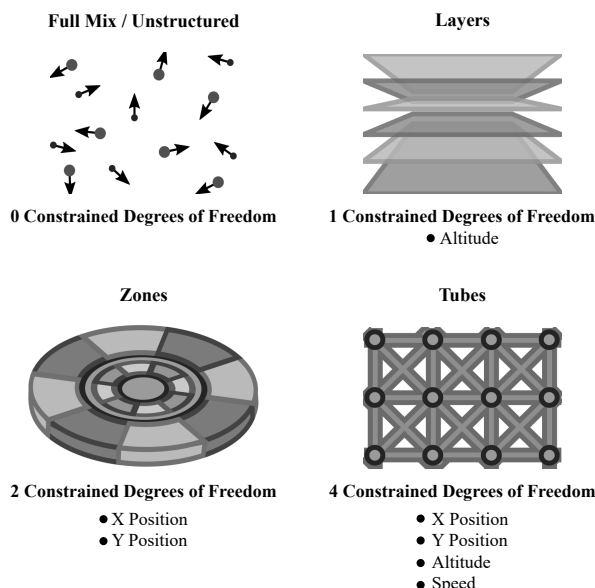

Figure 6.1: Four concepts of increasing structure were compared using simulation experiments to determine the effect of airspace design on the capacity of decentralized ATC in chapter 2. Note that the Full Mix concept is also known as unstructured airspace.

The results of these simulations were unexpected; since previous studies had focused on only airspace designs that closely resembled either Full Mix or Tubes, one of these two extreme options for structuring traffic was expected to lead to the highest capacity. The results, however, clearly indicated that a vertical segmentation of traffic, as used by Layers, led to the best balance of all considered metrics. This approach not only lowered relative velocities between aircraft, it also permitted direct horizontal routes. As such, the Layers concept led to the highest safety of all concepts, without unduly reducing route efficiency relative to the completely unstructured Full Mix design. In contrast, a strict horizontal structuring of traffic, as for Zones and Tubes, caused a mismatch between the imposed structure and the traffic demand pattern. This in turn caused artificial traffic density hot-spots, and reduced overall performance.

Of the different airspace designs considered, the highly structured Tubes concept led to the lowest capacity. This conclusion was emphasized by the results of simulation runs that used rogue aircraft. Such aircraft, which deliberately ignored concept dependent routing requirements, caused a break-down of the pre-planned routes used by Tubes to separate traffic, and resulted in a large number of unintended conflicts and intrusions. While all concepts were negatively influenced by the uncertainties caused by rogue aircraft and wind, these results indicated that the safety of highly structured and planned airspace concepts is particularly vulnerable to differences between the intended and actual flight trajectories.

Because of the empirical nature of the results, the conclusions drawn above are, to some degree, sensitive to the specific parameter settings selected for the four airspace concepts. However, given the magnitude of the differences in all of the results, as well as the consistency between results, it is unlikely that the overall trends are affected by different settings; capacity for decentralization was found to improve when structural constraints fostered a reduction of relative velocities between aircraft, and when direct horizontal routes were permitted. This conclusion is most applicable for traffic scenarios without distinct horizontal patterns. For traffic demand cases with discernible horizontal patterns, airspace concepts that permit flexible routing in the horizontal direction are also expected to perform well, since such structuring would not interfere with any demand pattern.

6.1.2. Safety Modeling

Given the supreme importance attached to the safety of air travel, it is unsurprising that many previous studies have developed analytical conflict count models to quantify the intrinsic safety provided by an airspace design [66–69, 101–103, 106]. Such models are often referred to as 'gas models' in literature. This approach is inspired by the collisions that occur between ideal gas particles, and it determines instantaneous system-wide conflict counts between aircraft as a measure of intrinsic airspace safety. However, most gas models developed previously have only considered conflicts involving cruising aircraft, and have relied on several assumptions that limit the type of traffic scenarios for which they are applicable. The second part

of this thesis addressed these limitations of existing gas models, using unstructured and layered airspace designs as case studies.

6.1.2.1. 3-D Analytical Conflict Count Models

Chapter 3 extended gas models for unstructured and layered airspace designs by taking into account the effects of both cruising *and* climbing/descending aircraft on conflict counts. The developed method groups aircraft according to flight phase, while also considering the interactions, as well as the proportion of aircraft, in different flight phases. This approach was combined with a simple method to compute both the horizontal and vertical components of the expected relative velocity in an airspace. The resulting analytical models could be used to compute the total 3-D conflict probability between aircraft as a function of traffic demand, the constraints imposed by a particular airspace design, and airspace parameters, such as traffic separation requirements and airspace area/volume.

Fast-time simulation experiments that were used to validate the modeling approach indicated high accuracies for both airspace designs. Furthermore, the models suggested, and the simulation results confirmed, that the improved safety performance of layered airspaces could be attributed to the two aspects that differentiated unstructured and layered designs: the use of predefined flight levels, and the use of heading-altitude rules. The models indicated that these two design elements of layered airspaces increased safety by reducing the number of combinations of two cruising aircraft and the average conflict probability between aircraft.

Although layered designs improved the overall safety of en route airspaces, the simulations also showed that there were no differences between unstructured and layered concepts in terms of the number of conflicts involving climbing/descending aircraft. In fact, the results clearly indicated that as the heading range per flight level is decreased, the *proportion* of conflicts involving climbing/descending aircraft is increased. This indicates that such conflicts become more influential than conflicts between cruising aircraft for layered airspaces with a narrow heading range per fight level. This result emphasizes the importance of taking into account all relevant aircraft flight phases when assessing the overall intrinsic safety of an airspace design. The 3-D models derived in chapter 3 were able to accurately capture this important effect.

6.1.2.2. Effect of Traffic Scenario Assumptions

Most analytical gas models described in literature, including the 3-D models derived in chapter 3, assume 'ideal' traffic scenario properties, namely equal ground speeds for all aircraft, as well as uniform aircraft heading, altitude and spatial distributions. In practice, however, a traffic scenario with this exact combination of properties is unlikely to occur. This calls into question the accuracy of such models for more realistic traffic scenarios.

Chapter 4 investigated the accuracy of analytical gas models for 'non-ideal' traffic scenarios. To this end, model predictions for unstructured and layered airspace designs were compared with the results of four fast-time simulation experiments with varying speed, heading, altitude and spatial distributions. In each experiment, one of the four traffic scenario assumptions was intentionally violated in order to determine the specific effect of each assumption on model accuracy.

This exercise revealed that non-ideal altitude and spatial distributions had the greatest impact on model accuracy, with some distribution shapes resulting in accuracies as low as 50%. This is because non-uniform altitude and spatial distributions resulted in traffic concentrations, either vertically or horizontally, which in turn caused a higher number of conflicts relative to the ideal case. The heading distribution also affected model accuracy, but the magnitude of its effect strongly depended on the shape of the distributed used. Moreover, in contrast to the altitude and spatial cases, non-ideal heading distributions led to a reduction of conflict counts. However, speed distribution only had a minor effect on accuracy. Speed distribution is expected to have a greater impact on airspace concepts for which overtaking conflicts are more common, such as layered airspaces with a very narrow heading range per flight level (narrower than those considered here). Nonetheless, these results strongly suggest that the predictions of analytical gas models should be considered with caution for non-ideal traffic scenarios.

To further generalize the models, chapter 4 also presented so called 'adjusted gas models' which used a numerical approach to relax the dependency of the models on the idealized scenario assumptions. In contrast to the purely analytical models, the numerically adjusted models were found to be very accurate for all tested conditions. Because the adjustments only affect the computation of certain model components, the basic structure of the adjusted models remain unchanged relative to the baseline analytical model. Therefore, in addition to providing a physical understanding of the relationships between the parameters that affect intrinsic airspace safety, the adjusted models can also be used to compute the highly accurate conflict count estimates necessary for practical airspace design applications.

6.1.3. Capacity Modeling

Because conventional capacity measurement methods relate to aspects that are not relevant for decentralized ATC, such as ATCo workload, most previous studies in this domain have used *qualitative* methods to determine the capacity limit of decentralized concepts. Such qualitative methods measure capacity *indirectly* by analyzing the variation of safety and efficiency metrics, as well as other relevant metrics, with traffic density. However this approach can result in biased capacity estimates because weighting factors are necessary to rank the relative importance of the considered metrics.

The third and final part of this thesis developed a *quantitative* and *direct* approach to measure the maximum theoretical capacity of decentralized airspace concepts. This was achieved using the notion of airspace stability, which considers the occurrence

6

and propagation of conflict chain reactions. In addition to traffic demand, conflict chain reactions are dependent on the routing constraints imposed by the selected airspace design, and on the conflict resolution actions commanded by the selected CD&R algorithm. Because chain reactions elongate aircraft trajectories, they are detrimental to both the safety and efficiency performance of the airspace. As such, capacity measurement from the perspective of airspace stability implicitly takes into account the combined effects of airspace design and airborne CD&R on airspace safety and efficiency, without the need for arbitrary weights.

Using the notion of airspace stability, *chapter 5* developed the Capacity Assessment Method for Decentralized ATC (CAMDA). This method consisted of six steps, and defined the capacity limit of decentralized airspace as the traffic density at which the Domino Effect Parameter (DEP), a measure of the number of conflict chain reactions, approaches infinity. A semi-empirical approach is used to identify the capacity limit by combining analytical models that described the intrinsic safety provided by an airspace design, i.e., using the output of chapter 3, with empirical models that described the actions of decentralized CD&R algorithms.

Chapter 5 demonstrated the CAMDA method using fast-time simulations of decentralized unstructured and layered airspace designs that used the state-based Conflict Detection (CD) method, and the Modified Voltage Potential (MVP) Conflict Resolution (CR) algorithm. As expected, layered airspaces led to higher capacities than the unstructured airspace design, reiterating the conclusion of chapter 2, as well as the safety trends noted in chapters 3 and 4. However, the capacities of the different layered designs tested, which varied in terms of the heading range allowed per flight level, did not follow the trends in safety. Although decreasing the heading range per flight level lowered the number of conflicts, a reduction of this parameter did not always improve capacity. Detailed analysis traced this unexpected result to the behavior of the MVP CR algorithm when it is used in conjunction with layered airspaces. This is because the distance between conflicting aircraft and their closest point of approach, and correspondingly, the length of the MVP commanded resolution path, increases as the heading range of layered airspaces is decreased. To summarize, the capacity of layered airspaces that use MVP for CR can be negatively affected by the increasing *inefficiency* with which conflicts are resolved as the heading range per flight level is decreased.

The simulations described in chapter 5 also studied how capacity was affected by a number of other factors such as CD parameters, CR dimension and CR priority. For all cases, the CAMDA method estimated the occurrence of conflict chain reactions with high accuracy, enabling capacity estimations using relatively non-intensive low density traffic simulations. Furthermore, because all the parameters of the CAMDA framework have a physical interpretation, the capacity effects of all tested conditions could be directly understood from the structure of the underlying CAMDA models. This in turn allows for a more systematic selection of the required experimental conditions when assessing the capacity limit of a new decentralized airspace design and/or CD&R algorithm.

6.1.4. Additional Considerations

Theoretical vs. Practical Capacity
It is important to realize that there is a clear distinction between the theoretical and the operationally relevant practical capacity of the airspace. The CAMDA method developed in this work focuses on the theoretical capacity limit. The theoretical capacity limit can be used as a metric to compare different airspace design options. Furthermore, the CAMDA approach makes it possible to understand how the features of a particular airspace design contribute to its theoretical capacity. However this theoretical capacity limit is hypothetical, as it represents a situation where aircraft never reach their destination, but are in a persistent state of conflict. This theoretical capacity limit on its own therefore has no operational relevance.

For an operational capacity limit, it is necessary to define thresholds on safety and efficiency. Here, thresholds on safety, e.g., target levels of safety (e.g. 10^{-7} incidents per hour), are dependent on what we as a society find an acceptable risk of an incident occurring. Efficiency limits are dictated by economic demands of the airspace users. Such targets are independent of the airspace design selected. Nevertheless, using such desired targets, it is possible to use the CAMDA relations to determine corresponding operational capacity for the selected airspace concept.

Extension to Other Airspace Designs
Although the safety and capacity models derived in this thesis have focused on unstructured and layered airspace designs, the underlying modeling methods can be extended to other airspace concepts. Any adaptations along these lines would require an analysis of how the constraints imposed by a particular airspace design affect the number of combinations of two aircraft, and the conflict probability between any two aircraft[2], since these two basic factors constitute the starting point for both the safety and capacity models discussed here. In fact, this approach was used to derive the models for layered airspaces using the models initially developed for the unstructured airspace concept.

The methods are also suitable for hybrid airspace designs. For such cases, the total airspace should be first discretized into its individual sub-elements. Subsequently, the safety and capacity modeling methods described in this thesis should be applied to each sub-element, while also considering all *possible interactions* between the different sub-elements. These steps mirror the approach used to generalize the safety models to take into account the effects of non-uniform spatial distributions of traffic; see section 4.4.4.

---

[2]It should be noted that conflict probability is in turn dependent on how an airspace design influences the average horizontal and vertical relative velocities between aircraft.

6.2. Recommendations for Future Work

This section describes opportunities for future research in the domain of decentralized ATC. Additionally, the expected societal impact of this work is briefly discussed.

6.2.1. Influence of Weather on Safety and Capacity

It is a well-known fact that bad weather can negatively affect airspace capacity by reducing the safety and efficiency of operations. In Europe for example, bad weather was one of the top three contributors to en route delays in 2016, costing airlines over 150 million Euros in lost revenue. The effect of weather on traffic flows is a complex topic, and it is the subject of many ongoing studies. Simply put, from the perspective of airspace design, bad weather cells can block access to large areas of airspace, and it can therefore cause traffic re-routings, decreasing the efficiency of travel. Additionally, bad weather, and strong winds in particular, can severely reduce aircraft maneuverability, and this can in turn decrease options for conflict resolution, affecting the safety of travel.

Although the empirical study described in chapter 2 of this thesis presented a preliminary analysis of the effects of stochastic conditions, such as weather, on the capacity of decentralized ATC, the quantitative models derived in subsequent chapters did not consider such effects. In fact, the simulations used to validate all models developed in this thesis only considered ideal weather conditions. Nonetheless, it is worth noting that the semi-empirical CAMDA capacity assessment method described in chapter 5 could, in theory, be used to quantify the capacity reductions caused by various weather phenomena, as long as such phenomena can be simulated with adequate realism. This is because conflict chain reactions, which are central to the CAMDA capacity definition, will invariably be affected by the type and the intensity of the weather conditions considered. Consequently, an analysis along these lines would be extremely valuable when evaluating the operational constraints affecting decentralized control.

6.2.2. Dynamic Airspace Reconfiguration

This thesis has limited its attention to airspace designs that remain static in time. But to maximize the efficiency with which the available airspace is utilized, it may be beneficial to dynamically reconfigure the constraints imposed by a particular airspace design to better match the demand pattern shifts that occur during the course of a day. This concept can be illustrated for the Layers airspace design; all layered designs considered here have assigned an equal number of flight levels to each heading interval. This strategy of assigning flight levels results in a uniform distribution of aircraft altitudes only for traffic scenarios which also exhibit a uniform distribution of aircraft headings. For other heading distributions, the vertical distribution of traffic will be uneven, and this has been shown to decrease the intrinsic

safety provided by layered designs; see Figure 4.16. But, by carefully reconfiguring the airspace structure by assigning a greater number of flight levels to popular travel directions, it may still be possible to realize a uniform distribution of aircraft altitudes for scenarios with non-uniform heading distributions.

Although such dynamic reconfigurations can be advantageous in terms of capacity, it is unclear how the safety of operations can be guaranteed during configuration changes, and when and what configurations should be selected. This is an interesting avenue for future research that deserves further analysis.

6.2.3. Tailored Conflict Resolution Algorithms for Layered Airspaces

The results presented in chapter 5 indicated that the capacity of layered airspaces was bottlenecked by the CR algorithm used in this work because it unnecessarily increased the length of conflict resolution trajectories for shallow angle conflicts. The resulting decrease in efficiency outweighed the safety benefits offered by layered airspaces when the heading range per flight level is decreased. It is hypothesized that the capacity limits of layered airspaces can be further increased over the levels found in this thesis by developing a conflict resolution algorithm that prioritizes the efficiency of conflict resolution paths. This may be achieved using resolution algorithms that aim to solve a conflict as quickly as possible rather than using the 'shortest-way-out' strategy used here. Research in this direction is already being conducted at TU Delft as an extension to [52].

6.2.4. Reference Traffic Scenarios

Fast-time simulations have become ubiquitous in ATC research for analysis and design purposes, and they have been used in all technical chapters of this thesis. The conclusions drawn using this approach are, to some degree, dependent on the traffic scenarios considered. However, despite the popularity of fast-time simulations, methods to generate standardized traffic scenarios have not been studied in detail in the past. This makes it very difficult to even compare the results of identical ATC studies that have used fast-time simulations.

To overcome this issue, it is recommended to develop a library of reference traffic scenarios. Such a library should contain a multitude of scenarios for different use cases, given the wide range of operational settings analyzed using simulations. For example, different sets of scenarios would be needed to evaluate the performances of high altitude en route airspaces when compared to those needed for low altitude terminal airspaces. In addition to specifying origin-destination pairs, these reference scenarios should also specify default traffic demand volumes that take into account the predicted growth of air traffic in the future. If the methods used to generate reference scenarios are made open-source, then they can be continuously updated as the needs of the research community change, for example when new aircraft types are introduced. In addition to making research more compara-

ble, reference traffic scenarios would also make the results of simulation studies more transparent. This recommendation is inspired by the goals of the AHMED project.

6.2.5. Extension to Centralized ATC

This study has focused on developing safety and capacity modeling methods for future decentralized operations. But it is worth noting that some aspects of this thesis could also be extended to analyze the performance of the current centralized ATC system. This is particularly the case for the three dimensional conflict count models derived here to quantify the intrinsic safety of an airspace design. As mentioned above, such adaptations should analyze how the currently used airspace structures affect both the number of combinations of two aircraft, and the average conflict probability between any two aircraft, since these two factors constitute the starting point for all models discussed in this work.

Because conflict chain reactions can also occur in today's mode of operations, it may also be possible to develop a capacity assessment framework for centralized ATC that is comparable to the CAMDA method derived here for decentralized ATC. Such research should be preceded by a human-in-the-loop study that uses experienced ATCos to determine the likelihood of conflict chain reactions for a wide range of real operational conditions, and for a wide range traffic demands.

6.2.6. Societal Impact of this Research

Despite the capacity constraints faced by today's centralized ATC system, in the short-term, decentralized control is unlikely to be applied towards improving commercial air transport operations for both technical as well as political reasons. However, the decentralized ATC concept is unlikely to be confined to the research domain for much longer thanks to the rapid emergence of *unmanned and personal aerial vehicles*. The incredible traffic volumes forecasted for these new aircraft types, and the clean sheet approach to ATC that is required to facilitate their operation, has provided the incentives necessary for aviation authorities to investigate some important aspects of decentralization, such as self-separation (referred to as 'detect and avoid' by the unmanned community), for the growing field of urban airspace design. Recent publications outlining the latest plans for urban airspaces confirm that this is indeed the case [55, 56]. Because of the generic nature of the airspace designs and the quantitative safety and capacity models discussed in this thesis, the results of this work can be generalized beyond the specific conditions that have been considered here, for instance for the lower speeds anticipated for unmanned traffic. Therefore, the methods developed in this thesis to analyze and model the capacity of decentralized ATC could be useful towards the design of new concepts that enable low altitude urban air transport operations.

7

Conclusions

Based on the results presented in the preceding chapters, the following final conclusions are drawn in relation to the three open problems that have limited the further development of the decentralized Air Traffic Control (ATC) concept, namely airspace design, safety modeling and capacity modeling:

On Airspace Design

1. *Capacity for decentralization is maximized when a layered airspace design is used* to separate traffic with different travel directions at different flight levels. This airspace design improves performance over completely unstructured airspace by decreasing the average conflict probability between aircraft, while allowing flexible routing in the horizontal direction.

2. *Over-constraining the horizontal paths of aircraft can trigger artificial traffic concentrations* at the intersections of structural elements and reduce airspace capacity. Therefore, horizontal constraints should be avoided as much as possible, unless they can be tailored to match the observed horizontal traffic demand pattern.

3. *Robustness to uncertainties is significantly reduced when decentralization using time-based separation is combined with a predefined and fixed three-dimensional route structure.* For such airspace designs, uncertainties, such as wind and rogue aircraft, can cause unintended conflicts and intrusions, which in turn reduce airspace safety and capacity.

On Safety Modeling

4. *The intrinsic safety provided by an airspace design is influenced by the number of combinations of two aircraft and the average conflict probability between any two aircraft.* Both factors are affected by the constraints imposed by a particular airspace design, and such models are often referred to as 'gas models' in literature.

5. *When modeling the overall intrinsic safety provided by an airspace design, it is essential to take into account the interactions that occur between aircraft in all flight phases*, and not just those between cruising aircraft. This is particularly important for layered airspaces as the proportion of conflicts involving climbing/descending aircraft increases as the heading range per flight level decreases.

6. *Analytical gas models assume 'ideal' traffic scenario properties, and accuracy is high for the ideal case.* But accuracy decreases for non-ideal traffic scenarios, and it is the lowest for non-ideal altitude and spatial distributions.

7. *Numerical 'adjustments' can be used to generalize gas models and increase their accuracy for non-ideal traffic scenarios.* The adjustments apply to both factors of gas models, and this approach increased accuracy for non-ideal scenarios to the levels found with the analytical model for the ideal traffic scenario.

On Capacity Modeling

8. *The Capacity Assessment Method for Decentralized ATC (CAMDA) defines the maximum theoretical capacity of the airspace as the traffic density at which conflict chain reactions become uncontrollable*. Because conflict chain reactions are central to the CAMDA capacity definition, this approach implicitly takes into account the safety and efficiency of travel when estimating capacity.

9. *CAMDA is a semi-empirical method*, but all its parameters have a physical interpretation. Consequently, the effect of a number of factors on capacity can be directly understood from the structure of the underlying models. This in turn allows for a more systematic selection of the experimental conditions required when comparing different airspace designs and/or CD&R algorithms in terms of capacity.

10. *The capacity of decentralized ATC is dependent on both the selected airspace design and the selected CD&R algorithm.* Here airspace design affects the safety and efficiency of the planned flight routes, whereas CD&R algorithm contributes to the safety and efficiency of the actually flown routes. Therefore, an optimization of capacity requires an optimization of both airspace design and CD&R algorithm, as well as an optimization of the pairing between them.

A

Traffic Scenario Generation

Fast-time simulations have been used throughout this thesis for two main purposes. In chapter 2, simulations were used to empirically study the dynamics of decentralized air traffic operations for the specific purpose of analyzing the airspace structure-capacity relationship. Chapters 3-5, on the other hand, used simulations to validate the quantitative safety and capacity models developed in this work. Because of this versatility, fast-time simulations have become extremely common as a tool for analysis and design purposes in Air Traffic Control (ATC) research.

In addition to modeling aircraft systems and kinematics, to perform fast-time simulations, it is necessary to generate traffic scenarios. Simply put, traffic scenarios describe the creation times, deletion times, and routes of all aircraft in a simulation. In other words, traffic scenarios represent the input conditions used by fast-time simulations to numerically calculate and propagate the motion of aircraft.

The goal of this appendix is to describe the design of the traffic scenario generator that has been developed for this thesis. Even though fast-time simulations are ubiquitous in ATC research, as of the writing of this thesis, there are no standardized procedures to generate scenarios, and different studies have used different methods to produce scenarios (and these are often not well documented). For this reason, traffic scenario generation continues to be, unfortunately, more of an 'art' than a 'science'. Consequently, some of the design choices discussed in this appendix are based on what has been found to 'work' in practice, often using trial-and-error, for the specific needs of this study. For this reason, this appendix should not be viewed as a comprehensive guide on traffic scenario generation; it simply describes the scenario generation process used here for the sake of completeness. Nonetheless, to make the descriptions that follow tangible, the scenarios used in chapter 5 are used as an illustrative example (other chapters use identical traffic scenario generators).

A

A.1. Overview of Scenario Generation Process

The traffic scenario generator developed for this thesis consists of five sequential steps; see Figure A.1.
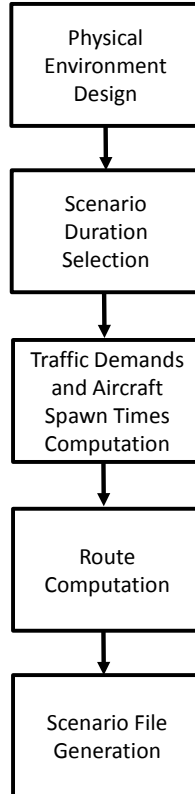
Figure A.1: The five steps of the traffic scenario generator developed for this study

The scenario generator makes use of several assumptions and input parameters. These aspects are discussed next. Subsequently, the details of the five steps of the scenario generator are presented.

A.2. Baseline Assumptions

The scenario generator makes use of the following five assumptions. These assumptions can also be viewed as baseline design choices.

En Route Scenarios Only
The scope of this thesis is limited to decentralized en route operations; see section 1.5. Therefore, the scenario generator discussed here only computes the routes

of aircraft within en route airspaces. In other words, take-off, initial climb, final descend and landing flight phases are not taken into account.

Three-Dimensional Scenarios and Flight Profiles

Although only the trajectories of aircraft in en route airspaces are considered, the approach used here produces three-dimensional scenarios. Therefore, all aircraft flight profiles consist of: 1) a climbing segment through so a called transition airspace that is assumed to exist between low-altitude centralized and high-altitude decentralized airspaces; 2) a cruising segment towards the destination; and 3) a descending phase to exit from decentralized en route airspace. Figure A.2 displays an example aircraft flight profile which consists of these three segments.

Constant Density Scenarios

The scenarios produced here builds up traffic volume from zero to a desired value, after which traffic density is maintained at the desired value; see Figure A.3. Consequently, the scenarios have to be combined with an experiment design that utilizes multiple traffic demand levels if the rate of change of a dependent variable, such as safety and efficiency metrics, with density needs to be evaluated. The method used here to define multiple traffic demand levels is described in section A.6.

Finite Airspace Volume

All simulated traffic are assumed to fly within a predefined and finite volume of airspace. This implies that the creation and deletion points of all aircraft are located within this predefined volume, i.e., aircraft do *not* fly outside the boundaries of the simulated sector. In fact the scenario generator expects aircraft to be deleted as they descend through the lower boundary of the simulated sector in order to maintain traffic density at the desired level.

Offline Scenario Generation

To ensure that all experiment conditions, for example all tested conflict detection settings, are subjected to the same traffic demand patterns, all scenarios need to be generated offline prior to the actual simulations. Therefore, the scenario generator converts the computed aircraft routes into text files which can subsequently be loaded into the selected air traffic fast-time simulator during run-time. In this study, the TMX and BlueSky fast-time simulators have been used. Both simulators expect the same scenario file format, and use the same scenario commands. Section A.8 describes how the scenarios produced here should be converted to text files such that they can be used by these two ATC simulators.

A.3. Input Parameters

In addition to the above assumptions, several input parameters are expected by the scenario generator. These are listed in Table A.1, along with the corresponding values used by the traffic scenarios of chapter 5. Most of these parameters are used for sizing the physical environment of the simulations; see section A.4. Additionally, all parameters related to densities are used to define the specific traffic demand scenarios required for simulation; see section A.6 for more details.

Table A.1: Input parameters of the traffic scenario generator
and corresponding values used in chapter 5
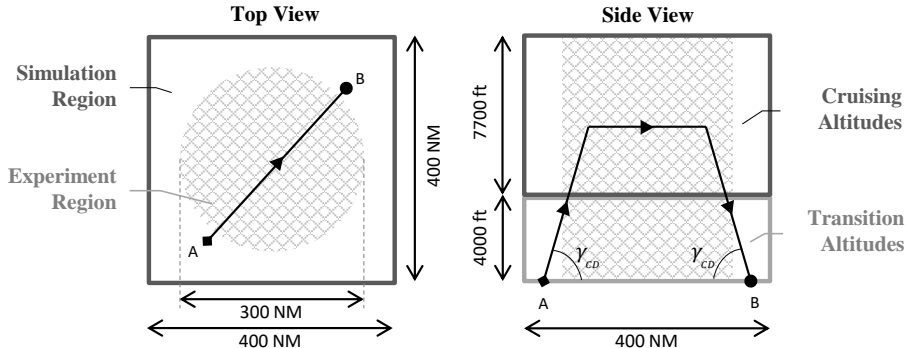
Parameter	Value	Description
D_{min}	200 [NM]	Min. flight distance in sector
D_{max}	250 [NM]	Max. flight distance in sector
$\bar{D}$	225 [NM]	Avg. flight distance in sector
S_h	5 [NM]	Max. horizontal separation in all experiments
S_v	1000 [ft]	Max. vertical separation in all experiments
t_l	5 [mins]	Max. look-ahead time for CD in all experiments
$\bar{V}$	400 [kts]	Avg. ground speed of all a/c
ρ_{min}	5 [ac/10,0000 NM²]	Min. traffic demand
ρ_{max}	50 [ac/10,0000 NM²]	Max. traffic demand
N_{dens}	10	Number of traffic demand scenarios
N_{fl}	8	Number of flight levels (only valid for Layers)
γ_{cd}	2.82^o	Climb/descend angle for all traffic
Z_{min}	4000 [ft]	Altitude of lowest flight level above lower simulation boundary

A.4. Design of Physical Environment

The first step of the scenario generation process is to design the physical environment of the simulation. The scenario generation process described here aims to size a decentralized en route airspace sector similar to the one shown in Figure A.2.

In the vertical direction, the sector is divided in two parts; an upper 'cruising' zone, and a lower 'transition' zone. As the name suggests, aircraft cruise towards their respective destinations in the cruising zone. In this study, the vertical height of this zone is determined based on the number of flight levels used by layered airspace designs, N_{fl}, and the height of each flight level, ζ. The latter parameter is dependent on the the vertical separation requirement, S_v. This is because a design requirement for layered airspaces is that $\zeta >= S_v$ in order to prevent conflicts between aircraft cruising in adjacent flight levels. In this work, the maximum value used for $S_v = 1000$ ft. Consequently, ζ is set to 1100 ft; the extra 100 ft was required to prevent so called 'false' conflicts that can sometimes occur when aircraft level-off at their desired cruising altitude. Because the lower and upper boundaries of the cruising zone act as flight levels, the total height of the cruising zone can be calculated using N_{fl} and ζ:

$$\text{Height of Cruising Zone} = \left(N_{fl} - 1 \right) \zeta \tag{A.1}$$

Figure A.2: Top and side views of the simulation's physical environment, with dimensions as used in chapter 5. The trajectory of an example flight is shown.

The transition zone is defined to be the region of airspace between low altitude centralized airspaces and high altitude decentralized airspaces. In the simulation, all aircraft are created, or spawned, at the lower boundary of the transition zone. Subsequently, they climb into the cruising zone. At the end of their flights, aircraft once again descend through the transition zone. Descending aircraft are *deleted* as they cross the lower boundary of the transition zone. The deletion of aircraft is an important aspect for the scenario generator design considered here; old aircraft need to be deleted so that traffic density is maintained at the required level when new aircraft are introduced into the simulation. In the BlueSky and TMX ATM simulators, aircraft deletion can be controlled via the *AREA* command.

No specific rationale is used here to size the transition zone. Experience has shown that a transition zone that is approximately half the height of the cruising zone can effectively prevent short term conflicts which can sometimes occur between new aircraft and aircraft that already cruising. Since the cruising zone has a height of 7700 ft, see Figure A.2, the transition zone was assigned a height of 4000 ft in chapter 5 (3850 ft rounded to the nearest 1000 ft).

In the horizontal direction, the simulated sector was designed to have a square-shaped cross-section. Since the starting and end points of all flights are assumed be located in the simulated sector, see section A.2, horizontal sizing is dependent on the expected flight distances of aircraft. To ensure that there is sufficient variation between the possible trajectories of aircraft, the following rule of thumb is used:

$$\text{Horizontal Square Length} = 2\, D_{min} \tag{A.2}$$

It should be noted that D_{min} is used for horizontal sizing, and not D_{max}. This is because the horizontal cross-sectional area is directly proportional to the number of instantaneous aircrafts needed to realize the desired traffic densities. Therefore, using D_{max} would result in an unnecessarily large simulation area, as well as an

A

unnecessarily large number of instantaneous aircrafts to realize the required densities. This would in turn increase the computational load when performing the actual fast-time simulations, without any benefits in terms of results.

In the horizontal plane, Figure A.2 shows that the physical environment is divided into separate 'simulation' and 'experiment' regions. Although traffic is simulated throughout the entire simulation region, this distinction is necessary because no traffic is simulated outside the considered sector. Therefore, aircraft near the edges of the simulation region are less likely to interact with other flights relative to aircraft near the center of the sector. To solve this issue, following the simulation design described in [92], a smaller cylindrical 'experiment region' is defined at the center of the simulation region. The gap between the experiment and simulation regions needs to be greater than the average conflict detection look-ahead distance so that aircraft in the experiment region can easily conflict with other aircraft from all directions. The average look-ahead distance can be computed as:

$$\text{Gap Between Simulation and Experiment Regions} >= \bar{V} t_l \qquad \text{(A.3)}$$

Here, $\bar{V}$ is the average speed of all aircraft in the simulation, and t_l is the conflict detection look-ahead time. For the values listed in Table A.1, this results in a look-ahead distance of 33.3 NM. Correspondingly, the diameter of the experiment region was selected to be 300 NM, since this results in a gap of 50 NM between the simulation and experiment regions. Because of this design, only the paths of aircraft within the experiment region, and only conflicts with closest points of approach within the experiment region, should be considered when analyzing the results of the simulations.

It should be noted that square and circular shaped cross-sections were selected arbitrarily for the simulation and experiment regions for the scenarios used in chapter 5. The subsequent steps of the scenario generator are not dependent on these specific shape choices. The only requirement is that convex shapes are selected for both regions.

A.5. Scenario Duration

The traffic scenario design described here consists of three phases: a pre-logging phase, a logging phase, and a 'run down' phase; see Figure A.3. To determine the total duration of a scenario, it is, therefore, necessary to determine the durations of each of these three component phases.

Scenarios always begin with a pre-logging phase. During this phase, traffic volume is built up from zero to the desired level. Because aircraft are introduced into the simulation at a constant rate (see section A.6 for more details on this), the amount of time required to realize the desired traffic density is equivalent to the average duration of a flight, $\bar{t}_f = \frac{\bar{D}}{\bar{V}}$. Using the values for $\bar{V}$ and $\bar{D}$ listed in Table A.1, it
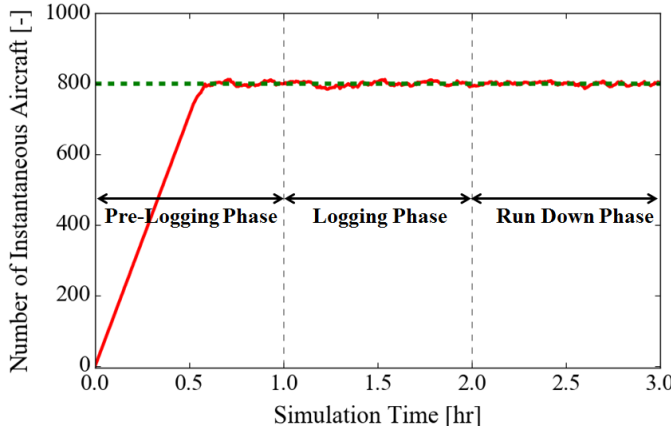
Figure A.3: The total scenario duration is divided into three phases. The red line indicates the actual traffic volume, and the green line represents the target traffic volume.

takes approximately 35 minutes to realize the desired traffic demand for the scenario settings used in chapter 5. The duration of the pre-logging phase must be greater than this value. This is because logging should only commence once the traffic is allowed to settle at the desired density for some time. This is particularly important for simulations which use tactical conflict resolutions; this additional buffer is needed to prevent any artificial conflict chain reactions that are triggered during the traffic volume build up period from skewing the results during the logging phase. For this reason, in chapter 5, the total pre-logging phase is selected to be 1 hour.

Subsequently, the logging phase can begin. During the logging phase, all relevant traffic characteristics should be logged into text files for analysis after all experiment runs. The duration of the logging phase should be greater than the maximum flight time of an aircraft in the simulation. For the scenarios used in chapter 5, the maximum flight time is approximately 40 minutes (computed using the input parameters listed in Table A.1). Therefore, the duration of the logging phase is set to be 1 hour.

To allow aircraft created at the end of the logging phase to finish their flights, and thus prevent abnormally short flights from skewing the results, the simulation ends with a run down phase. As indicated in Figure A.3, traffic demand is held constant at the required level during the run down phase so that the logs obtained from a particular simulation can be attributed to a particular traffic density for the entire duration of a scenario log. This final phase is only required if efficiency related metrics need to be analyzed. As for the logging phase, the duration of the run down phase must be greater than the maximum flight time. Therefore, the duration of the run down phase is also set to be 1 hour in chapter 5.

As mentioned above, the total duration of a scenario can be computed as a summation of the durations of each simulation phase. As explained above, in chapter 5, each phase was set to have a duration of 1 hour, resulting in a total of $T = 3$ hours for a complete scenario. Using this information, and the spawn interval of aircraft needed realize the desired instantaneous traffic density, it is possible to determine the number of aircraft that need to be simulated during an entire scenario. These aspects are discussed next.

A.6. Traffic Demands and Aircraft Spawn Times

The third step in the scenario generation process is to determine the traffic demands used for simulation, and to determine corresponding the aircraft spawn, or creation, times for each demand case.

A.6.1. Traffic Demand Selection

If the goal of an experiment is to empirically study the rate of change of a dependent measure with traffic density, then it is necessary to repeat the simulations for multiple traffic demand conditions. In most cases, the span of densities selected for simulation should include today's peak traffic demand. In 2017, the maximum traffic density in en route airspaces ($>= 18,000$ ft) over the Netherlands was approximately 32 aircraft per $10,000$ NM^2 (computed using logged ADS-B data). Therefore, ten traffic densities between 5-50 aircraft per $10,000$ NM^2 were selected for the experiments performed in chapter 5; see Table A.2.

Table A.2: Traffic demand scenarios used for the simulations in chapter 5

#	Traffic Density [ac per 10,000 NM²]	No. of Instantaneous A/C
1	5.0	80.0
2	6.5	103.3
3	8.3	133.5
4	10.8	172.4
5	13.9	222.6
6	18.0	287.5
7	23.2	371.3
8	30.0	479.6
9	38.7	619.4
10	50.0	800.0

Note that the values given in Table A.2 are for the full 'simulation region'; see Figure A.2.

Table A.2 shows that there are more low density scenarios than high density scenarios. In fact, the densities selected in chapter 5 are geometrically spaced in this

manner to reduce the total computational load of the corresponding simulation experiments. To space the densities selected for simulation as a geometric sequence, the common ratio, r, between consecutive demand conditions is computed using the minimum and maximum traffic demands, ρ_{min} and ρ_{max}, and the number of traffic demand conditions required, N_{dens}:

$$\log r = \frac{\log \rho_{max} - \log \rho_{min}}{N_{dens} - 1} \tag{A.4}$$

Table A.1 gives the values used in chapter 5 for the three input parameters of the above equation.

The next step is to compute the number of instantaneous aircraft, N_{inst}, corresponding to the desired traffic demand densities. To do this, the following simple relationship between N_{inst}, traffic density, ρ, and area, A, is used:

$$N_{inst} = \rho A \tag{A.5}$$

It should be noted that the area of the full simulation region is used when evaluating the above equation. The magnitude of this area can be calculated with the aid of Figure A.2, and it equals $160,000$ NM^2. Using this approach, the number of instantaneous aircraft corresponding to each demand condition is also displayed in Table A.2.

A.6.2. Spawn Rate Calculation

As mentioned above, the scenario generator considered here aims to maintain the desired traffic density during the logging and run down phases of the simulation, i.e., to produce scenarios with density-time profiles matching Figure A.3. To produce such scenarios, aircraft need to be replaced at the same rate at which they are deleted. This rate, referred to as the spawn rate, Ω, can be calculated using the following simple logic. Since $\bar{V}$ is the average speed and $\bar{D}$ is the average distance flown by aircraft in the simulation, the average time taken by a flight to cross the simulation region is $\bar{t}_f = \frac{\bar{D}}{\bar{V}}$. Since aircraft are deleted when they fly out of the simulation region, the *rate* with which aircraft need to be introduced into the simulation to ensure that there is always 1 aircraft within the simulation region at all times is the inverse of the average flight time, or $\frac{\bar{V}}{\bar{D}}$. Correspondingly, the rate at which aircraft need to be introduced to ensure that there is always N_{inst} aircraft within the simulation region is:

$$\Omega = \frac{\bar{V}}{\bar{D}} N_{inst} = \frac{\rho \bar{V}}{\bar{D} A} N_{inst} \tag{A.6}$$

A

By introducing aircraft into the simulation at the rate described by the above equation, it is possible to achieve the desired number of instantaneous aircraft after $\frac{\bar{D}}{\bar{V}}$ minutes, i.e., after the after average flight time, $\bar{t}_f$.

A.6.3. Total Number of Aircraft in One Scenario and Aircraft Spawn Times

The total number of aircraft needed for one complete scenario, N_{total}, can be computed using the total scenario duration, T, and the spawn rate of aircraft, Ω, using the following simple expression:

$$N_{total} = T\Omega \tag{A.7}$$

The spawn interval between each aircraft is equal to the inverse of the spawn rate, i.e,. $\frac{1}{\Omega}$. The spawn interval can be used to divide the total duration of the simulation, T, into N_{total} segments to determine the spawn time of each aircraft. Because aircraft are unlikely to enter a sector at a constant time interval in real life, a uniformly distributed random number, between 0 and half the spawn interval, can be added to the spawn times of aircraft to reduce the predictability of the simulation. This 'spawn time randomization' was done for all the scenarios used in this thesis.

A.7. Route Computation

The most important step of the scenario generator is to compute the routes of all aircraft. Route computation is heavily dependent on the constraints imposed on traffic motion by an airspace design. Since the vast majority of this thesis has focused on unstructured and layered airspace designs, this appendix will focus on route computation for these two direct routing airspace concepts (direct routing in the horizontal direction).

An overview of the route computation process is shown in Figure A.4. This flowchart is mostly self-explanatory. Nonetheless, the following paragraphs discuss some key aspects of the route computation process.

A
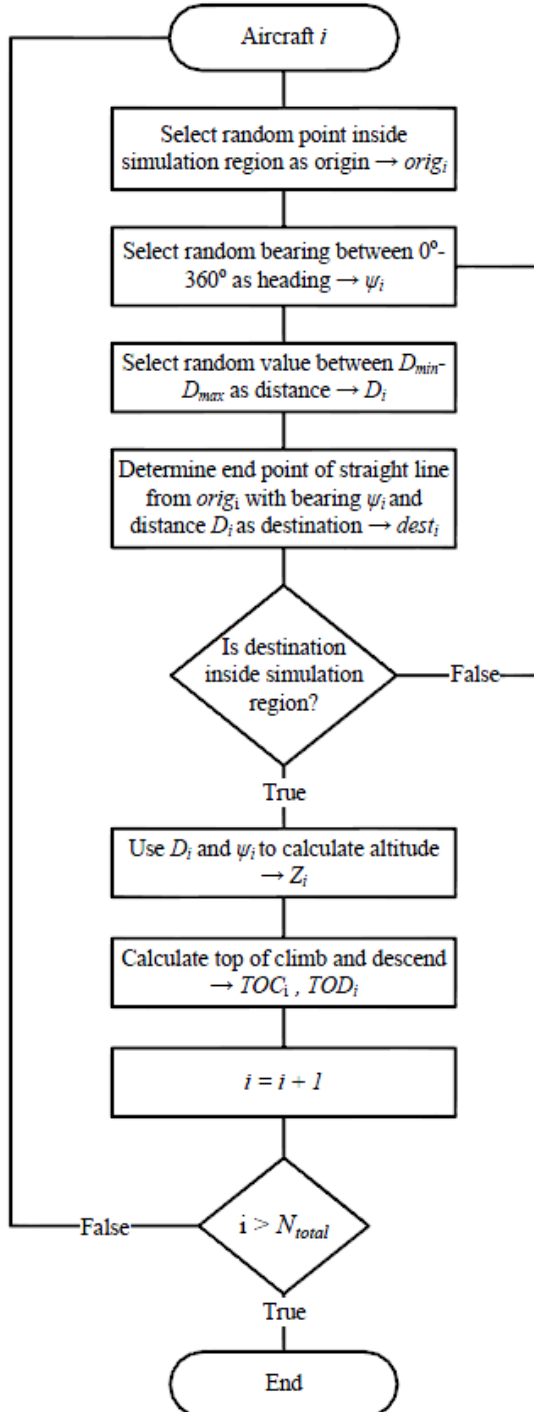
Figure A.4: Flowchart describing the route computation process

A.7.1. Origin and Destination Selection

As mentioned previously, the origins and destinations of all aircraft are located within the 'simulation region', at the lower boundary of the 'transition region'; see Figure A.2. Therefore, any latitude/longitude combination within the simulation region can be selected as the origin of an aircraft, and random combinations can be determined using a random number generator. Random number of generators, of the desired distribution, are also used to determine an aircraft's heading and its flight distance. Subsequently, the destination of an aircraft is computed as the end-point of a straight line that extends from the selected origin, with a length corresponding to the selected distance, and a bearing corresponding to the selected heading. This can be done using the following geometrical equations:

$$lat_{dest} = \arcsin\left[\cos\left(\frac{D_i}{R_E}\right)\sin(lat_{orig}) + \sin\left(\frac{D_i}{R_E}\right)\cos(lat_{origin})\cos(\psi_i)\right] \quad \text{(A.8a)}$$
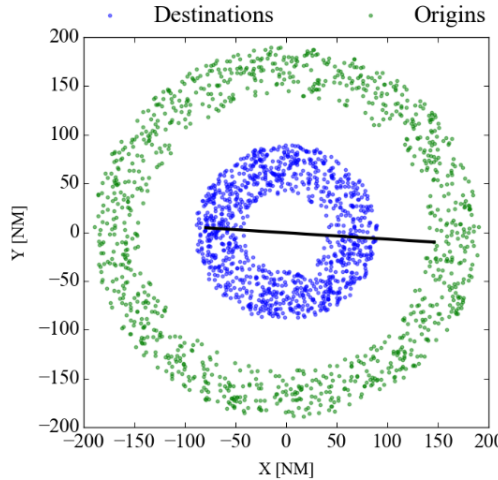
$$lon_{dest} = lon_{orig} + \arctan\left(\frac{\sin(\psi_i)\cos(lat_{orig})\sin\left(\frac{D_i}{R_E}\right)}{\cos\left(\frac{D_i}{R_E}\right) - \sin(lat_{orig})\sin(lat_{dest})}\right) \quad \text{(A.8b)}$$

Here, lat and lon represent latitude and longitude, respectively, whereas D_i and ψ_i are an aircraft's flight distance and heading, respectively. Additionally, the subscripts $orig$ and $dest$ stand for 'origin' and 'destination'.

If the destination computed by the above equation is within the simulation region, then it can be accepted. If the destination is outside the simulation region, it has to be discarded. Subsequently, the above process is repeated until a distance and heading combination is found that results in a destination that is inside the simulation region.

It should be noted that random number generators describing any distribution can be used to select origins, headings and destinations. For instance, if a scenario with normally distributed heading angles is desired, then such a scenario can be realized by using a normally distributed random number generator when selecting aircraft headings. The same goes for the distance distribution, which indirectly affects the altitude distribution of aircraft. This approach was used to produce so called 'non-ideal' traffic scenarios in chapter 4.

To produce scenarios with non-uniform spatial distributions, it is necessary to apply additional constrains when selecting the origins and destinations of traffic. For instance, to produce scenarios with traffic density hot spots at the center of the simulation region, the origins and destinations of traffic should be distributed within two concentric rings as shown in Figure A.5. This arrangement of origins and destinations forces aircraft to fly through the center of the simulation region, thereby creating a traffic density hot spot. By adjusting the radii of the two concentric circles, the intensity of the hot spot can be controlled; smaller radii result in 'hotter' hot spots.

Figure A.5: To create traffic density hot spots, aircraft origins (green) and destinations (blue) need to be distributed within concentric rings. An example trajectory is shown.

A.7.2. Altitude Computation

Although both unstructured and layered airspace designs use the same direct horizontal routes, the two airspace concepts differ in terms of the vertical flight profiles of aircraft. In unstructured airspace, the cruising altitude of an aircraft, $Z_{ua,i}$, is directly proportional to its trip distance, D_i:

$$Z_{ua,i} = Z_{min} + \frac{Z_{max} - Z_{min}}{D_{max} - D_{min}} (D_i - D_{min}) \qquad (A.9)$$

Here, Z_{min} and Z_{max} are the minimum and maximum altitudes allowed for cruising aircraft in the simulation. Comparably, D_{min} and D_{max} are the minimum and maximum trip distances of aircraft in the simulation.

On the other hand, for layered airspaces, the cruising altitude of an aircraft, $Z_{lay,i}$, depends on both its heading, ψ_i, and its trip distance, D_i, as indicated by the following heading-altitude rule:

$$Z_{lay,i} = Z_{min} + \zeta \left[\left\lfloor \frac{D_i - D_{min}}{D_{max} - D_{min}} \kappa \right\rfloor \beta + \left\lfloor \frac{\psi_i}{\alpha} \right\rfloor \right] \qquad (A.10)$$

Here, β is the number of flight levels needed to define one complete set of layers, and κ is the number of complete layer sets. These two parameters are defined as $\beta = 360^o/\alpha$ and $\kappa = L/\beta$, where L is the total number of available flight levels, and α is the heading range permitted per flight level. Note that the second term of equation A.10 computes the cruising altitude of an aircraft as an *integer multiple* of

A

the vertical spacing between flight levels, ζ, using the the floor operator ('$\lfloor \rfloor$'). For all layered airspaces considered in this study, $\zeta = 1,100$ ft and $L = 8$. Correspondingly, for most layered airspaces considered here, $\kappa > 1$. For layered concepts with $\kappa > 1$, equation A.10 uses trip distances to determine cruising altitudes such that short flights remain at lower altitudes, while longer flights use higher layer sets.

A.7.3. Aircraft Speed

Although not explicitly mentioned in Figure A.4, route computation also involves selecting the ground speed of each aircraft, V_i. Aircraft are required to fly with constant ground speeds throughout their flight. However, different aircraft in the simulation may have different ground speeds. Similar to the headings and distances flown by aircraft, the V_i can be selected using a random number generator of any desired distribution. The speed is necessary to compute the top of climb and descend locations (see below).

A.7.4. Top of Climb and Descend

In addition to determining the origins, destinations and cruising altitudes of aircraft, it is necessary to compute the top of climb and descend locations to completely define the route of an aircraft. The process of computing the top of climb of an aircraft is identical to that required to determine its the top of descend. Therefore, only the procedure used to determine the top of climb is described below in detail.

To compute the latitude and longitude of the top of climb of an aircraft, it is necessary to know its climb angle, γ_{cd}, and its vertical speed, $V_{Z,i}$ during climb. While the former is an input variable to the scenario generator, see Table A.1, the latter can be computed using its speed, V_i (determined in the previous step):

$$V_{Z,i} = V_i \sin\left(\gamma_{cd}\right) \tag{A.11}$$

Next, using $V_{Z,i}$ and the cruising altitude of the aircraft, Z_i, the climb time, t_{climb}, and the horizontal distance flown during the climb, $D_{climb,i}$, can be computed:

$$
\begin{aligned}
t_{climb,i} &= \frac{Z_i}{V_{Z,i}} & \text{(A.12a)} \\
D_{climb,i} &= V_i t_{climb,i} & \text{(A.12b)}
\end{aligned}
$$

A

Finally, the latitude and longitude of the top of climb location can be computed using following two geometrical equations:

$$lat_{TOC} = \arcsin\left[\cos\left(\frac{D_{climb,i}}{R_E}\right)\sin(lat_{orig}) + \sin\left(\frac{D_{climb,i}}{R_E}\right)\cos(lat_{origin})\cos(\psi_i)\right] \quad \text{(A.13a)}$$

$$lon_{TOC} = lon_{orig} + \arctan\left(\frac{\sin(\psi_i)\cos(lat_{orig})\sin\left(\frac{D_{climb,i}}{R_E}\right)}{\cos\left(\frac{D_{climb,i}}{R_E}\right) - \sin(lat_{orig})\sin(lat_{TOC})}\right) \quad \text{(A.13b)}$$

Note that the above equations are identical to those used previously to determine the latitude and longitude of the destination of an aircraft. The only difference is that $D_{climb,i}$ is used here instead of the total flight distance, D_i.

The top of descend can be calculated using a similar approach to that described above for the top of climb. The only difference is that the procedure should be applied backwards from the destination. The top of descend point is *not* needed for experiments *with* tactical conflict resolution. This is because conflict resolution may cause aircraft to overshoot their top of descend, and specifying it in a scenario file may, therefore, cause such aircraft to fly backwards. Instead, for cases with conflict resolution, the fast-time simulator should compute the top of descend in real time based on the actual location of the aircraft with respect to its destination.

A.8. Scenario File Generation

The previous steps of the scenario generator computed all the parameters needed to describe the complete routes of aircraft, and their spawn times. This final step describes how these parameters should be written into standardized text files that can be understood by the BlueSky and TMX fast-time simulators.

A.8.1. Scenario Files

Each scenario file lists the routes and spawn times of all aircraft for one particular traffic demand case. Both BlueSky and TMX simulators use identical commands and command arguments for scenarios. Table A.3 describes the six commands that are necessary to define each aircraft's route within the context of the scenarios described here. Figure A.6 shows the implementation of these commands for two arbitrary flights. Here it can be seen that each command is preceded by the spawn time of the corresponding aircraft in hh:mm:ss.ss format. Additionally, the top of descend waypoint is neglected as the scenarios shown here were used in an experiment that used tactical conflict resolution. Moreover, all speeds are specified in Calibrated Air Speed (CAS). For a more detailed description of the scenario command syntax needed for describing aircraft routes, the reader is referred to: `https://github.com/ProfHoekstra/bluesky/wiki/Command-Reference`

A

Table A.3: Scenario commands needed to specify the routes of each aircraft for the BlueSky simulator

#	Command	Syntax	Arguments
1	Create Aircraft	CRE	Call sign, Aircraft type, Origin lat, Origin lon, heading, altitude, Speed (CAS)
2	Set Origin	ORIG	Call sign, Origin lat, Origin lon
3	Set Destination	DEST	Call sign, Destination lat, Destination lon
4	Add TOC Waypoint	ADDWPT	Call sign, TOC lat, TOC lon, TOC altitude, Speed at TOC (CAS)
5	Activate LNAV	LNAV	Call sign, ON (optional command)
6	Activate VNAV	VNAV	Call sign, ON (optional command)

```
# AC0193 Direct Distance = 227.4 NM
01:02:48.35>CRE,AC0193,B744,-0.75664317,1.54963544,332.15373221,0.0,400.00000000
01:02:48.35>ORIG,AC0193,-0.75664317,1.54963544
01:02:48.35>DEST,AC0193,2.58825882,-0.21827490
01:02:48.35>ADDWPT,AC0193,-0.29081038,1.30355120,9500.00000000,351.12305673
01:02:48.35>LNAV,AC0193,ON
01:02:48.35>VNAV,AC0193,ON

# AC0194 Direct Distance = 232.82 NM
01:03:23.69>CRE,AC0194,B744,-0.77330066,-0.72194947,72.5378518893,0.0,400.00000000
01:03:23.69>ORIG,AC0194,-0.77330066,-0.72194947
01:03:23.69>DEST,AC0194,0.38979758,2.97272491
01:03:23.69>ADDWPT,AC0194,-0.63349436,-0.27755971,8400.00000000,356.66641535
01:03:23.69>LNAV,AC0194,ON
01:03:23.69>VNAV,AC0194,ON
```

Figure A.6: An example scenario file for the BlueSky fast-time ATM simulator for two arbitrary flights. Note that all commands are preceded by the spawn time of aircraft. Lines that begin with the '#' symbol are comment lines, and they are not executed by BlueSky.

A.8.2. Batch Files

A full experiment usually consists of multiple traffic scenarios. To sequentially execute all the scenarios of an experiment without manual intervention, the BlueSky simulator uses so called 'batch' files. Batch files contain calls to the scenario and simulation settings files that are needed for a particular experiment. Figure A.7 displays an example batch file with calls to two arbitrary simulations. These two runs are repetitions of the same traffic demand, but using different simulation settings.

In Figure A.7, it can be seen that three different commands are used in a batch file: SCEN, PCALL and HOLD. The SCEN command is used to name a simulation run, and this name is also used to name the logs of a particular run. For instance in Figure A.7, the two simulations are named 'Scenario-OFF' and 'Scenario-ON', and therefore, the log files corresponding to these two simulations will also contain the words 'Scenario-ON' and 'Scenario-OFF'.

```
00:00:00.00>SCEN  Scenario-ON
00:00:00.00>PCALL Inst80-Rep6.scn
00:00:00.00>PCALL Settings-CRON.scn
05:30:00.00>HOLD

00:00:00.00>SCEN  Scenario-OFF
00:00:00.00>PCALL Inst80-Rep6.scn
00:00:00.00>PCALL Settings-CROFF.scn
05:30:00.00>HOLD
```

Figure A.7: An example batch file for the BlueSky fast-time ATM simulator for calls to two arbitrary scenarios

The PCALL command is used to load the traffic scenarios and settings files. As mentioned above, both simulations shown in Figure A.7 use the same traffic demand condition, namely, 'INST-80-Rep6', but use different settings files. The first simulation run uses tactical conflict resolution, and therefore, this simulation is performed using the 'Settings-CRON' settings file. The second simulation does not use conflict resolution, and therefore, it is performed using the 'Settings-CROFF' settings file. In addition to activating/deactivating conflict detection and resolution algorithms, settings files can also specify many other characteristics of the simulation including the simulation time step, start and end times for logging, traffic separation requirements and experiment area definitions. In addition to automating the execution of multiple simulation runs in sequence, the ability to repeat identical scenarios with different settings is a useful feature of the batch mode of BlueSky.

Finally, the HOLD command is used to indicate the time at which BlueSky should stop a particular simulation run, and start the following run. To ensure that a simulation run is fully completed before starting the following run, the HOLD command should be executed at a very late time; in the example shown in Figure A.7, the command is executed 5 hours and 30 minutes after a simulation has started since all aircraft are guaranteed to have finished their flights after this duration (for the scenarios considered here).

A.9. Additional Considerations

Two Dimensional Scenarios
The scenario generator described in this appendix aims to generate three dimensional scenarios. But, the same basic design can also be used to create two dimensional scenarios, i.e., scenarios focusing on only the cruise phase of flight. This can be achieved by simply having only one flight level for all cruising traffic. Nonetheless, aircraft should still be spawned at a lower altitude and be required to climb into the cruising level. Although logging can be restricted to the single cruising flight level, this approach can prevent very short term conflicts between just spawned aircraft and pre-existing cruising traffic. Once all aircraft have finished their flights, they can be deleted as they descend below the cruising flight level.

A

A word of caution; it is the opinion of the author that two dimensional simulations lead to incomplete conclusions. Therefore, 2-D simulations should only be used for initial testing purposes, for example, for testing the implementation of a new conflict resolution algorithm. They should not be used to study the dynamics of the air traffic system, or to evaluate the safety or capacity of a new airspace design. Experience has shown that two dimensional simulations oversimplify the actual interactions that occur between aircraft in real life, and that these interactions can have a significant impact on safety and capacity. For instance, the three dimensional simulations performed in this thesis have shown that climbing/descending aircraft trigger the vast majority of conflicts in layered airspaces (over 70% of conflicts for the conditions tested here). Simulations without climbing/descending aircraft would, therefore, significantly overestimate the safety performance of layered airspaces.

'Bouncing-Out' Effect

When performing simulations with conflict resolution, it is possible that aircraft are bounced out of the experiment region for part of their flights. Since logging is only performed in the experiment region, this 'bouncing-out' effect can distort the results. This problem can not be solved completely. But it can be mitigated to some degree by forcing aircraft to recover to their pre-conflict destination after resolving a conflict, and by using as large an experiment region as possible within the simulation region; Figure A.2 displays the difference between these two regions. Also aircraft should not be deleted if they leave the simulation region horizontally. They should only be deleted when they leave the simulation region vertically. This gives a chance for aircraft that are bounced out to re-enter the experiment region after conflict resolution.

Naming of Simulation Runs

The labels used to name a simulation run should clearly identify the most important experiment conditions used by that run. For example, the names used by the two simulation runs displayed in Figure A.7 clearly indicates whether a particular run is performed with or without conflict resolution. This is because, in most cases, the logs of a simulation run assume the same name as the simulation run itself. Therefore, this approach to naming simulation runs makes it much easier to analyze the results of a simulation during post-processing.

Activation of Conflict Resolution Algorithms

If tactical conflict resolution is used, it should be activated right from the start of a scenario, and not just before the logging phase begins. This is because a sudden activation of conflict resolution can trigger artificial conflict chain reactions, which can in turn negatively affect the results of an experiment. Moreover, it is more realistic to activate conflict resolution right from the start of a scenario.

Scenario Repetitions

Because each scenario represents only one of many possible realizations of a traffic demand condition, each demand condition has to be repeated multiple times using different origin-destination combinations. As a rule of thumb, the number of repe-

titions performed should be at least equivalent to the number of levels of the main independent variable of an experiment. For instance, if an experiment is performed to study the safety differences between five different airspace designs, then each traffic demand conditions should be repeated a minimum of five times.

References

[1] M. Nolan, Fundamentals of Air Traffic Control, Chapter 1 History of ATC, 5th Edition, Delmar Cengage Learning, 2010.

[2] G. Gilbert, Historical Development of the Air Traffic Control System, IEEE Transactions on Communications 21 (5) (1973) 364–375. doi:10.1109/TCOM.1973.1091699.

[3] T. L. Kraus, Celebrating 75 years of Federal Air Traffic Control, Tech. rep., FAA (2016).

[4] FAA, Photo Album – Air Traffic Control (2014).
URL https://www.faa.gov/about/history/photo_album/air_traffic_control/

[5] S. Kahne, I. Frolow, Air traffic management: evolution with technology, IEEE Control Systems 16 (4) (1996) 12–21. doi:10.1109/37.526911.

[6] N. Tofukuji, An enroute ATC simulation experiment for sector capacity estimation, IEEE Transactions on Control Systems Technology 1 (3) (1993) 138–143. doi:10.1109/87.251881.

[7] U. Metzger, R. Parasuraman, The Role of the Air Traffic Controller in Future Air Traffic Management: An Empirical Study of Active Control versus Passive Monitoring, Human Factors: The Journal of the Human Factors and Ergonomics Society 43 (4) (2001) 519–528.
doi:10.1518/001872001775870421.
URL http://hfs.sagepub.com/content/43/4/519

[8] P. Brooker, Future air traffic management: strategy and control philosophy, Aeronautical Journal 107 (1076) (2003) 589–598.
URL
http://cat.inist.fr/?aModele=afficheN&cpsidt=15198022

[9] A. Majumdar, W. Y. Ochieng, G. McAuley, J. Michel Lenzi, C. Lepadatu, The Factors Affecting Airspace Capacity in Europe: A Cross-Sectional Time-Series Analysis Using Simulated Controller Workload Data, The Journal of Navigation 57 (03) (2004) 385–405.
doi:10.1017/S0373463304002863.

[10] S. Loft, P. Sanderson, A. Neal, M. Mooij, Modeling and Predicting Mental Workload in En Route Air Traffic Control: Critical Review and Broader Implications, Human Factors: The Journal of the Human Factors and

Ergonomics Society 49 (3) (2007) 376–399.
doi:10.1518/001872007X197017.
URL http://hfs.sagepub.com/content/49/3/376

[11] P. H. Kopardekar, A. Schwartz, S. Magyarits, J. Rhodes, Airspace Complexity Measurement: An Air Traffic Control Simulation Analysis, International Journal of Industrial Engineering: Theory, Applications and Practice 16 (1) (2009) 61–70.
URL http://journals.sfu.ca/ijietap/index.php/ijie/article/view/18

[12] Performance Review Commission, Eurocontrol Performance Review Report 2016, Tech. Rep. PRR2016, Eurocontrol (2016).
URL http://www.eurocontrol.int/news/performance-review-report-2016

[13] Magill, S. A. N., Effect of Direct Routing on ATC Capacity, in: USA/Europe Air Traffic Management R&D Seminar, Orlando, 1998.
URL http://www.atmseminar.org/seminarContent/seminar2/papers/p_022_APMMA.pdf

[14] P. Dell'Olmo, G. Lulli, A new hierarchical architecture for Air Traffic Management: Optimisation of airway capacity in a Free Flight scenario, European Journal of Operational Research 144 (1) (2003) 179–193.
doi:10.1016/S0377-2217(01)00394-0.
URL http://www.sciencedirect.com/science/article/pii/S0377221701003940

[15] J. M. Hoekstra, R. C. J. Ruigrok, R. N. H. W. van Gent, Free Flight in a Crowded Airspace?, in: Proceedings of the 3rd USA/Europe Air Traffic Management R&D Seminar, Naples, 2000.

[16] SESAR, Sesar European ATM Masterplan 2015, Tech. rep. (2015).

[17] FAA, NextGen Implementation Plan 2016, Tech. rep. (2016).

[18] SESAR Consortium, The Concept of Operations at a glance, Tech. rep., Single European Sky (2007).

[19] FAA and Eurocontrol, Principles of operation for the use of airborne seapration assurance systems, Tech. rep. (2001).

[20] J. M. Hoekstra, Designing for safety: the free flight air traffic management concept, PhD Dissertation, Delft University of Technology, Delft (Nov. 2001).
URL http://resolver.tudelft.nl/uuid:d9f6078a-0961-403f-871e-cad365ee46a9

[21] Radio Technical Commission for Aeronautics, Minimum aviation system performance standards for automatic dependent surveillance broadcast (ADS-B), Tech. rep., RTCA (1998).

[22] W. Chung, R. Staab, A 1090 Extended Squitter Automatic Dependent Surveillance - Broadcast (ADS-B) Reception Model for Air-Traffic-Management Simulations, in: AIAA Modeling and Simulation Technologies Conference and Exhibit, American Institute of Aeronautics and Astronautics, 2006. doi:10.2514/6.2006-6614.
URL https://arc.aiaa.org/doi/abs/10.2514/6.2006-6614

[23] FAA, Review of the ADS-B system and development of ADS-B flight inspection requireemnts, methodologies and procedures, Tech. Rep. OU/AEC 08-09TM15689/0007-1 (2008).

[24] Eurocontrol, ADS-B and WAM deployment in Europe, Tech. rep. (2013).
URL https://www.eurocontrol.int/tags/ads-b

[25] T. Langejan, E. Sunil, J. Ellerbroek, J. Hoekstra, Effect of ADS-B Characteristics on Airborne Conflict Detection and Resolution, in: Proccedings of the 6th Sesar Innovation Days, 2016.

[26] T. L. Verbraak, J. Ellerbroek, J. Sun, J. M. Hoekstra, Large-Scale ADS-B Data and Signal Quality Analysis, in: Proceedings of the 12th USA/Europe Air Traffic Management R&D Seminar, 2017.

[27] M. V. Clari, R. Ruigrok, J. Hoekstra, Cost-benefit study of Free Flight with airborne separation assurance, in: AIAA Guidance, Navigation, and Control Conference and Exhibit, American Institute of Aeronautics and Astronautics, 2000.
URL http://arc.aiaa.org/doi/abs/10.2514/6.2000-4361

[28] M. Jardin, Air Traffic Conflict Models, in: AIAA 4th Aviation Technology, Integration and Operations (ATIO) Forum, American Institute of Aeronautics and Astronautics, 2004.
URL http://arc.aiaa.org/doi/abs/10.2514/6.2004-6393

[29] M. R. Jardin, Analytical Relationships Between Conflict Counts and Air-Traffic Density, Journal of Guidance, Control, and Dynamics 28 (6) (2005) 1150–1156. doi:10.2514/1.12758.
URL http://dx.doi.org/10.2514/1.12758

[30] J. M. Hoekstra, R. N. H. W. van Gent, R. C. J. Ruigrok, Designing for safety: the 'free flight' air traffic management concept, Reliability Engineering & System Safety 75 (2) (2002) 215–232.
doi:10.1016/S0951-8320(01)00096-5.
URL http://www.sciencedirect.com/science/article/pii/S0951832001000965

[31] Radio Technical Commission for Aeronautics, Final Report of RTCA Task Force 3 Free Flight Implementation, Tech. rep., RTCA (1995).

[32] J. Krozel, M. Peters, K. Bilimoria, A decentralized control strategy for distributed air/ground traffic separation, in: AIAA Guidance, Navigation, and Control Conference and Exhibit, American Institute of Aeronautics and Astronautics, 2000.
URL http://arc.aiaa.org/doi/abs/10.2514/6.2000-4062

[33] K. Bilimoria, K. Sheth, H. Lee, S. Grabbe, Performance evaluation of airborne separation assurance for free flight, in: AIAA Guidance, Navigation and Control Conference, AIAA-2000-4269, 2000.
doi:10.2514/6.2000-4269.
URL http://arc.aiaa.org/doi/abs/10.2514/6.2000-4269

[34] K. Bilimoria, H. Lee, Properties of air traffic conflicts for free and structured routing, in: AIAA Guidance, Navigation, and Control Conference and Exhibit, American Institute of Aeronautics and Astronautics, 2001.
URL http://arc.aiaa.org/doi/abs/10.2514/6.2001-4051

[35] T. Prevot, V. Battiste, E. Palmer, S. Shelden, Air traffic concept utilizing 4d trajectories and airborne separation assistance, in: AIAA Guidance, Navigation, and Control Conference, AIAA-2003-5770, 2003.
doi:10.2514/6.2003-5770.
URL http://arc.aiaa.org/doi/pdf/10.2514/6.2003-5770

[36] S. Mondoloni, D. Kozarsky, T. Breunig, S. Green, Distributed Air/Ground Traffic Management (DAG-TM) Benefit Mechanisms, in: AIAA's 3rd Annual Aviation Technology, Integration, and Operations (ATIO) Forum, American Institute of Aeronautics and Astronautics, 2003.
URL http://arc.aiaa.org/doi/abs/10.2514/6.2003-6807

[37] J. M. Hoekstra, R. N. H. W. v. Gent, J. M. Hoekstra, R. C. J. Ruigrok, R. C. J. Ruigrok, Conceptual design of Free Flight with airborne separation assurance, 1998, pp. 98–4239.

[38] M. Ballin, D. Wing, M. Hughes, S. Conway, Airborne separation assurance and traffic management - Research of concepts and technology, in: Guidance, Navigation, and Control Conference and Exhibit, American Institute of Aeronautics and Astronautics, 1999.
URL http://arc.aiaa.org/doi/abs/10.2514/6.1999-3989

[39] M. Ballin, J. Hoekstra, D. Wing, G. Lohr, NASA Langley and NLR Research of Distributed Air/Ground Traffic Management, in: AIAA Aircraft Technology, Integration, and Operations (ATIO) Conference, AIAA-2002-5826, American Institute of Aeronautics and Astronautics, 2002.
doi:10.2514/6.2002-5826.
URL http://arc.aiaa.org/doi/abs/10.2514/6.2002-5826

[40] B. Korn, C. Edinger, S. Tittel, D. Kügler, T. Pütz, O. Hassa, B. Mohrhard, Sectorless atm—a concept to increase en-route efficiency, in: Digital

Avionics Systems Conference, 2009. DASC'09. IEEE/AIAA 28th, IEEE, 2009, pp. 2–E.

[41] B. Birkmeier, B. Korn, D. Kügler, Sectorless atm and advanced sesar concepts: Complement not contradiction, in: Digital Avionics Systems Conference (DASC), 2010 IEEE/AIAA 29th, IEEE, 2010, pp. 2–D.

[42] A. R. Schmitt, C. Edinger, B. Korn, Balancing controller workload within a sectorless atm concept, CEAS Aeronautical Journal 2 (1-4) (2011) 35–41.

[43] Ruigrok, R. C. J, M. Clari, The impact of aircraft intent information and traffic separation assurance responsibility on en-route airspace capacity., in: 5th FAA/EUROCONTROL ATM R&D Seminar, 2003.

[44] D. Wing, R. Vivona, D. Roscoe, Airborne Tactical Intent-Based Conflict Resolution Capability, in: 9th AIAA Aviation Technology, Integration, and Operations Conference (ATIO), American Institute of Aeronautics and Astronautics, 2009.
URL http://arc.aiaa.org/doi/abs/10.2514/6.2009-7020

[45] M. S. Eby, A Self-Organizational Approach for Resolving Air Traffic Conflicts, Lincoln Laboratory Journal 7 (2) (1994) 239–254.
URL http://trid.trb.org/view.aspx?id=524235

[46] R. Lachner, Collision avoidance as a differential game: real-time approximation of optimal strategies using higher derivatives of the value function, in: Computational Cybernetics and Simulation 1997 IEEE International Conference on Systems, Man, and Cybernetics, Vol. 3, 1997, pp. 2308–2313 vol.3. doi:10.1109/ICSMC.1997.635270.

[47] K. Bilimoria, B. Sridhar, G. Chatterji, Effects of conflict resolution maneuvers and traffic density on free flight, in: Guidance, Navigation, and Control Conference, American Institute of Aeronautics and Astronautics, 1996.
URL http://arc.aiaa.org/doi/abs/10.2514/6.1996-3767

[48] R. Irvine, Comparison of pair-wise priority-based resolution schemes through fast-time simulation, in: 8th Innovative Research Workshop & Exhibition, EEC, 2009.
URL http://publish.eurocontrol.int/eec/gallery/content/public/document/eec/conference/paper/2009/007_Comparison_of_resolution_schemes_by_FTS.pdf

[49] J. K. Kuchar, L. C. Yang, A Review of Conflict Detection and Resolution Modeling Methods, IEEE Transactions on Intelligent Transportation Systems 1 (2000) 179–189.

[50] Y. I. Jenie, E. v. Kampen, J. Ellerbroek, J. M. Hoekstra, Taxonomy of Conflict Detection and Resolution Approaches for Unmanned Aerial Vehicle in an Integrated Airspace, IEEE Transactions on Intelligent Transportation Systems 18 (3) (2017) 558–567. doi:10.1109/TITS.2016.2580219.

[51] J. Ellerbroek, M. Visser, S. B. Van Dam, M. Mulder, M. M. van Paassen, Design of an airborne three-dimensional separation assistance display, Systems, Man and Cybernetics, Part A: Systems and Humans, IEEE Transactions on 41 (5) (2011) 863–875.
URL `http://ieeexplore.ieee.org/xpls/abs_all.jsp?arnumber=5682415`

[52] J. Ellerbroek, Airborne Conflict Resolution in Three Dimensions, Ph.D. thesis, Delft University of Technology, Faculty of Aerospace Engineering (Sep. 2013).
URL `http://resolver.tudelft.nl/uuid:96c65674-06d4-410c-87c2-b981af95211e`

[53] R. C. J. Ruigrok, J. M. Hoekstra, Human factors evaluations of Free Flight: Issues solved and issues remaining, Applied Ergonomics 38 (4) (2007) 437–455. `doi:10.1016/j.apergo.2007.01.006`.
URL `http://www.sciencedirect.com/science/article/pii/S000368700700018X`

[54] J. Hoekstra, F. Bussink, Free Flight: How low can you go?, 2002.

[55] SESAR Joint Undertaking, European Drones Outlook Study-Unlocking the value for Europe, Tech. rep., SESAR (2016).

[56] SESAR Joint Undertaking, U-Space Blueprint, Tech. rep., SESAR (2017).

[57] E. Sunil, J. Hoekstra, J. Ellerbroek, F. Bussink, D. Nieuwenhuisen, A. Vidosavljevic, S. Kern, Metropolis: Relating Airspace Structure and Capacity for Extreme Traffic Densities, in: USA/Europe Air Traffic Management R&D Seminar, Lisbon, 2015.

[58] P. Kopardekar, J. Rios, T. Prevot, M. Johnson, J. Jung, J. Robinson, Unmanned aircraft system traffic management (utm) concept of operations, in: Proceeding of the 16th AIAA Aviation Technology, Integration, and Operations Conference, 2016. `doi:AIAA2016-3292`.

[59] V. Bulusu, R. Sengupta, Z. Liu, Unmanned aviation: To be free or not to be free?, in: 7th International Conference on Research in Air Transportation, 2016.

[60] V. Bulusu, R. Sengupta, V. Polishchuk, L. Sedov, Cooperative and non-cooperative uas traffic volumes, in: Unmanned Aircraft Systems (ICUAS), 2017 International Conference on, IEEE, 2017, pp. 1673–1681.

[61] L. Sedov, V. Polishchuk, Centralized and Distributed UTM in Layered Airspace, in: Proceedings of the 8th International Conference on Research in Air Transportation (ICRAT 2018), 2018.

[62] N. Peinecke, A. Kuenz, Deconflicting the urban drone airspace, in: 2017 IEEE/AIAA 36th Digital Avionics Systems Conference (DASC), 2017, pp. 1–6. `doi:10.1109/DASC.2017.8102048`.

[63] F. Maracich, Flying free flight: pilot perspective and system integration requirement, IEEE Aerospace and Electronic Systems Magazine 21 (7) (2006) 3–7. `doi:10.1109/MAES.2006.1684261`.

[64] K. Wichman, L. Lindberg, L. Kilchert, O. Bleeker, Four-Dimensional trajectory based air traffic management, in: AIAA Guidance, Navigation, and Control Conference, AIAA-2004-5413, 2004, p. 11.
`doi:10.2514/6.2004-5413`.
URL `http://arc.aiaa.org/doi/pdf/10.2514/6.2004-5413`

[65] J. Klooster, S. Torres, D. Earman, M. Castillo-Effen, R. Subbu, L. Kammer, D. Chan, T. Tomlinson, Trajectory synchronization and negotiation in Trajectory Based Operations, in: IEEE/AIAA Digital Avionics Systems Conference (DASC), 2010, pp. 1.A.3–1–1.A.3–11.
`doi:10.1109/DASC.2010.5655536`.

[66] R. L. Ford, On the Use of Height Rules in Off-route Airspace, The Journal of Navigation 36 (02) (1983) 269–287.
`doi:10.1017/S037346330002498X`.
URL
`http://journals.cambridge.org/article_S037346330002498X`

[67] P. G. Reich, Analysis of Long-Range Air Traffic Systems: Separation Standards—I, The Journal of Navigation 19 (01) (1966) 88–98.
`doi:10.1017/S037346330004056X`.

[68] S. Ratcliffe, R. L. Ford, Conflicts between Random Flights in a Given Area, The Journal of Navigation 35 (01) (1982) 47–74.
`doi:10.1017/S0373463300043101`.
URL
`http://journals.cambridge.org/article_S0373463300043101`

[69] S. Endoh, Aircraft collision models, Ph.D. thesis, Massachusetts Institute of Technology, Flight Transportation Laboratory (1982).
URL `http://dspace.mit.edu/handle/1721.1/68072`

[70] Hoekstra, J., Maas, J., Tra, M., Sunil, E., How Do Layered Airspace Design Parameters Affect Airspace Capacity and Safety?, in: Proceedings of the 7th International Conference on Research in Air Transportation, 2016.

[71] Coisabh, North atlantic tracks for the westbound crossing of february 24, 2017, with the new rlat tracks shown in blue (2017).
URL `https://en.wikipedia.org/wiki/North_Atlantic_Tracks`

[72] R. C. J. Ruigrok, R. N. H. W. v. Gent, J. M. Hoekstra, The Transition Towards Free Flight: A Human Factors Evaluation of Mixed Equipage, Integrated Air-Ground, Free Flight ATM Scenarios, SAE Technical Paper 1999-01-5564, SAE International, Warrendale, PA (Oct. 1999).
URL http://papers.sae.org/1999-01-5564/

[73] Maas, J., Sunil, E., Ellerbroek, J., Hoekstra, J.M., The Effect of Swarming on a Voltage Potential-Based Conflict Resolution Algorithm, Philadelphia, 2016, submitted.

[74] E. Sunil, J. Ellerbroek, J. Hoekstra, A. Vidosavljevic, M. Arntzen, F. Bussink, D. Nieuwenhuisen, Analysis of Airspace Structure and Capacity for Decentralized Separation Using Fast-Time Simulations, Journal of Guidance, Control, and Dynamics 40 (1) (2017) 38–51. doi:10.2514/1.G000528.
URL http://dx.doi.org/10.2514/1.G000528

[75] P. U. Lee, J. Mercer, B. Gore, N. Smith, K. Lee, R. Hoffman, Examining airspace structural components and configuration practices for dynamic airspace configuration, in: AIAA Guidance, Navigation, and Control Conference, AIAA-2008-7228, 2008, pp. 18–21.
doi:10.2514/6.2008-7228.
URL http://arc.aiaa.org/doi/pdf/10.2514/6.2008-7228

[76] N. A. Doble, R. Hoffman, P. U. Lee, J. Mercer, B. Gore, N. Smith, K. Lee, Current airspace configuration practices and their implications for future airspace concepts, in: AIAA Aviation Technology, Integration and Operations (ATIO) Conference, AIAA-2008-8936, Anchorage, 2008.
doi:10.2514/6.2008-8936.
URL http://arc.aiaa.org/doi/pdf/10.2514/6.2008-8936

[77] Joint Planning and Development Office, Concept of operations for the Next Generation Air Transportation System, Tech. rep., FAA (Jun. 2007).

[78] J. Krozel, M. Peters, K. Bilimoria, C. Lee, J. Mitchell, System performance characteristics of centralized and decentralized air traffic separation strategies, in: USA/Europe Air Traffic Management R&D Seminar, 2001.

[79] International Civil Aviation Organization, Annex 2, Rules of the Air, Tech. rep. (Jul. 2005).

[80] F. Bussink, J. Hoekstra, B. Heesbeen, Traffic manager: a flexible desktop simulation tool enabling future ATM research, in: IEEE Digital Avionics Systems Conference (DASC), Vol. 1, IEEE, 2005, pp. 3.B.4 − 31–10.
doi:10.1109/DASC.2005.1563344.
URL http://ieeexplore.ieee.org/xpls/abs_all.jsp?arnumber=1563344

[81] A. Nuic, D. Poles, V. Mouillet, BADA: An advanced aircraft performance model for present and future ATM systems, International Journal of

Adaptive Control and Signal Processing 24 (10) (2010) 850–866.
URL http:
//onlinelibrary.wiley.com/doi/10.1002/acs.1176/abstract

[82] P. Hart, N. Nilsson, B. Raphael, A Formal Basis for the Heuristic
Determination of Minimum Cost Paths, IEEE Transactions on Systems
Science and Cybernetics 4 (2) (1968) 100–107.
doi:10.1109/TSSC.1968.300136.

[83] D. Delahaye, S. Puechmorel, Air traffic complexity: towards intrinsic
metrics, in: USA/Europe Air Traffic Management R&D Seminar, 2000.

[84] Vidosavljevic, A., Delahaye, D., Sunil, E., Bussink, F., Hoekstra, J.M.,
Complexity Analysis of the Concepts of Urban Airspace Design for
Metropolis Project, in: ENRI International Workshop on ATM/CNS, 2015.

[85] G. J. Ruijgrok, Elements of Aviation Acoustics, Chapter 9 Noise Measures,
Delft University Press, 2004.
URL http:
//www.iospress.nl/book/elements-of-aviation-acoustics/

[86] E. R. Boeker, E. Dinges, B. He, G. Fleming, C. J. Roof, P. J. Gerbi, A. S.
Rapoza, J. Hemann, Integrated Noise Model (INM) Version 7.0, Tech. Rep.
FAA-AEE-08-01 (Jan. 2008).
URL http://trid.trb.org/view.aspx?id=1355723

[87] M. Arntzen, R. Aalmoes, F. Bussink, E. Sunil, J. M. Hoekstra, Noise
computation for future urban air traffic systems, in: Inter-Noise Congress:
Implementing Noise Control Technology, 2015.
URL http://repository.tudelft.nl/view/ir/uuid:
2da75f98-756a-4a71-a84f-35e1c72d3a9b/

[88] E. Sunil, J. Ellerbroek, J. M. Hoekstra, J. Maas, Three-dimensional conflict
count models for unstructured and layered airspace designs, Transportation
Research Part C: Emerging Technologies 95 (2018) 295–319.
doi:10.1016/j.trc.2018.05.031.
URL http://www.sciencedirect.com/science/article/pii/
S0968090X1830771X

[89] P. Dell'Olmo, G. Lulli, A new hierarchical architecture for Air Traffic
Management: Optimisation of airway capacity in a Free Flight scenario,
European Journal of Operational Research 144 (1) (2003) 179–193.
doi:10.1016/S0377-2217(01)00394-0.
URL http://www.sciencedirect.com/science/article/pii/
S0377221701003940

[90] J. J. Rebollo, H. Balakrishnan, Characterization and prediction of air traffic
delays, Transportation Research Part C: Emerging Technologies
44 (Supplement C) (2014) 231–241.

doi:10.1016/j.trc.2014.04.007.
URL http://www.sciencedirect.com/science/article/pii/
S0968090X14001041

[91] S. M. Green, K. D. Bilimoria, M. G. Ballin, Distributed air/ground traffic
management for en route flight operations, Air Traffic Control Quarterly
9 (4) (2001) 259–285.
URL https://arc.aiaa.org/doi/abs/10.2514/atcq.9.4.259

[92] J. Krozel, M. Peters, K. Bilimoria, C. Lee, J. Mitchell, System performance
characterisitcs of centralized and decentralized air traffic separation
strategies, in: USA/Europe Air Traffic Management R&D Seminar, 2001.

[93] A. Barnett, Free-Flight and en Route Air Safety: A First-Order Analysis,
Operations Research 48 (6) (2000) 833–845.
doi:10.1287/opre.48.6.833.12394.
URL http://pubsonline.informs.org/doi/citedby/10.1287/
opre.48.6.833.12394

[94] NMD/NSD Operations Roadmap Team, European Free Route Airspace
Developments, Tech. rep., Eurocontrol (2015).

[95] R. Irvine, H. Hering, Towards Systematic Air Traffic Management in a
Regular Lattice, in: 7th AIAA ATIO Conf, 2nd CEIAT Int'l Conf on Innov and
Integr in Aero Sciences, 17th LTA Systems Tech Conf; followed by 2nd
TEOS Forum, 2007, p. 7780.
URL http://arc.aiaa.org/doi/pdf/10.2514/6.2007-7780

[96] K. Leiden, S. Peters, S. Quesada, Flight level-based dynamic airspace
configuration, in: Proceedings of the 9th AIAA Aviation Technology,
Integration and Operations (ATIO) Forum. American Institute of
Aeronautics and Astronautics, 2009.
URL http://arc.aiaa.org/doi/pdf/10.2514/6.2009-7104

[97] R. A. Paielli, A Linear Altitude Rule for Safer and More Efficient Enroute Air
Traffic, Air Traffic Control Quarterly 8 (3).
URL http://www.aviationsystemsdivision.arc.nasa.gov/
publications/2000/Paielli_ATCQ_Alt-Rules_2000.pdf

[98] Norman Davidson, Statistical Mechanics, Dover Publications, 2003.

[99] B. L. Marks, Air Traffic Control Separation Standards and Collision Risk,
Tech. Rep. MATH 91 (1963).
URL https://trid.trb.org/view.aspx?id=618712

[100] P. G. Reich, Analysis of Long-Range Air Traffic Systems: Separation
Standards—III, The Journal of Navigation 19 (3) (1966) 331–347.
doi:10.1017/S0373463300047445.
URL https://www.cambridge.org/core/journals/

```
journal-of-navigation/article/
analysis-of-longrange-air-traffic-systems-separation-standardsiii/
F66DD3220162FC9B49774AA13DC0ED07
```

[101] P. Brooker, Future Air Traffic Management: Quantitative En Route Safety
Assessment Part 2 – New Approaches, The Journal of Navigation 55 (3)
(2002) 363–379. `doi:10.1017/S037346330200187X`.
URL `https://www.cambridge.org/core/journals/`
`journal-of-navigation/article/`
`future-air-traffic-management-quantitative-en-route-safety-assessment`
`415EBE595C2FCAEFC5014B21270E4721`

[102] F. Netjasov, Framework for airspace planning and design based on conflict
risk assessment: Part 1: Conflict risk assessment model for airspace
strategic planning, Transportation Research Part C: Emerging Technologies
24 (2012) 190–212. `doi:10.1016/j.trc.2012.03.002`.
URL `http://www.sciencedirect.com/science/article/pii/`
`S0968090X12000435`

[103] F. Netjasov, O. Babić, Framework for airspace planning and design based on
conflict risk assessment: Part 3: Conflict risk assessment model for airspace
operational and current day planning, Transportation Research Part C:
Emerging Technologies 32 (2013) 31–47.
`doi:10.1016/j.trc.2013.04.002`.
URL `http://www.sciencedirect.com/science/article/pii/`
`S0968090X13000752`

[104] W. Graham, R. H. Orr, Terminal Air Traffic Model with Near Midair Collision
and Midair Collision Comparison, Tech. rep., US Department of
Transportation-Air Traffic Control Advisory Committee (1969).

[105] P. D. Flanagan, K. E. Willis, Frequency of airspace conflicts in the mixed
terminal environment, Tech. rep., US Department of Transportation - Air
Traffic Control Advisory Committee (1969).

[106] K. Datta, R. M. Oliver, Predicting risk of near midair collisions in controlled
airspace, Transportation Research Part B: Methodological 25 (4) (1991)
237–252. `doi:10.1016/0191-2615(91)90006-5`.
URL `http://www.sciencedirect.com/science/article/pii/`
`0191261591900065`

[107] Dimitrios Milios, Probability Distributions as Program Variables, Master's
thesis, University of Edinburgh (2009).
URL `http://www.inf.ed.ac.uk/publications/thesis/online/`
`IM090722.pdf`

[108] J. Hoekstra, J. Ellerbroek, BlueSky ATC Simulator Project: an Open Data
and Open Source Approach, in: Proceedings of the 7th International
Conference on Research in Air Transportation, 2016.

[109] I. Metz, J. Hoekstra, J. Ellerbroek, D. Kugler, Aircraft Performance for Open Air Traffic Simulations, in: AIAA Modeling and Simulation Technologies Conference, 2016.

[110] Sunil, E., Þórðarson, O., Ellerbroek, J., Hoekstra, J.M., Analyzing the Effect of Traffic Scenario Properties on Conflict Count Models, in: Prodeedings of the 8th International Conference on Research in Air Transportation (ICRAT '18), 2018.

[111] P. K. Menon, G. D. Sweriduk, B. Sridhar, Optimal Strategies for Free-Flight Air Traffic Conflict Resolution, Journal of Guidance, Control, and Dynamics 22 (2) (1999) 202–211. `doi:10.2514/2.4384`.
URL `http://arc.aiaa.org/doi/abs/10.2514/2.4384`

[112] J. C. Clements, The optimal control of collision avoidance trajectories in air traffic management, Transportation Research Part B: Methodological 33 (4) (1999) 265–280. `doi:10.1016/S0191-2615(98)00031-9`.
URL `http://www.sciencedirect.com/science/article/pii/S0191261598000319`

[113] C. A. Zúñiga, M. A. Piera, S. Ruiz, I. Del Pozo, A CD&CR causal model based on path shortening/path stretching techniques, Transportation Research Part C: Emerging Technologies 33 (2013) 238–256.
`doi:10.1016/j.trc.2011.11.010`.
URL `http://www.sciencedirect.com/science/article/pii/S0968090X11001628`

[114] Sunil, E., Hoekstra, J.M., Ellerbroek, J., Bussink, F., The Influence of Traffic Structure on Airspace Capacity, in: Proceedings of the 7th International Conference on Research in Air Transportation (ICRAT 2016), 2016.

[115] Rahman, Q.I., Schmeisser, G., Characterization of the speed of convergence of the trapezoidal rule, Numerische Mathematik 57 (1) (1990) 123–138.
`doi:https://doi.org/10.1007/BF01386402`.

[116] J. Sander, M. Ester, H.-P. Kriegel, X. Xu, Density-Based Clustering in Spatial Databases: The Algorithm GDBSCAN and Its Applications, Data Mining and Knowledge Discovery 2 (2) (1998) 169–194.
`doi:10.1023/A:1009745219419`.
URL `https://doi.org/10.1023/A:1009745219419`

[117] Sunil, E., Ellerbroek, J., Hoekstra, J.M., CAMDA: Capacity Assessment Method for Decentralized Air Traffic Control, in: Prodeedings of the 8th International Conference on Research in Air Transportation (ICRAT '18), 2018.

[118] Sunil, E., Ellerbroek, J., Hoekstra, J.M., Maas, J., Three-Dimensional Conflict Count Models for Unstructured and Layered Airspace Designs, submitted to Transportation Research Part C: Emerging Technologies.

[119] Sunil, E., Ellerbroek, J., Hoekstra, J.M., Maas, J., Modeling Airspace Stability and Capacity for Decentralized Separation, in: Proceedings of the 12th USA/Europe Air Traffic Management R&D Seminar, 2017.

Samenvatting

Het huidige systeem van luchtverkeersleiding (LVL) is gebaseerd op een gecentraliseerde besturingsarchitectuur. Fundamenteel is dit systeem sterk afhankelijk van handmatig ingrijpen door menselijke luchtverkeersleiders (LVLDs) om veilige operaties te garanderen. De capaciteit van dit systeem is daarom nauw verbonden met de maximale werklast die door LVLDs getolereerd kan worden. Hoewel dit systeem tot nu toe heeft voorzien in de behoeften van de luchtvaart, wijzen de wereldwijde meldingen van toenemende vertragingen en congestie samen met het tekort aan LVLDs, welke de werkdruk van de LVLDs nog verergert, erop dat het huidige gecentraliseerde operationele model snel zijn maximale capaciteit nadert.

Om de voorspelde toename in verkeersdrukte het hoofd te bieden, hebben veel onderzoekers een overgang voorgesteld naar een paradigma van gedecentraliseerde verkeersscheiding in het en-route luchtruim. In dit gedecentraliseerde luchtruim is elk afzonderlijk vliegtuig verantwoordelijk voor zijn eigen separatie met al het omringende verkeer. Om decentralisatie mogelijk te maken, zijn aanzienlijke onderzoeken gewijd aan de ontwikkeling van nieuwe algoritmen voor geautomatiseerde conflictdetectie en -oplossing in de lucht (CD&O), waarbij sommige studies zelfs dergelijke algoritmen testen met echte vliegtuigbemanningen.

Ondanks meer dan twee decennia aan onderzoek dat de theoretische voordelen laat zien, moet decentralisatie echter nog worden ingezet in het veld. Vanuit technisch oogpunt heeft een gebrek aan inzicht in drie open vraagstukken, namelijk het ontwerp, de modellering van de veiligheid, en de modellering van de capaciteit van het luchtruim, de verdere ontwikkeling en uitvoering ervan belemmerd. Het doel van dit onderzoek is om deze drie problemen aan te pakken om gedecentraliseerde LVL dichter bij de realiteit te brengen. Daarom is de centrale deel van dit proefschrift verdeeld in drie delen, waarbij elk deel een van de drie bovengenoemde problemen aanpakt.

Het eerste deel van deze studie richtte zich op het ontwerpen van een gedecentraliseerd luchtruim. Hoewel het huidige gecentraliseerde LVL-systeem in elementen zoals luchtwegen en sectoren gebruikt in het ontwerp, is door eerdere studies nog niet in detail onderzocht hoe het gebruik van vergelijkbare opties gedecentraliseerde operaties kan optimaliseren. Er bestaat zelfs geen consensus in de bestaande literatuur omtrent de vraag of een bepaalde vorm van verkeersstructuur ook gunstig is voor gedecentraliseerde LVL, waarbij verschillende studies over dit onderwerp lijnrecht tegenovergestelde conclusies hebben. Om een beter begrip te krijgen van de relatie tussen het ontwerp van het luchtruim en de capaciteit van gedecentraliseerde LVL, gebruikte dit onderzoek versnelde simulaties om empirisch vier concepten met toenemende structuur van het luchtruim met elkaar te vergelijken. De

vier concepten, variërend van een volledig ongestructureerd concept van enkel di-
recte routes, tot een zeer gestructureerd buisnetwerk met behulp van 4D-trajecten,
werden onderworpen aan meerdere niveaus van verkeersdrukte binnen dezelfde si-
mulatieomgeving, voor zowel nominale als niet-nominale condities.

De resultaten van deze simulaties waren hoogst onverwacht: aangezien eerdere
studies zich hadden gericht op alleen volledig ongestructureerde en volledig ge-
structureerde luchtruimontwerpen, werd verondersteld dat een van deze twee ex-
treme ontwerpopties tot de hoogste capaciteit zou leiden. De simulatieresultaten
gaven echter aan dat een gelaagd luchtruimontwerp, dat voorschriften van koers-
hoogte gebruikte om kruisende vliegtuigen verticaal te scheiden op basis van hun
reisrichting, resulteerde in de beste balans van alle statistieken in het luchtruim die
in overweging werden genomen. Deze benadering van het organiseren van het ver-
keer verlaagde niet alleen de relatieve snelheden tussen vliegtuigen, maar liet ook
directe horizontale routes toe. Als zodanig leidde het gelaagde luchtruimconcept
tot de hoogste veiligheid van alle geteste ontwerpen, zonder de route-efficiëntie
ten opzichte van het volledig ongestructureerde ontwerp onnodig te verminderen.
Deze laatste ontwerpoptie resulteerde in de op één na beste capaciteit. In tegen-
stelling tot dit, zorgden concepten die het verkeer strikte horizontale beperkingen
oplegden voor een onevenwicht tussen de opgelegde structuur en het patroon van
het verkeer. Dit leidde op zijn beurt tot kunstmatige concentraties van verkeer
die de algemene prestaties en capaciteit verminderden. Samenvattend verbeterde
de capaciteit van decentralisatie toen structurele beperkingen een verlaging van
de relatieve snelheden bevorderden en wanneer directe horizontale routes waren
toegestaan.

Het tweede deel van dit proefschrift ontwikkelde wiskundige conflictmodellen die
de intrinsieke veiligheid van een luchtruimontwerp kwantificeerden, met behulp van
casestudy's met ongestructureerde en gelaagde luchtruimconcepten. Hier verwijst
het begrip van intrinsieke veiligheid naar het vermogen van een luchtruimontwerp
om conflicten te voorkomen, alleen door de beperkingen die het oplegt aan het
verkeer. De modellen die hier worden behandeld, worden in de literatuur vaak
'gasmodellen' genoemd. Zoals de naam al aangeeft, behandelt deze modellerings-
methode conflicten tussen vliegtuigen die lijken op de botsingen die zich voordoen
tussen ideale gasdeeltjes. Hoewel dergelijke modellen veel worden gebruikt binnen
LVL-onderzoek, hebben de meeste eerdere gasmodellen zich alleen geconcentreerd
op conflicten tussen kruisende vliegtuigen, waardoor hun toepassingen werden be-
perkt.

Dit proefschrift breidt daarom de gasmodellen zodanig uit dat ze rekening houden
met de effecten van zowel kruisend als klimmend/dalend verkeer op het aantal
getelde conflicten. De ontwikkelde methode groepeerde vliegtuigen door middel
van de vluchtfase, terwijl ook rekening werd gehouden met de interacties, evenals
het aandeel van vliegtuigen, in verschillende vluchtfasen. Dit werd gecombineerd
met een eenvoudige, maar nieuwe methode om zowel de horizontale als verticale
componenten van de gewogen gemiddelde relatieve snelheid in het luchtruim te
berekenen. Experimenten met versnelde tijd toonden aan dat de resulterende 3D-

modellen het aantal conflicten met hoge nauwkeurigheid schatte voor zowel onge-structureerde als gelaagde ontwerpen, voor alle geteste omstandigheden. Boven-dien gaven de resultaten ook aan dat klimmende en dalende vliegtuigen betrokken zijn bij de overgrote meerderheid van conflicten voor gelaagde luchtruimten met een klein koersbereik per vluchtniveau. Dit laatste resultaat benadrukte het belang van het in acht nemen van alle relevante vluchtfasen bij het beoordelen van de intrinsieke veiligheid van een luchtruimontwerp.

In aangrenzend onderzoek werd ook het effect van de eigenschappen van het ver-keersscenario op de nauwkeurigheid van de gasmodellen geëvalueerd. De analyti-sche gasmodellen die eerder zijn beschreven, maken gebruik van een aantal geïdea-liseerde aannames in gedrag van het verkeer die niet altijd resulteren in realistische acties, in het bijzonder de veranderingen van de snelheid, koers, hoogte en loca-ties van een vliegtuig. Dit onderzoek probeert deze beperking aan te pakken door te onderzoeken wat de effecten van zulke aannames van scenario's hebben op de nauwkeurigheid van het analytisch gasmodel met behulp van versnelde simulaties. Daarnaast ontwikkelde en testte dit werk zogenaamde numerieke 'modelaanpas-singen' die de afhankelijkheid van de modellen op de aannames van het scenario versoepelden. Net als voorheen werden conflictmodellen voor ongestructureerde en gelaagde luchtruimten gebruikt als casestudy's voor deze doeleinden.

De resultaten van deze versnelde simulaties gaven aan dat niet-ideale hoogte en ruimtelijke verdelingen van het verkeer een drastisch negatief effect hadden op de analytische nauwkeurigheid van het model, terwijl niet-ideale koersverdelingen een kleiner negatief effect hadden. Daarentegen had de verdeling van de grondsnel-heid geen betekenisvolle invloed op het aantal conflicten voor de hier beschouwde ontwerpen van het luchtruim. Het effect nam echter wel toe in omvang, omdat het koersbereik per vliegniveau afnam voor gelaagd luchtruim. De simulatieresul-taten gaven ook aan dat de numerieke modelaanpassingen die in dit proefschrift zijn ontwikkeld, de nauwkeurigheid van de meer realistische scenario's verbeterden tot de niveaus die werden gevonden met het analytische model voor de instellingen van het ideale scenario. Naast een fysiek inzicht in de factoren die de intrinsieke luchtruimveiligheid beïnvloeden, kunnen de aangepaste conflictmodellen daarom ook worden gebruikt als hulpmiddelen bij het ontwerpen van luchtruim.

Het derde en laatste deel van dit proefschrift ontwikkelde een kwantitatieve me-thode om de maximale capaciteit van gedecentraliseerde luchtruimconcepten te bepalen. De methode die hier wordt behandeld, genaamd Capaciteit evAluatie Methode voor geDecentraliseerde LVL ('Capacity Assessment Method for Decen-tralized ATC' (CAMDA)), definieert capaciteit als de verkeersdichtheid waarbij zich ketens van conflicten ongecontroleerd door het gehele luchtruim voortbewegen. Deze kritische dichtheid werd geïdentificeerd met behulp van een semi-empirische benadering, waarbij analytische modellen die de intrinsieke veiligheid van een lucht-ruimontwerp beschrijven, worden gecombineerd met empirische modellen die de acties van CD&O-algoritmen beschrijven. Omdat keten van conflicten zowel de vei-ligheid als de efficiëntie van reizen beïnvloeden, beschouwt de aanpak van CAMDA capaciteit als een intrinsieke eigenschap van het luchtruim.

De CAMDA-methode wordt hier gedemonstreerd met behulp van versnelde simula-
ties van gedecentraliseerde ongestructureerde en gelaagde luchtruimontwerp waar-
bij gebruik werd gemaakt van een op toestand gebaseerde methode voor con-
flictdetectie en een op spanningspotentieel gebaseerd algoritme voor conflictoplos-
sing. De resultaten van de simulatie bevestigden de voorspellingen van de CAMDA-
modellen: de capaciteit bleek hoger te zijn voor een gelaagd luchtruim omdat het
vooraf gedefinieerde regels gebruikt voor vluchtniveaus en koershoogte van het
kruisverkeer. Deze twee ontwerpelementen verminderden het aantal mogelijke
combinaties van twee vliegtuigen en de gemiddelde conflictkans tussen vliegtuigen
in vergelijking met ongestructureerd luchtruim, die op hun beurt de maximale ca-
paciteit voor gelaagd luchtruim verhoogden. De simulaties gaven ook aan dat de
sterke koppeling tussen het geselecteerde luchtruimontwerp en het geselecteerde
CD& O-algoritme moet worden geoptimaliseerd om de capaciteit van het decentrale
luchtruim te maximaliseren.

De simulaties die werden gebruikt om CAMDA te demonstreren, werden ook ge-
bruikt om het effect op de capaciteit te bestuderen van de dimensie van de con-
flictoplossing, de prioriteit voor de conflictoplossing en de snelheidsverdeling van de
vliegtuigen. Voor alle onderzochte gevallen schatte CAMDA het optreden van con-
flictketenreacties met hoge nauwkeurigheid, en maakte daarom capaciteitsschat-
tingen mogelijk met behulp van relatief niet-intensieve verkeerssimulaties met lage
dichtheid. Omdat alle CAMDA-parameters een fysieke interpretatie hebben, kun-
nen bovendien de effecten van alle geteste condities op de capaciteit direct worden
begrepen vanuit de structuur van de onderliggende modellen. Om deze redenen
kan de CAMDA-methode, naast het verschaffen van een vergelijkende capaciteit-
smeetwaarde, ook worden gebruikt om systematisch de experimentele condities te
selecteren die nodig zijn om de maximale capaciteitslimiet van gedecentraliseerde
luchtruimontwerpen te beoordelen.

Hoewel de veiligheids- en capaciteitsmodellen die in dit werk zijn ontwikkeld, zich
hebben gericht op ongestructureerde en gelaagde luchtruimontwerpen, is het be-
langrijk om te beseffen dat de onderliggende modelleringsmethoden ook van toe-
passing zijn op andere concepten van een luchtruim. Bij elke aanpassing moet
worden geanalyseerd hoe de beperkingen die een bepaald luchtruimontwerp op-
legt, het aantal mogelijke combinaties van twee vliegtuigen beïnvloedt, alsook de
gemiddelde conflictkans tussen twee vliegtuigen. Dit laatste omdat deze twee ba-
sisfactoren het startpunt zijn voor alle veiligheids- en capaciteitsmodellen die hier
worden besproken. Uitbreidingen van de modellen voor andere luchtruimontwer-
pen zijn een interessante manier om verder onderzoek te doen.

Hier moet wel opgemerkt worden dat alle kwantitatieve modellen beschreven in dit
proefschrift zijn gevalideerd onder ideale weersomstandigheden. Aangezien van het
weer bekend is dat het de veiligheid en de capaciteit van het luchtruim beïnvloedt,
moet de nauwkeurigheid van de afgeleide modellen voor andere, meer realistische
weersomstandigheden worden overwogen in toekomstig onderzoek. In dit verband
is het de moeite waard te erkennen dat de semi-empirische CAMDA methode om de
capaciteit te beoordelen, in theorie kan worden gebruikt om de capaciteitsverlagin-

gen te kwantificeren die door verschillende fenomenen worden veroorzaakt, zolang dergelijke verschijnselen met voldoende realisme kunnen worden gesimuleerd. Het gebruik van de CAMDA-methode om de effecten van operationele beperkingen, zoals het weer, op capaciteit te beoordelen, vormt daarom een ander interessant onderwerp voor verdere analyse.

Ten slotte is het noodzakelijk om de praktische toepassingen van dit onderzoek te overwegen. Voordat de luchtvaartautoriteiten, welke gefocust zijn op veiligheid, overtuigd kunnen worden van een radicale transformatie van het luchtruimontwerp voor kruisende vliegtuigen van een gecentraliseerd naar een gedecentraliseerd vorm, is het waarschijnlijk dat er meer praktische ervaring moet worden opgedaan met gedecentraliseerde LVL. Dankzij de snelle opkomst van onbemande en persoonlijke vliegtuigen, kan het mogelijk zijn om dit in de nabije toekomst zo praktisch mogelijk te maken. De ongelooflijke verkeersvolumes die voor deze nieuwe vliegtuigtypen zijn voorspeld, en het ontwerp vanaf een compleet lege pagina van de LVL die nodig is om hun activiteiten te vergemakkelijken, hebben de luchtvaartautoriteiten de nodige prikkels gegeven om belangrijke aspecten van decentralisatie, zoals zelfscheiding, voor het ontwerp van het groeiend gebied van stedelijk luchtruim. Vanwege de generieke aard van de ontwerpen van luchtruim en van de kwantitatieve veiligheids- en capaciteitsmodellen die in dit proefschrift worden besproken, kunnen de resultaten van dit werk worden veralgemeniseerd boven de specifieke omstandigheden die hier zijn overwogen. Bijvoorbeeld voor de lagere snelheden die verwacht worden voor onbemande vliegtuigen. Daarom zouden op korte termijn de methoden die in dit proefschrift zijn ontwikkeld om de capaciteit van gedecentraliseerde ATC te analyseren en te modelleren, nuttig kunnen zijn bij het ontwerpen van nieuwe concepten die de luchtvaart in stedelijke omgevingen op lage hoogte mogelijk maken.

Nomenclature

Acronyms

ACC	Area Control Center
ADS-B	Automatic Dependent Surveillance Broadcast
ANSP	Air Navigation Service Provider
APM	Aircraft Performance Models
ATC	Air Traffic Control
ATCo	Air Traffic Controller
ATM	Air Traffic Management
BADA	Base of Aircraft Data
CAMDA	Capacity Assessment Method for Decentralized ATC
CD	Conflict Detection
CD&R	Conflict Detection and Resolution
CP	Conflict Prevention
CPA	Closest Point of Approach
CR	Conflict Resolution
DEP	Domino Effect Parameter
FAA	Federal Aviation Administration
FMS	Flight Management System
FRA	Free Routing Airspace
IFR	Instrument Flight Rules
INM	Integrated Noise Model
IPR	Intrusion Prevention Rate
L180	Layers Concept With $\alpha = 180^o$
L360	Layers Concept With $\alpha = 360^o$
L45	Layers Concept With $\alpha = 450^o$
L90	Layers Concept With $\alpha = 90^o$
LDEN	Loudness Day Evening Night
MTOW	Maximum Take-Off Weight
MVP	Modified Voltage Potential
NAT-OTS	North Atlantic Organized Track System
NLR	Netherlands Aerospace Center
PASAS	Predictive Airborne Separation Assurance System
PATS	Personal Aerial Transportation System

RNAV   Area Navigation
RQ   Research Question
RTA   Required Time of Arrival
RTCA   Radio Technical Commission for Aeronautics
SESAR   Single European Sky ATM Research
TBO   Trajectory Based Operations
TMA   Terminal Maneuvering Area
TMX   Traffic Manager
TWR   Air Traffic Control Tower
UA   Unstructured Airspace

Greek Symbols

α Heading range per flight level [^{o}]
β No. of flight levels in 1 layer set
Γ Thrust vector [lbf]
γ Flight path angle [^{o}]
κ Number of layer sets
ω Proportion of climbing/descending aircraft
ψ Aircraft heading [^{o}]
ρ Density [ac/NM^2]
ρ_{max} Maximum theoretical airspace capacity [ac/NM^2]
ε Proportion of cruising aircraft
ζ Vertical spacing between layers [ft]

Roman Symbols

$\mathbf{P}_{ij}$ Relative position vector between a/c i and j[NM]
$\mathbf{s}$ Displacement vector [NM]
$\mathbf{V}_{r,ij}$ Relative velocity vector between a/c i and j [kts]
A Airspace area [NM^2]
B Airspace volume [ft^3]
C Conflict count
CX Complexity metric
D Trip distance [NM]
D_{cdr} Extra distance flown due to conflict detection & resolution [NM]
D_{ij} Normalized distance between a/c i and j [NM]
DEP Domino Effect Parameter
I Intrusion (count)
IPR Intrusion Prevention Rate
k Model accuracy parameter
L Total No. of flight levels

LA	A-weighted noise metric [dB(A)]
$LA_{eq}68$	Contour area of A-weighted noise metric at 68 dB(A) [NM^2]
N	No. of aircraft
n_s	Number of samples
p	Average Conflict probability between any two aircraft
PR	Convergence indicator
PR	Proximity indicator
$R1$	Number of conflicts that were avoided with conflict resolution
$R2$	Number of conflicts that occurred with and without conflict resolution
$R3$	Number of additional conflicts that occurred because of conflict resolution
$S1$	Set of all conflicts without conflict resolution
$S2$	Set of all conflicts with conflict resolution
S_h	Horizontal separation requirement [NM]
S_v	Vertical separation requirement [ft]
SCX	Structural complexity metric
T	Analysis time interval [s]
t	Time [s]
t_l	Conflict look-ahead time [s]
V	Aircraft velocity magnitude [kts]
V_r	Relative velocity magnitude [kts]
W	Work Done [MJ]
Z	Altitude [ft]

Subscripts

h	Horizontal
v	Vertical
$2d$	Two dimensional
$3d$	Three dimensional
LAY	Layered airspace
UA	Unstructured airspace
cd	Climbing/Descending aircraft
cr	Cruising aircraft
$inst$	Instantaneous
max	Maximum
min	Minimum
sev	Severity
$total$	Total (during analysis time interval)

Acknowledgements

Deciding to pursue a PhD at C&S was an easy decision for me; I jumped at the chance as soon as it was presented! Looking back, this period of my life has been very important to me on both a personal and academic level. In addition to studying and working at a world renowned university, I've had opportunities afforded to very few; from working with well-known scientists and engineers as part of the pan-European Metropolis project, to the immensely satisfying and productive mini 'sabbatical' at ENAC Toulouse. None of this would have been possible without the support of many amazing people at C&S and beyond, and so I want use these final pages to express my heart-felt thanks to everyone that helped me on this incredible journey.

First of all, I need to express my sincere gratitude to Prof. dr. ir. Jacco M. Hoekstra. Jacco not only gave me the opportunity to do a PhD, he also gave me many useful ideas and tips throughout my research. I still remember very clearly the eureka moment that you had during the preliminary MSc thesis presentation of Martijn Tra when you came up with the initial ideas needed to derive the conflict count models developed in this thesis. I also want to thank you for initiating, and continuously contributing to the BlueSky ATM simulator, which was used for most of the fast-time simulations performed in this thesis. Aside from academic aspects, I also learnt many useful life lessons from Jacco, most importantly time management. It still amazes me how you find the time to be actively involved in research and coding BlueSky while also having a full teaching schedule throughout the year. Your excitement for ATM research has been contagious, and I am sure that many life lessons and technical skills that I learnt from you will continue to help me in my future career and life.

I also want to deeply thank my daily supervisor and co-promotor Dr. ir. Joost Ellerbroek. In addition to performing the tasks of a daily supervisor, Joost was like an 'academic big brother' to me. And like all good big brothers, Joost used his own previous experiences to help me avoid many mistakes, and helped me to safely navigate through the challenging PhD process. His advice on how to write scientific articles and peer-review response letters contributed significantly to the publications that resulted from this PhD. Additionally, Joost, as a major BlueSky contributor, was always available for quick bug fixes and new feature implementations that significantly that were required for this work. I am also extremely grateful for our weekly Monday morning meetings that were extremely useful for solving many technical problems, and for your tips on staying productive through the difficult times of the PhD.

One of the most enjoyable aspects of my PhD was the chance to be part of the Metropolis project back in 2014. Metropolis was my first exposure to the ATM world, and I learned a lot about ATM research by being part of this project. The project even contributed heavily towards the 2nd chapter of this thesis. Because of this, I would like to specially thank everyone involved in the project: Jacco and Joost from TU Delft; Frank, Dennis, Roalt Pim, and Marieke from the NLR; Andrija, Daniel and Georges from ENAC; and Oliver and Stefan from DLR. The project was only a success because of the commitment that all of you showed.

I am extremely grateful to both Dr. Andrija Vidosavljevic and to Prof. dr. Daniel Delahaye for inviting me for a mini three month sabbatical at ENAC in Toulouse, France, towards the end of the PhD. Toulouse and ENAC were a very welcome change of scenery that helped me to focus and finish the technical components of my research. I also met many friendly fellow researchers at ENAC that made my stay very enjoyable and lively, most notably Ruixin Wang and Ji Ma, with whom I had many fun Friday evening trips to the city center. I also remember with great fondness the many interesting conversations that Andrija and I had during the very delicious lunch breaks at ENAC, and the truly wonderful hike organized by Daniel through the Pyrenees, something I would have never done on my own. You were both very generous and warm hosts, and I am extremely thankful for this wonderful opportunity.

I would also like to thank my MSc thesis supervisors: Dr. Jan Smisek, Dr. ir. Renee van Paassen, and Prof. dr. ir. Max Mulder. The very seamless experience that I had with the three of you during my MSc thesis made my decision to do a PhD, and to do it here at C&S, a no-brainer!

My PhD experience was made complete and extremely pleasant by all the students and staff of C&S. I really enjoyed attending all the long coffee breaks, tasty barbecues, exciting basketball tournaments, loud vrijmibos, FULL POWER pool games, delightful dinners, super Chinese new year parties, and the many other social gatherings that were organized by Stabilo and the PhD board. I thank all my fellow PhD students and our one post-doc for their great comradery (in no specific order): Junzi, Wei, Sherry, Tommaso, Joao, Peng, Hann Woei, Jerom, Dyah, Jan Smisek, Jan Comans, Laurens, Sophie, Yazdi, Jaime, Ye Zhou, Ye Zhang, Yingshi, Tao, Ewoud, Matej, Henry, Julia, Jia, Liguo, Deniz, Maarten, Rolf, Lodewijk, Tim, Kasper, Ivan, Kimberly, Kirk, Dirk, Neno, Isabel, Annemarie, Shuai, Sihao, Shuo, Mario, Diana, Jelmer, Tom, Daniel, Ying, Bo, Yingfu Paolo, Ezgi, Malik, Mariam, Yke, Sarah, Anne, Gustavo, Sjoerd and Herman. I also thank all my office mates in both Sim 0.04 and room 3.21 (blue tower) for the many stimulating conversations on politics, economics, and a wide range of other non-work related topics. These interesting and enlightening talks were useful distractions when the work was not proceeding according to plan! I also want to thank all the staff members of C&S, all whom were very friendly and helpful: Daan, Clark, Erik-Jan, Coen, Olaf, Andries, Harold, Alwin, Guido, Bart, Ferdinand, Christophe, Marilena, Bob, Xander and Hans. Because of all you I was able to have some sort of work-life balance during the PhD without which I would have surely gone insane!

At a recent C&S pub quiz, one of the questions was: "Who is the most important person at C&S?". The answer was of course, without a doubt, our very friendly and efficient group secretary Bertine Markus. You can always be confident that if Bertine is on the job, it will be done very well and quickly! Over the years, Bertine was always happy to help me through the bureaucracy of being an international student, and has also written countless 'student-proof' letters on my behalf. Thank you Bertine for all the hard work that you did for me! I always really appreciated your efforts!

I also extend a very special thanks to Jerom Maas. Jerom was initially my MSc thesis student, but to my great benefit, he continued to help me with my research during his PhD, even though his own PhD topic was on a completely different topic! I have never heard of another case where this has happened, and I am truly appreciative all the time you spent helping me, especially to derive the conflict count models presented in chapter 3. I also had the very good fortune of supervising several other talented MSc students, all of whom have contributed in some shape or form to this thesis (in chronological order): Dennis Mischon, Martijn Tra, Thom Langejan, Suthes Balasooriyan and Ólafur Þórðarson.

A very interesting side-task that I had during the PhD was to be the C&S representative on the board of Aerospace Engineering PhD students of TU Delft. I am thankful to Prof. Dr. Dick Simons for this honor. Organizing the various activities of the board, including the yearly social and scientific events, with the other esteemed board members Roberto, Maurice, Tomas, Morteza, Svenja and Fardin, was always great fun! I am also very happy that Dirk van Baelen has become our new C&S representative on the board and has become its chairman. Under his astute leadership, he has taken the board to even greater heights! Dirk also generously helped me to translate the summary of this thesis to Dutch.

Last, but certainly not least, I thank my parents and my little brother. You have always supported me unconditionally through all walks of life, instilled all that is good in me, and have always believed in me even when I didn't believe in myself. I couldn't have done this without you, and I am where I am today because of you; this achievement is as much yours as it is mine. To my fiancée Kavya: you only entered my life towards the end of this PhD process, but the love and affection you have shown me has meant the world to me. I look forward to our shared lives together, and to all the adventures that we will have in the future!

Delft and TU Delft has been my home for the last ten years, and I have met so many remarkable people here that have helped me throughout my studies. Unfortunately, I couldn't mention you all here, but I thank you all very, very much from the bottom of my heart! I am forever in your service!

Emmanuel Sunil
Delft, 25th of October 2018

Curriculum Vitae

EMMANUEL SUNIL

24 - 12 - 1989   Born in Thodupuzha, Kerala, India

Education

2014 – 2018   **PhD. Aerospace Engineering**
Delft University of Technology, Delft, The Netherlands
2011 – 2014   **MSc. Aerospace Engineering**
Delft University of Technology, Delft, The Netherlands
2008 – 2011   **BSc. Aerospace Engineering**
Delft University of Technology, Delft, The Netherlands
2006 – 2008   **Advanced Level (CIE)**
Trivandrum International School, Trivandrum, India

Experience

2018 – Ongoing   **R&D Engineer**
Nationaal Lucht- en Ruimtevaartlaboratorium (NLR)
Amsterdam, The Netherlands
April – June   **Visiting Researcher**
2018   Ecole Nationale de l'Aviation Civile (ENAC)
Toulouse, France
2014 – 2015   **Research Engineer Metropolis Project**
Delft University of Technology, Delft, The Netherlands
July – October   **Research Intern myCopter Project**
2012   Max Planck Institute for Biological Cybernetics
Tübingen, Germany
2011 – 2012   **Vehicle Dynamics Engineer**
Formula Student Team Delft, Delft, The Netherlands

Awards and Accomplishments

2015 – 2016   **Board member** of the Aerospace Engineering PhD
student society of TU Delft
June 2016   **Best paper award** at the FAA/Eurocontrol International
Conference for Research in Air Transportation

List of Publications

Journal Articles

5. **Emmanuel Sunil**, Joost Ellerbroek and Jacco Hoekstra, *"Airspace Stability-Based Capacity Assessment Method for Decentralized Air Traffic Control"*, in Elsevier Transportation Research Part C: Emerging Technologies (in preparation)

4. **Emmanuel Sunil**, Joost Ellerbroek, Jacco Hoekstra and Ólafur Þórðarson, *"Effect of Traffic Scenario Characteristics on the Accuracy of Conflict Count Models"*, in Elsevier Transportation Research Part C: Emerging Technologies (in preparation)

3. **Emmanuel Sunil**, Joost Ellerbroek, Jacco Hoekstra and Jerom Maas, *"Three Dimensional Conflict Count Models for Unstructured and Layered Airspace Designs"*, in Elsevier Transportation Research Part C: Emerging Technologies, Vol. 95, Pg. 295-319, October 2018

2. **Emmanuel Sunil**, Joost Ellerbroek, Jacco Hoekstra, Andrija Vidosavljevic, Michael Arntzen, Frank Bussink and Dennis Nieuwenhuisen, *"Analysis of Airspace Structure and Capacity for Decentralized Separation Using Fast Time Simulations"*, in AIAA Journal of Guidance Control and Dynamics, Vol. 40, No. 1, Pg. 38-51, January 2017

1. Jan Smisek, **Emmanuel Sunil**, Marinus M. Van Paassen, David Abbink and Max Mulder, *"Neuromuscular System Based Tuning of a Haptic Shared Control Interface for UAV Teleoperation"*, in IEEE Transactions on Human Machine Systems, Vol. 47, No. 4, Pg. 449-461, October 2016

Conference Proceedings

15. **Emmanuel Sunil**, Joost Ellerbroek and Jacco Hoekstra, *"CAMDA: Capacity Assessment Method for Decentralized Air Traffic Control"*, Presented at the 8th International Conference on Research in Air Transportation (ICRAT), February 2018

14. **Emmanuel Sunil**, Ólafur Þórðarson, Joost Ellerbroek and Jacco Hoekstra, *"Analyzing the Effect of Traffic Scenario Properties on Conflict Count Models"*, Presented at the 8th International Conference on Research in Air Transportation (ICRAT), February 2018

13. Jacco Hoekstra, Joost Ellerbroek, **Emmanuel Sunil** and Jerom Maas, *"Geovectoring: Reducing Traffic Complexity to Increase the Capacity of UAV airspace"*, Presented at the 8th International Conference on Research in Air Transportation (ICRAT), February 2018

12. **Emmanuel Sunil**, Joost Ellerbroek, Jacco Hoekstra and Jerom Maas, *"Modeling Airspace Stability and Capacity for Decentralized Separation"*, Presented at the 12th USA Europe Air Traffic Management Research and Development Seminar (ATM), June 2017

11. Martijn Tra, **Emmanuel Sunil**, Joost Ellerbroek and Jacco Hoekstra, *"Modeling the Intrinsic Safety of Unstructured and Layered Airspace Designs"*, Presented at the 12th USA Europe Air Traffic Management Research and Development Seminar (ATM), June 2017

10. Thom Langejan, **Emmanuel Sunil**, Joost Ellerbroek and Jacco Hoekstra, *"Effect of ADSB Characteristics on Airborne Conflict Detection and Resolution"*, Presented at the 6th SESAR Innovation Days, November 2016

9. **Emmanuel Sunil**, Jacco Hoekstra, Joost Ellerbroek, Frank Busink, Andrija Vidosavljevic, Daniel Delhaye and Dennis Nieuwenhuisen, *"The Influence of Traffic Structure on Airspace Capacity"*, Presented at the 7th International Conference on Research in Air Transportation (ICRAT), June 2016

8. **Emmanuel Sunil**, Jerom Maas, Joost Ellerbroek and Jacco Hoekstra, *"The Relationship Between Traffic Stability and Capacity for Decentralized Airspace"*, Presented at the 7th International Conference on Research in Air Transportation (ICRAT), June 2016

7. Jacco Hoekstra, Jerom Maas, Martijn Tra and **Emmanuel Sunil**, *"How Do Layered Airspace Design Parameters Affect Airspace Capacity and Safety"*, Presented at the 7th International Conference on Research in Air Transportation (ICRAT), June 2016

6. Jerom Maas, **Emmanuel Sunil**, Joost Ellerbroek and Jacco Hoekstra, *"The Effect of Swarming on a Voltage Potential Based Conflict Resolution Algorithm"*, Presented at the 7th International Conference on Research in Air Transportation (ICRAT), June 2016

5. Andrija Vidosavljevic, Daniel Delahaye, **Emmanuel Sunil**, Frank Bussink and Jacco Hoekstra, *"Complexity Analysis of the Concepts of Urban Airspace Design for METROPOLIS Project"*, Presented at ENRI International Workshop on ATM and CNS (EIWAC), November 2015

4. Michael Arntzen, Roalt Aalmoes, Frank Bussink, **Emmanuel Sunil** and Jacco Hoekstra , *"Calculation of futuristic metropolitan noise due to aircraft"*, Presented at Internoise, August 2015

3. **Emmanuel Sunil**, Jacco Hoekstra, Joost Ellerbroek, Frank Bussink, Dennis Nieuwenhuisen, Andrija Vidosavljevic and Stefan Kern, *"Metropolis Relating Airspace Structure and Capacity for Extreme Traffic Densities"*, Presented at the 11th USA Europe Air Traffic Management Research and Development Seminar (ATM), June 2015

2. Roalt Aalmoes, YS Cheung, **Emmanuel Sunil**, Jacco Hoekstra and Frank Bussink, *"A conceptual third party risk model for personal and unmanned aerial vehicles"*, Presented at the International Conference on Unmanned Aircraft Systems, June 2015

1. **Emmanuel Sunil**, Jan Smisek, Marinus M van Paassen and Max Mulder, *"Validation of a Tuning Method for Haptic Shared Control Using Neuromuscular System Analysis"*, Presented at IEEE Systems Man and Cybernetics conference, October 2014

Posters

1. **Emmanuel Sunil**, Joost Ellerbroek, and Jacco Hoekstra, *"An Empirical Analysis of Airspace Structure and Capacity for Decentralized Separation"*, Presented at the 6th Sesar Innovation Days (SID), November 2016